

Infrared Spectroscopic Studies of Polystyrene Emulsion Polymers: Effect of Oxidation During Polymerization

J. N. SHAW and M. C. MARSHALL,
School of Chemistry, University of Bristol, Bristol, England

Synopsis

Infrared spectroscopy was employed to study the nature of the structural changes which occurred through oxidation during the emulsion polymerization of styrene. Aliphatic carboxylic, amino, and phosphate emulsifiers and hydrogen peroxide and potassium persulfate initiators were employed for polymer preparation. In addition, a polystyrene dispersion prepared in the absence of any emulsifier or stabilizer was examined. Irrespective of the nature of the initiator-emulsifier combination employed, all of the polymer spectra revealed bands at 1705 and 1770 cm^{-1} . The band at 1705 cm^{-1} was assigned in part to the carbonyl stretching mode of dimeric carboxylic acid, formed by oxidation, in the polystyrene chains. Absorption at 1770 cm^{-1} , which was very weak, was tentatively attributed to the carbonyl stretching mode of the monomeric form of this acid. The structure of the acid endgroup was not established, but the results obtained suggest that it was possibly a phenylacetic acid residue or a residue with a similar structure.

INTRODUCTION

Extensive use has been made of infrared spectroscopy for the purpose of establishing the molecular structure of polymers.^{1,2} The availability of relevant information in the literature facilitates spectroscopic studies of polymers which have undergone structural changes by, for example, oxidation. Hitherto, oxidative changes have in the main been investigated on samples obtained by oxidation after polymerization,³⁻¹⁵ and most studies appear to have been performed on oxidized polyethylene.^{3-5, 8, 9, 11, 12} As far as can be ascertained, the oxidative changes in polymers which occur during polymerization have been investigated only to a limited extent.^{16, 17} Moreover, although some spectroscopic studies have been performed on the bulk polymer,^{10, 16, 17} it would appear that emulsion-polymerized polystyrene has received little attention.

The present work was concerned with a spectroscopic examination of polystyrene latices prepared with the use of hydrogen peroxide and potassium persulfate as initiators, and aliphatic carboxylic, amino, and phosphate emulsifiers. Previous electrokinetic and radiotracer studies¹⁸⁻²⁰ indicated that the emulsifiers could be removed from the polymer by

extensive dialysis to leave particles with surface carboxyl groups of pK value 4.60. Dye interaction (with Rhodamine 6GBN) and potentiometric titration studies²¹ have also provided evidence for the presence of these groups. The latter were found to be an integral part of the polymer chains and were presumably formed by oxidation during polymerization. Polystyrene particles prepared in aqueous solution and in the absence of any emulsifier or stabilizer also contained the same acidic groups. Infrared spectroscopy was employed in an effort to obtain more direct evidence for the presence of these carboxyl endgroups on the emulsion polymers.

EXPERIMENTAL

Polystyrene Dispersions

The latices employed in the present work, with the initiator-emulsifier combinations used to prepare them are listed in Table I. Dispersion I

TABLE I
Polystyrene Samples Used

Designation	Particle diameter, A.	Initiator/emulsifier Combination
Latex B	1030 \pm 82	H ₂ O ₂ /sodium dodecanoate
F	2480 \pm 85	H ₂ O ₂ /sodium monododecylphosphate
G	2300 \pm 25	H ₂ O ₂ /dodecylamine hydrochloride
H	2640 \pm 50	K ₂ S ₂ O ₈ /sodium dodecanoate
Dispersion I	11300 \pm 1200	H ₂ O ₂ /no emulsifier

was prepared in the absence of any emulsifier or stabilizer by polymerizing the monomer in water with hydrogen peroxide as initiator. The procedure used for the production of the emulsion polymers has been previously described.^{18,22} The emulsions were not purged with nitrogen before polymerization. Latex B was employed for previous studies^{23,24} and is typical of latices prepared with the use of sodium dodecanoate as emulsifier and hydrogen peroxide as the initiator. All of the latices were extensively dialyzed to remove the emulsifiers.

Treatment of Materials

Two aliquots of latex B, numbered B1 and B2, were treated as follows.

Latex B1. Sample B1 was obtained by coagulating latex B with hydrochloric acid and repeatedly washing the polymer with warm, dilute sodium hydroxide, hydrochloric acid, and double-distilled water. The polymer was dried *in vacuo* in the presence of hydrochloric acid so as to ensure that most of the carboxyl groups in the polymer chains¹⁸⁻²⁰ would be un-ionized.

Latex B2. The treatment employed for this latex was the same as that for B1 except that in this case the polymer was dried in the presence of 10 ml. of a 0.01M solution of sodium hydroxide. Thus the sodium salt of some, if not all, of the polymeric carboxyl groups was formed.

Latexes F, G, H, and Dispersion I. The solid polymer from latexes F, G, H and dispersion I was washed as described above and dried in the presence of hydrochloric acid.

Measurement of Spectra

The spectra were recorded with a Unicam SP 100 spectrophotometer equipped with a sodium chloride prism. Although some measurements were made in the spectral region 2500–4000 cm^{-1} , in the main the studies were confined to the region 1500–1900 cm^{-1} . Scale expansion, both ordinate and abscissa, was also employed.

Spectra were obtained on the solid polymer in the form of thin films of arbitrary thickness. The films were produced by casting a solution of polymer in carbon tetrachloride onto the rock salt window and removing the solvent *in vacuo*. Pressed disks of the dried materials were occasionally employed. It was found that samples in both forms produced identical spectra.

In order to establish with some certainty the bands due to the oxidation products in the polymer, a compensation technique was used. The normal polystyrene peaks were compensated with a sample of the pure polymer (Distillers Company light-scattering standard) which was designated "standard polystyrene." The spectrum of this material did not exhibit any bands which could be attributed to oxidation products. The compensating film of the standard sample was gradually increased in thickness until the appropriate polystyrene bands in the spectra of the latexes were compensated to the required degree. The nomenclature C₁, C₂, etc., denotes an increasing degree of compensation. This procedure did not reveal bands which were not already present in the spectra.

RESULTS AND DISCUSSION

Standard Polystyrene

The unexpanded spectrum of the standard polystyrene sample is presented in Figure 1a. It appears to be in agreement with the spectra of amorphous polystyrene obtained by other workers.^{25,26} Bands in the region of 1700 cm^{-1} are of particular interest, since it is in this region that carbonyl groups produced by oxidation would be expected to absorb. Bands at 1945, 1875, 1802, 1745, and 1675 cm^{-1} are attributable²⁵ to combinations of the CH out-of-plane deformation vibrations characteristic of the phenyl group. The band at 1603 cm^{-1} is characteristic of the benzene ring. Clearly, the spectrum does not reveal any bands which could be attributed to carbonyl vibrations and therefore the standard polystyrene sample was eminently suitable for compensation purposes.

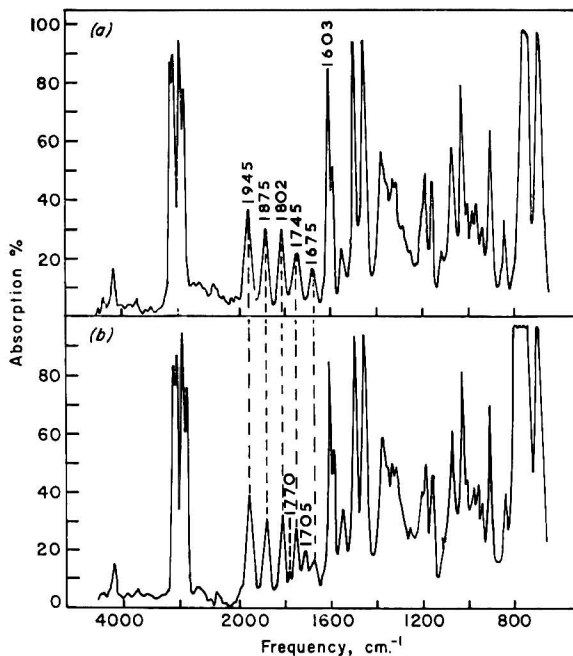


Fig. 1. Infrared spectra of (a) standard polystyrene sample and (b) latex B1 in the range 800–4000 cm^{-1} .

Uncompensated and Unexpanded Spectrum of Latex B1

The spectrum of latex B1, shown in Figure 1b, contains weak bands at 1770 and 1705 cm^{-1} . The latter were not present in the spectrum of the standard polymer. Although the absorption at 1705 cm^{-1} is comparatively weak, it is significantly stronger than that at 1675 cm^{-1} . The 1705 cm^{-1} band can be assigned to a carbonyl stretching vibration.²⁷

Expanded and Compensated Spectra of Latices B1 and B2

The expanded and compensated spectra of samples B1 and B2, in the region 1500–1800 cm^{-1} , are compared in Figures 2a and 2b. The film thickness of the samples was so chosen that the intensities of the characteristic polystyrene bands would be of equal magnitude in both spectra. It can be seen that the third compensation, C_3 , removed the absorption at 1802, 1745, and 1675 cm^{-1} in each spectrum. Absorption at 1770 and 1705 cm^{-1} was unaffected in each case. In addition, the compensation technique resolved very weak bands at 1630 and 1608 cm^{-1} . The former is probably attributable to the C=C stretching mode of residual styrene^{27,28} in the emulsion polymer.

Although the band at 1705 cm^{-1} is common to both spectra, the intensity of this band in the spectrum of latex B1 (Fig. 2a) is significantly greater than it is in that of latex B2 (Fig. 2b). This difference would be expected if the polymer contained carboxylic acid groups, since in the

case of B2, owing to the treatment with alkali, some of these groups would be ionized and consequently a reduced acid carbonyl absorption at 1705 cm.^{-1} would be anticipated. In the spectra of carboxylic acids the carbonyl stretching mode at about 1700 cm.^{-1} disappears on salt formation and is replaced by the asymmetric ($1610\text{--}1550\text{ cm.}^{-1}$) and symmetric ($1420\text{--}1330\text{ cm.}^{-1}$) modes of the carboxylate ion.²⁷

The fact that the 1705 cm.^{-1} band in the spectrum of B2 was not removed suggests that either all of the acid groups did not ionize, or that

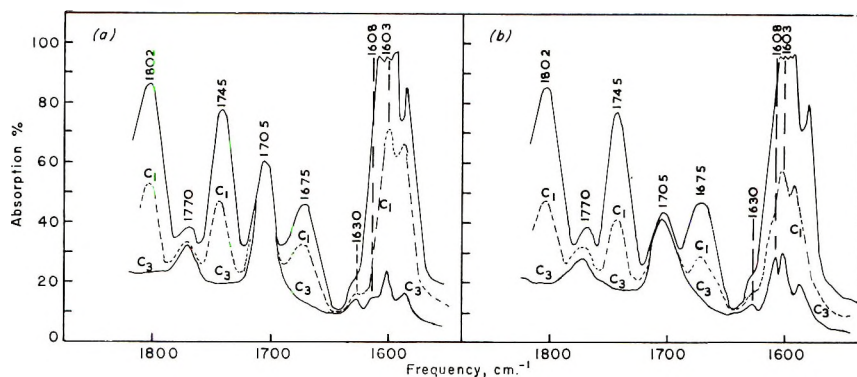


Fig. 2. Comparison of the infrared spectra of (a) latex B1 and (b) latex B2 in the range $1600\text{--}1800\text{ cm.}^{-1}$.

some other carbonyl-containing structures such as ketones or aldehydes, or both, contributed to this absorption. Although it occurs in both spectra and is weak, the band at 1608 cm.^{-1} appears to be stronger in that for sample B2 than in the spectrum of B1 and may possibly be ascribed to the asymmetric mode of the carboxylate ion²⁷ in the polymer chains. This, however, is a tentative assignment. The corresponding symmetric mode could not be detected; in any case the latter is rather less characteristic than asymmetric vibration.^{27,29} The absorption at 1770 cm.^{-1} in the spectra is considered later.

Latex B1 with Added Dodecanoic Acid

Expanded and compensated spectra indicating the effects produced by added dodecanoic acid are presented in Figures 3a and 3b. For the latter, the concentrations of added acid were, respectively, 2.50×10^{-5} and 1.35×10^{-4} mole acid/g. polymer. The same film thickness was employed for both spectra. As before, complete compensation of the bands at 1802 and 1675 cm.^{-1} was effected, but there was significant residual absorption at 1745 cm.^{-1} . Figure 3b shows that the higher concentration of the added acid produced the higher intensity at this frequency. Although the band at 1770 cm.^{-1} was unaffected for both acid concentrations, the intensity of the 1705 cm.^{-1} band appeared to be enhanced in each spectrum.

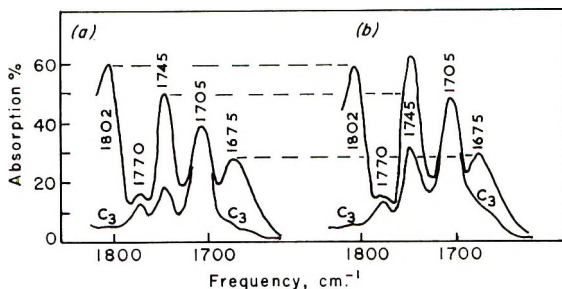


Fig. 3. Infrared spectra in the range 1620–1800 cm^{-1} , showing the effects produced on the addition of dodecanoic acid to latex B1: (a) 2.50×10^{-3} mole acid added/g. polymer; and (b) 1.35×10^{-4} mole/g. polymer.

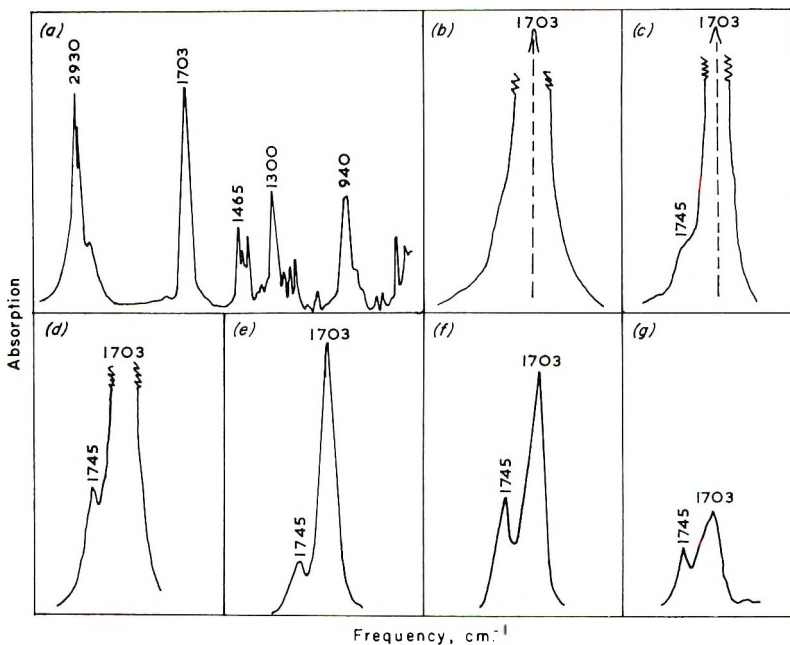


Fig. 4. Infrared spectra of dodecanoic acid: (a) in the range 700–3600 cm^{-1} , obtained from a thin film; (b)–(g) from solutions of the acid in carbon tetrachloride, (b) 0.25*M*, (c) 0.01*M*, (d) 0.025*M*, (e) 0.005*M*, (f) 0.001*M*, (g) 0.0002*M*.

With progressively greater additions of acid, spectra were obtained in which the acid carbonyl intensity increased until eventually it masked the bands between 1770 and 1675 cm^{-1} and had a maximum at 1703 cm^{-1} ; a spectrum of dodecanoic acid, which agrees with those obtained by others,^{29–32} is presented in Figure 4a.

Thus, when the acid concentration was low, the carbonyl absorption occurred mainly at 1745 cm^{-1} , suggesting that the acid was predominantly in the monomeric form.²⁷ Since the relevant data did not appear to be available in the literature, this conclusion was checked by determining

the spectra of solutions of dodecanoic acid in carbon tetrachloride over the concentration range $0.25\text{--}2 \times 10^{-4}M$. The results obtained are presented in Figures 4*b*–4*g*. The spectra show that as the concentration of acid decreased the band at 1745 cm^{-1} became more resolved. This band can be assigned to the carbonyl stretching mode of the monomeric acid,²⁷ while the absorption at 1703 cm^{-1} is due to the dimeric form.²⁷

Spectra of Latices F and G

The spectrum of latex F, presented in Figure 5*a*, exhibits, as expected on the basis of previous studies,^{18–21} similar features to those of the spectrum of latex B1. Absorption was observed at 1770, 1705, 1630, and 1608 cm^{-1} . The band at 1705 cm^{-1} provides evidence for the presence of oxidation products in this emulsion polymer also.

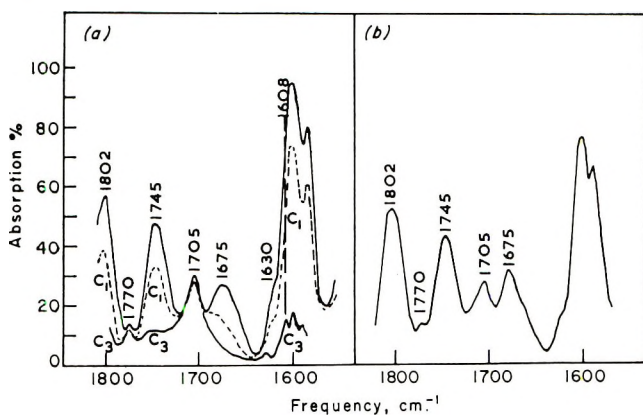


Fig. 5. Infrared spectra of (a) latex F and (b) latex G, in the range $1600\text{--}1800\text{ cm}^{-1}$.

It may be seen from Figure 5*b* that the spectrum of latex G exhibits bands at 1770 and 1705 cm^{-1} . In this case the polystyrene vibrations were not compensated.

Spectra of Latex H and Dispersion I

Latex H was prepared by using potassium persulfate as the initiator, but the presence of the 1705 cm^{-1} band in the spectrum of this polymer (Fig. 6*a*) indicates that oxidation occurred during the polymerization. The spectrum was not compensated. Absorption which might be attributable to —O—SO_3^- ions in the polymer chains could not be detected. This result was anticipated since it was previously shown²⁰ that the polymer contained about five times more carboxyl groups than sulfate ions. The band at 1770 cm^{-1} is present in this spectrum also.

Electrokinetic studies^{18–20} on dispersion I revealed that the polystyrene particles contained carboxylic acid groups. Since no emulsifier was used for the preparation of this polymer these groups must have been produced by polymer oxidation during polymerization. The uncompensated spec-

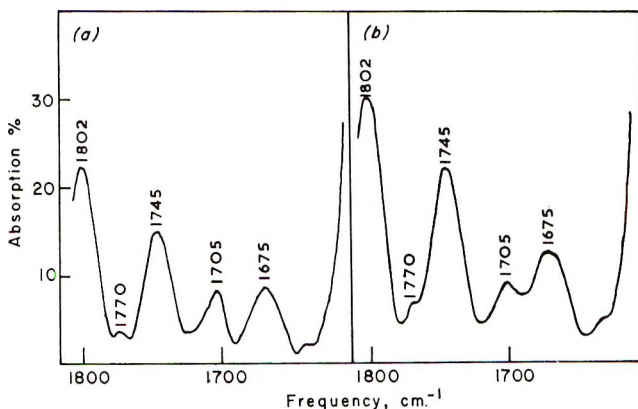


Fig. 6. Infrared spectra of (a) latex H and (b) dispersion I, in the range 1600–1800 cm^{-1} .

trum in Figure 6b shows the presence of a carbonyl band at 1705 cm^{-1} and also a band at 1770 cm^{-1} .

Band Assignments

Absorption at 1705 cm^{-1} . On the basis of the evidence provided by the spectra of latices B1 and B2 (Figs. 2a and 2b), at least some of the absorption at 1705 cm^{-1} can be assigned to a dimeric carboxylic acid.²⁷ Since on treatment with alkali, however, the band was not removed it seems probable that the presence of aryl aldehyde or alkyl ketone, or both, in the polymer contributed to the intensity at this frequency.

The precise structure of the acid in the emulsion polymers is not known. As the results obtained from the addition of dodecanoic acid to latex B1 (Figs. 3 and 4) show, the band at 1705 cm^{-1} is not due to the presence of residual emulsifier in this polymer. This conclusion is strongly supported by the spectrum for dispersion I (Fig. 6b), during the preparation of which no emulsifier was used.

An acid could possibly be formed by the oxidation of an endgroup such as $\text{HOCH}_2-(\text{C}_6\text{H}_5)\text{CH}-$ to give $\text{HOOC}-(\text{C}_6\text{H}_5)\text{CH}-$, and thus a phenylacetic acid residue would be produced. The carbonyl-stretching frequency of dimeric phenylacetic acid has been recently reported to occur at $1697 \pm 3 \text{ cm}^{-1}$ by Flett²⁹ and at about 1706 cm^{-1} (interpolated from the published spectrum) by Hadzi.³³ The $\text{p}K$ value of the latter is 4.33³⁴ while that of acid in the emulsion polymers was found to be 4.60.¹⁸⁻²¹ However, the difference between the two figures may not be of particular significance because the $\text{p}K$ of the polymeric acid is an intrinsic value. Thus the presence of phenylacetic acid residues or acid residues with a similar structure could conceivably account for the present results.

Absorption at 1770 cm^{-1} . The intensity of the band 1770 cm^{-1} in all of the spectra examined was very weak and it is therefore difficult to make an unequivocal assignment. This band may be due to the

presence of the monomeric form of the acid endgroups in the polymer. Although this assignment is tentative, it is of interest to note that the carbonyl-stretching frequency of monomeric phenylacetic acid has been reported³⁵ to occur at 1763 cm.^{-1} .

Absorption at 1608 cm.^{-1} . A tentative assignment of this band, which occurs in the spectra of latices B1, B2, and F, to the asymmetric mode of the carboxylate ion has already been made.

Absorption Between 2500 and 3600 cm.^{-1} . The stretching bands of the hydroxyl group associated with carboxylic acids occur in this region. However, during the present study, bands which could be ascribed to the free (about 3500 cm.^{-1}) or hydrogen-bonded (2750 – 2500 cm.^{-1}) hydroxyl group were not detected. The inherent weakness of these bands,²⁷ coupled with the low concentration of acid in the polymers (e.g., latex B²¹ contained 3.57×10^{-5} mole acid/g. polymer) probably precluded their detection. The fact that the carbonyl band at 1705 cm.^{-1} had a relatively low intensity supports this conclusion.

CONCLUSIONS

The primary purpose of the spectroscopic examination of the latices was to establish that oxidation of the polymer occurred during polymerization, and to identify, if possible, the oxygen-containing structures formed. Although the absorption in the spectral regions of interest was relatively weak, the results obtained indicate that, irrespective of the nature of the initiator or emulsifier employed, polymer oxidation did occur, and that carboxylic acid groups were produced in the polymer chains.

Indeed, many other authors^{3-6,8,9,11,12,15,36} have demonstrated by infrared spectroscopy that carboxylic acid is produced in polymers by oxidation, although the techniques employed were rather different from those used here in that the oxidation was carried out on the preformed polymer. The spectra obtained in the present study suggest that the acidic groups in the polystyrene were phenylacetic acid residues or residues with a similar structure.

Financial support from the Dyestuffs Division, Imperial Chemical Industries, Manchester, and the Science Research Council is gratefully acknowledged.

References

1. S. Krimm, *Fortschr. Hochpolymer. Forsch.*, **2**, 51 (1960); in *Vibrational Spectra at High Polymers* (*J. Polymer Sci. C*, **7**), G. Natta and G. Zerbi, Eds., Interscience, New York, 1964, p. 3.
2. R. Zbinden, *Infrared Spectroscopy of High Polymers*, Academic Press, New York, 1964.
3. L. H. Cross, R. B. Richards, and H. A. Willis, *Discussions Faraday Soc.*, **9**, 235 (1950).
4. F. M. Rugg, J. J. Smith, and R. C. Bacon, *J. Polymer Sci.*, **13**, 535 (1954).
5. A. W. Pross and R. M. Black, *J. Soc. Chem. Ind. (London)*, **69**, 115 (1950).

6. J. E. Field, D. E. Woodford, and S. D. Gehman, *J. Polymer Sci.*, **15**, 51 (1955).
7. W. C. Sears and W. W. Parkinson, *J. Polymer Sci.*, **21**, 325 (1956).
8. H. C. Beachell and S. P. Nemphos, *J. Polymer Sci.*, **21**, 113 (1956).
9. H. C. Beachell and G. W. Tarbet, *J. Polymer Sci.*, **45**, 451 (1960).
10. J. C. Spitzbergen and H. C. Beachell, *J. Polymer Sci. A*, **2**, 1205 (1964).
11. J. P. Luongo, *J. Polymer Sci.*, **42**, 139 (1960).
12. G. D. Cooper and X. Prober, *J. Polymer Sci.*, **44**, 397 (1960).
13. S. S. Stivala, L. Reich, and P. G. Kelleher, *Makromol. Chem.*, **59**, 28 (1963).
14. S. S. Stivala, E. B. Kapan, and L. Reich, *J. Appl. Polymer Sci.*, **9**, 3557 (1965).
15. S. D. Burow, D. T. Turner, G. F. Pezdirtz, and G. D. Sands, *J. Polymer Sci. A-1*, **4**, 613 (1966).
16. A. A. Miller and F. R. Mayo, *J. Am. Chem. Soc.*, **78**, 1017 (1956).
17. N. Grassie and N. A. Weir, *J. Appl. Polymer Sci.*, **9**, 963, 975, 989, 999 (1965).
18. R. H. Ottewill and J. N. Shaw, *Kolloid-Z.*, in press.
19. R. H. Ottewill and J. N. Shaw, *Kolloid-Z.*, in press.
20. J. N. Shaw, paper presented before the Division of Polymer Chemistry at the Symposium on New Concepts in Emulsion Polymers, American Chemical Society Meeting, New York, September 12-16, 1966; *J. Polymer Sci. C*, in press.
21. J. N. Shaw, to be published.
22. J. N. Shaw, Ph.D. thesis, University of Cambridge, 1965.
23. J. N. Shaw and R. H. Ottewill, *Nature*, **208**, 681 (1955).
24. R. H. Ottewill and J. N. Shaw, paper presented at the Discussion of the Faraday Society on Colloid Stability in Aqueous and Non-aqueous Media, University of Nottingham, September, 1966; *Discussions Faraday Soc.*, in press.
25. C. Y. Liang and S. Krimm, *J. Polymer Sci.*, **27**, 241 (1958).
26. M. Takeda, K. Jimura, A. Yamada, and Y. Imamura, *Bull. Chem. Soc., Japan*, **32**, 1150 (1959).
27. L. J. Bellamy, *Infra-red Spectra of Complex Molecules*, Methuen, London, Wiley, New York, 1958.
28. Yu. Pao-shan, V. N. Nikitin, and M. V. Vol'kenshtein, *Zh. Fiz. Khim.*, **36**, 681 (1962).
29. M. St. C. Flett, *Spectrochim. Acta*, **18**, 1537 (1962).
30. M. St. C. Flett, *J. Chem. Soc.*, **1951**, 962.
31. D. Hadzi and N. Sheppard, *Proc. Roy. Soc. (London)*, **A216**, 247 (1953).
32. R. N. Jones, *Can. J. Chem.*, **40**, 301, 321 (1962).
33. D. Hadzi, *Boll. Sci. Fac. Chim. Ind. Bologna*, **21**, 23 (1963).
34. R. P. Bell and A. T. Kuhn, *Trans. Faraday Soc.*, **59**, 1789 (1963).
35. M. Oki and H. Iwamura, *Bull. Chem. Soc. Japan*, **35**, 283 (1962).
36. R. H. Boundy and R. F. Boyer, *Styrene, Its Polymers, Copolymers, and Derivatives*, Reinhold, New York, 1952, p. 535.

Received February 27, 1967

Prod. No. 5416A

Polymerization of Tetrahydrofuran by $\text{AlEt}_3\text{-H}_2\text{O}$ Promoter System: Rate of Propagation Reaction

TAKEO SAEGUSA, HIROSUKE IMAI, and SHU-ICHI MATSUMOTO,
Department of Synthetic Chemistry, Kyoto University, Kyoto, Japan

Synopsis

Kinetic studies were carried out on the polymerization of tetrahydrofuran with catalyst systems of aluminum alkyl-epichlorohydrin. As aluminum alkyl species AlEt_3 , $\text{AlEt}_3\text{-H}_2\text{O}$ (1:0.1 to 1:1.0), and "oxyaluminum ethyl" were employed. The polymerizations with these catalysts are characterized by a mechanism of stepwise addition without chain transfer or termination, which is expressed by the kinetic relation $R_p = k_p[\text{P}^*](\text{[M]} - \text{[M]}_e)$, where [M] and [M]_e are the instantaneous and equilibrium concentrations of monomer and $\text{[P}^*]$ is the concentration of propagating species calculated from the amount and molecular weight of the product polymer. The determination of the rate constant k_p for these catalysts has shown that the polymerization rate varied considerably with the change of aluminum alkyl species, i.e., with the water-to-aluminum ratio, but the propagation rate constant itself varied very little. The variation of polymerization rate was, therefore, attributed primarily to the differences in concentration of the propagating species, i.e. the efficiency of the catalyst in forming propagating species. The catalyst efficiency was closely related to the acid strength of the aluminum alkyl species, which was estimated from the magnitude of shift of the xanthone carbonyl band in the infrared spectrum of its coordination complex with aluminum alkyl. The maximal catalyst efficiency was attained at about $[\text{H}_2\text{O}]/[\text{AlEt}_3] = 0.75$.

INTRODUCTION

It was established in a previous paper¹ that the polymerization of tetrahydrofuran (THF) catalyzed by a mixture of $\text{AlEt}_3\text{-H}_2\text{O}$ (2:1) and epichlorohydrin (ECH) proceeds through a stepwise addition mechanism in which the propagating chain continues to grow without chain termination or chain transfer. The concentration of propagating species remains unchanged after the induction period. On the basis of the equilibrium polymerization mechanism the rate of propagation R_p is expressed by

$$R_p = k_p[\text{P}^*](\text{[M]} - \text{[M]}_e) \quad (1)$$

where [M] and [M]_e are instantaneous and equilibrium monomer concentrations, respectively, and $\text{[P}^*]$ is the concentration of propagating species. According to these findings, the propagation rate constant can be determined from the value of $\text{[P}^*]$, which is given from the amount and the molecular weight of the polymer product according to

$$[\text{P}^*] = [(\text{polymer in g.})/(\text{mol. wt.})] \times [1/(\text{vol. of react. syst.})] \quad (2)$$

The purpose of this study was to examine the effect of the $[\text{H}_2\text{O}]/[\text{AlEt}_3]$ ratio of catalyst on the polymerization kinetics in relation to the change in its acid character. Polymerization with the system oxyaluminum ethyl² and ECH was also studied, and its kinetics was compared with that of $\text{AlEt}_3\text{-H}_2\text{O}$.

EXPERIMENTAL

Materials and Polymerization Technique

The materials and technique were described in the previous paper.¹ The $\text{AlEt}_3\text{-H}_2\text{O}$ system and oxyaluminum ethyl were prepared as described previously.

Infrared Analysis of Catalyst-Xanthone Complex

To a catalyst solution in methylene dichloride a solution of xanthone (1 mole-% of AlEt_3 used in the preparation of catalysts) in methylene dichloride was added and stirred for 1 hr. at room temperature under nitrogen. The infrared spectrum was taken at room temperature with a potassium bromide cell filled with nitrogen.

RESULTS AND DISCUSSION

Polymerization with $\text{AlEt}_3\text{-ECH}$ System

The THF polymerization with the binary catalyst system of $\text{AlEt}_3\text{-ECH}$ at 0°C. showed a comparatively long induction period (about 3 hr.) followed by slow propagation. The kinetic data with varying compositions

TABLE I
Polymerization of THF by $\text{AlEt}_3\text{-ECH}$

$[\text{M}]_0$, mole/l.	$[\text{AlEt}_3]_0$, mole/l.	$[\text{ECH}]_0$, mole/l.	$[\text{P}^*] \times 10^3$, mole/l.	$R_p \times 10^4$, mole/l.-sec.	$k_p \times 10^3$, l/mole- sec.	$[\text{P}^*]/$ $[\text{AlEt}_3]_0$ $\times 10^3$
Polymerization at 0°C.						
11.7	0.370	0.278	0.166	0.0955	5.90	0.449
11.8	0.372	0.196	0.181	0.0978	5.46	0.487
11.9	0.292	0.141	0.134	0.0738	5.71	0.461
12.1	0.164	0.127	0.0962	0.0511	5.29	0.586
12.2	0.131	0.127	0.0965	0.0544	5.60	0.735
					(avg. 5.59)	
Polymerization at 25°C.						
11.8	0.198	0.132	0.113	0.360	40.0	0.571
11.7	0.238	0.132	0.132	0.482	46.6	0.555
11.4	0.427	0.163	0.141	0.465	44.1	0.331
11.4	0.461	0.147	0.097	0.319	43.1	0.210
11.3	0.489	0.133	0.153	0.526	46.4	0.313
					(avg. 44.0)	

of catalysts are shown in Table I. The propagation rate constant was determined according to the equation.¹

$$-d[\text{M}]/dt = k_p[\text{P}^*]([\text{M}] - [\text{M}]_e) \quad (3)$$

where $[\text{M}]_e$, the equilibrium monomer concentration, was 1.7 mole/l. at 0°C .² and $[\text{P}^*]$ was obtained from the amount and molecular weight of polymer product according to eq. (2).

It can be seen that the propagation rate constant k_p does not change in spite of wide variation in the initial concentrations of the catalyst components. The concentration of propagating species, $[\text{P}^*]$, is quite small in comparison with the initial concentration of AlEt_3 . The ratio of $[\text{P}^*]/[\text{AlEt}_3]$, which is the efficiency of the formation of propagating species based upon AlEt_3 , is in the vicinity of 0.5×10^{-3} .

In the calculation of k_p at 25°C . a value of 3.3 mole/l. of $[\text{M}]_e$ at 25°C . was adopted.³ Compared with the polymerization at 0°C ., the overall polymerization rate is considerably increased at 25°C ., but the concentration of the propagating species, i.e. the catalyst efficiency, is not increased by the rise in reaction temperature. Therefore, the increase in polymerization rate is ascribed chiefly to the increase in the propagation rate constant.

Polymerization with $\text{AlEt}_3\text{-H}_2\text{O-ECH}$ Systems

Previously we have shown that the catalyst activity of AlEt_3 for cationic polymerization is much enhanced on treatment with a controlled amount of water.⁴⁻⁸ The catalyst activation by the addition of water in the THF polymerization was examined kinetically in the present study. Table II shows the results of polymerization with the ternary catalyst system $\text{AlEt}_3\text{-H}_2\text{O-ECH}$ having various $[\text{H}_2\text{O}]/[\text{AlEt}_3]$ ratios. Here the catalyst efficiency was determined from the amount of AlEt_3 employed in the cata-

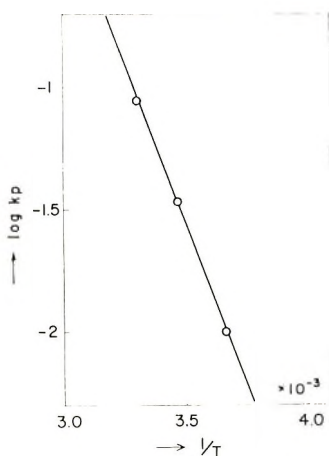


Fig. 1. Bulk polymerization of THF with system $\text{AlEt}_3\text{-H}_2\text{O}$ (1:0.5) and ECH: Arrhenius plot of propagation rate constant.

lyst preparation. It is indicated that the overall rate of polymerization, R_p , is increased with the increase of the $[\text{H}_2\text{O}]/[\text{AlEt}_3]$ ratio up to 0.75 and then it is decreased; the propagation rate constant k_p , however, is not much affected by the change in this ratio. The modification of the catalyst by the reaction with water causes an increase in the concentration of the propagating species ($[\text{H}_2\text{O}]/[\text{AlEt}_3]$ up to 0.75), to which the increase in the overall rate of polymerization is mainly ascribed; in other words, the catalyst efficiency, $[\text{P}^*]/[\text{AlEt}_3]$, is increased by the increase of the $[\text{H}_2\text{O}]/[\text{AlEt}_3]$ ratio to the maximum at about $[\text{H}_2\text{O}]/[\text{AlEt}_3] = 0.75$.

TABLE II
Polymerization of THF by AlEt_3 - H_2O -ECH:
Bulk Polymerization at 0°C.

$[\text{M}]_0$, mole/l.	$[\text{AlEt}_3]_0$, mole/l.	$[\text{ECH}]_0$, mole/l.	$[\text{P}^*] \times 10^3$, mole/l.	$R_p \times 10^4$, mole/l.- sec.	$k_p \times 10^3$, l./mole- sec.	$[\text{P}^*]/$ $[\text{AlEt}_3]_0$ $\times 10^3$
Concn. ^a 1:0.1						
12.3	0.113	0.128	0.403	0.372	9.17	3.57
12.0	0.282	0.128	0.814	0.777	9.97	2.89
12.1	0.226	0.128	0.782	0.681	9.06	3.47
						(avg. 9.40)
Concn. 1:0.25						
12.0	0.288	0.128	1.69	1.75	11.2	5.85
11.7	0.240	0.128	1.35	1.37	11.0	5.62
12.1	0.192	0.128	1.34	1.36	11.0	6.95
						(avg. 11.1)
Concn. 1:0.5						
12.2	0.234	0.0284	1.90	1.81	10.1	8.09
11.8	0.389	0.141	2.15	1.97	9.74	5.51
11.9	0.346	0.141	2.44	2.18	9.78	7.06
12.0	0.260	0.141	1.60	1.59	10.5	6.18
12.2	0.173	0.141	0.973	0.933	9.77	5.62
						(avg. 9.98)
Concn. 1:0.75						
12.1	0.234	0.128	2.90	3.44	12.9	12.4
12.1	0.195	0.128	2.85	2.91	11.0	14.6
12.3	0.117	0.128	1.72	1.76	10.6	14.6
						(avg. 11.5)
Concn. 1:1						
12.2	0.244	0.0847	2.66	2.03	8.29	10.9
11.8	0.381	0.141	2.27	1.79	8.52	5.96
11.9	0.338	0.141	2.17	1.67	8.36	6.42
						(avg. 8.39)

^a Concentration, $[\text{AlEt}_3]:[\text{H}_2\text{O}]$.

The effect of the reaction temperature in the THF polymerization with the ternary catalyst system AlEt_3 - H_2O (2:1) and ECH was also examined. As in the polymerization with AlEt_3 -ECH, the propagation rate constant k_p was increased by the rise in the reaction temperature, whereas the catalyst efficiency was not changed. From the linear relationship in the

Arrhenius plot in Figure 1, the activation energy ΔE_p and the frequency factor A_p of the propagation reaction were calculated:

$$\Delta E_p = 12 \text{ kcal./mole}$$

$$A_p = 5.2 \times 10^7 \text{ l./mole-sec.}$$

Here the calculation of k_p values at three different temperatures (0, 15, and 30°C.) was made according to eq. (3), with the use of the values of the equilibrium monomer concentration given by Ofstead.³

Polymerization with Oxyaluminum Ethyl-ECH System

In a previous paper² oxyaluminum ethyl, Al(O)Et , was prepared by the reaction of oxyaluminum chloride with AlEt_3 , and its structure was assumed to resemble the $\text{AlEt}_3\text{-H}_2\text{O}$ system. Oxyaluminum ethyl was shown to induce the THF polymerization in the presence of a small amount of ECH. For a comparison of the catalyst behavior of oxyaluminum ethyl and that of the $\text{AlEt}_3\text{-H}_2\text{O}$ system the kinetics of the polymerization with oxyaluminum ethyl-ECH was studied. The results are shown in Table III.

It is indicated that the k_p value with oxyaluminum ethyl-ECH is almost the same as that with $\text{AlEt}_3\text{-H}_2\text{O-ECH}$ and that the catalyst efficiency of oxyaluminum ethyl is somewhat higher than that of $\text{AlEt}_3\text{-H}_2\text{O}$ (1:0.75). Here the catalyst efficiency of oxyaluminum ethyl has been calculated on the basis of the amount of aluminum atom.

TABLE III
Polymerization of THF by Oxyaluminum Ethyl-ECH System:
Bulk Polymerization at 0°C.

$[\text{M}]_0$, mole/l.	$[\text{AlEt}_3]_0$, mole/l.	$[\text{ECH}]_0$, mole/l.	$[\text{P}^*] \times 10^3$, mole/l.	$R_p \times 10^4$, mole/l.-sec.	$k_p \times 10^3$, l./mole-sec.	$[\text{P}^*]/$ $[\text{AlEt}_3]_0$ $\times 10^3$
12.3	0.133	0.127	2.12	2.16	7.78	16.0
12.3	0.106	0.127	2.17	1.57	7.35	20.5
12.3	0.118	0.141	1.93	1.72	9.15	16.1

Acid Character of AlEt_3 and $\text{AlEt}_3\text{-H}_2\text{O}$ System

The relationship between the catalyst behavior of $\text{AlEt}_3\text{-H}_2\text{O}$ and its acid character was examined. It has already been shown that AlEt_3 and $\text{AlEt}_3\text{-H}_2\text{O}$ have acid sites that are responsible for the catalysis in the THF polymerization.⁸ However, the type of acid sites in $\text{AlEt}_3\text{-H}_2\text{O}$, i.e. of Brönsted acid, Lewis acid, or both, has not been established. The acid character of this system was first examined by the complex formation with 2,6-dimethyl-4-pyrone by infrared spectroscopy. In the spectrum of a mixture of $\text{AlEt}_3\text{-H}_2\text{O}$ (1:1) and 2,6-dimethyl-4-pyrone there could be detected no band of OH group which was to be formed by the protonation of a carbonyl group of pyrone with a Brönsted type of acid.⁹ This observation

indicates that the $\text{AlEt}_3\text{-H}_2\text{O}$ (1:1) reaction proceeds almost completely, leaving no detectable amount of acidic hydrogen.

According to Cook's method,¹⁰ the Lewis acid strengths of some of these catalysts were then examined in relation to the catalyst behaviors in polymerization. Xanthone was employed as a reference Lewis base, and the magnitude of shift of the xanthone carbonyl absorption ($\Delta\nu_{\text{C=O}}$) in the infrared spectrum caused by complex formation with a Lewis acid was taken as a measure of Lewis acid strength. It is known that no shift of the carbonyl band of xanthone is caused by protonic (Brönsted) acid.¹⁰

Table IV shows the acid strengths and the kinetic data. Here catalyst efficiencies, $[\text{P}^*]/[\text{catalyst}]$, are the mean values of bulk polymerizations with a fairly large amount of ECH. It has been shown that in the polymerization with $\text{AlEt}_3\text{-H}_2\text{O}$ (2:1) and ECH the $[\text{P}^*]$ is proportional to the initial amount of ECH, $[\text{ECH}]_0/[\text{AlEt}_3]_0$, in the region <0.07 . However, in the region where the amount of ECH is fairly large, >0.3 , $[\text{P}^*]$ is no longer affected by this ratio.¹

TABLE IV
Lewis Acid Strengths and Catalytic Behaviors of Alkylaluminum Catalysts in the Polymerization of THF: Bulk Polymerization at 0°C. with ECH as Promoter

Catalyst	$\Delta\nu_{\text{C=O}}$, ^a cm. ⁻¹	$k_p \times 10^3$, ^b l./mole-sec.	$[\text{P}^*]/$ $[\text{AlEt}_3]$ ^b
AlEt_3	83	5.59	0.00056
$\text{AlEt}_3\text{-H}_2\text{O}$, concn.:			
1:0.1	—	9.40	0.0033
1:0.25	—	11.1	0.0061
1:0.5	88	9.98	0.0078
1:0.75	109	11.5	0.014
1:1	103	8.39	0.0078
Al(O)Et	113	8.09	0.018

^a Shift in carbonyl-stretching absorption of xanthone by complex formation with a catalyst.

^b Average value of data in Tables II and III.

It is shown in Table IV that the Lewis acid strength of $\text{AlEt}_3\text{-H}_2\text{O}$ is increased by the increase in the $\text{H}_2\text{O}/\text{AlEt}_3$ ratio up to 0.75 while the propagation rate constant varies very little. On the other hand, the catalyst efficiency, which is defined as the ratio of concentration of propagating species to that of Lewis acid catalyst, varies with the nature of the catalyst. In the polymerization with $\text{AlEt}_3\text{-H}_2\text{O}$ the catalyst efficiency, based upon the amount of AlEt_3 , is increased as the $[\text{H}_2\text{O}]/[\text{AlEt}_3]$ ratio is increased, up to 0.75. In our previous paper,⁸ the number of acid sites in AlEt_3 and in $\text{AlEt}_3\text{-H}_2\text{O}$ were determined by titration with pyridine using butter yellow indicator. This value, being of the order of 0.1 to 0.5 per mole of AlEt_3 , was much higher than that of the catalyst efficiency in the THF polymerization. In view of the fact that the catalyst efficiencies of AlEt_3 and $\text{AlEt}_3\text{-H}_2\text{O}$

are quite small in the present polymerization, the catalyst site responsible for the formation of propagating species is presumed to be quite specific.

References

1. H. Imai, T. Saegusa, S. Matsumoto, T. Tadasa, and J. Furukawa, *Makromol. Chem.*, **102**, 222 (1967).
2. H. Imai, S. Ohsugi, T. Saegusa, and J. Furukawa, *Makromol. Chem.*, **81**, 119 (1965).
3. E. A. Ofstead, *Polymer Preprints*, **6**, 674 (1965).
4. T. Saegusa, H. Imai, and J. Furukawa, *Makromol. Chem.*, **53**, 203 (1962).
5. T. Saegusa, H. Imai, and J. Furukawa, *Makromol. Chem.*, **64**, 224 (1963).
6. T. Saegusa, H. Imai, and J. Furukawa, *Makromol. Chem.*, **65**, 60 (1963).
7. T. Saegusa, H. Imai, and J. Furukawa, *Makromol. Chem.*, **79**, 207 (1964).
8. H. Imai, T. Saegusa, and J. Furukawa, *Makromol. Chem.*, **81**, 92 (1965).
9. D. Cook, *Can. J. Chem.*, **41**, 505 (1963).
10. D. Cook, *Can. J. Chem.*, **41**, 522 (1963).

Received March 14, 1967

Revised July 5, 1967

PVC-Rubber Blends. VI. The Structure*

P. ZÍTEK and J. ZELINGER, *Department of Rubber and Plastics
Technology, Technical University, Prague, Czechoslovakia*

Synopsis

The dependence of the dynamic shear modulus of blends of polyvinyl chloride and rubber on the temperature and concentration of the rubber was investigated. For a calculation of a theoretical value of the modulus a formula recently derived by Uemura and Takayanagi was adopted. This formula is based on the assumption of a two-phase system, in which one phase is a continual matrix and the other is discrete spherical particles, and of perfect adhesion between the phases. Most of the theories that clarify the part played by rubber in rubber-modified vitreous materials are based on these assumptions. In most cases we have found a good conformity between the theoretical and experimental values of the modulus. In a certain system with an outstanding impact strength, however, a severe discrepancy has been found. This implies that the present structural explanation of the high impact strengths of two-phase systems is not quite generally applicable.

Introduction

The modification of vitreous polymers by means of rubberlike materials is a routine technological procedure, which has already been applied for many years in the adjustments of physical-mechanical properties. The explanation of the function of rubber in these materials remains, however, unsatisfactory. The problem has been dealt with by numerous authors, and several mechanisms of the effect of rubber have been presented. All these published theories are based on two assumptions: the rubber takes the shape of discrete spherical particles evenly dispersed in the hard matrix, and there exists a perfect adhesion between the two phases. Uemura and Takayanagi¹ started from the same basic assumptions in deriving equations for distinguishing the obvious elastic constant of the two-phase system from the elastic constant of its components. For the case in which the frequency of the applied tension is small and the wavelength in the medium is sufficiently small in comparison with the size of the dispersed particles the authors¹ have adjusted the equation to the form

$$G^* = G_1^* \frac{(7 - 5\nu_1)G_1^* + (8 - 10\nu_1)G_2^* - (7 - 5\nu_1)(G_1^* - G_2^*)\nu_2}{(7 - 5\nu_1)G_1^* + (8 - 10\nu_1)G_2^* - (8 - 10\nu_1)(G_1^* - G_2^*)\nu_2} \quad (1)$$

*For Parts I to V see the *Scientific Papers* from the Institute of Chemical Technology, Prague, (Sborník, Vysoká Škola Chem.-Technol., Part C, **9**, 63-118, 1966).

where G^* is the complex shear modulus of the system, G_1^* and G_2^* are the complex shear moduli of the suspending medium and the suspended particles, respectively, ν_1 is Poisson's ratio for the medium, and ν_2 is the volume fraction of the particles.

Uemura and Takayanagi have verified the validity of this equation by applying it to ABS terpolymers, and they obtained a satisfactory conformity of the theoretical curves with the experimental results.

The aim of our work was first to verify the validity of the formula with blends of PVC and rubber and then to apply it as a medium for studying, in the structure of some of these blends, derivations from theoretical assumptions.

Experimental

For a description of the materials used of the preparation of samples the reader is referred to Zelinger's paper,² from which most of the experimental data on the complex dynamic shear modulus G^* were taken. Series of blends with 5, 10, 20, 30, and 40% by volume of rubber were prepared, different types of rubber being used. Measurements of the real component of the modulus, G' , and the mechanical damping, $\tan \delta$, were taken on a torsional pendulum of standard design at frequencies ranging from 0.1 to 3 cps. The imaginary component, G'' , of the complex modulus G^* is equal to $G' \tan \delta$. The average error of the value of G' is $\pm 2\%$ and that of the value of G'' is $\pm 10\%$. Poisson's ratio for the medium was assumed to be 0.40.³

Results

The validity of eq. (1) for PVC modified with rubberlike substances was above all verified with blends of PVC and chlorinated polyethylene. The curves of moduli G' and G'' (T) and the dependence of G' and G'' (ν) show that the equation is valid for blends, especially at the lower concentrations of chlorinated polyethylene, see Figure 1. At the higher concentrations of

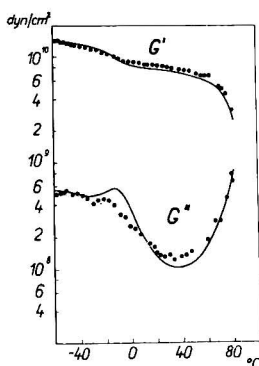


Fig. 1. Curves of G' and G'' for PVC-chlorinated polyethylene blend. Volume fraction of chlorinated polyethylene is 0.20: (●) experimental points; (—) theoretical curves.

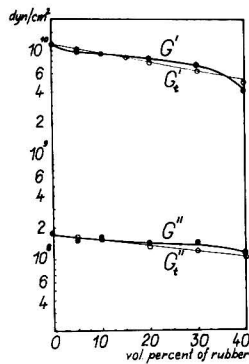


Fig. 2. Curves of G' and G'' for PVC-chlorinated polyethylene blend at 20°C.: (●) experimental points; (○) theoretical points.

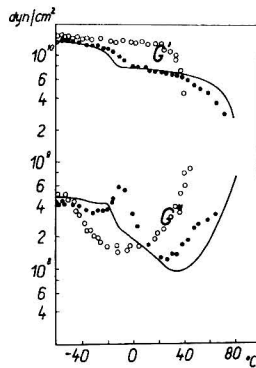


Fig. 3. Curves of G' and G'' for PVC-NBR 40 blend, where volume fraction of rubber is 0.20: (○) experimental points for routinely prepared blend; (●) experimental points for blend of pulverized PVC and NBR 40; (—) theoretical curves.

chlorinated polyethylene the discrepancy between the experimental and theoretical results increases; see Figure 2. This discrepancy, according to Uemura and Takayanagi, can be explained by the fact that with the increasing volume fraction of chlorinated polyethylene the interaction between the rubber-like particles is increasing and the particles are, under these conditions, not of a perfectly spherical shape. Both these phenomena violate the validity of eq. (1).

Further work was conducted in an endeavor to separate from each other with accuracy the influence of the two basic theoretical assumptions from which eq. (1) is derived: that is to say, primarily the effect of the existence of two phases of a certain geometry and, secondarily, that of perfect adhesion between the phases. That is why we made measurements with blends in which the rubber-like phase always satisfied mainly one of the assumptions. In the first case were measured a number of blends of PVC and NBR 40 (40% acrylonitrile). Here, owing to the solubility of rubber in PVC, the divergence of both phases into a molecular scale had been

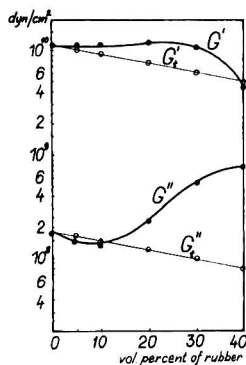


Fig. 4. Curves of G' and G'' for PVC-NBR 40 blend at 20°C.: (●) experimental points; (○) theoretical points.

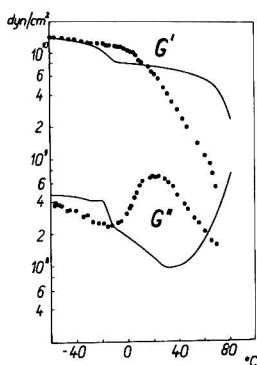


Fig. 5. Curves of G' and G'' for PVC-NBR 40 blend rolled at 90 to 100°C., where volume fraction of NBR 40 is 0.20: (●) experimental points; (—) theoretical curves.

anticipated. The effect of the solubility of rubber on the curves of the moduli G' and $G''(T)$ in comparison with the theoretical curves becomes evident in Figure 3. It is obvious that near the softening temperature of the blend in question the experimental values of G' and G'' exceed the theoretical values. More conspicuous are the deviations caused by the solubility of rubber in PVC that are shown in Figure 4; the values of G' and G'' are considerably higher than their theoretical curves. The decrease in the value of G' at a 40% volume fraction of rubber to below the theoretical value is due to the fact that the blend is at the comparative temperature of 20°C. in the transition zone.

In an endeavor to approximate also the system PVC-NBR 40 to the theoretical assumption of the existence of two independent phases with a perfect adhesion between the rubber phase and the coherent phase, the dissolubility and dispersion of NBR 40 were studied. Three different methods were used:

(a) The molding of test samples from blends of pulverized PVC and NBR 40 without preliminary rolling (Fig. 3).

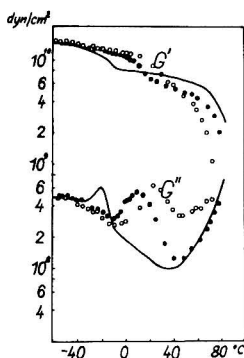


Fig. 6. Curves of G' and G'' for blends of PVC and NBR 40 vulcanized with 0.5 and 1.0% dicumylperoxide (DCP), where volume fraction of rubber is 0.20: (O) experimental points, 0.5% DCP; (●) experimental points, 1.0% DCP; (—) theoretical curves.

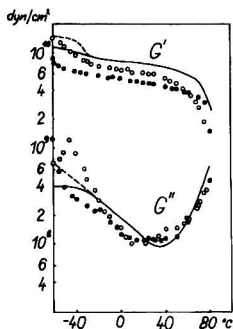


Fig. 7. Curves of G' and G'' for PVC-natural rubber and PVC-chloroprene rubber blends, where volume fraction of rubber is 0.20: (●) experimental points for PVC-NR; (○) experimental points for PVC-chloroprene rubber; (—) theoretical curves for PVC-NR; (---) theoretical curves for PVC-chloroprene rubber.

(b) The rolling of blends of PVC and the rubber at low temperatures, 90 to 100°C. (Fig. 5).

(c) The vulcanization of the rubber to varying degrees with dicumylperoxide and the subsequent rolling of the blend at 160°C. (Fig. 6).

It is evident in all these cases that the decrease of the dispersion of NBR 40 brings about an approximation of the experimental values to the theoretical. The conformity is especially conspicuous when the pulverized components are molded: that is, when the approximately spherical particles of NBR 40 with a perfect adhesion to PVC caused by the dispersion of their surfaces in the coherent phase have been preserved (Fig. 3).

In another case, blends of PVC-natural rubber and PVC-chloroprene rubber were compared (Figs. 7 and 8). The theoretical assumption of the existence of two independent phases is satisfied here, but the adhesion of the phases, owing to the great discrepancy demonstrated, for instance, by the solubility parameter $\Delta\delta = 1.4 \text{ cal.}^{1/2}/\text{cm.}^{-2/2}$, is negligible. In accor-

dance with this, conspicuously lower values of G' were measured than the theoretical ones. The comparison of the curves for natural rubber and for chloroprene rubber shows that with the increasing discrepancy of

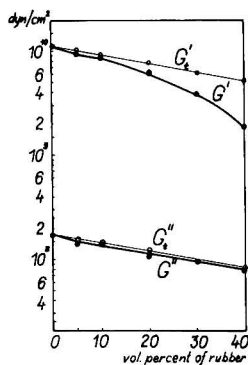


Fig. 8. Curves of G' and G'' for PVC-chloroprene rubber blend at 20°C.: (●) experimental points; (○) theoretical points.

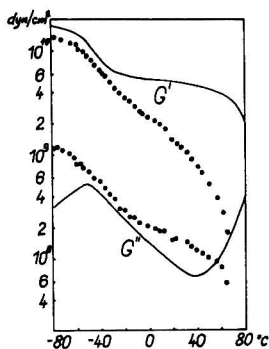


Fig. 9. Curves of G' and G'' for PVC-NBR 18 blend, where volume fraction of rubber is 0.40: (●) experimental points; (—) theoretical curves.

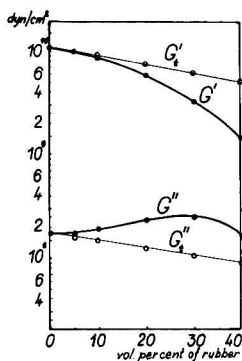


Fig. 10. Curves of G' and G'' for PVC-NBR 18 blend at 20°C.: (●) experimental points; (○) theoretical points.

rubber the negative deviations of the experimental values of G' are more pronounced.

Interesting results have been gained with blends of PVC and NBR 18. It is a known fact that the copolymer butadiene-acrylonitrile of about 20% acrylonitrile is a suitable modifier for PVC and even in small concentration considerably increases its toughness. As Figures 9 and 10 show, the moduli G' and G'' do not, in spite of this, absolutely conform to the theory.

It is obvious that the deviations from theory cannot be specified on the basis of the aforementioned criteria. Blends of PVC and NBR 18 do not, according to results achieved by dynamic measurements, behave as homogeneous substances (with one transition zone and a relatively high value of the real component G'), nor do they behave as obviously heterogeneous ones (with two distinct transition zones and a relatively low modulus G' at 20°C.). It may be stated that these blends have one transition zone (with gradually decreasing G' and high G''), covering the entire range of the measurements carried out and extending to below the softening temperature of the given type of rubber (T_s for NBR 18 is -54°C.). To this corresponds also the embrittlement temperature (the transition between the brittle and tough fracture) which, at 20% NBR 18, is more than 10°C. lower than the embrittlement temperature of neat rubber.

Discussion

As the graphs indicate, the conditions of the validity of the equation expressing the existence of spherical particles of the rubber phase and their absolute adhesion to the coherent phase have been fulfilled nearly absolutely with blends of PVC and chlorinated polyethylene (Figs. 1 and 2). With blends of PVC and natural or chloroprene rubber and, finally with NBR 40, were found deviations from the theoretical curves. These deviations correspond even to the lower value of the toughness of the blends.

Figures 9 and 10 demonstrate, however, that the validity of the assumptions is not generally acceptable. The PVC-NBR 18 blends do not meet the theoretical assumptions of the equation, although even at small concentrations of NBR 18 a material of great toughness is gained without the existence of two one-component phases and, moreover, the blends retain their tough quality at temperatures at which the rubber phase is already in a glasslike state. It follows that in this case a new structure has been created, differing both from the assumed two-phase system and from a one-phase system. As measurements of PVC-NBR 40 of limited dispersion show, this structure forms at the transition from one state to the other. It is, at the same time, extremely advantageous for absorbing the energy released in huge reformation processes, no matter what type of absorption is to take place.

Summary

The application of the equation for the computation of the elastic constants of complex system and the elastic constants of the individual components has proved to be a valuable means of investigating the structure of PVC-rubber blends. It has been found that the structure of certain blends does not conform to the assumptions adopted in the interpretation of their impact toughness. It is particularly the structure of the PVC-NBR 18 blends that must be investigated in detail because of their exceptional character and outstanding mechanical properties.

The authors wish to express their thanks to J. Maláč, M.Sc., for his valuable assistance in the mathematical processing of the data.

References

1. S. Uemura and M. Takayanagi, *J. Appl. Polymer Sci.*, **10**, 113 (1966).
2. J. Zelinger, *J. Polymer Sci.*, in press.
3. S. Newman and S. Strella, *J. Appl. Polymer Sci.*, **9**, 2297 (1965).

Received January 27, 1967

Revised August 2, 1967

Sorption of Water Vapor by Poly(vinyl Alcohol): Influence of Polymer Crystallinity

AKIRA TAKIZAWA, TAKAO NEGISHI, and KINZO ISHIKAWA,
*Faculty of Textile Technology, Tokyo Institute of Technology,
Tokyo, Japan*

Synopsis

The influence of crystallinity on water sorption behavior by poly(vinyl alcohol) (PVA) was studied by using a PVA of low crystallinity (15% crystalline by x-ray analysis) and an annealed sample therefrom (46%) crystalline. With the increase of crystallinity, the sigmoid shape (which is a characteristic for the sorption isotherm of the low crystalline polymer) diminishes. The B.E.T. plots of the isotherms are linear between the relative vapor pressures of 0.1 and 0.4 as usual, and deviate from straight lines in the higher pressure range in the direction of a larger sorbed quantity than that predicted by the B.E.T. theory. This tendency is regarded as a kind of dissolution, and the Flory-Huggins interaction parameter χ_1 was calculated. In both polymers, the χ_1 versus pressure relation has a maximum, while overall χ_1 values are smaller in the polymer of low crystallinity. The maximum point (which lies in the higher pressure region in case of the less crystalline sample) is considered to be a transition point from a phenomenon controlled mainly by an adsorption mechanism to a phenomenon controlled mainly by a dissolution mechanism. Accordingly, the separation of the isotherm into adsorption and a dissolution components was made, and the polymer fraction which contributes to the dissolution mechanism versus pressure relation was calculated. The result indicates that the crystalline region observed by x-ray analysis may partly contribute to the dissolution process at room temperature.

INTRODUCTION

To describe certain sorption isotherms for polar amorphous polymer-polar small molecule systems, the statistical thermodynamics of solution accompanied by adsorption seems to be adequate. Especially, for the experimental isotherms of protein-water and cellulose nitrate-acetone systems, the theory of solution accompanied by adsorption gives a constant interaction parameter χ_1 to each system, and the parameter agrees with that obtained by another method.¹

For the quantitative development of the problem, it is desirable to study the adsorption behavior of water by a polymer which is simpler in chemical structure and more highly sorptive than proteins. Poly(vinyl alcohol) (PVA) has been selected for this purpose. However, this polymer shows a tendency to crystallize even under conditions of freeze-drying of the aqueous solution. However, PVA powder of 15% crystallinity (by x-ray analysis) was obtained (this figure is extremely low compared with others²⁻⁴).

Accordingly, in this paper, the influence of crystallinity on water adsorption by poly(vinyl alcohol) has been studied. Adsorption isotherms have been determined accurately by using the above PVA sample of low crystallinity and its annealed sample, and analyses of the adsorption mechanism have been made on the basis of various theories.

EXPERIMENTAL

Apparatus

The sorption apparatus is essentially of the same type as that of Fogiel-Heller's gravimetric-volumetric one⁵ except for a few points. As is shown in Figure 1, each mercury cut-off valve has a screw-type greaseless stopcock (Kern Chemical Corp., Los Angeles 18, Calif.) provided with a fluorocarbon rubber diaphragm, instead of a conventional vacuum stopcock. These greaseless stopcocks are effective for isolating each part of the apparatus by filling mercury inside the cocks. Thus even if any damage should occur in any part of the apparatus, other parts remain intact. To make the experiment more efficient, four sorption chambers are installed in a series.

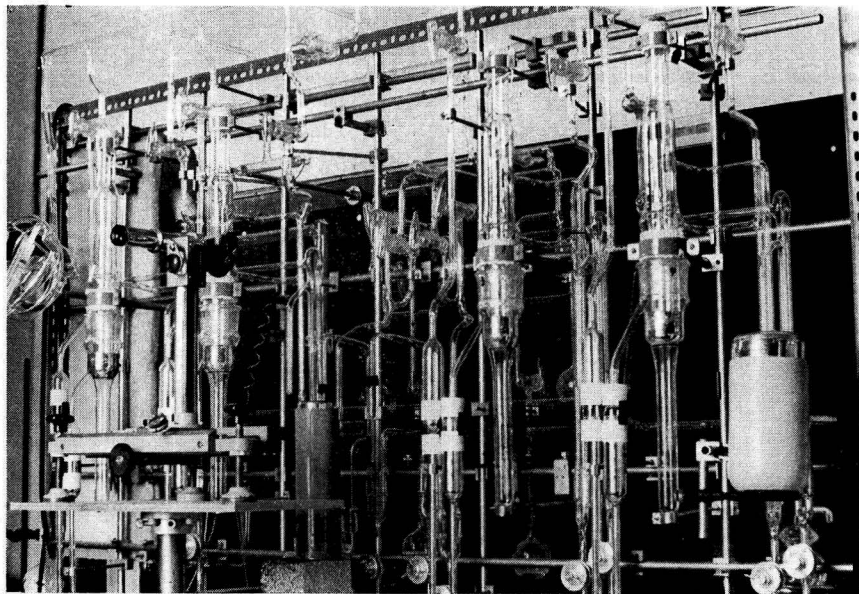
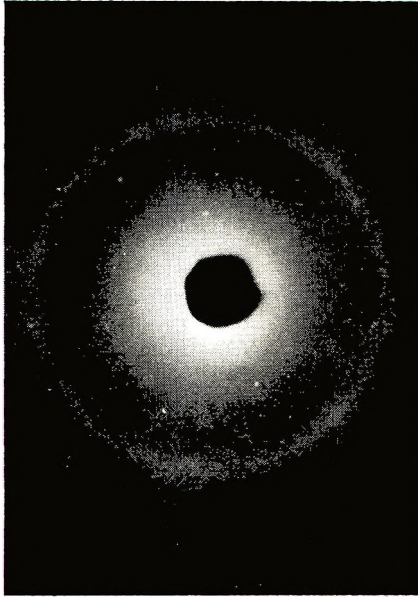


Fig. 1. Adsorption apparatus.

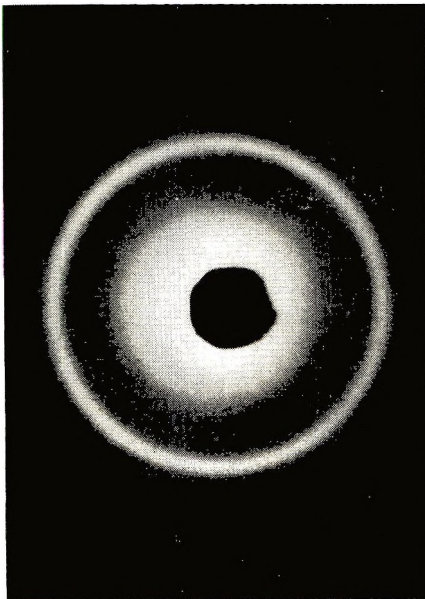
Materials

A poly(vinyl alcohol) manufactured by the Kurashiki Rayon Company, Ltd. (Japan), having a degree of polymerization of 1700 by the viscosity measurement, was used.

As a result of a study of freeze-drying conditions (that is, PVA concentration in aqueous solution and freeze-drying temperature), a sample was prepared by freezing of the 1% PVA aqueous solution at about -72°C . (Dry



(a)



(b)

Fig. 2. X-ray diffraction patterns of: (a) 15% crystalline poly(vinyl alcohol); (b) 46% crystalline poly(vinyl alcohol).

Ice-methyl alcohol bath) and subsequent vacuum drying. The x-ray diffraction pattern of the sample is shown in Figure 2*a*, and the crystallinity calculated by the usual method is 15%. Annealing of this sample for 15 min. at 160°C. increased its crystallinity to 46% by x-ray analysis (Fig. 2*b*). It has been confirmed that these figures are almost the same as those obtained by density observations.

Water was distilled three times before introduction of water to the sorption chamber.

Procedure

Approximately 40 mg. of the PVA sample was placed in a quartz pan of 0.5 cc. capacity and attached to a calibrated quartz helix balance housed in the sorption chamber. The system containing the sample was outgassed by continuous pumping at 10^{-6} mm. Hg for 5 days at $25.0 \pm 0.1^\circ\text{C}$., which is the temperature of the actual sorption experiment. No change in weight was observed beyond 3 days.

After each introduction of water vapor by the differential method, it took 3-4 days for sorption equilibrium to be attained.

RESULTS AND DISCUSSION

Sorption isotherms for the two samples are shown in Figure 3. (Higher pressure regions are shown in Figs. 6 and 7.) The less crystalline sample shows a higher value of water adsorbed, over the whole pressure range, compared with the literature data.²⁻⁴ At a relative vapor pressure of 0.9,

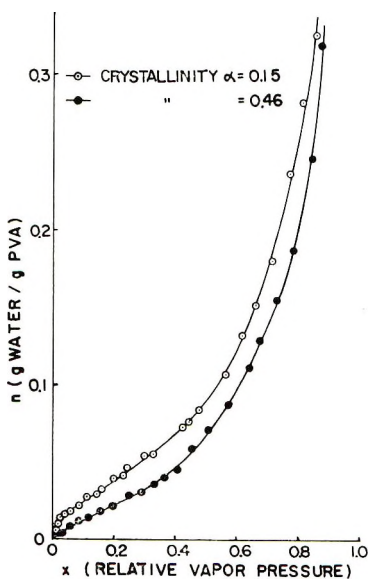


Fig. 3. Adsorption isotherms for 15% and 46% crystalline PVA.

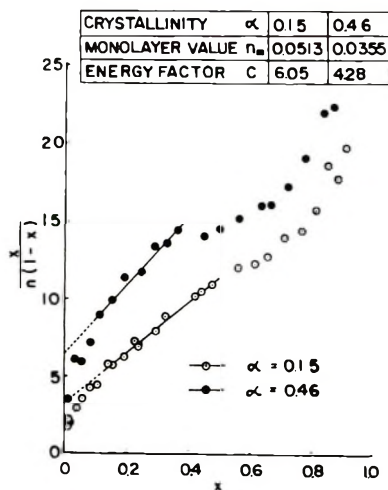


Fig. 4. B.E.T. plots of the isotherms of Fig. 3.

the weight of water sorbed for this sample is 1.7 times the value³ for the polymer of crystallinity 0.29 which has shown the highest sorbed quantity.

With the increase of crystallinity, a sigmoid shape (which is a characteristic of the polymer of low crystallinity) disappears, and the isotherm becomes rather concave upwards over the whole range of relative vapor pressure. Similar sorption isotherms are observed for highly crystalline nylon 66 and nylon 6-water systems.⁶ The sigmoid shape corresponds to the usual adsorption mechanism, such as the B.E.T. model, and the isotherms which are concave upwards are considered to represent a solution mechanism. As the sample of low crystallinity has many unbonded polar groups, the adsorption mechanism seems to be the main feature especially in the low pressure range. On the other hand, in the highly crystalline sample there are few unbonded groups because of the strong interactions among polar groups. Accordingly, in the highly crystalline sample, it is likely that the random mixing of water with nonpolar segments of the polymer becomes more prominent than the adsorption of water by unbonded polar groups. Thus, the isotherm represents principally a solution mechanism of the water-nonpolar segment system. This behavior will be discussed more quantitatively below.

Figure 4 represents plots of the isotherms according to the B.E.T. equation [eq. (1)]:⁷

$$x/[n(1-x)] = (1/n_m C) + [(C-1)/n_m C]x \quad (1)$$

where n is the weight in grams of water vapor sorbed per gram of polymer, n_m is the weight of water vapor sorbed to form a monomolecular layer, x is the relative vapor pressure, and C is a constant which is related to the average net heat of sorption for the monolayer. The B.E.T. plots of the isotherms are linear between the relative pressures of 0.1 and 0.4 as usual.

The monolayer value n_m and the energy factor C are also given in Figure 4. Both n_m and C values are larger in the sample of low crystallinity. However, n_m values are extremely small as compared with the numbers of polar groups based on the amorphous fraction of the polymer. (For example, when the crystallinity is 0.154, the corresponding value of the polar groups is 0.595 g./g.) The difference of C values between two samples may be due to the difference of the interactions among polar groups in the amorphous region.

The B.E.T. plots for both samples deviate from straight lines in the relative vapor pressure range beyond 0.4 in the direction of there being too much adsorption at a given x value to conform to eq. (1). This tendency is unusual, because almost all other adsorbents show smaller n values than those predicted by the B.E.T. theory in that range. This phenomenon can be explained reasonably in terms of the increase of adsorption sites (polar groups) which are newly disclosed during the sorption process. Thus, on going from lower to higher cohesive energy regions in succession, the crystalline part achieves a more stable solvated state by the dissolving action of water. In other words, the crystalline regions are gradually disordered to the solvated (amorphous) state which corresponds to the lower chemical potential than those in the original states.

To clarify the situation more quantitatively, application of the Flory-Huggins' solution theory [eq. (2)] was made, and the interaction parameter χ_1 was calculated:

$$\ln x = \ln v_1 + (1 - v_1) + \chi_1(1 - v_1)^2 \quad (2)$$

where v_1 is the volume fraction of polymer and x is the relative vapor pressure. Essentially, the statistical thermodynamics of polymer solution is based on relatively small molecular interactions. Accordingly, the interaction parameter χ_1 in the present case is in the nature of the experimental parameter because of the strong interaction between water and PVA and also of the presence of the crystalline region of PVA. In the calculation of the volume fraction of polymer v_1 , 0.7762 and 0.7633 were used, respectively, for partial volumes of low and high crystallinity. These values were obtained by extrapolating the specific volume of water adsorbed PVA versus water concentration relations² to zero concentration. The contribution due to the elastic deformation to the total free energy change⁸ was neglected, since the apparent interaction parameter χ_1 decreased with v_1 . The calculation of the volume fraction of polymer or water was based on the total polymer (including both crystalline and amorphous portions) in the same way as the treatment of Rowen and Simha,⁹ because the examination using only the amorphous portion as the polymer yielded an illogical result, i.e., a lower χ_1 value than that of dilute polymer solution.

The calculated χ_1 value versus relative vapor pressure relations are shown in Figure 5. Overall χ_1 values are smaller in the less crystalline polymer, which shows higher affinity to water than the highly crystalline polymer. In both cases, χ_1 has a maximum value, and the corresponding x

value is smaller in the more crystalline sample than in the less crystalline sample.

The increasing trend of χ_1 (i.e., decreasing trend of affinity between water and polymer) up to a maximum is due to the contribution of adsorp-

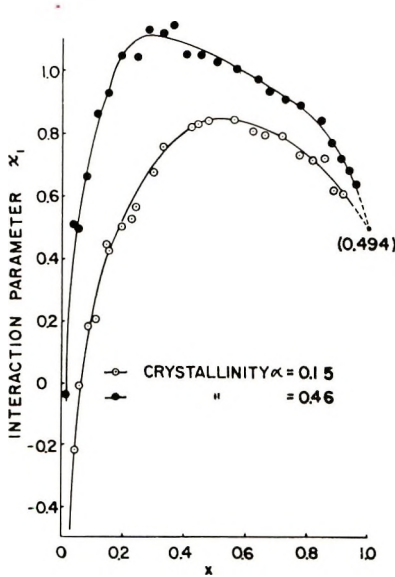


Fig. 5. Interaction parameter χ_1 of Flory-Huggins' equation vs. relative vapor pressure relations for 15% and 46% crystalline PVA.

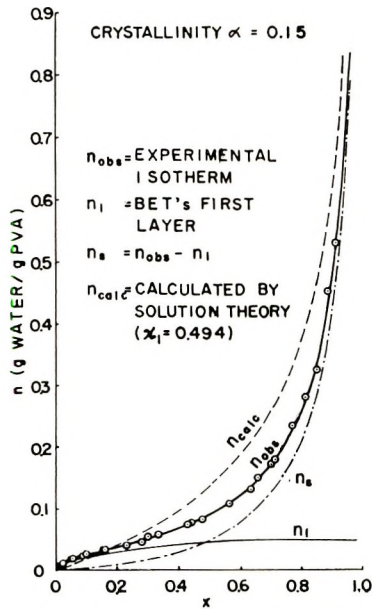


Fig. 6. Separation of experimental isotherm into adsorption part n_1 and dissolution part n_s . n_{calc} is the curve calculated by Flory-Huggins' theory with $\chi_1 = 0.494$. Crystallinity 46%.

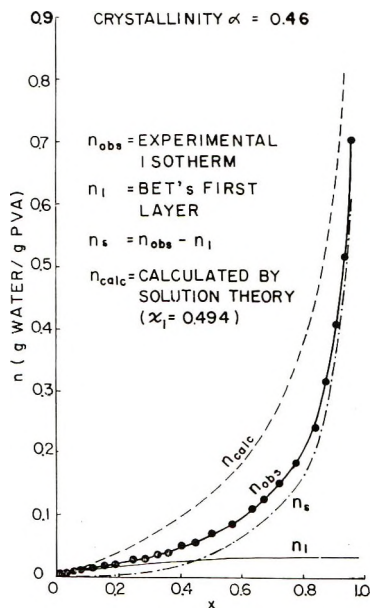


Fig. 7. Separation of experimental isotherm into adsorption part n_1 and dissolution part n_s . n_{calc} is the curve calculated by Flory-Huggins' theory with $\chi_1 = 0.494$. Crystallinity 15%.

tion mechanism which diminishes gradually with the increase of x . This explanation will be understood considering that among the interaction energies which compose the interaction parameter χ_1 , the interaction energy between polymer segments (w_{22} in the Flory's notation) is not needed in case of adsorption. Referring to Figure 4, it may be considered that the decreasing tendency of χ_1 in the higher pressure region beyond the maximum is due to the effect of the newly disclosed polar groups; in other words, a melting phenomenon of the aggregate occurs on going from lower to higher cohesive energy region. This behavior is a kind of dissolution process. Therefore, the maximum point is regarded as a transition point from a phenomenon controlled mainly by an adsorption mechanism to a phenomenon controlled mainly by a dissolution mechanism. Thus, the value of water sorbed at this x shows roughly a measure of unbonded polar groups, and the values are given to be 0.095 g./g. and 0.03 g./g., respectively, for the samples of low and high crystallinity. These values are also small compared with the corresponding values of polar groups calculated from the noncrystallinity. It means that the amorphous region does not necessarily contribute to the adsorption on the whole.

To elucidate the mechanism more clearly, the fraction which contributes to the dissolution mechanism was calculated. According to the previous paper,¹ it is adequate to divide an isotherm into an adsorption part and a dissolution part. The dissolution part can be obtained by subtracting the Langmuir-type adsorption isotherm from the experimental isotherm.¹ In

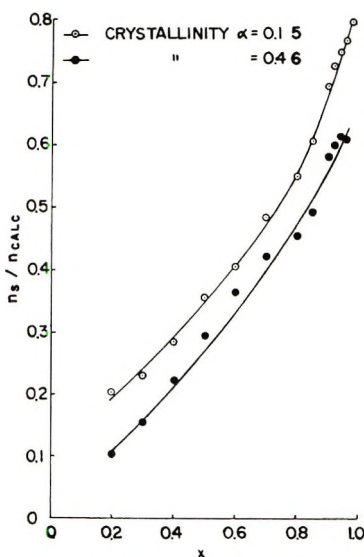


Fig. 8. n_s/n_{calc} vs. relative vapor pressure.

the present case, for the Langmuir type isotherm, the B.E.T.'s first layer n_1 [eq. (3)] is used:

$$n_1 = n_m Cx/[1 + (C - 1)x] \quad (3)$$

where n_m and C values are to be obtained from Figure 4. The processes of subtraction are shown in Figures 6 and 7 for 15% and 46% crystalline PVA, respectively. The dissolution curve (n_s versus x relation) corresponds to the water content coexisting with the amorphous region at a given chemical potential ($\ln x$).

On the other hand, the χ_1 value for a PVA-water solution was determined to be 0.494 by the osmotic pressure observation.¹⁰ From this value and the Flory-Huggins' equation [eq. (2)], the v_1 versus x relation and the corresponding n_{calc} versus x relation can be calculated. (In this case, referring to the ratio of adsorption part to the total sorbed water, n_{calc} is based on the total polymer.) Since the above χ_1 value (0.494) corresponds to the liquid state of polymer segments, n_{calc} is the water content which coexists with the completely amorphous polymer at a certain chemical potential ($\ln x$).

The ratio of experimental n_s to n_{calc} expresses the amorphous fraction which contributes to the dissolution process at that x (chemical potential). In other words, this ratio versus x relation (Fig. 8) can be regarded as an integration curve of lateral order distribution.^{11,12} Although both samples show a similar tendency, differentiation of the curves of Figure 8 may show that the more crystalline sample has the maximum of distribution at higher chemical potential.

It is noteworthy that the more crystalline sample, which has 54% non-crystalline material, by x-ray, does mix with water by more than 60%

fraction of the total polymer. Namely, the crystalline region observed by x-ray analysis may contribute to some extent to the dissolution process.

References

1. A. Takizawa, *J. Phys. Chem.*, **71**, 1611 (1967).
2. H. Tadokoro, S. Seki, and I. Nitta, *Bull. Chem. Soc. Japan*, **27**, 451 (1954).
3. H. Tadokoro, S. Seki, and I. Nitta, *Bull. Chem. Soc. Japan*, **28**, 559 (1955).
4. P. M. Hauser and A. D. McLaren, *Ind. Eng. Chem.*, **40**, 112 (1948).
5. W. Heller and A. Fogiel, *J. Phys. Chem.*, **70**, 2039 (1966).
6. H. W. Starkweather, Jr., *J. Appl. Polymer Sci.*, **2**, 129 (1959).
7. S. Brunauer, *Adsorption of Gases and Vapors*, Princeton Univ. Press, Princeton, N. J., 1943, p. 154.
8. T. Kawai, *J. Polymer Sci.*, **37**, 181 (1959).
9. J. W. Rowen and S. Simha, *J. Phys. Colloid Chem.*, **53**, 921 (1949).
10. A. Nakajima, *Polyvinyl Alcohol*, Society of High Polymers, Japan, 1955, p. 347.
11. J. A. Howsmon and W. A. Sisson, *Cellulose and Cellulose Derivatives*, Part I, E. Ott, H. M. Spurlin, and M. W. Graffin, Eds., Interscience, New York, 1954, Chap. 4B.
12. H. Maeda, *J. Soc. Fiber Sci. Tech., Japan*, **12**, 6 (1956).

Received May 10, 1967

Revised July 18, 1967

Effects of Mercaptides on the Butyllithium-Initiated Polymerization of Methyl Methacrylate

TAKUJI HIRAHARA, TOYOTOSHI NAKANO, and YUJI MINOURA,
Research Institute for Atomic Energy, Osaka City University, Osaka, Japan

Synopsis

The effects of mercaptides on the butyllithium-initiated polymerization of methyl methacrylate in toluene were investigated. The rates of polymerization were decreased by the addition of mercaptides, possibly owing to the formation of a relatively stabilized complex between the mercaptides and the active center of the polymerizing monomer. The stereoregularity was also affected by the addition of mercaptides. The effects increased in the order of increase in the bulk of the alkyl group of the mercaptides: *n*-propyl < isopropyl < *tert*-butyl < phenyl. The effects of mercaptides on the stereoregularity were larger than those of the analogous oxygen compounds. The concentrations of butyllithium and monomer had no effect on the stereoregularity.

INTRODUCTION

Hitherto many studies on the stereoregularity in the anionic polymerizations of vinyl monomers have been reported. It is known that the stereoregular polymerization of polar monomers is influenced by the following conditions:¹ (1) size and electronegativity of the metal in the catalyst, (2) polar character of the monomer, (3) nature of the groups attached to the metal in the catalyst, (4) polymerization temperature, (5) solvent. As for the polymerization of certain vinyl monomers with alkali metal alkyls, lithium and its alkyls are generally good stereospecific catalysts, and the stereoregularity of product decreases in the order of increase in the size and electropositivity of the metal:²⁻³ Li > Na > K.

Those catalysts having bulkier alkyl groups such as *tert*-hexyl alcoholate⁴ and Grignard reagents⁵ such as *i*-BuMgBr form highly isotactic poly(methyl methacrylate).

As for the vinyl monomers, styrene,⁶ acryl esters,⁷⁻¹¹ vinyl ketones,¹² thiolacrylates,¹² and acrylamides¹³ form stereoregular polymers under appropriate conditions. The stereoregularity of the acryl esters decreases in the order of decrease in the bulk of the ester group:¹⁴ *tert*-butyl > *sec*-butyl > isobutyl > *n*-butyl.

Moreover, the polymerization temperature and solvent affect the stereoregularity. Highly stereospecific catalysts are relatively insensitive to changes in temperature, but the stereoregulating ability of less stereospecific catalysts is changed greatly by changing the temperature.^{1,5} Inert solvents are normally required for stereoregular polymerization.

The effects of additives on anionic polymerizations have also been reported by some workers. The addition of alkoxides in the butyllithium-initiated polymerization of methyl methacrylate (MMA) increases the overall rates of polymerization and isotacticity of the product.¹⁵ The effects of lithium butoxide on the butyllithium-initiated polymerization of styrene¹⁶ have also been reported. In this case both the initiation rate and the propagation rate are decreased by the addition of BuOLi.

Lithium hydroxide, when added in the butyllithium-initiated polymerization of styrene, also increases the isotacticity greatly.¹⁷ In this paper, the effects of the addition of various lithium mercaptides, the sulfur analogs of alkoxides, in the butyllithium-initiated polymerization of methyl methacrylate in toluene at -30°C . were investigated.

The effects of the concentrations of butyllithium (BuLi) and the monomer on the stereoregularity were also studied, and a comparison of the effects of the mercaptides with those of the analogous alkoxides was made.

EXPERIMENTAL

Reagents

Methyl Methacrylate. Commercially available monomer was distilled with steam. The inhibitor was removed with care by washings with 10% sodium hydroxide solution and then water. The monomer was dried with anhydrous sodium sulfate and then distilled under a nitrogen atmosphere at reduced pressure and its middle fraction was collected and kept in a dark place.

This fraction was freshly distilled immediately before use over calcium hydride at $45\text{--}45.5^{\circ}\text{C}$. under a pressure of 100 mm. Hg.

Toluene. Analytical grade reagent was washed successively with concentrated sulfuric acid and then with water. It was distilled twice over sodium wire after drying over calcium chloride and refluxing with sodium wire.

Mercaptans. Commercially available products were distilled immediately before use: thiophenol, $86.2\text{--}86.5^{\circ}\text{C}/5$ mm. Hg; *n*-propylmercaptan, 67°C .; isopropylmercaptan, $52.5\text{--}53^{\circ}\text{C}$.; *tert*-butylmercaptan, $63.7\text{--}64.0^{\circ}\text{C}$.

***n*-Butyllithium.** Commercially available product was obtained as a dilute solution in pentane. The concentration was checked before use by the double titration method described by Gilman and Haubein.¹⁸

Phenol. Commercially available product was distilled at $61.0\text{--}61.2^{\circ}\text{C}$. under a pressure of 9 mm. Hg.

***tert*-Butanol.** A good grade of commercial alcohol¹⁹ was stirred over anhydrous calcium chloride at 60°C . for several hours and then distilled in a moisture-free apparatus. Its middle fraction was distilled at 82.4°C . just before use.

Polymerization

The polymerizations were carried out in sealed glass tubes at -30°C . Precautions were taken to remove traces of water in all the polymerizations.

Small quantities of the appropriate mercaptans were added, prior to the monomer addition, at room temperature, to solutions of BuLi in toluene. Lithium mercaptides were formed by the reaction of known quantities of the mercaptans with a known excess of BuLi, as in eq. (1).



It was thus possible to prepare an initiator solution containing constant concentrations of BuLi and lithium mercaptides. The reaction mixture was poured into a large excess of methanol containing dilute hydrochloric acid after the desired length of time and filtered off.

The polymers obtained were dried under reduced pressure at room temperature to constant weight.

Intrinsic Viscosity [η]

The viscosities of the polymers were measured by means of an Ubbelohde viscometer at 30°C.

Measurement of Stereoregularity by Infrared Spectra

The infrared spectra of the polymers obtained were scanned over the region 4000–400 cm^{-1} on a Perkin-Elmer Model 337 double-beam spectrometer under standard scanning conditions. Thin films were prepared from benzene solutions of poly(methyl methacrylate) by evaporating the solvent. As a diagnostic parameter, the J values were determined according to the method of Goode et al.²⁰

Measurement of Tacticity by Nuclear Magnetic Resonance

To obtain more detailed results on the stereoregularity, the high-resolution nuclear magnetic resonance (NMR) spectra of these poly(methyl methacrylates) were measured in chloroform solution by using a 60 Mcycle/sec. Varian A 60 A spectrometer at 60°C. The tacticity of the poly(methyl methacrylate) was obtained from the bands due to the absorption by the protons of the α -methyl group according to the method of Bovey and Tiers.²¹

RESULTS AND DISCUSSION

The effects of lithium thiophenoxide on the BuLi-initiated polymerization of methyl methacrylate were investigated, and the effects of the mercaptide on the rate of the polymerization are shown in Figure 1. The overall rate of the polymerization was decreased by the addition of lithium thiophenoxide, possibly owing to the formation of a relatively stabilized complex ion pair between the mercaptide and the active center end of the polymerizing monomer.

The effects of the mercaptide on the stereoregularity are also shown in the parentheses in Figure 1. The conversion had almost no effect on the stereoregularity for the polymerization in the presence of the mercaptide,

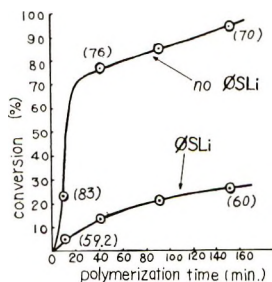


Fig. 1. Effect of $\text{C}_6\text{H}_5\text{SLi}$ on the rate of polymerization. $[\text{BuLi}] = 1.37 \times 10^{-2}$ mole/l.; $[\text{C}_6\text{H}_5\text{SLi}] = 1.37 \times 10^{-2}$ mole/l.; $[\text{MMA}] = 1.87$ mole/l.; in toluene, -30°C . Numbers in parentheses are J values.

whereas the conversion had a considerable effect on the stereoregularity for the polymerization in the absence of the mercaptide.

A complete explanation of the results does not appear to be possible owing to their complexity. But in the absence of the mercaptides, the rate of polymerization was quite high, and a toluene solution of the polymer at higher conversion was extremely viscous. Therefore this seems to favor the stereospecific polymerization.²² However, in the presence of the mercaptide, the rate of polymerization was low, possibly owing to formation of a relatively stabilized complex between the mercaptide and the active center end as mentioned above.

The effects of the concentration of lithium thiophenoxide on the BuLi-initiated polymerization of methyl methacrylate in toluene at -30°C . are shown in Table I. As the solubility in toluene was low, the polymerizing systems were quite heterogeneous at higher concentrations. The addi-

TABLE I
Effect of $\text{C}_6\text{H}_5\text{SLi}$ on the Stereoregularity of PMMA^a

$\text{C}_6\text{H}_5\text{SLi}$, mole/l.	Conversion, %	J value	Tacticity			$[\eta]$, dl./g.
			I , %	H , %	S , %	
0	93.8	72	48	29	23	0.485
2.27×10^{-2}	50.1	55	79	18	3	1.026
6.80×10^{-2}	29.8	56	74	23	3	0.576
27.2×10^{-2}	10.0	56	71	26	3	0.359

^a Conditions: $[\text{BuLi}] = 6.8 \times 10^{-2}$ mole/l.; $[\text{MMA}] = 1.87$ mole/l.; in toluene, -30°C ., 2 hr.

tion of small quantities of lithium thiophenoxide greatly increased the isotacticity of the poly(methyl methacrylate) obtained, as shown in Table I. However, on further addition of lithium thiophenoxide, the isotacticity of the polymer gradually decreased, possibly owing to the decrease in the rate of polymerization with increase in the concentration of the mercaptide. In most cases the intrinsic viscosity $[\eta]$ of the polymer formed in the presence of the mercaptide was lower than that of the

polymer obtained in the absence of the mercaptide. But no simple relation was found between the intrinsic viscosity and the concentration of the mercaptide. The effects of other mercaptides such as $n\text{-C}_3\text{H}_7\text{-SLi}$, $i\text{-C}_3\text{H}_7\text{-SLi}$ and $\text{tert-C}_4\text{H}_9\text{SLi}$ were also investigated under comparable conditions to those for lithium thiophenoxide, and the results obtained are shown in Tables II-IV.

By the addition of these mercaptides, the rates of polymerization were also decreased and the isotacticity of the poly(methyl methacrylate) increased as in the case of lithium thiophenoxide. But the effects of these mercaptides on the isotacticity were not so large as in the case of the thiophenoxide. The effect of the mercaptides on the stereoregularity

TABLE II
Effect of $n\text{-PrSLi}$ on the Stereoregularity of PMMA^a

$n\text{-PrSLi}$, mole/l.	Conversion, %	J value	Tacticity			$[\eta]$, dl./g.
			I , %	H , %	S , %	
0	93.8	72	48	29	23	0.485
2.27×10^{-2}	93.8	68	52	26	22	0.701
6.80×10^{-2}	86.8	70	52	26	22	0.524
27.2×10^{-2}	82.2	63	55	27	18	0.240

^a Conditions: $[\text{BuLi}] = 6.8 \times 10^{-2}$ mole/l.; $[\text{MMA}] = 1.87$ mole/l.; in toluene, -30°C ., 2 hr.

TABLE III
Effect of $i\text{-PrSLi}$ on the Stereoregularity of PMMA^a

PrSLi , mole/l.	Conversion, %	J value	Tacticity			$[\eta]$, dl./g.
			I , %	H , %	S , %	
0	93.8	72	48	29	23	0.485
2.27×10^{-2}	82.1	67	47	31	22	0.322
6.80×10^{-2}	80.8	66	52	29	19	0.590
27.2×10^{-2}	31.3	61	62	28	10	0.163

^a Conditions: $[\text{BuLi}] = 6.8 \times 10^{-2}$ mole/l.; $[\text{MMA}] = 1.87$ mole/l.; in toluene, -30°C ., 2 hr.

TABLE IV
Effect of tert-BuSLi on the Stereoregularity of PMMA^a

tert-BuSLi , mole/l.	Conversion, %	J value	Tacticity			$[\eta]$, dl./g.
			I , %	H , %	S , %	
0	93.8	72	48	29	23	0.485
2.27×10^{-2}	82.4	67	54	29	17	0.344
6.80×10^{-2}	55.3	65	60	28	12	0.143
27.2×10^{-2}	17.6	63	66	26	8	0.256

^a Conditions: $[\text{BuLi}] = 6.8 \times 10^{-2}$ mole/l.; $[\text{MMA}] = 1.87$ mole/l.; in toluene, -30°C ., 2 hr.

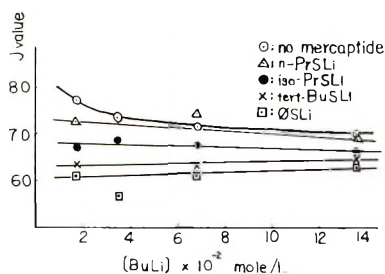


Fig. 2. Effect of BuLi concentration on stereoregularity of PMMA: (O) no mercaptide; (Δ) *n*-PrSLi; (\bullet) *i*-PrSLi; (\times) *tert*-BuSLi; (\square) C_6H_5SLi . [Mercaptide] = 6.80×10^{-2} mole/l.; [MMA] = 1.87 mole/l.; in toluene, $-30^\circ C.$; 2 hr.

decreased in the order of decrease in the bulk of the alkyl group of the mercaptide: phenyl-SLi > *tert*-butyl-SLi > isopropyl-SLi > *n*-propyl-SLi.

These data agree with the reports^{4,5,12,13} that the stereoregularity of the polymerization is determined by the rigidity of the complex formed at the active center end of the polymerizing monomer.

The effect of the concentration of BuLi on the tacticity was also investigated under otherwise constant conditions; the results are shown in Figure 2. As can be seen from Figure 2, the concentration of BuLi had almost no effect on the stereoregularity with all these mercaptides. However, the *J* values obtained increased as mentioned above in the order of increase in the bulk of the alkyl group of the mercaptides independent of the concentration of BuLi.

The concentration of the monomer also had no effect on the stereoregularity, as in the case of changes in the concentration of BuLi.

From these results, it was concluded that the effects on the stereoregularity under these conditions were determined by the concentrations and the kind of the mercaptides and were independent of the concentrations of BuLi and methyl methacrylate.

The effects of the addition of analogous alkoxides in the BuLi-initiated polymerization of methyl methacrylate in toluene at $-30^\circ C.$ were also investigated. The effects of the alkoxides on the stereoregularity are shown in Table V, in which they are compared with the effects of the analogous

TABLE V
Effect of Alkoxides and Mercaptides on the Stereoregularity of PMMA^a

Alkoxide or mercaptide	Conversion, %	<i>J</i> value	$[\eta]$, dl./g.
<i>tert</i> -BuOLi	70.3	65	0.423
<i>tert</i> -BuSLi	54.5	62	—
C_6H_5OLi	94.5	58	0.704
C_6H_5SLi	39.5	54	—

^a Conditions: [alkoxide] = 6.8×10^{-2} mole/l.; [mercaptide] = 6.8×10^{-2} mole/l.; [BuLi] = 6.8×10^{-2} mole/l.; [MMA] = 0.94 mole/l.; in toluene, $-30^\circ C.$, 2 hr.

mercaptides. The J values obtained were in both cases higher for the analogous oxygen compounds: phenyl-OLi > phenyl-SLi; *tert*-butyl-OLi > *tert*-butyl-SLi. Therefore, the mercaptides had a greater effect than the analogous oxygen compounds on the stereoregularity in the BuLi-initiated polymerization of methyl methacrylate, possibly owing to the higher coordination character of the sulfur compounds as compared with the alkoxides, as can be seen from the fact that the rate of polymerization decreased when the mercaptides were added. The low solubility of mercaptides in toluene, in comparison with the alkoxides, would also promote the rigidity of the complex ion pair formed at the active center end of the polymerizing monomer.

The authors are grateful to Dr. T. Kakutani and H. Kurita, of the Asahi Kasei Co. Ltd., for the measurements and determinations of the tacticity of PMMA by the Varian NMR spectrometer.

References

1. M. L. Miller, *The Structure of Polymers*, Reinhold, New York, 1966, p. 382.
2. D. L. Glusker, E. Stiles, and B. Yoncoskie, *J. Polymer Sci.*, **49**, 297, 315 (1961).
3. D. Braun, M. Herner, U. Johnson, and W. Kern, *Makromol. Chem.*, **51**, 15 (1962).
4. D. Lim and J. Trekoval, paper presented at International Symposium of Macromolecular Chemistry, Paris, 1963.
5. H. Watanabe, *Kogyo Kagaku Zasshi*, **63**, 1628 (1960); *ibid.*, **65**, 1104 (1962).
6. W. Kern, *Nature*, **187**, 410 (1960).
7. T. G. Fox et al., *J. Am. Chem. Soc.*, **80**, 1768 (1958); *J. Polymer Sci.*, **31**, 173 (1958).
8. Rohm & Haas Co., Belg. Pat. 566, 713 (1958).
9. R. L. Miller, *J. Polymer Sci.*, **38**, 63 (1959).
10. A. Nishioka and H. Watanabe, *Kogyo Kagaku Zasshi*, **63**, 1628 (1960); *ibid.*, **64**, 720 (1961).
11. Y. Nakayama, T. Tsuruta, and J. Furukawa, *Kogyo Kagaku Zasshi*, **64**, 591, 1846 (1961).
12. J. Furukawa, *Polymer*, **3**, 487 (1962).
13. Y. Nakayama, T. Tsuruta, and J. Furukawa, *Makromol. Chem.*, **43**, 76 (1961); *ibid.*, **49**, 112, 136, 153 (1961); *ibid.*, **53**, 197 (1962).
14. T. Makimoto, T. Tsuruta, and J. Furukawa, *Makromol. Chem.*, **50**, 116 (1961).
15. D. M. Wiles and S. Bywater, *J. Phys. Chem.*, **68**, 1983 (1964).
16. J. E. L. Roovers and S. Bywater, *Trans. Faraday Soc.*, **62**, 1876 (1966).
17. D. J. Worsfold and S. Bywater, *Makromol. Chem.*, **65**, 245 (1963).
18. H. Gilman and A. H. Haubein, *J. Am. Chem. Soc.*, **66**, 1515 (1944).
19. R. E. Ireland and M. Chaykovsky, in *Organic Syntheses*, Vol. 41, Wiley, New York, 1961, p. 7.
20. W. E. Goode, F. H. Owens, R. P. Fellman, and W. H. Snyder, *J. Polymer Sci.*, **46**, 317 (1960).
21. F. A. Bovey and G. V. D. Tiers, *J. Polymer Sci.*, **44**, 173 (1960).
22. D. M. Wiles and S. Bywater, *Polymer*, **3**, 175 (1962).

Received June 6, 1967

Revised July 18, 1967

Vinyl Polymerization Initiated by Ceric Ion Reducing Agent Systems in Sulfuric Acid Medium

S. V. SUBRAMANIAN and M. SANTAPPA, *Department of Physical Chemistry, University of Madras, Madras, India*

Synopsis

Polymerization of the monomers, methyl acrylate (MA) and methyl methacrylate (MMA) was carried out in sulfuric acid medium at 15°C. with the redox initiator system, ceric ammonium sulfate-malonic acid. There was no induction period, and a steady state was attained in a short time. There was found to be no polymerization even after 1 hr. in the absence of the reducing agent R. The initiation was by the radical produced from the Ce^{4+} -malonic acid reaction. The rate of monomer disappearance was proportional to $[M]^{1.5}$, $[R]^{0.5}$, and $[Ce^{4+}]^{0.3-0.5}$, and the rate of ceric disappearance was directly proportional to $[R]$ and $[Ce^{4+}]$. Chain lengths of the polymers were directly proportional to $[M]$ and inversely to $[R]^{1/2}$ and $[Ce^{4+}]^{1/2}$. The experimental results were explained by a kinetic scheme involving the following steps: (a) oxidation of the substrate to give the primary radical which reacts with Ce^{4+} to give the products, (b) initiation by the primary radical, (c) propagation, and (d) termination of the growing polymer radicals by the mutual type. For the polymerization of acrylonitrile (AN) by the redox system, ceric ammonium sulfate-cyclohexanone (CH), in sulfuric acid at 15°C., the scheme was modified to include linear type of termination by Ce^{4+} , along with the mutual termination to explain the results especially under conditions with $[Ce^{4+}] \geq [CH]$.

INTRODUCTION

Ceric salts or ceric salt-reducing agent systems were used as initiators of vinyl polymerization. Venkatakrishnan and Santappa¹ studied the polymerization of methyl acrylate initiated by ceric perchlorate. Ananthanarayanan and Santappa² studied in detail the thermal polymerization of methyl acrylate, methyl methacrylate, and acrylonitrile initiated by Ce^{4+} in aqueous perchloric, nitric, and sulfuric acid media. Lalitha and Santappa³ used redox systems of ceric ion with various alcohols (reducing agents) as initiators. Mino et al.⁴ studied the polymerization of acrylamide initiated by the ceric nitrate-3-chloro-1-propanol redox system and observed that at constant hydrogen and nitrate ion concentrations, the rate of polymerization was independent of ceric ion concentration. Katai et al.⁵ made a detailed kinetic study of polymerization of acrylonitrile initiated by the ceric sulfate-ethylene glycol redox system. It was concluded that initiation was both by Ce^{4+} and the primary radical from the substrate, and termination was exclusively by Ce^{4+} . Ananthanarayanan and Santappa⁶ carried out polymerization of methyl acrylate initiated by

the redox system Ce^{4+} -HCHO in perchloric acid medium. Previous studies by different investigators revealed that the rates of initiation of vinyl monomers by various ceric salts were in the order, ceric perchlorate > ceric nitrate > ceric sulfate, and the chain lengths of polymers initiated by the above ceric salts were in the reverse order. It was envisaged that in the vinyl systems polymerized by redox type initiator involving Ce^{4+} , the direct interaction of Ce^{4+} with the monomer and the growing polymer radical could be brought under control by suitable adjustments of concentrations of the reactants, temperature etc., so that such reactions might either be suppressed or eliminated if necessary. For elucidation of these points, a study of kinetics of polymerization of methyl acrylate (MA) and methyl methacrylate (MMA) initiated by the ceric ammonium sulfate-malonic acid redox system in sulfuric acid was carried out, and a brief account of this has already been reported.⁷ The study of the kinetics of polymerization of acrylonitrile (AN) initiated by the ceric ammonium sulfate-cyclohexanone (CH) redox pair was also carried out.

EXPERIMENTAL

Materials

The monomers, methyl acrylate (Rohm and Haas, U.S.A.), methyl methacrylate (B.D.H.), and acrylonitrile (American Cyanamide Co.) were purified by standard methods, i.e., distilled twice in an atmosphere of nitrogen under reduced pressure before use. Water doubly distilled over alkaline permanganate and passed through the ion exchange resin Biodiminrolit was used. Ceric ammonium sulfate (Atomic Energy Establishment, India), sulfuric acid (Analar, Basic Synthetic Chemicals, India), potassium hydrogen sulfate (Analar B.D.H.) were used. Malonic acid (E. Merck) was used as such for preparation of solutions. Cyclohexanone was dried over anhydrous sodium sulfate, fractionally distilled, the middle fraction (b.p. 155-156°C.) being collected. Solvents like benzene, acetone, chloroform, and dimethylformamide were fractionally distilled and the middle cuts were used. Deaeration of the system was done with nitrogen, previously freed from oxygen by passage through Fieser's solution.

Estimations

Ceric concentration was estimated by titration against standard ferrous ammonium sulfate solution in sulfuric acid medium with the use of ferroin indicator. The malonic acid concentration was determined by titration against standard sodium hydroxide with phenolphthalein as indicator.

Apparatus and Procedure

The reaction vessel was a glass tube, 6 in. in length and 2 in. in diameter, fitted with a B-24 ground joint head to which two glass tubes were fused; one bent at right angles at the top and reaching the bottom of the tube

was used as inlet for passing nitrogen gas through the reaction system, while the second shorter tube was used for addition of the oxidizing agent to the system. First, the reaction system (except the ceric salt solution) was taken in the reaction tube and deaerated; the ceric salt solution was then separately deaerated and added to the former. No induction period was observed. The reaction system was maintained at $15 \pm 0.1^\circ\text{C}$. in a thermostat usually for 10 min. The reaction was then frozen by addition of a known excess of ferrous ammonium sulfate solution to the system; the precipitated polymer was filtered off and used for computing rate of monomer disappearance, $-d[M]/dt$, while the filtrate was used for estimating the rate of ceric disappearance, $-d[\text{Ce}^{4+}]/dt$. Poly(methyl methacrylate) and poly(methyl acrylate) were purified by dissolving in acetone, reprecipitating by addition of methanol, filtering off, and drying the polymers. The procedure for polyacrylonitrile was similar, dimethylformamide and methanol being used as solvent and precipitant, respectively. The chain lengths n of the purified polymers were determined viscometrically, by using an Ubbelohde suspended-level dilution viscometer (Polymer Consultants Ltd., Colchester, U.K.) kept in a Kreb viscometric bath designed for precision viscometry. The following Mark-Houwink relationships were employed.

For poly(methyl methacrylate)⁸ in benzene at 25°C .:

$$n = 2.81 \times 10^3 [\eta]^{1.32}$$

For poly(methyl acrylate)⁹ in acetone at 20°C .:

$$n = 11.2 [\eta]^{1.22}$$

For polyacrylonitrile¹⁰ in dimethylformamide at 25°C .:

$$[\eta] = 2.34 \times 10^{-4} \bar{M}_v^{0.75}$$

RESULTS AND DISCUSSIONS

Polymerization of Methyl Acrylate and Methyl Methacrylate in Sulfuric Acid Medium Initiated by Ce⁴⁺-Malonic Acid System

Under conditions of low temperature (15°C .) it was found that there was no polymerization of the monomers (MMA, MA, or AN) even after 60 min. when ceric ammonium sulfate alone was used as an initiator, but with Ce⁴⁺-malonic acid redox initiator it was noticed that the polymerization reaction proceeded without any induction period.

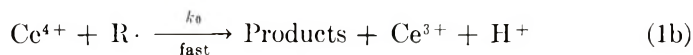
Kinetic Scheme. The following reaction scheme is found to explain satisfactorily the kinetic results obtained.

Reaction of ceric ion with reducing agent:

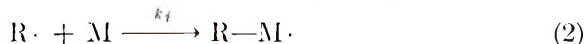


where R is reducing agent and R· is a primary radical.

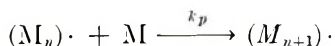
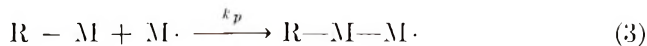
Reaction of primary radical with Ce^{4+} to give the products.



Initiation of polymerization by reaction of primary radical with monomer:



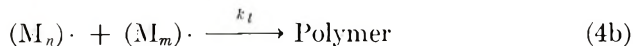
Propagation:



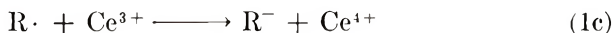
Termination by Ce^{4+} :



Mutual termination:



A possible alternative to step (1b) may be:



which may arise especially from a consideration of products of reaction (1a) still in the solvent cage and which means competition for $R\cdot$ between Ce^{4+} and Ce^{3+} . Occurrence of such a step would mean a decrease in the rate of ceric ion disappearance with time which was not observed in our experiments. Such an alternative step, it may be pointed out, was also not considered in the studies on oxidation of alcohols,^{11,12} aldehydes,¹³ ketones,¹⁴ etc. by Ce^{4+} by various workers.

Making the usual assumptions for the steady-state concentrations of free radicals (primary and chain) and the rate constants being independent of chain length, and considering only the mutual type of termination as effective under our experimental conditions, as evidence against linear termination (4a) appears under $-d[M]/dt$ below, we arrive at the eqs. (5), (6), and (7) for the rate of ceric disappearance, rate of monomer disappearance, and chain length n , respectively:

$$-d[Ce^{4+}]/dt = k_r[Ce^{4+}][R] \quad (5)$$

$$\frac{-d[M]}{dt} = \frac{k_p[M]^{3/2}}{k_i^{1/2}} \left\{ \frac{k_i k_r [R][Ce^{4+}]}{k_i[M] + k_0[Ce^{4+}]} \right\}^{1/2} \quad (6)$$

$$n = \frac{k_p[M]^{1/2} \{ k_0[Ce^{4+}] + k_i[M] \}^{1/2}}{(k_i k_r k_i)^{1/2} [Ce^{4+}]^{1/2} [R]^{1/2}} \quad (7)$$

Rate of Ceric Disappearance. The rate was found to be directly proportional to $[Ce^{4+}]$, $-d[Ce^{4+}]/dt$ versus $[Ce^{4+}]$ gave a straight line passing through the origin (Fig. 1). The rate was independent of the monomer

concentration which meant ceric ions were not involved in an initiation reaction of the type $M + Ce^{4+}$ or in a termination reaction of the type $M_n + Ce^{4+}$ (4a). The rate increased with first power of the malonic acid concentration (Fig. 1). Absence of complex formation between the substrate and ceric ion was revealed by the straight line plot of the rate against Malonic acid concentration passing through the origin; on the other hand formation of a complex and obedience to Michaelis-Menton¹⁵ kinetics would mean that a plot of $1/\text{rate}$ versus $1/[\text{substrate}]$ leaves an intercept on the ordinate. The rate was found to increase with increasing $[H_2SO_4]$ at constant ionic strength, μ ; the rate was unaffected with increasing

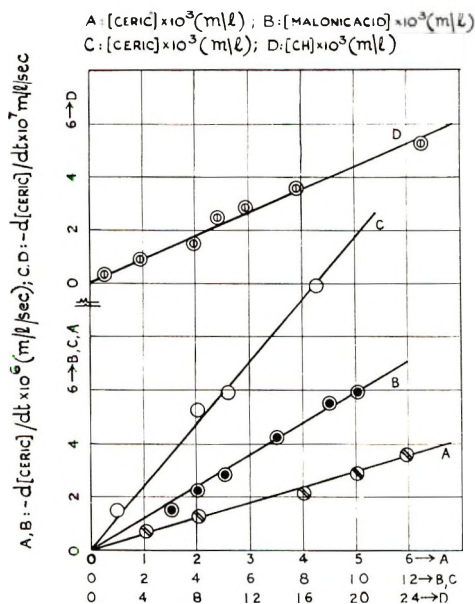
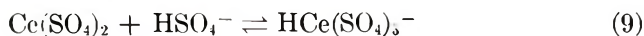
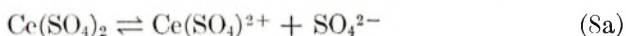


Fig. 1. Plots of (A) $-d[Ce^{4+}]/dt$ vs. $[Ce^{4+}]$ at $[\text{malonic acid}] = 5 \times 10^{-3}M$, $[\text{MMA}] = 0.0940M$; (B) $-d[Ce^{4+}]/dt$ vs. $[\text{malonic acid}]$ at $[Ce^{4+}] = 5 \times 10^{-3}M$, $[\text{MMA}] = 0.0940M$; (C) $-d[Ce^{4+}]/dt$ vs. $[Ce^{4+}]$ at $[\text{CH}] = 2.5 \times 10^{-2}M$, $[\text{AN}] = 0.4767M$; (D) $-d[Ce^{4+}]/dt$ vs. $[\text{CH}]$ at $[Ce^{4+}] = 4 \times 10^{-3}M$; $[\text{AN}] = 0.4767M$. For all cases, $[H_2SO_4] = 0.5M$; $\mu = 0.6M$; $T = 15^\circ C$.

$[H_2SO_4]$ if ionic strength was not kept constant; increasing ionic strength at constant $[H_2SO_4]$ showed that there was a fall in the rate. $KHSO_4$ was used for adjustments of μ . All these observations could be explained on the assumption that the reactive ceric species was a covalently bound neutral ceric sulfate molecule, $Ce(SO_4)_2$.¹¹ In solutions of ceric ammonium sulfate in sulfuric acid (1.0M) the following equilibria are recognized:



At constant μ (maintained by KHSO_4) the increase of rate with increase of $[\text{H}_2\text{SO}_4]$ or $[\text{H}^+]$ may be due to increase in the concentration of $\text{Ce}(\text{SO}_4)_2$ by operation of equilibria (Sa) and (8b). Similarly, retardation of rate by increase of μ at constant $[\text{H}^+]$ may be due to depletion of $\text{Ce}(\text{SO}_4)_2$ by operation of equilibrium (9). Further, the nonvariation of rates with increase of $[\text{H}_2\text{SO}_4]$ without keeping μ constant may be looked upon as nonvariation in $[\text{Ce}(\text{SO}_4)_2]$ by the opposing effects of $[\text{H}^+]$ and $[\text{HSO}_4^-]$ or by simultaneous operation of the equilibria (Sa), (8b), and (9).

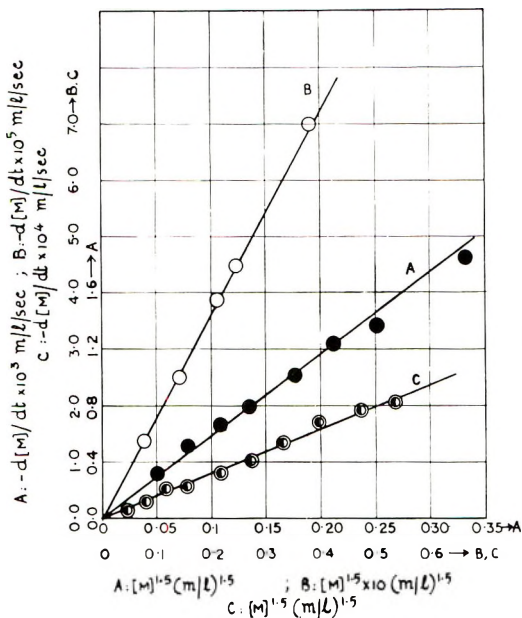


Fig. 2. Plots of $-d[M]/dt$ vs. $[M]^{1.5}$: (A) $[\text{Ce}^{4+}] = [\text{malonic acid}] = 5 \times 10^{-3}M$; $[\text{MA}] = 0.22M$; (B) $[\text{Ce}^{4+}] = [\text{malonic acid}] = 5 \times 10^{-3}M$; $[\text{MMA}] = 0.094M$ (C) $[\text{Ce}^{4+}] = 4 \times 10^{-3}M$, $[\text{CH}] = 2.5 \times 10^{-2}M$. For all cases, $[\text{H}_2\text{SO}_4] = 0.5M$; $\mu = 0.6M$; $T = 15^\circ\text{C}$.

Rate of Monomer Disappearance. The rate being dependent on $[M]^{1.5}$ (Fig. 2) is strong evidence for mutual termination rather than the linear type. The rate was also directly proportional to $[\text{malonic acid}]^{1/2}$ (Fig. 3); if linear termination (4a) were effective, $-d[M]/dt$ would have been directly proportional to $[\text{malonic acid}]$. Increasing $[\text{Ce}^{4+}]$ ($1.0 \times 10^{-4}M$ to $3.0 \times 10^{-3}M$) increased the rate; for $[\text{Ce}^{4+}] \geq 3.0 \times 10^{-3}M$, however the rate was independent of $[\text{Ce}^{4+}]$. The increase of rate with $[\text{Ce}^{4+}]$ (lower concentration range) may be understood in terms of initiation by $\text{Ce}^{4+} + \text{R}$, reaction (1a), and mutual termination (4b), and $-d[M]/dt$ being given by eq. (6). According to eq. (6) and assuming $k_0[\text{Ce}^{4+}] > k_i[M]$ at high $[\text{Ce}^{4+}]$:

$$R_p = -d[M]/dt = k_p(k_i k_t / k_0 k_t)^{1/2} [M]^{1.5} [R]^{1/2} \quad (10)$$

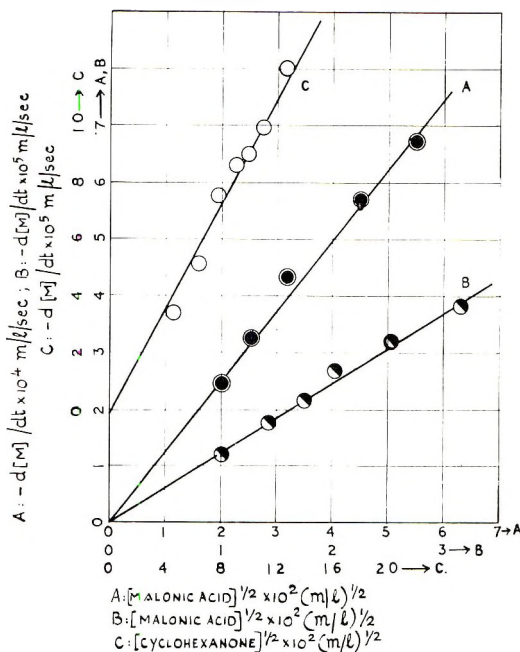


Fig. 3. Plots of: (A) $-d[M]/dt$ vs. $[\text{malonic acid}]^{1/2}$, $[\text{Ce}^{4+}] = 5 \times 10^{-3}M$, $[\text{MA}] = 0.221M$; (B) $-d[M]/dt$ vs. $[\text{malonic acid}]^{1/2}$, $[\text{Ce}^{4+}] = 5 \times 10^{-3}M$, $[\text{MMA}] = 0.0940M$; (C) $-d[M]/dt$ vs. $[\text{CH}]^{1/2}$, $[\text{Ce}^{4+}] = 4 \times 10^{-3}M$, $[\text{AN}] = 0.4767M$. For all cases, $[\text{H}_2\text{SO}_4] = 0.5M$; $\mu = 0.6M$; $T = 15^\circ\text{C}$.

It may be mentioned here that under conditions $k_0[\text{Ce}^{4+}] > k_i[\text{M}]$ plus termination (4a) $>$ (4b) at high $[\text{Ce}^{4+}]$, the rate would be independent of $[\text{Ce}^{4+}]$ but dependent on $[\text{M}]^2$ and $[\text{R}]$. As the experimental rate is strictly dependent on $[\text{R}]^{1/2}$ and on $[\text{M}]^{3/2}$, termination by (4a) must be ruled out. It may be added here that under conditions of high $[\text{Ce}^{4+}]/[\text{substrate}]$ ratio, rates were very high and subject to errors. The non-dependence of $-d[\text{M}]/dt$ on $[\text{Ce}^{4+}]$ at high concentration of the latter therefore follows from the eqs. (4). In the range where the rate was dependent on $[\text{Ce}^{4+}]$, the reciprocal of eq. (6) and rearrangement gives eq. (11):

$$\frac{[\text{M}]^2}{R_p^2} = \frac{k_t}{k_p^2 k_7 [\text{R}][\text{Ce}^{4+}]} + \frac{k_0 k_t}{k_p^2 k_7 k_i [\text{R}][\text{M}]} \tag{11}$$

The plot of $[\text{M}]^2/R_p^2$ against $[\text{Ce}^{4+}]^{-1}$ (Fig. 4) and a plot of $[\text{M}]^2/R_p^2$ against $[\text{M}]^{-1}$ (Fig. 4) were linear with intercepts on the ordinates. The effects of increasing $[\text{H}^+]$ or μ on $-d[\text{M}]/dt$ were similar to those on $-d[\text{Ce}^{4+}]/dt$. The increase of $-d[\text{M}]/dt$ with increasing $[\text{H}_2\text{SO}_4]$ at constant μ , independence of rate with increase in $[\text{H}_2\text{SO}_4]$ when μ was not maintained constant, the decrease of rate with increase of μ by addition of KHSO_4 at constant $[\text{H}_2\text{SO}_4]$, etc., were all indicative that neutral species, $\text{Ce}(\text{SO}_4)_2$, were indeed the active species.

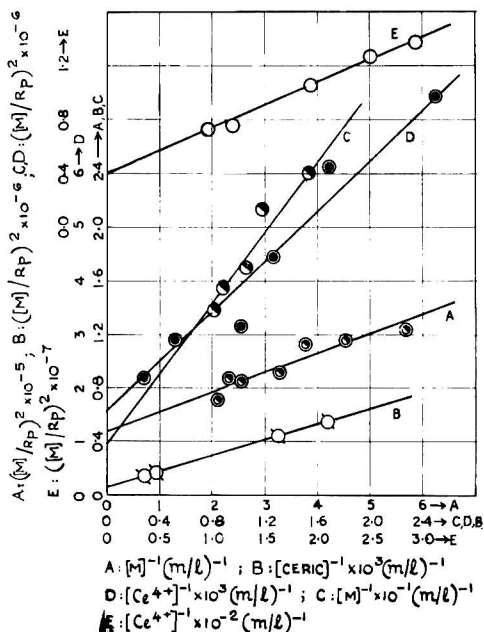


Fig. 4. Plots of: (A) $([M]/R_p)^2$ vs. $[M]^{-1}$, $[\text{Ce}^{4+}] = [\text{malonic acid}] = 5 \times 10^{-3}M$; (B) $([M]/R_p)^2$ vs. $[\text{Ce}^{4+}]^{-1}$, $[\text{malonic acid}] = 5 \times 10^{-3}M$, $[\text{MA}] = 0.221M$; (C) $([M]/R_p)^2$ vs. $[M]^{-1}$, $[\text{Ce}^{4+}] = [\text{malonic acid}] = 5 \times 10^{-3}M$; (D) $([M]/R_p)^2$ vs. $[\text{Ce}^{4+}]^{-1}$, $[\text{malonic acid}] = 5 \times 10^{-3}M$, $[\text{MMA}] = 0.0940M$; (E) $([M]/R_p)^2$ vs. $[\text{Ce}^{4+}]^{-1}$, $[\text{CH}] = 2.5 \times 10^{-2}M$; $[\text{AN}] = 0.4767M$. For all cases $[\text{H}_2\text{SO}_4] = 0.5M$; $\mu = 0.6M$; $T = 15^\circ\text{C}$.

Chain Lengths. Chain lengths were directly proportional to $[M]$ and inversely to $[\text{Ce}^{4+}]^{1/2}$ and $[\text{malonic acid}]^{1/2}$ (Table I). The presence of carboxyl group in the polymer was expected, if the initiator were the primary radical $\text{HOOC}-\dot{\text{C}}-\text{COOH}$. An attempt was therefore made to estimate the chain length of poly(methyl methacrylate) of low molecular weight by titration of the carboxyl endgroups ($\bar{M}_n \sim 11,500$), and a comparison of the latter with the viscometric chain length ($\sim 10,000$) indicated that there were four COOH groups per chain. This fact lent further support to termination of the mutual type.

Rate Constant. The value of k_t ($=0.22$ l./mole-sec.) was obtained from the slope of the plot of k_{obs} against $[\text{malonic acid}]$, k_{obs} being the pseudo first-order rate constant for ceric ion disappearance at a particular malonic acid concentration. Values of the composite constant, $k_p(k_i/k_0k_t)^{1/2}$ were obtained under conditions of high $[\text{Ce}^{4+}]$ from slope of the plot of $-d[M]/dt$ against $[M]^{1.5}$ (Fig. 2) and from plots of $([M]/R_p)^2$ versus $[M]^{-1}$ or $[\text{Ce}^{4+}]^{-1}$ (Fig. 4). From a plot of $([M]/R_p)^2$ against $[\text{Ce}^{4+}]^{-1}$, it would be seen that (intercept/slope) $= k_0/k_t$. From the value of the slope $(k_i/k_p^2k_t)$ and by substituting for k_t , parameter $k_p/k_t^{1/2}$ was obtained. Values of all parameters (Table II) depend on measurements of $-d[M]/dt$ which are accurate to within 1% and of $-d[\text{Ce}^{4+}]/dt$ which are accurate

TABLE I
Effect of [M], [Ce⁴⁺], and [Malonic Acid] on Chain Length for
the Ceric Ammonium Sulfate–Malonic Acid Redox System in Sulfuric Acid*

[Ceric] × 10 ³ , mole/l.	[Malonic acid] × 10 ³ , mole/l.	MMA		MA	
		[M], mole/l.	<i>n</i> (PMMA)	[M], mole/l.	<i>n</i> (PMA)
5	5	0.0846	65	0.133	1779
5	5	0.0940	132	0.177	2320
5	5	0.1034	320	0.221	2819
5	5			0.266	4339
5	5			0.354	5164
5	5			0.399	5636
5	0.1	0.094	815	0.221	16,550
5	0.2	0.094	624	0.221	14,370
5	0.4	0.094	398	0.221	9759
5	0.6	0.094	313	0.221	9072
5	0.8	0.094		0.221	7785
5	1.0	0.094	281	0.221	7381
0.2	5.0	0.094		0.221	
0.3	5.0	0.094		0.221	12,720
0.4	5.0	0.094	1005	0.221	—
0.6	5.0	0.094	511	0.221	10,750
0.8	5.0	0.094	409	0.221	8984
1.0	5.0	0.094	347	0.221	—
2.0	5.0	0.094	—	0.221	6646
2.0	5.0	0.094	—	0.221	6646
3.0	5.0	0.094	137	0.221	—

* [H₂SO₄] = 0.5M; μ = 0.6M; 15°C.

TABLE II
Rate Parameters for Ceric Ammonium Sulfate–Malonic Acid
Redox System (Sulfuric Acid Medium)

Monomer	Value of $k_p(k_i/k_0k_t)^{1/2}$			k_0/k_t	Value of $k_p/k_t^{1/2}$	
	From plot of R_p vs. [M] ^{1.5}	From plot of $([M]/R_p)^2$ vs. [M] ⁻¹	From plot of $([M]/R_p)^2$ vs. [Ce ⁴⁺] ⁻¹		From plot of $([M]/R_p)^2$ vs. [M] ⁻¹	From plot of $([M]/R_p)^2$ vs. [Ce ⁴⁺] ⁻¹
MMA	0.073	0.082	0.077	60	0.596	0.600
MA	0.205	0.242	0.285	70	1.532	1.100

to within ±0.1%, and therefore the order of magnitudes of the parameters may be considered accurate to within ±1%.

Polymerization of Acrylonitrile in Sulfuric Acid Medium Initiated by Ce⁴⁺–Cyclohexanone (CH) Redox System

Rate of Monomer Disappearance. Under the conditions, [CH]/[Ce⁴⁺] ≈ 6, the experimental results were found to be explained by the same mechanism as the one proposed for the system, ceric ammonium sulfate–

TABLE III
Rate Parameters for Ceric Ammonium Sulfate-Cyclohexanone Redox System with AN in H₂SO₄ Medium

Temp., °C.	$k_r \times 10^3$, l./mole-sec.	Value of $k_p' \left(\frac{k_r k_i}{k_0 k_t} \right)^{1/2}$			Value of $k_t/k_p k_t'$ ^a		
		From plot of $-d[M]/dt$ vs. [m] 1.5	From plot of $-d[M]/dt$ vs. [R] ^{1/2}	(k_0/k_t)	From plot of $R_p/[M]^2$ vs. [M]	From plot of $R_p/[M]^2[R]$ vs. [R]	From plot of $R_p[Ce^{4+}]/[M]^2$ vs. $[Ce^{4+}]^{-2}$
5	1.920	—	—	—	5.870	—	4.978
15	5.584	2.530×10^{-3}	2.762×10^{-3}	53	5.437	5.199	4.098

^a Value of k_t' (oxidative termination of the polymer radical by Ce⁴⁺) = 2.58×10^4 l./mole-sec. was obtained from $k_t/k_p k_t'$, assuming the literature values of $k_p = 1.45 \times 10^4$ l./mole-sec. and $k_t = 2 \times 10^9$ l./mole-sec.

malonic acid-MA (or MMA) in sulfuric acid. Thus the rate was proportional to $[M]^{1.5}$ (Fig. 2) and to $[CH]^{1/2}$ (Fig. 3). Similarly, values of the composite constants, $k_p(k_t/k_0k_i)^{1/2}$, k_0/k_i , and $k_p/k_t^{1/2}$ were evaluated (Table III).

Under the conditions $[CH]/[Ce^{4+}] \ll 1$, it was found that the rate was dependent on $[M]^{1.7}$; an increase in $[Ce^{4+}]$ keeping $[CH]$ constant was thus found to change the nature of the termination mechanism from one of pure mutual type to mutual plus linear termination types [eqs. (4a), (4b)].

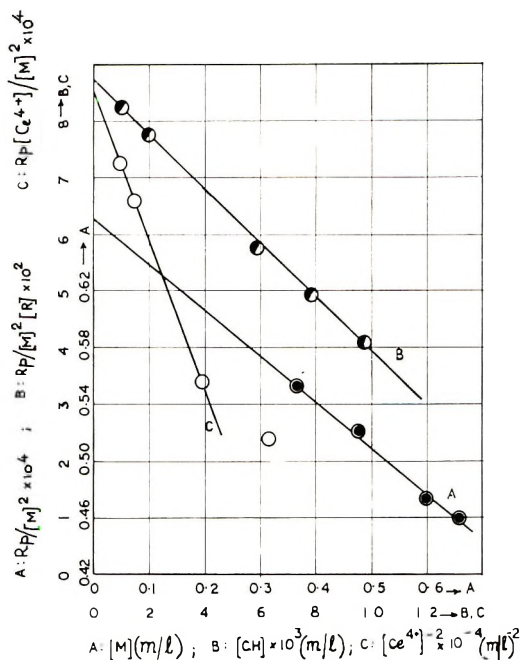


Fig. 5. Plots of: (A) $R_p/[M]^2$ vs. $[M]$, $[Ce^{4+}] = [CH] = 1 \times 10^{-2}M$; (B) $R_p/[M]^2 [R]$ vs. $[R]$, $[Ce^{4+}] = 4 \times 10^{-3}M$, $[AN] = 0.4767M$; (C) $R_p[Ce^{4+}]/[M]^2$ vs. $[Ce^{4+}]^{-2}$, $[CH] = 2.5 \times 10^{-2}M$, $[AN] = 0.4767M$. For all cases, $[H_2SO_4] = 0.5M$; $\mu = 0.6M$; $T = 15^\circ C$.

Absence of polymerization without the reducing agent, even after 1 hr., indicated that initiation was purely by the primary radical produced from the reaction of Ce^{4+} with cyclohexanone. R_p for pure linear termination would have been proportional to $[M]^2$ and for pure mutual termination to $[M]^{1.5}$, whereas experimentally it was proportional to $[M]^{1.7}$. Hence linear termination alone or pure mutual termination did not conform to the experimental results. A scheme consisting of initiation by the primary radical termination by mutual as well as by Ce^{4+} was found to explain all the results satisfactorily in this particular case. $-d[Ce^{4+}]/dt$ would still be given by eq. (5), but R_p would be given by eq. (12):

$$R_p = \frac{-d[M]}{dt} = \frac{k_p}{k_t' [Ce^{4+}]} \left(\frac{k_i k_r}{k_0} \right) [R][M]^2 - \left(\frac{k_p k_t}{\{k_t' [Ce^{4+}]\}^3} \right) \left(\frac{k_i k_r}{k_0} \right)^2 [R]^2 [M]^3 \quad (12)$$

Thus a plot of $R_p/[M]^2$ against $[M]$ was linear with a negative slope S and an intercept I (Fig. 5), and the parameter $k_i k_p k_t = S/I^2$ was calculated. This value was also obtained from plots of $R_p/[M]_2[R]$ versus $[R]$ and $R_p[Ce^{4+}]/[M]^2$ versus $[Ce^{4+}]^{-2}$. The order of magnitudes of various parameter (Table III) may be considered accurate within $\pm 1\%$ for reasons stated earlier.

References

1. S. Venkatakrisnan and M. Santappa, *Makromol. Chem.*, **27**, 51 (1958).
2. V. S. Ananthanarayanan and M. Santappa, *J. Appl. Polymer Sci.*, **9**, 2437 (1965).
3. J. Lalitha and M. Santappa, *Vignana Parishad Anusandhana Patrika*, **4**, 139 (1961).
4. G. Mino, S. Kaizermann, and E. Rasmussen, *J. Polymer Sci.*, **38**, 393 (1959).
5. A. A. Katai, V. K. Kulshrestha, and R. H. Marchessault, in *Fourth Cellulose Conference (J. Polymer Sci. C, 2)*, R. H. Marchessault, Ed., Interscience, New York, 1963, p. 403.
6. V. S. Ananthanarayanan and M. Santappa, *Proc. Indian Acad. Sci.*, **62**, 150 (1965).
7. S. V. Subramanian and M. Santappa, *Current Sci. (India)*, **35**, 437 (1966).
8. J. H. Baxendale, S. Bywater, and M. G. Evans, *J. Polymer Sci.*, **1**, 237 (1946).
9. N. Fuhrman and R. B. Mesrobian, *J. Am. Chem. Soc.*, **76**, 3281 (1954).
10. W. H. Stockmayer and R. H. Cleland, *J. Polymer Sci.*, **17**, 473 (1955).
11. S. S. Muhammed and K. Vijayachander Rao, *Bull. Chem. Soc. Japan*, **36**, 944 (1963).
12. G. Mino, S. Kaizermann, and E. Rasmussen, *J. Am. Chem. Soc.*, **81**, 1494 (1959).
13. G. Hargreaves and L. H. Sutcliffe, *Trans. Faraday Soc.*, **51**, 1105 (1955).
14. J. Shorter and C. N. Hinshelwood, *J. Chem. Soc.*, **1950**, 72, 3276, 3425; *ibid.*, **1962**, 1860.
15. L. Michaelis and M. Menton, *Biochem.*, **3**, 49 (1913).
16. F. S. Dainton, and R. S. Eaton, *J. Polymer Sci.*, **39**, 313 (1959).

Received May 16, 1967

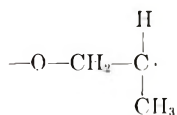
Revised July 19, 1967

Electron Spin Resonance Study of Polyglycols

F. C. THRYION, *Department of Chemistry*, and M. D. BAIJAL, *Department of Chemical Engineering, Laval University, Quebec, P. Q., Canada*

Synopsis

Polyethylene glycols and polypropylene glycols were irradiated with gamma-rays from a ^{60}Co source at 77°K. Electron spin resonance spectra of the free radicals produced were recorded. It was found that the rupture in the polymer chain takes place at $\text{C}-\text{C}$ and $\text{C}-\text{O}$ bonds. The radicals identified were $-\text{O}-\dot{\text{C}}\text{H}_2$ in polyethylene glycols and mainly



in polypropylene glycols. Thermal decay of these radicals followed a second-order law, and the decay constant calculated was $k = 2.32 \times 10^9 \text{ cm}^3 \text{ mole}^{-1} \text{ sec}^{-1}$. A complete discussion of the results is presented.

INTRODUCTION

Irradiated polyolefins (polyethylene¹⁻⁵ and polypropylene⁶⁻⁸ have been studied widely by electron spin resonance spectroscopy (ESR). In these systems scission generally takes place at the $\text{C}-\text{H}$ bond. The resulting radicals have been well identified.

Polyolefin oxides (polyglycols) which have some structural resemblance with polyolefins have not been given very much attention by ESR yet. It was thought that it would be interesting to follow the character of radicals in polyglycols.

In this study ESR spectra were recorded of polyethylene glycols (PEG), and polypropylene glycols (PPG). Identification of radicals suggested that the rupture takes place at $\text{C}-\text{C}$ and $\text{C}-\text{O}$ bonds. Thermal decay was also studied. Details are given in the following sections.

EXPERIMENTAL

PEG-200,⁹ PPG-425,⁹ and PPG-1000 (Union Carbide) were viscous liquid polymers, while PEG-4000 (Fluka AG) was a crystalline solid polymer. The samples' purity was checked by infrared spectroscopy and gel permeation chromatography. Weighed samples were loaded in Suprasil tubes and then evacuated at 10^{-4} torr for several hours. Irradiation was accom-

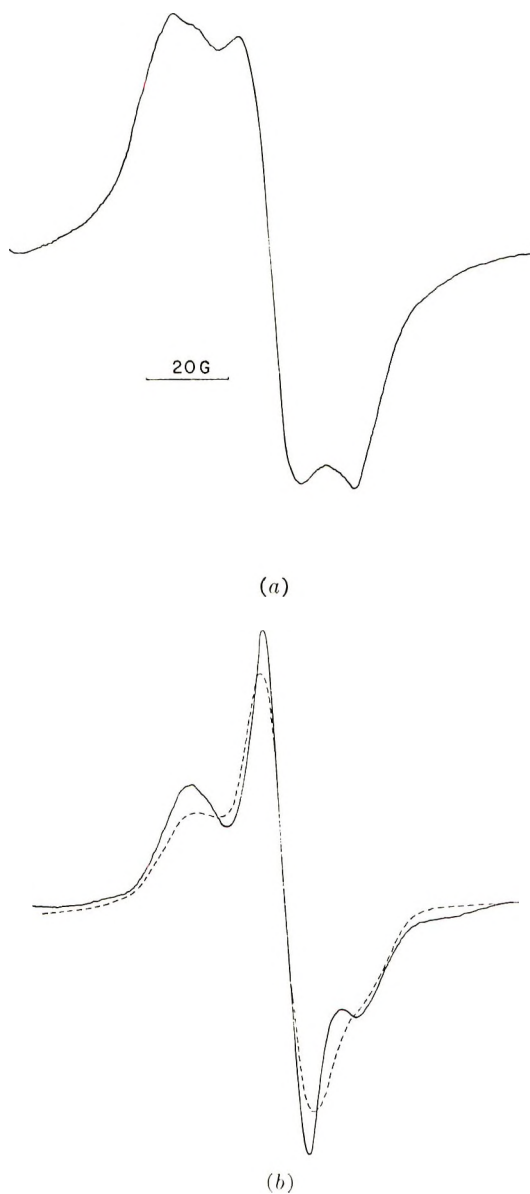


Fig. 1. ESR spectra of PEG: (a) PEG-200 at 123°K.; (b) PEG-200 (—) and PEG-4000 (---) at 173°K.

plished with a typical gamma cell consisting of a ^{60}Co source having an energy output of 1.78×10^{20} e.v. liter $^{-1}$ min. $^{-1}$ (determined by dosimetry with ferrous sulfate). The samples were irradiated for 5 hr. at 77°K.

The free-radicals spectra were obtained with a Varian (Model 4500-10A, X-Band) EPR Spectrometer, which was equipped with a variable-temperature cavity and cooling system. Temperature control was maintained

within $\pm 0.5^\circ\text{C}$. The first-derivative spectra were obtained with an X-Y recorder.

The radicals' concentration was determined by calibration with diphenylpicrylhydrazine in benzene.

RESULTS AND DISCUSSION

Polyethylene Glycols

With an increase of temperature the PEG-200 spectrum changes in an irreversible manner; see Figure 1(a and b). This change might have been

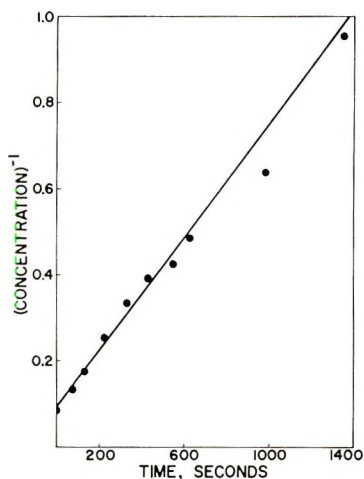


Fig. 2. Thermal decay of radicals in PEG-200 at 203°K .; relative concentration vs time.

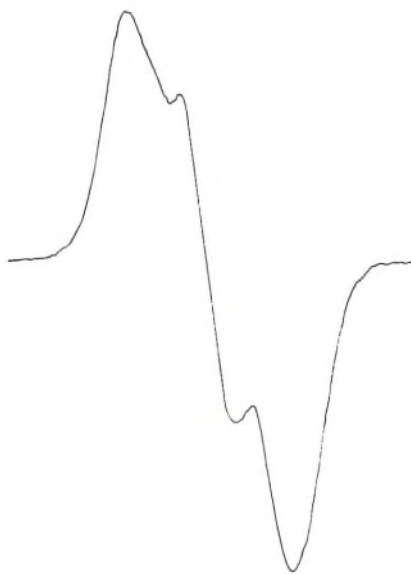


Fig. 3. PEG-200 at 203°K .

caused by the reorganization of the vitreous matter damaged by radiation. It may be noted here that PEG-1000 did not show this behavior. Therefore, the identification of the radicals is based on the spectra given in Figure 1*b*.

With regard to Figure 1*b*, then, one sees that the central line of Peg-4000 is less broad than that of PEG-200. To explain this, one might think of superposition of a singlet and a doublet, but this seems unlikely if one compares the distance between the lines of the so-called doublet and the proton

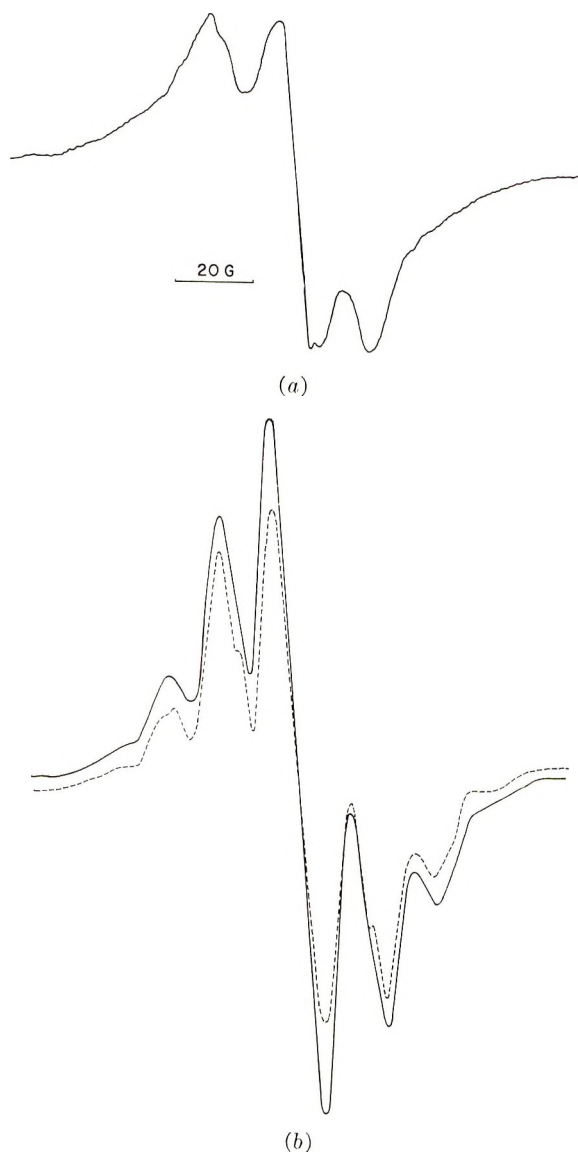


Fig. 4. See caption p. 509.

coupling constant for hydrocarbons of this kind. A triplet with the intensity ratio 1:2.2:1, which is very close to that observed for the interaction of an odd electron with two equivalent protons, suggests that a $-\text{O}-\dot{\text{C}}\text{H}_2$ radical is responsible for these spectra.

In support of such assignment the triplet spectrum of irradiated methanol^{10,11} may be mentioned. The radical identified was $\text{HO}-\dot{\text{C}}\text{H}_2$. The triplet splitting was $18G$,¹¹ as compared to $17.2 \pm 0.2G$ for PEG.

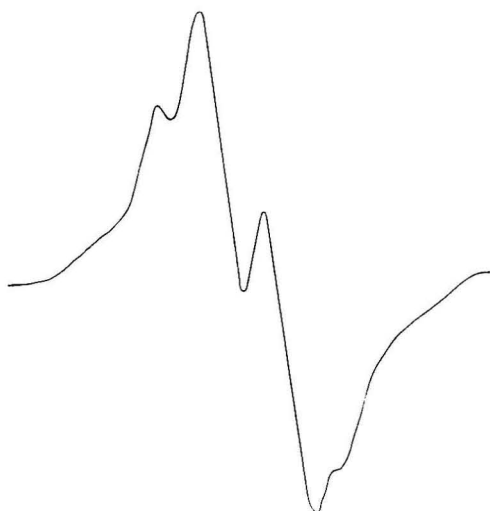
Further support may be derived from the spectrum of polyoxymethylene¹²⁻¹⁵ (POM). In POM the singlet was assigned to $-\text{CH}_2-\text{O}\cdot$, the doublet to $-\text{O}-\dot{\text{C}}\text{H}-\text{O}-$, and the triplet to $-\text{O}-\dot{\text{C}}\text{H}_2$. Triplet splitting was reported to be $19G$ ¹² and 17 to $18G$.¹⁴

If, as suggested above, a $-\text{O}-\dot{\text{C}}\text{H}_2$ radical is produced, then the other radical formed by the same bond rupture should be located close by,⁴ owing to the cage effect. This should give a second-order thermal decay, as such was observed experimentally; see Figure 2.

The greater intensity of the central line of the triplet might have been caused by traces of a singlet due to $-\text{CH}_2-\text{O}\cdot$ radical.

The narrowness of the central line in crystalline PEG-4000 should be due to antiparallel orientation of the nuclear magnetic moments of the two hydrogen atoms. It is well known that the anisotropic broadening is partly quenched in this case. This property is less evident in the vitreous state, where the broadening is larger.

The spectrum shown in Figure 3 is not sufficiently well resolved to explain the changes observed when the temperature was raised to the disappearance point of radicals.



(c)

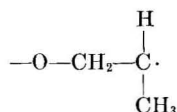
Fig. 4. ESR spectra of PPG: (a) PPG-425 at 123°K .; (b) PPG-1000 at (—) 143°K . and (---) 183°K . (c) PPG-1000 at 213°K .

Polypropylene Glycols

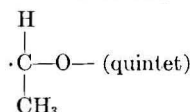
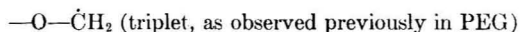
PPG-425 and PPG-1000 give different spectra, as shown in Figure 4. The marked similarity between the spectra reproduced in Figures 1a and 4a may be noted here.

Since it is difficult to obtain information from the PPG-425 spectrum, the following discussion is based on the PPG-1000 spectrum.

PPG-1000 gives a well-resolved seven-line spectrum [Fig. 4(b)] with a 15.5G proton hyperfine constant. The radical



where the interaction between an odd electron with six equivalent protons lead to a seven-line spectrum, satisfies the experimental observation. However, the possibility of other kinds of radicals is not ruled out. From Figure 4b in the broken-line spectrum it is evident that, as the temperature is increased from 143 to 183°K., the lines neighboring the central line have superimposed spectra. It seems likely that additional radicals,



are produced as a result of C—C bond rupture. The above discussion and

the possibility of a singlet ($-\overset{|}{\text{C}}-\text{O}\cdot$) may now be used to explain the greater intensities of the central lines ($-\text{ : 7 : 16 : 2 : 30 : 4 : 15 : 7 : 7 : -$) in the PPG-1000 spectrum.

With the increase of temperature the spectrum of PPG-1000 [Fig. 4b and 4c] changes from an odd to an even number of lines. This indicates that the radicals postulated are secondary radicals, produced when the temperature is raised.

Disappearance and Decay of Radicals

The temperatures of disappearance of radicals were found to be >323°K. (PEG-4000), 203°K. (PEG-200), and 213°K. (PPG-425 and PPG-1000). They are in good agreement with data available on heat-capacity measurements,¹⁶ dilatometry,¹⁷ and glass-transition points.¹⁸

Thermal decay of radicals in PEG and PPG was found to be second-order with a decay constant of $k = 2.32 \times 10^5 \text{ cm.}^3 \text{ mole}^{-1} \text{ sec.}^{-1}$ (Fig. 2). It seems likely that diffusion is not the main process. Further, the radicals formed as a result of bond rupture probably lie close to each other without recombining. As the temperature is increased, the molecular fragments orient themselves and thus start the decay process.

The $G(R)$ values calculated were low, 0.2 to 0.5. The minimal value was that of PEG-4000.

The authors wish to thank the National Research Council of Canada for postdoctoral fellowships. Special thanks are due L. P. Blanchard for his continued support, J. L. Savard for research assistance, and J. Herman for encouragement. Assistance from the Solid State Research Center is also gratefully acknowledged.

References

1. S. Ohnishi, S. Sugimoto, and I. Nitta, *J. Chem. Phys.*, **37**, 1283 (1962).
2. S. Ohnishi, I. Ikeda, M. Kashiwagi, and I. Nitta, *Polymer*, **2**, 119 (1961).
3. D. Libby and M. G. Ormerod, *J. Phys. Chem. Solids*, **18**, 316 (1961).
4. E. J. Lawton, J. S. Balwit, and R. S. Powell, *J. Chem. Phys.*, **33**, 395 (1960).
5. I. Auerbach, *Polymer*, **7**, 283 (1966).
6. B. Smaller and M. S. Matheson, *J. Chem. Phys.*, **28**, 1169 (1958).
7. H. Yoshida and B. Ranby, *Acta Chem. Scand.*, **19**, 72 (1965).
8. H. Fischer and K. H. Hellwege, *J. Polymer Sci.*, **56**, 33 (1962).
9. L. P. Blanchard and M. D. Baijal, *J. Polymer Sci. B*, **4**, 837 (1966).
10. C. Chachaty and E. Hayon, *J. Chim. Phys.*, **61**, 1115 (1964).
11. V. A. Roguniskii, A. G. Kotov, and S. Ya. Pshezhetskii, *Russ. J. Phys. Chem.*, **39**, 248 (1965).
12. H. Yoshida and B. Ranby, *J. Polymer Sci. A*, **3**, 2289 (1965).
13. Yu. D. Tsvetkov, Yu. N. Molin, V. V. Voevodskii, *Vysokomolekul., Soedin.*, **1**, 1805 (1959).
14. R. Marx and C. Chachaty, *J. Chim. Phys.*, **59**, 527 (1961).
15. H. Sasakura, N. Takeuchi, and T. Mizuno, *J. Phys. Soc. (Japan)*, **17**, 572 (1962).
16. R. H. Beaumont, B. Clegg, G. Gee, J. B. M. Herbert, D. J. Marks, R. C. Roberts, and D. Sims, *Polymer*, **7**, 401 (1966).
17. D. J. Marks, Ph.D. Thesis, Manchester Univ., 1961.
18. B. Wunderlich, "Melting of Polymers," Wayne State Univ. Polymer Conf. lecture, 1967.

Received April 25, 1967

Revised July 12, 1967

The Synthesis of Some Optically Active *C*-Methylated 2-Oxohexamethyleneimines

C. G. OVERBERGER* and GORDON M. PARKER, *Department of Chemistry, Institute of Polymer Research, Polytechnic Institute of Brooklyn, Brooklyn, New York 11201*

Synopsis

Three new, optically active, methyl-substituted 2-oxohexamethyleneimines were prepared by cyclization of the respective optically active *C*-methylated 6-aminohexanoic acids. The active forms of the amino acids used for the preparation of (-)-3-methyl-2-oxohexamethyleneimine and (-)-7-methyl-2-oxohexamethyleneimine were obtained by resolution of their diastereomeric quinine salts. *s*-(+)-5-methyl-2-oxohexamethyleneimine was synthesized without racemization from optically pure 2-isopropylidene-5-methylcyclohexanone (pulegone).

INTRODUCTION

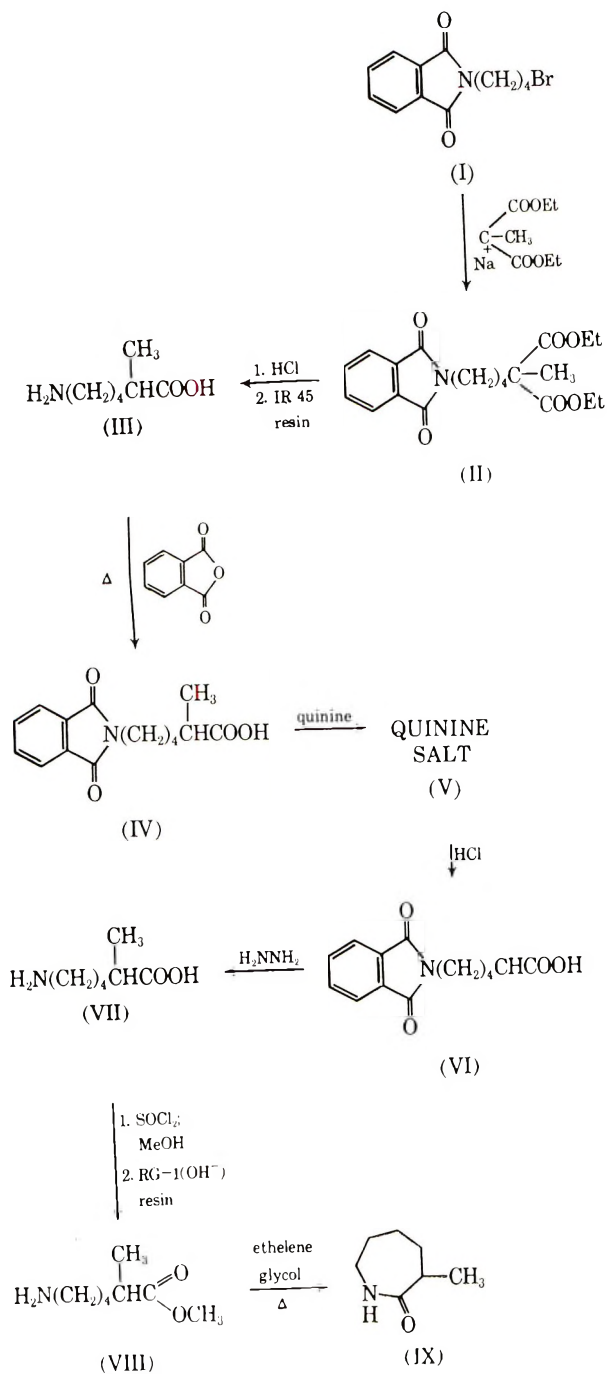
Wallach¹ was the first to report on optically active *C*-methylated 2-oxohexamethyleneimine. He synthesized a mixture of 4-methyl- and 6-methyl-2-oxohexamethyleneimines from naturally occurring, optically active 2-isopropylidene-5-methylcyclohexanone (pulegone) by hydrolytic cleavage of the double bond followed by oxime formation and Beckmann rearrangement. The 4-methyl-2-oxohexamethyleneimine was separated in pure form from mixture by repeated recrystallization, whereas the more soluble 6-methyl-2-oxohexamethyleneimine was obtained in a somewhat pure form from the mother liquor.

Our preparations reported here include the synthesis of the previously unreported, optically active 3-methyl-, 5-methyl-, and 7-methyl-2-oxohexamethyleneimines.

To prepare optically active 3-methyl-2-oxohexamethyleneimine it was necessary first to obtain the racemic 6-amino-2-methylhexanoic acid and to resolve and, then, after cyclization to (-)-3-methyl-2-oxohexamethyleneimine, to remove some racemized product by recrystallization. The synthetic procedure for preparing the resolved 6-amino-2-methylhexanoic acid was developed by Jabloner.²

4-Bromobutylphthalimide (I) was prepared by a standard Gabriel synthesis from 1,4-dibromobutane and potassium phthalimide. This was condensed with diethyl methylmalonate to give ethyl-2-carbethoxy-2-

* Present address: Department of Chemistry, University of Michigan, Ann Arbor, Michigan 48104.



methyl-6-phthalimidohexanoate (II). Cleavage of the phthalimido and ester groups with hydrochloric acid, followed by the removal of HCl from the amino acid hydrochloride with an exchange resin, gave a good yield of the racemic 6-amino-2-methylhexanoic acid (III).

Prior to resolution the amino acid (III) was converted to 6-phthalimido-2-methylhexanoic acid (IV) by being heated in bulk with phthalic anhydride and a diastereomeric salt prepared by dissolving (IV) with quinine in ethyl acetate. Twenty-eight recrystallizations of the quinine salt (V) gave a single diastereomeric isomer, which was hydrolyzed to (+)-6-phthalimido-2-methylhexanoic acid (VI) by treatment with aqueous hydrochloric acid.

Adams and Fle³ have shown for the preparation of 4-amino-2-methylbutyric acid that the phthalimido group may be removed with hydrazine without racemization of the center of asymmetry adjacent to the acid function. This procedure was useful in preparing optically pure (+)-6-amino-2-methylhexanoic acid (VII) from the phthalimido acid (VI). The optical purity of the recovered amino acid may be demonstrated by recrystallizing from a 10:1 ethanol-water solution. The racemic 6-amino-2-methylhexanoic acid is more soluble in this solution than the optically active form (VII), and if any racemization had occurred during the removal of the phthalimido group with hydrazine, it could have been observed in a change of rotation for (+)-6-amino-2-methylhexanoic acid (VII) on recrystallization, and no such change was observed.

Esterification of the amino acid (VII) was carried out under very mild conditions so as to prevent any racemization of the asymmetric center. The amino acid (VII) was reacted with thionyl chloride in methanol at -10° and methyl-6-amino-2-methylhexanoate (VIII), was obtained by treating the amino ester hydrochloride intermediate with a basic ion-exchange resin.

Cyclization of methyl-6-amino-2-methylhexanoate to 2-oxohexamethyleneimine by adding the amino ester slowly to ethylene glycol maintained at 180° has been reported by Saotome.⁴ The temperature used in the similar cyclization of methyl-6-amino-2-methylhexanoate (VIII) to (-)-3-methyl-2-oxohexamethyleneimine (IX) was reduced to 155° , but even at this temperature approximately 13% of the asymmetric centers are racemized in 4 hr. The optically active (-)-3-methyl-2-oxohexamethyleneimine (IX) was more soluble than the racemate in the only suitable recrystallization solvent found, i.e., hexane, and the optically pure (-)-3-methyl-2-oxohexamethyleneimine (IX) could be isolated only by recovery from the mother liquor after recrystallization.

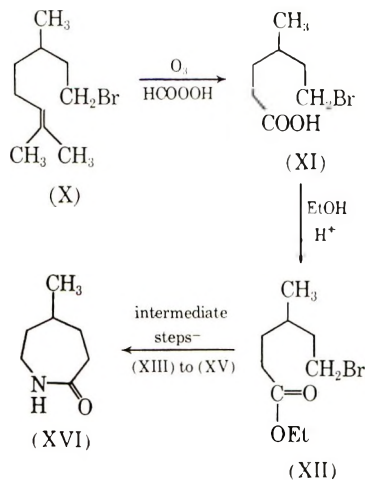
Optically active 5-methyl-2-oxohexamethyleneimine was prepared from optically pure 2-isopropylidene-5-methylcyclohexanone (pulegone). The synthesis of citronellyl bromide (X) was carried out according to the procedure of Lukes et al.⁵ The remainder of the synthesis is outlined below.

Citronellyl bromide (X) was ozonized, and the ozonide was oxidatively decomposed with performic acid to give 4-methyl-6-bromohexanoic acid (XI).

Optically active citronellol, the immediate precursor to citronellyl bromide in Lukes' synthesis, is available commercially; it has been shown by Pino,⁶ however, that it is only 75% optically pure. The synthesis of optically pure citronellol from a known 100% optically pure starting material, e.g., pulegone, was therefore necessary.

This is an unstable acid which, on standing at room temperature, would slowly lose hydrogen bromide and form either the lactone or low molecular weight polyester. The acid (XI) was converted to *n*-(-)-ethyl-4-methyl-6-bromohexanoate (XII) for increased stability by a standard Fisher esterification. This ester, after reaction with potassium phthalimide in dimethylformamide, gave a 48% yield of *s*-(-)-ethyl-6-phthalimido-4-methylhexanoate (XIII). Complete hydrolysis of (XIII) with concentrated HCl, followed by the removal of HCl from the amino acid hydrochloride intermediate with an exchange resin, resulted in a good yield of *n*-(-)-6-amino-4-methylhexanoic acid (XIV).

Methyl-6-amino-4-methylhexanoate (XV) was prepared from (XIV) in the same manner that methyl-6-amino-2-methylhexanoate (VIII) was prepared from 6-amino-2-methylhexanoic acid (VII). Cyclization of the amino ester (XV) was accomplished by slowly adding the ester to hot ethylene glycol. The product, *s*-(+)-5-methyl-2-oxohexamethyleneimine (XVI), was very hygroscopic and very soluble in all common solvents. Purification was effected by preparative vapor-phase chromatography.

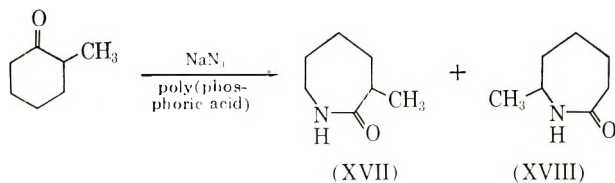


An alternate route to the optically active 6-amino-4-methylhexanoic acid (XIV) was also available. 4-Methylcyclohexanone may be converted to the oxime, followed by a Beckmann rearrangement to the single product, racemic 5-methyl-2-oxohexamethyleneimine. This cyclic amide may be hydrolyzed to 6-amino-4-methylhexanoic acid, and 6-phthalimido-4-methylhexanoic acid is prepared by heating the amino acid in bulk with phthalic anhydride. With the exception of the position of the methyl

group this is the same molecule that after reaction with quinine served as the means of preparing the active (+)-6-amino-2-methylhexanoic acid (VII).

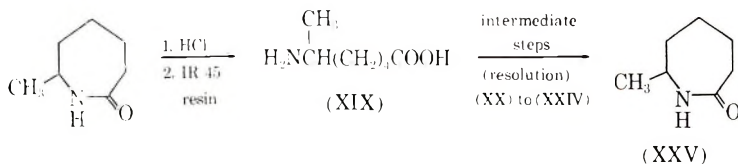
Three diastereomeric salts were prepared from 6-phthalimido-4-methylhexanoic acid using quinine, ephedrine, and dexadrine. Each of these is probably suitable for the resolution, but the small rotation of the active ethyl ester of 6-phthalimido-4-methylhexanoic acid, $[\alpha]_D^{25} = -3.37^\circ$ and the even smaller rotation of a single isomer of 6-amino-4-methylhexanoic acid, 0.9° , makes it difficult to demonstrate the completeness of such a resolution.

Optically active 7-methyl-2-oxohexamethyleneimine was prepared from (+)-6-amino-6-methylhexanoic acid. The initial step in this synthesis was the preparation of racemic 7-methyl-2-oxohexamethyleneimine (XVIII) from 2-methylcyclohexanone by reaction with sodium azide in poly(phosphoric acid) as shown:



Conley⁷ had reported that this reaction gave only one product (XVIII), but a second isomer was also isolated. The single isomer (XVIII) was obtained only after the distillation product was recrystallized from hexane.

Schaffler and Ziegenbein⁸ proved that the Beckmann rearrangement of 2-methylcyclohexanone oxime gave both (XVII) and (XVIII) by taking advantage of the slower rate of the saponification of (XVII). This technique proved to be useful here too. Part of the mixture of products was refluxed with aqueous base for 2 hr., and a small yield of pure 3-methyl-2-oxohexamethyleneimine (XVII) was isolated by ether extraction. The substance (XVII) showed no melting-point depression when mixed with a sample of 3-methyl-2-oxohexamethyleneimine, prepared by the usual cyclization procedure from racemic 6-amino-2-methylhexanoic acid (III). The synthesis was quite similar to the synthesis of (-)-3-methyl-2-oxohexamethyleneimine (IX).



Racemic 7-methyl-2-oxohexamethyleneimine (XVIII) was first hydrolyzed with concentrated hydrochloric acid, and the amino acid hydrochloride was converted to racemic 6-amino-6-methylhexanoic acid (XIX) with an ion-exchange resin. 6-Phthalimido-6-methylhexanoic acid (XX) was prepared by heating (XIX) in bulk with phthalic anhydride. A crystalline

diastereomeric salt (XXI) readily formed when (XX) was mixed with quinine in ethyl acetate. Thirty recrystallizations of the quinine salt (XXI) gave a single diastereomeric isomer, which was hydrolyzed to (–)-6-phthalimido-6-methylhexanoic acid (XXII) by treatment with aqueous hydrochloric acid. The phthalimido group was removed through the reaction of (XXII) with hydrazine hydrate in refluxing ethanol, giving (+)-6-amino-6-methylhexanoic acid (XXIII). Cyclization to the desired (–)-7-methyl-2-oxohexamethyleneimine (XXV) was carried out in the same manner as has been described for the preparation of (–)-3-methyl-2-oxohexamethyleneimine (IX). The amino ester hydrochloride and the amino ester (XXIV) were not characterized, but the hygroscopic cyclization product (XXV) was purified by preparative vapor-phase chromatography for characterization.

EXPERIMENTAL

All melting points are corrected. The analyses (with two exceptions, noted below) were made by Alfred Bernhardt, Mikroanalytisches Laboratorium, Mulheim, West Germany.

Ethyl 2-Carboxy-2-methyl-6-phthalimidohexanoate (II)

This material was prepared according to the procedure of Manasse and Gabriel⁹ under the conditions employed for a malonic ester synthesis on a related compound.

From 295.7 g. (1.70 moles) of diethylmethyl malonate and 455 g. (1.61 moles) of 4-bromobutylphthalimide (I) was obtained 374.2 g. (62.5%) of ethyl 2-carboxy-2-methyl-6-phthalimidohexanoate; b.p., 212 to 216° (0.65 mm.); m.p., 46 to 47.5°.

ANAL. Calcd. for C₂₀H₂₅NO₆: C 63.97%, H 6.37%. Found: C 63.75%, H 6.42% (obtained by Jabloner, who first prepared this material⁹).

Racemic 6-Amino-2-methylhexanoic Acid (III)

Ethyl 2-carboxy-2-methyl-6-phthalimidohexanoate (II), 370 g. (0.99 mole), was suspended in 2100 ml. of concentrated hydrochloric acid, and the hydrochloric acid was refluxed for 48 hr. At this point the oily phase was completely gone, and a large quantity of white crystals of phthalic acid had settled out of solution. The solution was cooled, and the phthalic acid was removed by filtration. The volume of the liquid was reduced to 600 ml., and the solution was stored at 0° for several days. This procedure yielded an additional crop of phthalic acid, which also was removed by filtration. The remaining water was removed under vacuum, yielding a yellow oil, which crystallized after several days under vacuum. The crude yield of this hydrochloride was 99.5%, which was not characterized but was converted to the amino acid by the procedure of Meyers and Miller¹⁰ for the preparation of 6-amino-hexanoic acid, except that Amberlite IR-45 resin was used instead of IR-4b.

The amino acid hydrochloride, 176 g. (0.97 mole), was dissolved in 2 liters of water and passed through a resin-filled column 24 in. in length and 2 in. in diameter. The amino acid was eluted with an additional 3 liters of water. The volume of the solution was reduced to 300 ml., and 900 ml. of absolute ethanol and 1,500 ml. of ether were added to give a white crystalline product; total yield, 128.5 g. (91.3%); m.p., 225 to 227° (lit.⁸ m.p., 228 to 230°, prepared from 3-methyl-2-oxohexamethyleneimine by acid hydrolysis).

Racemic 6-Phthalimido-2-methylhexanoic Acid (IV)

6-Amino-2-methylhexanoic acid (III), 120 g. (0.83 mole), was mixed with 127 g. (0.86 mole) of phthalic anhydride, heated slowly in an open vessel to 220°, and then slowly allowed to cool. Vacuum distillation of the products yielded 196.3 g. (90%) of the desired racemic 6-phthalimido-2-methylhexanoic acid; b.p., 209 to 211° (0.35 mm.); m.p., 89 to 91°.

ANAL. Calcd. for C₁₅H₁₇NO₄: C 65.43%, H 6.24%, N 5.09%. Found: C 65.56%, H 6.24%, N 5.11% (obtained by Jabloner, who first prepared this material²).

(+)-6 Phthalimido-2-methylhexanoic Acid (VI)

Racemic 6-phthalimido-2-methylhexanoic acid (IV), 200 g. (0.73 mole), was dissolved in 6 liters of boiling ethyl acetate, and to this solution was added 236 g. (0.73 mole) of quinine. After the dissolving was complete, the solution was cooled and allowed to stand in a refrigerator for 2 days. The crystalline precipitate weighed 384 g. (88%); m.p., 141 to 145°. Twenty-eight recrystallizations from ethyl acetate gave 65.1 g. (33.8%) of the resolved diastereoisomer (V); m.p., 152 to 153°.

The quinine salt (V), 65.1 g. (0.108 mole), was dissolved in 870 ml. of boiling benzene and shaken with 775 ml. of 12% aqueous hydrochloric acid in a separatory funnel. The aqueous layer was separated and twice extracted with 150 ml. portions of benzene. The combined benzene extracts were evaporated to dryness, and the residue was dissolved in 210 ml. of hot benzene and filtered. Addition of a large excess of hexane (b.p., 66 to 69°) to the filtered solution yielded a white, flocculant precipitate, (+)-6-phthalimido-2-methylhexanoic acid. The yield after filtration was 28.96 g. (96.5%); m.p., 83 to 84°; $[\alpha]_D^{25} = 9.77^\circ$ (c 4.50, chloroform) [51%; m.p., 89 to 90°; $[\alpha]_D^{25} = +5.1^\circ$ (c 3.21, benzene)].²

The infrared spectrum of the resolved product (VI) is approximately equivalent to that of the racemic 6-phthalimido-2-methylhexanoic acid (2).

(+) 6-Amino-2-methylhexanoic Acid (VII)

The procedure used was similar to that of Adams and Fle³ for the preparation of 4-amino-2-methylbutyric acid.

(+)-6-Phthalimido-2-methylhexanoic acid (VI), 28.9 g. (0.105 mole), was dissolved in 270 ml. of warm ethanol, and 6.91 g. (0.138 mole) of hydrazine hydrate in 30 ml. of ethanol was added. Reaction was imme-

diate, and a white precipitate formed. The mixture was refluxed for 1 hr., and then the ethanol was removed under vacuum. The white residue was taken up in 500 ml. of water, and the pH of this solution was adjusted to 5.0 with glacial acetic acid. On standing overnight a large crop of phthaloyl hydrazide precipitated and was removed by filtration. The filtrate was evaporated under vacuum, and the white crystalline residue was dissolved in a boiling mixture of 500 ml. of ethanol and 20 ml. of water. This solution, on standing in a refrigerator, yielded 6.42 g. of the amino acid. The physical constants were identical for the two crops; m.p., 205 to 206°; $[\alpha]_D^{25} = +13.78^\circ$ (c 6.67, water). The combined yield was 83.4%.

ANAL. Calcd. for $C_7H_{15}O_2N$: C 57.90%, H 10.41%, N 9.65%. Found: C 57.83%, 57.86%; H 10.22%, 10.33%; N 9.67%, 9.71%.

(-)-3-Methyl-2-oxohexamethyleneimine (IX)

Thionyl chloride, 8.4 ml. (0.116 mole), was added dropwise to 65 ml. of methanol maintained at -10° . This was followed by the addition of 11.5 g. (0.079 mole) of (+)-6-amino-2-methylhexanoic acid (VII). Stirring was continued at -10° for 30 min., and the solution was warmed to 20° and maintained at this temperature for an additional 30 min. The addition of a large excess of anhydrous ether gave a fine white precipitate of (+)-methyl-6-amino-2-methylhexanoate hydrochloride, 12.51 g. (87.5%). This hydrochloride was not characterized but was dissolved in 50 ml. of methanol, and Rexyn RG-1 (OH⁻) resin, which had been thoroughly washed in methanol, was added until the solution was negative for chloride ion with a 1% solution of silver nitrate in methanol. The resin was filtered off, and the methanol was removed under vacuum, leaving a colorless oil of methyl 6-amino-2-methylhexanoate (VIII). This oil was diluted to 25 ml. with ether and divided into two approximately equal fractions. Fraction no. 1 was added dropwise over a period of 3 hr. to 20 ml. of ethylene glycol maintained at 160°C . The reaction mixture was then heated for an additional 1 hr. at 165° . Fraction no. 2 was treated in the same manner with an initial reaction temperature of 150 to 155° and a final hour of heating at 155° . The resultant brown solutions were each extracted for 24 hr. with benzene in a liquid-liquid extractor, the benzene was removed under vacuum, and in each case the solid residues were vacuum-distilled through a 3 in. column packed with nichrome turnings (Podbielniak Helipak); b.p., 104 to 105° (1.9 mm.). The combined yield was 5.27 g. (52%). Both fractions had a wide melting range; m.p., 82 to 95° ; $[\alpha]_D^{25} = -18.27^\circ$ (fraction no. 1, c 4.4, chloroform); -19.90° (fraction no. 2, c 4.4 chloroform).

After repeated recrystallizations from *n*-hexane, 1.02 g. (19.3%) of (-)-3-methyl-2-oxohexamethyleneimine was obtained; m.p., 86 to 90° ; $[\text{X}]_D^{25} = 26.77$ (c 4.5, chloroform). The infrared spectrum of this material differs slightly from its racemic counterpart by having additional absorptions at 1640, 1070, 760, and 745 cm.^{-1} and by lacking the absorption at 800 cm.^{-1} present in the spectrum of racemic 3-methyl-2-oxohexamethyl-

eneimine. The structure was confirmed by racemization to the known racemic 3-methyl-2-oxohexamethyleneimine of m.p. 94 to 96°.

Racemization of (-)-3-Methyl-2-oxohexamethyleneimine (IX)

Partially resolved (-)-3-methyl-2-oxohexamethyleneimine (IX), 0.5 g. (0.00392 moles) $[\alpha]_{\text{D}}^{25} = -22.80^{\circ}$ (c 5.0, chloroform), was mixed in a polymerization tube with 4.8 mg. (0.000189 mole) of a 54.1% dispersion of sodium hydride in mineral oil under a nitrogen atmosphere. The tube was partially evacuated and heated to 120°, so that the reaction forming the salt of the (-)-3-methyl-2-oxohexamethyleneimine would take place. Hydrogen was evolved rapidly, and the reaction was complete in 2 min. The tube was flushed with nitrogen, sealed with a serum cap, and heated to 145° for 30 min. After cooling, the solid product was broken up in a small sublimator and sublimed at 65° and 3×10^{-4} mm. to give 0.45 g. (90%) of racemic 3-methyl-2-oxohexamethyleneimine; $[\alpha]_{\text{D}}^{25} = -0.08^{\circ}$ (c 4.5, chloroform); m.p., 95 to 96°. This material showed no melting-point depression when mixed with an authentic sample of racemic 3-methyl-2-oxohexamethyleneimine.

R-(-)-Citronellyl bromide (X)

This was the procedure of Lukes.⁵ Since our physical constants differ slightly from those reported, a typical experiment is outlined.

From citronellol, 85 g. (0.54 mole), and phosphorus tribromide, 85 g. (0.31 mole), in the presence of pyridine, was obtained on distillation 65.6 g. (56.5%) of citronellyl bromide (X); b.p., 75 to 76° (2.1 mm.); $[\alpha]_{\text{D}}^{25} = -6.83^{\circ}$ (neat); $n_{\text{D}}^{20} = 1.4739$ (lit.:⁵ 43%; b.p., 111° (12 mm.); $[\alpha]_{\text{D}}^{25} = -6.93^{\circ}$ (neat); $n_{\text{D}}^{20} = 1.4756$).

Vapor-phase chromatography of citronellyl bromide (X) on a polyglycol column shows it to be at least 99.7% pure.

ANAL. Calcd. for $\text{C}_{10}\text{H}_{19}\text{Br}$: C 54.80%, H 8.74%, Br 36.46%. Found: C 54.72%, H 8.76%, Br 36.77%.

R-(-)-Ethyl 4-Methyl-6-bromohexanoate (XII)

R-(-)-Citronellyl bromide (X), 55.9 g. (0.26 mole), was dissolved in 820 ml. of methanol, and the solution was cooled and maintained at -68°. A stream of oxygen containing approximately 6% ozone by weight was bubbled into the solution at a rate of 0.06 ft.³/min. for 3.5 hr. The methanol was immediately removed, while cold, at a pressure of 0.5 mm. The remaining clear viscous oil was dissolved in 270 ml. of 88% formic acid, and 116 ml. of 30% hydrogen peroxide was added dropwise at room temperature. The solution was warmed slowly to 55° while being vigorously stirred and then increased spontaneously in temperature to 93°, when the solution refluxed. The spontaneous reaction was over in 10 min. and the temperature was maintained above 90° for an additional 15 min. with applied heat. The crude product was recovered by removing the water and

formic acid at 40° (0.5 mm.). An infrared spectrum of the product showed the characteristic absorption of saturated aliphatic acids at 1700 to 1725 cm.^{-1} . This acid (XI) was not characterized further but was dissolved in 600 ml. of absolute ethanol. To this solution were added 10 drops of concentrated sulfuric acid, and the solution was refluxed for 48 hr. After cooling, the ethanol solution was washed with 30 ml. of a saturated aqueous solution of sodium bicarbonate, and the ethanol was removed under vacuum. The crude ester was dissolved in ether, washed with water, and dried over anhydrous sodium sulfate, and the ether was removed under vacuum. Distillation of the product through a 10 in. column packed with glass helices yielded 37 g. (62%) of R-(−)-ethyl 4-methyl-6-bromohexanoate (XII); b.p., 76° (0.70 mm.).

Analysis on an analytical vapor-phase chromatograph with a succinate polyester column at 174° showed several impurities boiling close to the ester. A small sample of the ester was separated on a preparatory vapor-phase chromatography column (succinate polyester) for characterization: $[\alpha]_D^{25} = -3.58^\circ$ (c 4.5, chloroform), $n_D^{25} = 1.4590$.

ANAL. Calcd. for $\text{C}_{10}\text{H}_{17}\text{O}_2\text{Br}$: C 45.58%, H 7.23%, Br 33.70%. Found: C 45.83%, H 7.24%, Br 33.51%.

R-(−)-6-Amino-4-methylhexanoic Acid (XIV)

The use of dimethylformamide as a solvent for this Gabriel synthesis was similar to several syntheses carried out by Sheehan.¹¹

R-(−)-Ethyl 4-methyl-6-bromohexanoate (XII), 24.22 g. (0.102 mole), was dissolved in 90 ml. of dimethylformamide, and 18.90 g. (0.102 mole) of potassium phthalimide was added. The rapidly stirred mixture was heated at 100° for 24 hr., cooled, and diluted with 130 ml. of chloroform. The resulting solution was poured into 400 ml. of water. The chloroform phase was separated and combined with two 60 ml. chloroform extractions of the aqueous phase. The chloroform solution was washed with 70 ml. of 0.2*N* aqueous solution hydroxide and 50 ml. of water and dried over anhydrous sodium sulfate. The solution was filtered, the chloroform removed under vacuum, and the crude product vacuum distilled. The yield was 14.55 g. (47.7%) of s-(−)-ethyl 6-phthalimido-4-methyl hexanoate, (XIII); b.p., 176 to 177° (23 mm.). This material was hydrolyzed without further purification. Compound (XIII), 14.37 g. (0.0484 mole), was refluxed with 105 ml. of concentrated hydrochloric acid for 48 hr. The volume of the solution was reduced to 20 ml. by removing the condenser and allowing most of the water and hydrochloric acid to escape. After cooling, the precipitated phthalic acid was removed by filtration, and the filtrate was reduced to dryness under vacuum. The crude yield of the solid amino acid hydrochloride was 95%. This was not characterized but was dissolved in 100 ml. of water and passed through an ion-exchange column containing Amberlite IR-45 resin. The column was flushed with 200 ml. of water. The water solution of amino acid was reduced in volume to 15 ml. under vacuum, and the amino acid was

precipitated by adding 40 ml. of absolute ethanol and 100 ml. of ether. The yield of *r*-(-)-6-amino-4-methylhexanoic acid (XIV) was 4.68 g. (68%); m.p., 178 to 179°; $[\alpha]_D^{25} = -0.92^\circ$ (c 6.7, water).

ANAL. Calcd. for $C_7H_{13}O_2N$: C 57.90%, H 10.41%, N 9.65%. Found: C 57.92%, H 10.60%, N 9.58%.

s = (+)-5-Methyl-2-oxohexamethyleneimine (XVI)

Thionyl chloride, 3.75 ml. (0.052 mole), was added dropwise to 30 ml. of methanol, which was maintained at -10° . This was followed by 5.0 g. (0.034 mole) of *r*-(-) 6-amino-4-methylhexanoic acid (XIV). Stirring was continued at -10° for 30 min. and at room temperature for 30 min. more. Addition of a large excess of ether yielded a precipitate of 6.37 g. (94%) of the amino ester hydrochloride. This crude material showed both acid and ester carbonyl peaks in the infrared spectrum and had a melting point range of 75 to 82°. Without further purification 6.0 g. of this salt was treated with RG-1 (OH⁻) resin in the same manner as reported for the preparation of (-)-3-methyl-2-oxohexamethyleneimine (IX). The crude methyl 6-amino-4-methylhexanoate (XV) was not characterized but was dissolved in 8 ml. of ether and added over a period of 3 hr. to 20 ml. of ethylene glycol maintained at 165°. The solution was maintained at 165° for an additional hour and was then cooled and extracted with benzene in a liquid-liquid extractor for 20 hr. The benzene was removed under vacuum, and the product was vacuum-distilled, yielding 1.8 g. (50%) of *s*-(+)-5-methyl-2-oxohexamethyleneimine (XVI); b.p., 104 to 105° (1.2 mm.). Further purification by recrystallization was not possible, so the monomer was dissolved in a minimum of acetone and passed through a silicone oil column at 190° on a preparative vapor-phase chromatograph.

Purification was completed by subliming the monomer at 40° and 10^{-5} mm. This material was very hygroscopic; m.p., 44 to 46°; $[\alpha]_D^{25} = +29.44^\circ$ (c 2.4, chloroform).

ANAL. Calcd. for $C_7H_{13}ON$: C 66.10%, H 10.30%, N 11.02%. Found: C 66.09%, H 10.37%, N 10.88%.

Racemic 7-Methyl-2-oxohexamethyleneimine (XVIII)

This compound was prepared according to the procedure of Conley.⁷

From 71 g. (0.63 mole) of 2-methylcyclohexanone and 43 g. (0.66 mole) of sodium azide in 500 ml. of poly(phosphoric acid) was isolated after vacuum distillation 51.3 g. (64%) of a mixture of racemic 3-methyl- (XVII) and 7-methyl-2-oxohexamethyleneimines (XVIII); m.p., 60 to 85°. Five recrystallizations from hexane (b.p., 66 to 69°) gave 27.7 g. (54%) of racemic 7-methyl-2-oxohexamethyleneimine (XVIII); m.p., 90 to 92° (lit.⁸ m.p., 91 to 92°).

Racemic 3-Methyl-2-oxohexamethyleneimine (XVII)

A mixture of racemic 3- and 7-methyl-2-oxohexamethyleneimines of unknown composition, 37.5 g. (0.29 mole), was dissolved in 90 ml. of a 12% aqueous solution of sodium hydroxide. This basic solution was refluxed for 2 hr. and was then extracted with ether. Removal of the ether yielded 1.5 g. of crude crystalline material. After three recrystallizations from *n*-hexane 0.5 g. of 3-methyl-2-oxohexamethyleneimine was obtained as flat rectangular needles; m.p., 94 to 96°. A mixed melting-point determination with a sample of this lactam prepared by cyclization, m.p., 94 to 96°, showed no melting-point depression.

Racemic 6-Amino-6-methylhexanoic Acid (XIX)

This compound was previously prepared by Schaffler and Ziegenbein⁸ from racemic 7-methyl-2-oxohexamethyleneimine (XVIII) using sulfuric acid to open the ring. Hydrochloric acid was used here for the same purpose and was less difficult to remove completely in order to obtain the free amino acid.

Racemic 7-methyl-2-oxohexamethyleneimine (XVIII), 81 g. (0.64 mole), was dissolved in 900 ml. of concentrated hydrochloric acid and the solution refluxed for 3 hr. The water and excess hydrochloric acid were then removed under vacuum, giving a quantitative yield of the solid 6-amino-6-methylhexanoic acid hydrochloride. This material was not characterized but was dissolved in 2 liters of water and passed through a column 24 in. in length and 2 in. in diameter and filled with Amberlite IR-45 resin. The amino acid was eluted with an additional 2 liters of water. The volume of the solution was reduced to 370 ml., and 1100 ml. of absolute ethanol and 1,900 ml. of ether were added to precipitate 74 g. (80%) of a white crystalline solid, racemic 6-amino-6-methylhexanoic acid; m.p., 210 to 211° (lit.:⁸ m.p., 210 to 211°).

ANAL. Calcd. for $C_7H_{15}O_2N$: C 57.90%, H 10.41%, N 9.65%. Found: C 58.03%, H 10.19%, N 9.97%.

Racemic 6-Phthalimido-6-methylhexanoic Acid (XX)

Racemic 6-amino-6-methylhexanoic acid (XIX), 63.8 g. (0.44 mole), was mixed with 64 g. (0.43 mole) of phthalic anhydride and heated slowly to 195°. The temperature was maintained at 195° for 20 min., and the reaction mixture was then slowly allowed to cool. Vacuum distillation of the products yielded 107 g. (88.5%) of the desired 6-phthalimido-6-methylhexanoic acid; b.p., 210° (0.25 mm.); m.p., 87 to 88°. This material had principal absorptions in the infrared at 1730, 1710, 1615, and 718 cm^{-1} .

ANAL. Calcd. for $C_{17}H_{17}NO_4$: C 65.43%, H 6.24%, N 5.09%. Found: C 65.85%, H 5.99%, N 5.40%.

(-)-6-Phthalimido-6-methylhexanoic Acid (XXII)

Racemic 6-phthalimido-6-methylhexanoic acid (XX), 103 g. (0.374 mole), were dissolved in 5 liters of ethyl acetate, and to this solution was added 121.6 g. (0.374 mole) of quinine. Before the quinine salt would crystallize from solution, it was necessary to reduce the volume of the solution to 2 liters and cool it to 0°. The yield was 141.3 g. (63%); m.p., 111 to 114°. Thirty recrystallizations from ethyl acetate gave 28.3 g. (25.2%) of the resolved diastereoisomer; m.p., 117 to 119°.

This quinine salt, 28.0 g. (0.047 mole), was dissolved in 350 ml. of hot benzene and shaken with 300 ml. of 12% aqueous hydrochloric acid in a separatory funnel. The aqueous layer was separated and twice extracted with 100 ml. portions of benzene. The combined benzene extracts were evaporated to dryness, and the residue was dissolved in 100 ml. of hot benzene and filtered. Addition of a large excess of hexane (b.p., 66 to 69°) to the filtered solution yielded a white, flocculant precipitate of (-)-6-phthalimido-6-methylhexanoic acid. The yield was 11.85 g. (93%); m.p., 78 to 80°; $[\alpha]_D^{25} = -18.91^\circ$ (c 4.50, chloroform). The infrared spectrum of this isomer was essentially the same as its racemic counterpart.

(+)-6-Amino-6-methylhexanoic Acid (XXIII)

The procedure used was that of Adams and Fle³ for the preparation of 4-amino-2-methylbutyric acid, and was the same as reported in our preparation of (+)-6-amino-2-methylhexanoic acid (VII).

From 11.85 g. (0.043 mole) of (-)-6-phthalimido-6-methylhexanoic acid (XXII) and 2.85 g. (0.057 mole) of hydrazine hydrate was obtained 4.74 g. (76%) of a white crystalline precipitate of (+)-6-amino-6-methylhexanoic acid; m.p., 206 to 207.5°; $[\alpha]_D^{25} = +2.03^\circ$ (c 5.1, water). The infrared spectrum of this material differed from that of racemic 6-amino-6-methylhexanoic acid in the region from 1500 to 840 cm.⁻¹.

(-)-7-Methyl-2-oxohexamethyleneimine (XXV)

(-)-7-Methyl-2-oxohexamethyleneimine (XXV) was prepared from (+)-6-amino-6-methylhexanoic acid (XXIII) in the same manner that (-)-3-methyl-2-oxohexamethyleneimine (IX) was prepared from (+)-6-amino-2-methylhexanoic acid (VII).

From 4.25 g. (0.029 mole) of (XXIII) and 3.1 ml. (0.043 mole) of thionyl chloride was obtained an almost quantitative yield of the crude methyl 6-amino-6-methylhexanoate (XXIV), which after cyclization yielded 1.5 g. (41%) of (-)-7-methyl-2-oxohexamethyleneimine (XXV); b.p., 102 to 103° (2.0 mm.). Further purification of this lactam by recrystallization was not possible, so a sample of the monomer was dissolved in a minimum of acetone and passed through a silicone column at 190° on a preparative vapor-phase chromatograph. Purification was completed by subliming the monomer at 25° and 10⁻⁵ mm. This material was very hygroscopic; m.p., 51 to 53°; $[\alpha]_D^{25} = 15.92^\circ$.

ANAL. Calcd. for $C_7H_{13}ON$: C 66.10%, H 10.30%, N 11.02%. Found: C 66.04%, 66.26%; H 10.15%, 10.32%, N 10.90%, 10.86%.

References

1. O. Wallach, *Ann.*, **289**, 337 (1896); *idem*, *Ann.*, **346**, 253 (1906); *idem*, *Ann.*, **309**, 2 (1899).
2. H. Jabloner, dissertation for the degree of Doctor of Philosophy (Chemistry), Polytechnic Institute of Brooklyn, June 1963.
3. R. Adams and D. Fle, *J. Am. Chem. Soc.*, **81**, 4946 (1959).
4. K. Saotome, *J. Chem. Soc. Japan, Ind. Chem. Sec.*, **65**, 1059 (1962).
5. R. Lukes, A. Zabacova, and J. Plesek, *Croat. Chem. Acta*, **29**, 201 (1957).
6. P. Pino, F. Ciardelli, G. P. Lorenzi, and G. Montagnoli, *Makromol. Chem.*, **61**, 207 (1963).
7. R. T. Conley, *J. Org. Chem.*, **23**, 1330 (1958).
8. A. Schaffler and W. Ziegenbein, *Ber.*, **88**, 1374 (1955).
9. S. Gabriel and T. A. Manasse, *Ber.*, **32**, 1266 (1899).
10. C. Y. Meyers and L. E. Miller, *Organic Synthesis*, Vol. 32, Wiley, New York, 1944, p. 272.
11. J. C. Sheehan and W. A. Bolhofer *J. Am. Chem. Soc.*, **72**, 2786 (1950).

Received July 26, 1967

Effect of the Initiator Solvation on the Change in Polymerization Rates of Dioxolane and Tetrahydrofuran

M. KUČERA and K. MAJEROVÁ,

Research Institute of Macromolecular Chemistry, Brno, Czechoslovakia

Synopsis

The cocatalytical effects of water and ethanol on the cationic polymerization of dioxolane and tetrahydrofuran were studied. The ion pair $\sim\text{Si}^+\text{HSO}_4^-$ or $\sim\text{Si}^+\text{ClO}_4^-$ were used for initiating the polymerization. The dependence of the polymerization rate on the concentration of cocatalyst was examined with various temperatures, concentrations of monomer, solvents (heptane, tetrachloroethane, tetrachloroethane-heptane mixtures, and 1,4-dioxane), and concentrations of initiator. The abscissa of the maximum of the reaction rate in the dependence mentioned above was the criterion for evaluation of the effect of the reaction variables. The changes observed are small; nevertheless, they prove the share of all components of the polymerizing system in establishing solvation equilibria, which determine the number and the reactivity of active centers and, in fact, the reaction rate.

INTRODUCTION

In previous work¹⁻⁷ the polymerizations of trioxane (TOX), dioxolane (DOX), and tetrahydrofuran (THF) were shown to be conditioned by the initiator solvation. The solvating compound, i.e., the compound activating the initiator, can be a special substance present in the polymerizing medium or be a solvent and a monomer, or be a combination of these.⁷ The polymerization rate is a function of the state of the solvation equilibria formed in the given case.

The changes in the kinetics of the polymerization that are due to the initiator solvation entitle us to speak about a solvating agent as about a cocatalyst. Except for the case in which monomer or solvent is a "cocatalyst," the course of the polymerization depends very much on the character of a compound that activates the initiator. If a cocatalyst acts as a transfer agent at the same time, its concentration changes during polymerization. The whole process becomes nonstationary and, further, the molecular weight distribution of the product broadens.

In this communication we wish to point out the possibility of shifting the maximum in the cocatalyst concentration-reaction rate curve or of influencing quantitatively the dependence by a choice of polymerization conditions, or both.

EXPERIMENTAL

Most of the data about apparatus, materials, and procedures have been described in our previous papers.⁵⁻⁷ The preparation of the initiators $\sim\text{Si}^{\oplus}\text{HSO}_4^{\ominus}$ and $\sim\text{Si}^{\oplus}\text{ClO}_4^{\ominus}$ and the water-determination method⁸ also have been mentioned.⁵⁻⁷ Stirring of the content of dilatometers was found not to affect the shape of the curves; therefore most of the measurements were carried out on unstirred systems.

The way in which the results were evaluated is as follows. In some cases the relation between contraction and conversion was available. If so, the reaction rate was calculated from the maximum slope of the conversion-time curves. We did not measure the relations between conversion and contraction at all temperatures; in such cases the rate was read from the contraction curves. Therefore, the courses of the dependences presented cannot be directly compared with each other, but the abscissa of a maximum is not affected by that simplification, and it provides a direct comparison.

The measurements give a rather qualitative picture of the behavior of individual components and the effects of the factors studied. We suppose that the results cannot be used for quantitative calculation because of a

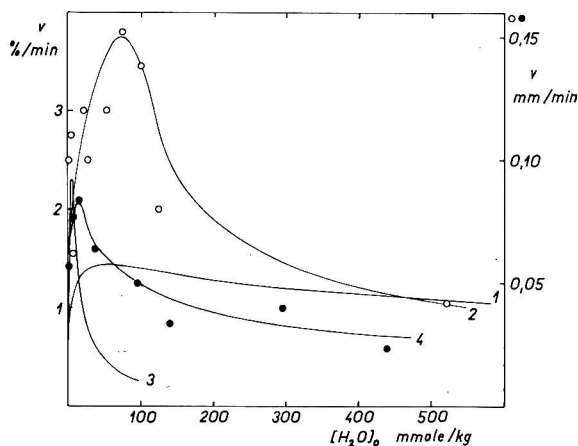


Fig. 1. Effect of temperature on position of maximum in "dependence" of DOX polymerization with $\sim\text{Si}^{\oplus}\text{HSO}_3^{\ominus}$ as initiator.

Curve	Point	Temp., °C.	Concentration, moles/kg.			
			DOX	Heptane	Tetrachloro- ethane	Initiator
1 ^a		70	13.7	—	—	0.114
2	○	30	13.7	—	—	0.100
3 ^a		70	3.1	0.35	4.2	0.107
4	●	30	3.1	0.35	4.2	0.166

^a See Kučera et al.⁶

great scattering of the values measured and because of small differences in the measured quantities.

RESULTS

The dependence of the reaction rate on the cocatalyst concentration (the term "dependence" is used instead of the full expression in the following text) has been measured under simplified conditions so far (water only was always used as a cocatalyst, the rate was determined at one temperature and in individual solvent, etc.). Therefore, it will be necessary to increase the number of experiments that cover further variables.

Polymerization of Dioxolane

The shifting of the maximum in the "dependence" with the concentration of DOX has been already described.⁶ Let us compare the quoted "dependence" with that measured at 30°C. (Fig. 1). The results were obtained by using $\sim\text{Si}^{\oplus}\text{HSO}_4^{\ominus}$ as initiator.

It was interesting to find out the effect of temperature on the shifting of the maximum with a more acid (more effective) initiator; the results with $\sim\text{Si}^{\oplus}\text{ClO}_4^{\ominus}$ are summarized in Figure 2. The maximum of the de-

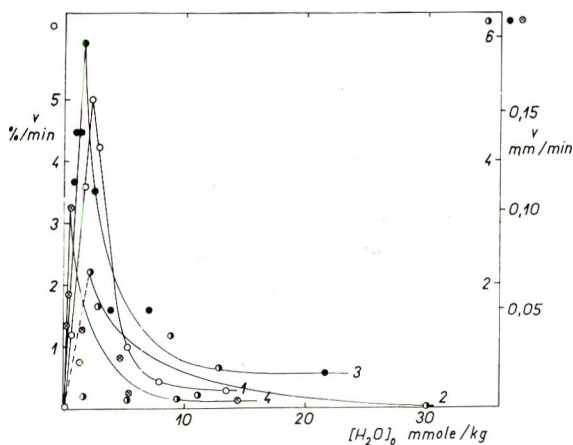


Fig. 2. Effect of DOX concentration on position of maximum in "dependence" with $\sim\text{Si}^{\oplus}\text{ClO}_4^{\ominus}$ as initiator.

Curve	Point	Temp., °C.	Concentration		
			DOX, moles/kg.	Heptane, moles/kg.	Initiator, mmoles/kg.
1	○	70	13.7	0	1.1
2	◐	0	13.7	0	0.18
3	●	0	8.4	3.9	0.54
4	⊙	0	5.4	5.9	6.3

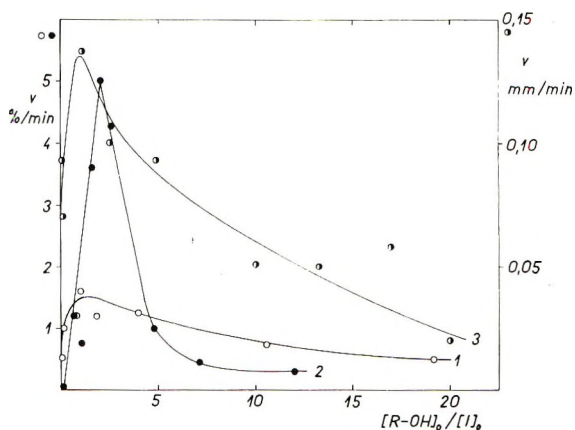


Fig. 3. Dependence of rate of DOX polymerization on ratio cocatalyst/initiator; DOX concentration, 13.7 moles/kg.

Curve	Point	Cocatalyst	Initiator concn., mmoles/kg.		Temp., °C.
			$\sim\text{Si}^{\oplus}\text{ClO}_4^{\ominus}$	$\sim\text{Si}^{\oplus}\text{HSO}_4^{\ominus}$	
1	○	H ₂ O		114	70
2	●	H ₂ O	1.1		70
3	◐	EtOH		100	30

pendence is shifted in both the sulfate and the perchlorate initiator polymerizations.

The displacement of the maximum with temperature is not very apparent. The effect of the temperature, however, may be masked by a factor that changed in consequence of the change of temperature and that, unfortunately, can be eliminated only with difficulty: namely, the concentration of the initiator. The effect of the initiator concentration on the

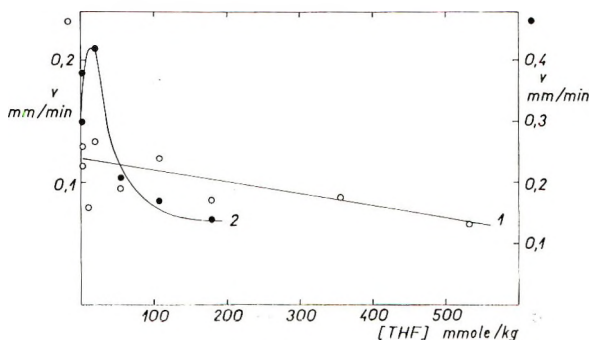


Fig. 4. Effect of THF on polymerization of DOX. DOX concentration, 13.7 moles/kg. Temperature, 30°C. Initiator concentration (mmoles/kg.): (curve 1) $\sim\text{Si}^{\oplus}\text{HSO}_4^{\ominus}$, 100; (curve 2) $\sim\text{Si}^{\oplus}\text{ClO}_4^{\ominus}$, 0.088. Initial water concentration (mmoles/kg.): (curve 1) 2.2; (curve 2) 2.3.

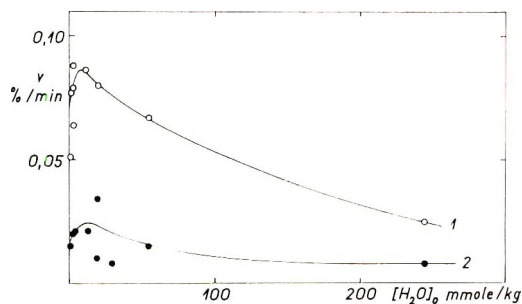


Fig. 5. Effect of initiator concentration on course of "dependence" in polymerization of THF at 0°C.

Curve	Point	Concentration, moles/kg.		
		THF	Heptane	Initiator
1	○	11.1	2.1	0.5
2	●	11.1	2.1	0.1

abscissa of the maximum measured is not expressive. This is illustrated by Figure 3, in which the dependence of the polymerization rate on the cocatalyst/initiator ratio is shown.

Water, however, is only a model of a cocatalyst; the same effect can be observed in the presence of ethanol (Figs. 3 and 4).

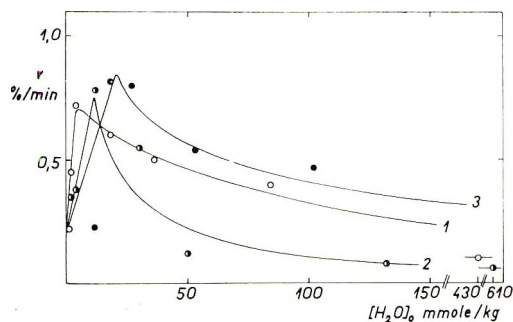


Fig. 6. Effect of temperature on position of maximum in the "dependence" in polymerization of THF.

Curve	Point	Temp., °C.	Concentration, moles/kg.			
			THF	Tetra- chloro- ethane	Heptane	Initiator
1	○	30	8.6	2.4	0.09	0.27
2	●	0	8.6	2.4	0.09	0.43
3	●	-78	8.6	2.4	0.09	1.20

From this point of view it was interesting to know whether THF could act as a cocatalyst. Yet THF was shown to be able to activate the initiator by itself.⁷ Its influence can be studied with $\sim\text{Si}^{\oplus}\text{HSO}_4^{\ominus}$ as initiator, with which THF does not polymerize, but it is also possible to use $\sim\text{Si}^{\oplus}\text{-ClO}_4^{\ominus}$, which initiates the polymerization of THF. The results of these experiments are shown in Figure 4.

Polymerization of Tetrahydrofuran

Unfortunately, it is not possible to study too fast or too slow reactions by means of our present experimental technique. For that reason we could not measure the polymerization rates of THF at such different initiator concentrations as would be desirable for determining the position of the maximum. Within the concentration range of $\sim\text{Si}^{\oplus}\text{ClO}_4^{\ominus}$ studied the maximum does not shift considerably (Fig. 5).

If the amount of the initiator has no great influence on the shifting of the maximum, it is possible to measure the effect of temperature on the course

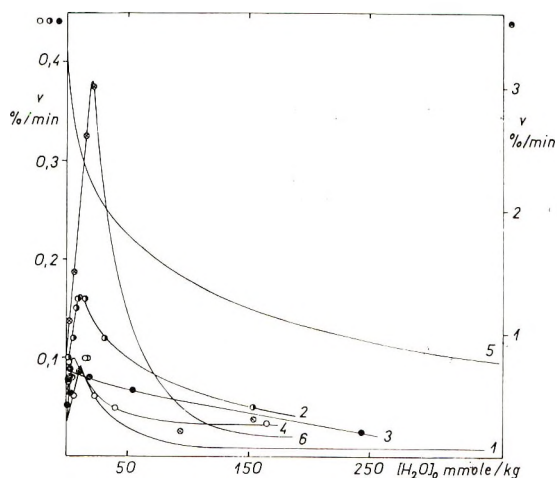


Fig. 7. Effect of solvents on course of "dependence" in polymerization of THF at 0°C.

Curve	Point	Concentration, moles/kg.				
		THF ^a	Tetra-chloro-ethane	Heptane	Dioxane	Initiator
1 ^a	●	8.6	2.4	0.09	—	0.43
2	●	5.0	3.7	0.14	—	0.85
3	●	11.1	—	2.05	—	0.5
4	○	8.0	—	4.3	—	0.5
5 ^b	○	13.8	—	—	—	0.32
6	⊙	10.0	—	—	3.2	0.15

^a See curve 2 in Fig. 6.

^b See curve 2 in Fig. 3 of Kučera et al.⁷

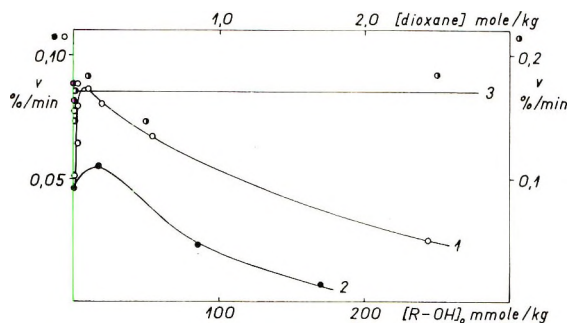


Fig. 8. Effect of the cocatalyst on "dependence" in the THF polymerization at 0°C.

Curve	Point	Cocatalyst	Concentration, moles/kg.		
			THF	Heptane	Initiator
1	○	H ₂ O	11.1	2.05	0.5
2	●	EtOH	11.1	2.05	0.27
3	◐	1,4-dioxane	13.8	—	0.25

of the "dependence" almost without any difficulty. In the measured interval of the temperature this effect is small (Fig. 6).

It is necessary to assume that a solvent also can influence the position of the maximum. The polymerization rates of THF in the presence of heptane or of mixtures of heptane and excesses of 1,1,2,2-tetrachloroethane were compared under the same conditions. In heptane the maximum of the "dependence" lies at lower concentrations than in the mixture. On the other hand, a small shifting of the maximum to the right may be observed in the case of 1,4-dioxane. The position of the maximum seems not to depend on the concentration of the monomer in the polymerization of THF. These assertions follow from the curves in Figure 7.

Likewise, other polar compounds than water, e.g., ethanol, are active as cocatalysts even in the polymerization of THF in the presence of a solvent (Fig. 8); the cyclic 1,4-dioxane, however, is entirely inert.

DISCUSSION

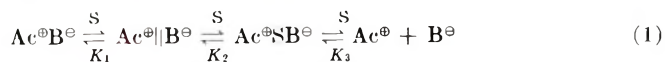
The course of the "dependence" changes quantitatively under the conditions investigated. These changes, however, are not great; the position of the maximum displaces only slightly. A greater change may be observed merely with a change of the whole affinity of the medium to water.

Now let us discuss the individual factors influencing the position of the maximum.

Temperature

In DOX and THF polymerizations the maxima shift slightly with decreasing temperature but definitely with increasing concentrations of water.

The shifting may be observed at all concentrations of the monomers (Figs. 1 and 6). This finding is unexpected. Considering the reactions in which the solvation equilibria are established,



(the position of this equilibrium corresponds to the observed reaction rate), the dependence of the equilibrium constants K on the temperature may be described by the Van't Hoff reaction

$$(d \ln K)/dT = \Delta H/RT^2 \quad (2)$$

Solvation is an exothermic process, a lower temperature corresponding to a higher K ; lower concentrations of a solvation compound—a cocatalyst—should yield the maximum reaction rate at lower temperatures. The dependence found is quite the reverse. For the present we cannot explain this disagreement. It is not excluded that at higher temperatures the less solvated units become the initiating centers. This view would be supported by a high activity of some initiators (catalysts) at high temperatures (in reactions in gaseous phase), at which the activation by solvation is questionable. The processes mentioned are opposite, so that they could compensate the effect of the temperature on the position of the maximum.

Concentration of Monomer

The shift of the maximum at the polymerization of DOX initiated by $\sim\text{Si}^{\oplus}\text{HSO}_4^{\ominus}$ is shown in Figure 1 (see also Kučera et al.⁶); by $\sim\text{Si}^{\oplus}\text{ClO}_4^{\ominus}$, in Figure 2. At DOX concentrations above 5.5 moles/kg. the position of the maximum is constant with decreasing concentration of the monomer of the water concentration at which the maximum rate is observed decreases. The shifting of the maximum was not ascertained in the polymerization of THF. The measurements, however, were carried out in mixtures with a high content of THF.

The explanation of the change in the position of the maximum with the concentration of DOX is evident from eq. (1). However, it is necessary to take into account that the equilibrium constants K_1 , K_2 , and K_3 are functions of the affinity of the system to the cocatalyst S. The equilibrium constants are expected to be lower, the higher the solubility of S in the reacting mixture; the ratio is probably not the same with all constants. These conclusions are demonstrated by the DOX polymerization. DOX is unlimitedly miscible with water; heptane and tetrachloroethane used as solvents have much less affinity to water. It is therefore evident that the part of the analytical concentration of S (H_2O), which can be used directly for activating the initiator, increases as the hydrophobic solvent substitutes for the hydrophilic monomer. The amount of water necessary to reach the maximum rate is smaller, the smaller the concentration of DOX in the mixture.

Solvent

The effect of the studied solvents or their mixtures on the course of the "dependence" corresponds chiefly to their greater or lesser affinity to water. The explanation is substantially the same as that one offered under "Concentration of Monomer." The effect of the solvents has been studied mainly in the polymerization of THF. The maximum shifts to smaller concentrations of water with the increase of the content of hydrophobic heptane in the mixture. A higher concentration of water was necessary to reach the maximum rate in the presence of hydrophilic 1,4-dioxane. The observed changes are very small (Fig. 7); the value of the abscissa of a maximum is loaded with a considerable relative error, which does not allow the derivation of quantitative relations from the results. Qualitatively, however, the shifting of the maximum is indisputable and proves the validity of the views given under "Concentration of Monomer."

Concentration of Initiator

The shifting of the maximum with the amount of the initiator was not observed in the concentration range studied (Fig. 5). Nevertheless, it cannot be excluded that the maximum of the reaction rate shifts with the concentration of the initiator; more exactly speaking, the abscissa of the maximum depends on the initiator/cocatalyst ratio. This would be supported by the measurements in Figure 3. In accordance with these results the position of the maximum would be a function of the quality of the initiator as well.

Type of Cocatalyst

There is no qualitative difference between water and ethanol, as shown in Figures 3 and 8. THF itself can activate the initiator.⁷ Therefore we studied the polymerization of DOX in the presence of THF; the results are summarized in Figure 4. THF retards polymerization when an initiator with which THF does not polymerize is used. With $\sim\text{Si}^{\oplus}\text{ClO}_4^{\ominus}$, however, it acts as a typical cocatalyst; a clearly expressed maximum may be observed in the "dependence."

The retarding effect of THF with $\sim\text{Si}^{\oplus}\text{HSO}_4^{\ominus}$ may be related to the formation of relatively stable oxonium complexes from THF and the initiator, and the cocatalytical effect of THF with $\sim\text{Si}^{\oplus}\text{ClO}_4^{\ominus}$ may be related to its share in the establishment of solvation equilibria according to eq. (1).

CONCLUSION

The variation of experimental conditions under which the DOX and THF polymerizations were performed caused neither a marked change of the maximum position in the "dependence" nor a qualitative change of its course. It provides proof of equilibrium processes by which the number

and the reactivity of initiation and growth centers and, hence, the reaction rate are determined.

References

1. M. Kučera and E. Spousta, *Makromol. Chem.*, **82**, 60 (1965).
2. M. Kučera and E. Hladký, *Collection Czechoslovak Chem. Commun.*, **32**, 3371 (1967).
3. M. Kučera, E. Hladký, and K. Majerová, in *Macromolecular Chemistry, Prague, 1965* (*J. Polymer Sci. C*, **16**), O. Wichterle and B. Sedláček, Chairmen, Interscience, New York, 1967, p. 257.
4. M. Kučera, E. Hladký, and K. Majerová, *Makromol. Chem.*, **97**, 146 (1966).
5. M. Kučera, E. Hladký, and K. Majerová, *J. Polymer Sci.*, A-1 **5**, 1881 (1967).
6. M. Kučera, E. Hladký, and K. Majerová, *J. Polymer Sci.*, A-1 **5**, 1889 (1967).
7. M. Kučera, E. Hladký, and K. Majerová, *J. Polymer Sci.*, in press.
8. M. Příbyl and Z. Slovák, *Mikrochim. Acta*, **6**, 1097 (1964).

Received June 7, 1967

Solution Properties of Cellulose Triacetate. II. Solubility and Viscosity Studies

P. HOWARD and R. S. PARIKH,
University of Surrey, London, England

Synopsis

The solubility of cellulose triacetate in a range of solvents was measured, and the results for tetrachloroethane, chloroform, and acetic acid were compared with those from initial phase separation in solvent-nonsolvent mixtures and viscosity-concentration studies. The correlation found between solubilities, precipitation values, and values of the Huggins viscosity constant is discussed with reference to the type of polymer-solvent interaction proposed previously to explain fractionation behavior. A qualitative comparison of solubility-swelling behavior was also made for a very low molecular weight cellulose triacetate sample in a wide range of solvents. Results are compared with those for higher molecular weight samples and discussed with regard to the cohesive-energy densities of solvent and polymer. Some attempt has been made to predict suitable solvents for cellulose triacetate, based on consideration of their molecular structures.

INTRODUCTION

It has been suggested earlier¹ that cellulose triacetate (not less than 62% AcOH content) dissolves in chloroform, tetrachloroethane, and acetic acid, forming hydrogen bonds with these solvents, the extent of such polymer-solvent interaction accounting for the poor fractionability observed in these systems. If such interaction is indeed a prerequisite of solubility, then this should be reflected in other solution properties of cellulose triacetate; the magnitude of these properties should be dependent on the proton-donating ability of the solvent. It was therefore thought desirable to carry out solubility, phase-separation and viscosity-concentration studies in tetrachloroethane, chloroform, and acetic acid, the results of which are described in the present work. An attempt has also been made to provide a theoretical basis for predicting suitable solvents while accounting for differences in solubility behavior between cellulose triacetate and other polymers of similar chemical nature.

The marked change in solubility behavior shown by cellulose acetate as its acetic acid content increases from 59 to 62.5% (triacetate), requiring the replacement of protophilic or amphiprotic solvents with protogenic ones, seems well established²⁻⁴ and is in keeping with the type of polymer-solvent interaction suggested. Certain anomalies, however, still exist, such as the reported solubility of cellulose triacetate in nitrobenzene⁵ and

also in ethyl acetate, acetone, dioxane, and pyridine.^{3,6} Such behavior probably can be attributed to a less acetylated "triacetate" or a fully acetylated cellulose having a very low molecular weight due to extensive degradation. The latter condition has been investigated in the present work by examining the solubility and swelling behavior of a very low molecular weight cellulose triacetate in a wide range of solvents. It might also be expected that such systems would, for relatively nonpolar solvents, move nearer to the theoretical conditions required by solubility theory.^{7,8} Thus it was desirable to see how far such solubility data could be correlated with solubility parameter values, and this aspect is examined in the present work.

EXPERIMENTAL

Materials

The higher molecular weight samples used in the present work were those described previously¹ and designated CT/1 ($\bar{M}_n = 28,000$; AcOH, 62.1%) and CT/2 ($\bar{M}_n = 38,200$; AcOH, 62.2%).

A very low molecular weight sample, CT/4, was prepared by acetylation under conditions that gave the triacetate, but the acetylation time was increased to 20 hr. The number-average molecular weight \bar{M}_n was determined with a Mechrolab vapor-pressure osmometer (Model 301A) calibrated with a chloroform solution of α -D-glucose pentaacetate. The value of \bar{M}_n determined in the same solvent was 6,420, being the mean of values 6570 and 6270 for two separately prepared solutions of 1.41 and 1.97 g. per 100 g. of solvent.

All solvents used in the present work were of Analar quality or else the best reagent grade and were used without further purification.

Solubility of High Molecular Weight Cellulose Triacetate CT/2

For acetic acid and nitrobenzene a small quantity of polymer was weighed out into a glass-stoppered flask, 15 or 25 ml. of solvent was pipetted in, and the mixture was shaken mechanically for 3 to 4 hr. The flask was then thermostatted overnight at 25°C., when undissolved polymer was either centrifuged or filtered off. The amount of dissolved polymer was obtained by careful evaporation of an aliquot of solution and drying of the residue to constant weight at 110°C. Runs were carried out in duplicate.

This method was impracticable in the case of chloroform and tetrachloroethane, since very viscous solutions were obtained, making filtration impossible and separation incomplete even after centrifuging; the following method was therefore employed. The saturation value was approximately obtained from preliminary experiments in which the solvent/polymer ratio was varied so as just to give a clear solution. A small amount of cellulose triacetate was then weighed out, and a volume of solvent calcu-

lated to give a slightly lower concentration of polymer in solution than the predetermined value was added to the flask. The flask was shaken and thermostatted at 25°C. as before, and the solution was again examined. A clear, homogeneous solution (absence of swollen phase) showed the saturation concentration to be between this and the previously assessed value, and experiments were repeated with gradually increased polymer/solvent ratios, until two successive runs just gave a slightly turbid solution. The mean of the two consistent values so obtained was taken as the limiting solubility at 25°C.

For bromoform, pyridine, dioxane, ethanol, and acetone an upper solubility limit was obtained by shaking a few milligrams of cellulose triacetate with 40–50 ml. of solvent and observing whether complete solution occurred after standing overnight at 25°C.

Solubility of Low Molecular Weight Cellulose Triacetate CT/4

A constant weight (53 ± 1 mg.) of dried sample was weighed out into a series of stoppered boiling-tubes, to which 20 ml. of solvent was added. The tubes were then thermostatted overnight (16 hr.) at 25°C., when the extent of polymer-solvent interaction was assessed visually from the extent of swelling or solubility, or both, in each case.

Precipitation Values

Stock solutions of 1.00 g. per 100 ml. were prepared from cellulose triacetate CT/2 in the solvents chloroform, tetrachloroethane, and acetic acid. Precipitant was then added dropwise to stirred aliquots of the stock solutions, contained in boiling tubes at 25°C., until the first appearance of turbidity. Stirring was continued for a few minutes, to avoid spurious effects due to localized precipitation, and if turbidity persisted, the volume of precipitant added was taken as the precipitation value for the solvent-nonsolvent system. The mean of at least two separately determined values was taken, and in cases in which the appearance of turbidity was more difficult to judge the mean values were based on three to four determinations.

Viscosity-Concentration Studies

Viscosity measurements were carried out in a dilution viscometer at 25°C., as described previously.¹

RESULTS

The solubilities of sample CT/2 in various liquids are shown in Table I and are mean values of the separately determined ones shown in parentheses. A qualitative comparison of the swelling-solubility behavior of the low molecular weight sample CT/4 in a range of solvents is shown in Table II. The solubility parameter values shown in this table were taken from the same source⁶ and are equal to the square roots of the cohesive-

energy densities. The value for cellulose triacetate calculated from Small's molar attraction constants⁹ was found to be $10.51 \text{ cal.}^{1/2} \text{ cc.}^{-1/2}$.

The results of the precipitation studies are summarized in Table III. Here a comparison has been made between a completely inert (aprotic)

TABLE I
Solubility of Cellulose Triacetate (CT/2) in
Various Solvents at 25°C.

Solvent	CT/2 dissolved g. per 100 ml. solvent*	
Tetrachloroethane	22.06	(21.92, 22.20)
Chloroform	11.44	(11.29, 11.59)
Acetic acid	1.87	(1.86, 1.87)
Nitrobenzene	0.008	(0.0006, 0.001)
Bromoform	<0.025	
Pyridine	<0.033	
Dioxane	<0.024	
Ethanol	<0.024	
Acetone	<0.020	

* Mean values (at left) of separately determined values (in parentheses).

TABLE II
Solubility of Cellulose Triacetate (CT/4) in Various Solvents at 25°C.

Solvent	Solubility parameter, $\text{cal.}^{1/2}/\text{cc.}^{1/2}$	0.053 g. polymer with 20 ml. solvent after 16 hr.
<i>n</i> -Hexane	7.3	No effect
Ethyl ether	7.4	No effect
Cyclohexane	8.2	No effect
Carbon tetrachloride	8.6	Slightly swollen
Toluene	8.9	Extremely swollen
Ethyl acetate	9.1	No effect
Tetrahydrofuran	9.1	Partly soluble; swollen residue
Benzene	9.2	Extremely swollen
Chloroform	9.3	Completely soluble
Methyl ethyl ketone	9.3	No effect
Chlorobenzene	9.5	Partly soluble; swollen residue
Tetrachloroethane	9.7	Completely soluble
Acetone	9.9	Completely soluble
Dioxane	10.0	Nearly all soluble; swollen residue
Nitrobenzene	10	Partly soluble; swollen residue
Pyridine	10.7	Partly soluble; fibrous residue
Acetonitrile	11.9	Partly soluble; swollen residue
Ethanol	12.7	No effect
Methanol	14.5	No effect

TABLE III
Precipitation Values for Cellulose Triacetate
(CT/2) Solutions at 25°C.

Solvent	Precipitation value ml. precipitant per 25 ml. soln.	
	Petroleum ether (100/120 fraction)	Ethyl ether
Tetrachlorethane	11.54 (11.70, 11.40, 11.52)	2.11 (2.12, 2.10)
Chloroform	7.6 (7.8, 7.4)	1.03 (1.00, 0.90, 1.20, 1.00)
Acetic acid	3.07 (3.13, 3.00)	0.75 (0.70, 0.80)

TABLE IV
Values of Huggins Constant and $[\eta]$ for Cellulose
Triacetates CT/1 and CT/2 at 25°C.

Solvent	Sample CT/1 ($\bar{M}_n = 28,600$)		Sample CT/2 ($\bar{M}_n = 38,200$)			
	$[\eta]$	Slope	k	$[\eta]$	Slope	k
Tetrachloroethane	0.500	0.0859	0.344	0.823	0.254	0.375
Chloroform	0.425	0.0814	0.450	0.715	0.218	0.427
Acetic acid	0.723	0.220	0.421	1.17	0.772	0.565

solvent and one which is protophilic, in this case ethyl ether. The precipitation values recorded are the mean of those shown in parentheses.

Plots of viscosity number η_{sp}/c versus concentration c within the range 0.1 to 1.1 g. per 100 ml. for cellulose triacetate samples CT/1 and CT/2 in

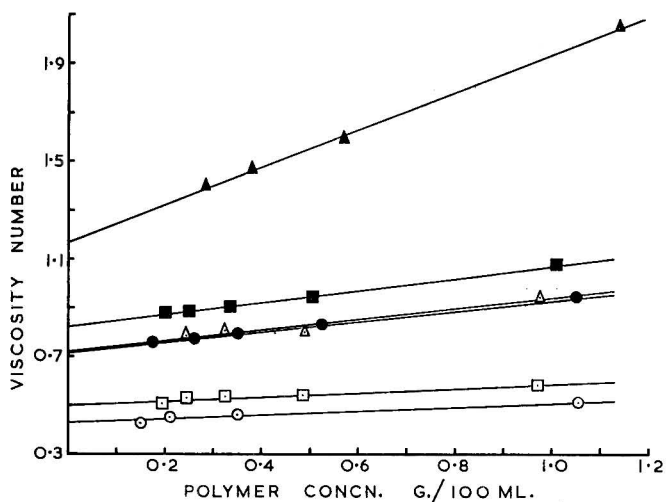


Fig. 1. Viscosity number versus concentration for cellulose triacetate samples: (○) CT/1 in chloroform; (●) CT/2 in chloroform; (□) CT/1 in tetrachloroethane; (■) CT/2 in tetrachloroethane; (△) CT/1 in acetic acid; (▲) CT/2 in acetic acid.

tetrachloroethane, chloroform, and acetic acid at 25°C. are shown in Figure 1. Values of the limiting viscosity number $[\eta]$ and the slope of the plots were calculated by the least-squares method. The Huggins constant k was evaluated from the relationship $\eta_{sp}/c = [\eta] + k[\eta]^2c$ proposed¹⁰ for dilute solutions, and the results are shown in Table IV.

DISCUSSION

Solubility Behavior

The solubility of a polymer in a given solvent is dependent on its average molecular weight, the degree and nature of substitution in the chain, and its degree of crystallinity. The influence of these factors is well illustrated in the case of cellulose and its derivatives. Cellulose itself is only soluble in solutions such as Schweitzer's reagent or zinc chloride, which are capable of forming complexes with it, while its insolubility in common solvents is attributed to its degree of crystallinity and intermolecular hydrogen bonding.

Far-hydrolyzed cellulose acetate (18–26% AcOH) is, however, soluble in water.¹¹ Here the original inherent crystallinity is largely destroyed, and the substituent ester groups allow the chains to move farther apart, while the free hydroxyl groups are sufficiently solvated to enable solubility to occur. On a further increase in the number of acetyl groups in the chain its solubility in water decreases, since the number of hydroxyl groups decreases, and at a stage corresponding approximately to the diacetate (44–52% AcOH) the acetylated cellulose is now soluble in solvents such as acetone, ethyl acetate, and phenol. At this point the cellulose acetate molecules show both acidic and basic characteristics (in the Lewis sense) and hence are soluble in both acidic and basic solvents. Further uniform substitution in the chain, giving a higher acetic acid content, brings about a progressive decrease in acetone solubility, until the fully acetylated triacetate is only soluble in acidic types of solvent such as chloroform or tetrachloroethane, which are capable of forming hydrogen bonds.

The results shown in Table I are in keeping with the type of interaction proposed, the solubilities of cellulose triacetate being in the order tetrachloroethane > chloroform > acetic acid \gg nitrobenzene, bromoform, pyridine, dioxane, ethanol, and acetone. The latter six are virtually non-solvents for the cellulose triacetate sample examined, although their behavior differs from that of the very low molecular weight sample (Table II); this is discussed later. Since in the case of the high molecular weight sample the entropy contribution to the solution process is relatively small, the enthalpy contribution predominates, and the solubility values in Table I are in the main determined by the proton-donating ability of the solvents. The highest solubility shown in tetrachloroethane can be attributed to the availability of two hydrogen atoms for hydrogen bonding with carbonyl

groups on the cellulose triacetate chain. It is significant that the solubility in chloroform is halved where only one proton in the solvent molecule is active. The marked effect of substituent atoms in the solvent molecule on the C—H polarization is shown by the virtual insolubility of cellulose triacetate in bromoform; this is in keeping with the order of electronegativity of the halogen atoms, and if fluoroform and iodoform were liquids, one would expect solubility values to be in the order fluoroform > chloroform > bromoform > iodoform. Despite the greater tendency of the C—OH than of the C—H group to act as a proton donor (apart from inductive effects of adjacent groups) acetic acid is seen to be a much poorer solvent (Table I) for cellulose triacetate. This fact is accounted for by the extensive dimerization of acetic acid, which reduces the effective concentration of proton-donor molecules.

The greater solubility of cellulose triacetate in both protophilic and aprotic solvents on reduction of its \bar{M}_n value from 38,200 to 6400 is evident from a comparison of Tables I and II. The difference is mainly attributed to an increase in the entropy of mixing arising from a greater randomization of a polymer-solvent mixture containing much shorter chains. Although only qualitative, the solubility results in Table II show that for solvents in which heats of mixing may be attributed mainly to dispersion forces (rather than hydrogen bonding) the degree of solubility or swelling can be correlated with solubility parameter values, as suggested by theory.^{7,8} Thus, for the solvents *n*-hexane, ethyl ether, cyclohexane, carbon tetrachloride, toluene, ethyl acetate, benzene, chlorobenzene, dioxane, nitrobenzene, pyridine, and acetonitrile the tendency to swell or dissolve increases with the solubility parameter value from 7.3 to 11.9, partial solubility being observed in the range 9.3–11.9 corresponding to the value of 10.5 for cellulose triacetate.

Reports of solubility in the literature have been mainly of a qualitative nature^{3,12-15} The results reported in Table I are in complete agreement with the qualitative observations of Malm et al.,¹⁵ while the quantitative results of Marvel et al.¹⁴ are clearly explained by the relative proton-donating abilities of their solvents. Lower solubilities reported by Marvel et al.¹³ for cellulose triacetate in chloroform (5.2 g. per 100 g.) and tetrachloroethane (5.8 g. per 100 g.) are probably due to the higher molecular weight of their sample. The partial solubility of highly acetylated samples (>60% AcOH) in acetone, pyridine, and dioxane reported by Howlett³ is not supported in the present work for a molecular weight as low as 38,200, although this is observed when \bar{M}_n is reduced to 6400 (Table II).

It is interesting to note that, where a quantitative comparison is available,^{13,14} cellulose triacetate is seen to be much less soluble than the vinyl-type polymers, such as poly(vinyl acetate) and poly(methyl methacrylate), in the same solvents. While molecular weight differences may be a contributing factor, the main cause probably lies in the molecular structure of the repeating unit and its influence on chain flexibility. It is useful in this respect to consider the dependence of the free energy of mixing of

polymer and solvent on the associated heat and entropy changes, expressed as ΔG_m , ΔH_m , and ΔS_m , respectively, in the relationship

$$\Delta G_m = \Delta H_m - T\Delta S_m$$

The conditions favoring a sufficiently negative value of ΔG_m to give a measurable polymer solubility would be a small or negative value for ΔH_m and a finite positive value for ΔS_m . In the case of protogenic solvents the heat evolved owing to polymer-solvent hydrogen bonding is expected to be about the same for poly(vinyl acetate) and poly(methyl methacrylate), although probably less than that for cellulose triacetate, and contributes favorably to the ΔG_m value. However, ΔS_m in each case will depend on the number of different configurations the polymer molecules can take up in solution without any appreciable change in energy. Cellulose and its derivatives are believed to have relatively stiff chains of large repeating units with very restricted rotation about the glucosidic linkages. The resultant lower value for ΔS_m than in the case of the more flexible vinyl-type polymer chain may well contribute to the lower solubility found for cellulose triacetate. Although more rotation about the C—C linkage may be possible for poly(vinyl acetate) and poly(methyl methacrylate), in the latter case the rotation may be less because of the steric effect of proximate methyl and acrylic groups with a resultant decrease in the number of different configurations the chains can take up in solution. In consequence one might expect the values of ΔS_m to be in the order poly(vinyl acetate) > poly(methyl methacrylate) \gg cellulose triacetate, which is the order of solubility for these polymers in proton-donor solvents, found by Marvel et al.^{13,14}

Precipitation Values

The amount of nonsolvent that must be added to a given polymer solution to just bring about initial phase separation of polymer, generally called the "precipitation value" or "solvent power number," has been used by various workers as a measure of the suitability or "goodness" of a solvent for a given polymer. To be more specific, precipitation values for a polymer dissolved in a range of solvents may be considered a measure of the degree of polymer-solvent interaction in many cases; higher values might thus be expected for decreasing values of the polymer-solvent interaction parameter χ , for which some evidence exists in the case of secondary cellulose acetate solutions.¹⁶

Comparison of precipitation values (Table III) for cellulose triacetate in the three solvents with the corresponding solubilities (Table I) clearly shows a correlation between them, the order in both cases being tetrachloroethane > chloroform > acetic acid. While both petroleum ether and ethyl ether give the same trend of precipitation values, in keeping with the solubilities, the difference between corresponding values for each solvent (Table III) provides further support for the existence of hydrogen bonding in these systems. Here the role of petroleum ether, as an aprotic nonsolvent, is that of a diluent, which reduces the extent of hydrogen bonding between

polymer and solvent enough to bring about insolubility. Ethyl ether, on the other hand, would be a much more effective precipitant since, because of its protophilic nature, it could effectively compete with cellulose triacetate in forming hydrogen bonds with the solvent as well as be a diluent. Limited support for an increase in precipitation value (and solubility) as the χ value decreases comes from osmotic pressure measurements in tetrachloroethane¹⁷ ($\chi = 0.29$) and chloroform¹ (mean value, $\chi = 0.34$), but so far a value for acetic acid solution has not been reported.

Results of initial phase-separation studies of cellulose triacetate, obtained by Moore and Russell,¹⁸ are consistent with those reported here for chloroform and tetrachloroethane; their higher precipitation values reported for the more acidic solvents *o*-cresol and *m*-cresol would be predicted from the type of polymer-solvent interaction proposed. It is interesting to note that higher precipitation values were obtained by these workers (*loc. cit.*) when hexane was replaced with toluene as precipitant. This behavior is clearly in keeping with the tendency of toluene to swell low molecular weight cellulose triacetate and the ineffectuality of hexane in that respect (Table II).

If a parallelism between precipitation value and solubility of cellulose triacetate in hydrogen-bonding solvents is accepted, then the present results, together with those of Moore and Russell (*loc. cit.*), would suggest that solvents can be listed as follows, in order of decreasing solubility of cellulose triacetate and decreasing order of thermodynamic solvent power (increasing χ values): *m*-cresol \gtrsim *o*-cresol \gg tetrachloroethane \gtrsim methylene chloride $>$ chloroform \gg acetic acid.

It seems clear that in any attempt to predict suitable solvents for cellulose triacetate their abilities to form hydrogen bonds with the polymer must be taken as necessary conditions. The useful classification of acidic (or electron acceptor) groups in order of increasing activity, made by Spurlin,¹⁹ might be used as a guide in selecting the best type of solvent for cellulose triacetate. For normal solvents containing substituent atoms or groups R, R₁, and R₂, where the inductive effect of group R is the same as the R₁ + R₂ combination, the ability of solvents to swell or dissolve cellulose triacetate should be in the order RSO₂H $>$ RCOOH $>$ RC₆H₄OH $>$ R₁R₂-CHCN $>$ R₁R₂CHNO₂ $>$ R₁R₂CHONO₂ $>$ RCHCl₂ $>$ R₁R₂CHCl, which is in fair agreement with the order of solubilities suggested above on the basis of precipitation values.

Viscosity-Concentration Relationship

The results obtained from viscosity studies in tetrachloroethane, chloroform, and acetic acid (Fig. 1 and Table IV) show that neither the limiting viscosity number nor the initial slope of the η_{sp}/c versus c is related in a simple manner to the precipitation value or solubility of cellulose triacetate in these solvents. While the values of the slope and $[\eta]$ are comparable for the better solvents, tetrachloroethane and chloroform, those for acetic acid are very much higher (Table IV) for both molecular weight samples.

This can probably be accounted for by a considerable increase in liquid structure due to hydrogen bonding between the polymer and the remaining free acetic acid molecules. The same effect was noted by Moore and Russell¹⁸ in the associated solvents *o*-cresol and *m*-cresol. The values for the Huggins constant, k , are seen to be higher in the poorer solvents, the trend being more marked for the higher molecular weight sample CT/2 (Table IV). This trend is in agreement with that reported by Alfrey et al. for poly(methyl methacrylate) in a range of solvent-nonsolvent mixtures,²⁰ but in the case of cellulose triacetate, at least, precipitation values are much more sensitive to changes in polymer solubility than are k values. The much smaller variation in k value between solvents for cellulose triacetate (Table IV) than between those for poly(methyl methacrylate),²⁰ also found by Moore and Russell (*loc. cit.*), supports the earlier assumption that the cellulose triacetate chain has a lower flexibility than has poly(methyl methacrylate) in solution.

References

1. P. Howard and R. S. Parikh, *J. Polymer Sci.*, **4**, 407 (1966).
2. I. Sakurada and T. Morita, *J. Soc. Chem. Ind. Japan*, **41**, 381 (1938).
3. F. Howlett, *J. Textile Inst.*, **35**, T123 (1944).
4. P. K. Choudhury and S. R. Palit, *J. Sci. Ind. Res. India*, **10B**, 110 (1951).
5. R. C. Weast and S. M. Selby, Eds., *Handbook of Chemistry and Physics*, 47th Ed. Chemical Rubber, Cleveland, Ohio, 1966-67.
6. J. Brandrup and E. H. Immergut, Eds., *Polymer Handbook*, Interscience, New York, 1966.
7. J. H. Hildebrand and R. L. Scott, *The Solubility of Nonelectrolytes*, Dover, New York, 1964.
8. G. Gee, *Trans. Faraday Soc.*, **40**, 468 (1944).
9. P. Small, *J. Appl. Chem.*, **3**, 71 (1953).
10. M. L. Huggins, *J. Am. Chem. Soc.*, **64**, 2716 (1942).
11. C. J. Malm, K. T. Barkey, M. Salo, and D. C. May, *Ind. Eng. Chem.*, **49**, 79 (1957).
12. W. Coltof, *J. Soc. Chem. Ind.*, **56**, T363 (1937).
13. C. S. Marvel, F. C. Dietz, and M. J. Copley, *J. Am. Chem. Soc.*, **62**, 2273 (1940).
14. C. S. Marvel, J. Harkema, and M. J. Copley, *J. Am. Chem. Soc.*, **63**, 1609 (1941).
15. C. J. Malm, J. W. Mench, D. L. Kendall, and G. D. Hiatt, *Ind. Eng. Chem.*, **43**, 688 (1951).
16. W. R. Moore, J. Russell, and J. A. Epstein, *Chem. Ind. (London)*, **1953**, 1339.
17. O. Hagger and A. J. H. van der Wyk, *Helv. Chim. Acta.*, **23**, 484 (1940).
18. W. R. Moore and J. Russell, *J. Colloid Sci.*, **9**, 338 (1954).
19. H. M. Spurlin, in *Cellulose and Cellulose Derivatives* (High Polymers, Vol. V), 2nd ed., Part 3, E. Ott, H. M. Spurlin, and M. W. Grafflin, Eds., Interscience, New York-London, 1955, pp. 63-74.
20. T. Alfrey, A. I. Goldberg, and J. A. Price, *J. Colloid Sci.*, **5**, 251 (1950).

Received June 9, 1967

Revised August 4, 1967

Linear Molecules Based on Dimethylgermanium and Dimethylsilicon Groups Bridged with Oxygen Atoms and Terminated with Chlorine Atoms

KURT MOEDRITZER and JOHN R. VAN WAZER,
*Central Research Department, Monsanto Company,
St. Louis, Missouri 63166*

Synopsis

This article deals with the equilibrated system $(\text{CH}_3)_2\text{SiCl}_2-(\text{CH}_3)_2\text{GeCl}_2-[(\text{CH}_3)_2\text{SiO}]-(\text{CH}_3)_2\text{GeO}$, which consists of a range of various chain, and some ring, molecules resulting from scrambling of the bridging oxygen with the monofunctional chlorine atoms between the dimethylgermanium and dimethylsilicon moieties. The proton nuclear magnetic resonance of the methyl groups (which do not exchange appreciably under the conditions employed) bonded to the germanium and silicon atoms shows that there is a strong preference of the chlorine atoms for being on the dimethylgermanium and the bridging group for being on the dimethylsilicon moiety at equilibrium. This means that thermodynamic factors alone cause the germanium atoms to be found as "unreacted" dimethyldichlorogermane with siloxane polymers or to be preferentially arranged at the ends of the chain molecules in the case of the mixed germoxane-siloxanes. The NMR fine structure is interpreted in these terms, and it is shown that the experimental data may be fitted by appropriate calculations based on only four equilibrium constants, which define the arrangement of neighboring atoms about any given atom in a molecule and the size distribution of the linear molecules.

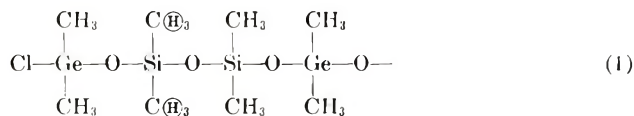
INTRODUCTION

Although there is considerable literature^{1,2} dealing with the "poly-metallosiloxanes," little if any quantitative work has been done on such systems. Further, it is not at all clear from reading the literature whether the reported chemical reactions were kinetically or thermodynamically controlled. In the work described here particular effort was made to ensure that the system was at equilibrium and, hence, that the reactions were thermodynamically controlled. The system $(\text{CH}_3)_2\text{SiCl}_2-(\text{CH}_3)_2\text{GeCl}_2-[(\text{CH}_3)_2\text{SiO}]-(\text{CH}_3)_2\text{GeO}$ described in this paper has as limiting cases the $(\text{CH}_3)_2\text{SiCl}_2-[(\text{CH}_3)_2\text{SiO}]$ system³ and the $(\text{CH}_3)_2\text{GeCl}_2-[(\text{CH}_3)_2\text{GeO}]$ system⁴ each of which by itself represents an entire family of compounds. These limiting-case systems have been described in previous publications^{3,4} from our laboratory and should be referred to for a full picture of the overall system.

EXPERIMENTAL SECTION

The reagents, preparation of equilibrium mixtures, and use of proton nuclear magnetic resonance (NMR) are the same as previously described.^{3,4} However, a new computer program⁵ has been developed to handle the statistical calculations underlying the evaluation from the equilibrium constants of the relative amounts of the various molecular fragments (graphs⁶) corresponding to the observed NMR peaks.

In this study we shall use the notation for segments of molecules that has been employed in recent publications^{3,4,6,7} from this laboratory, with the additional feature of the use of subscripts, subscript *1* referring to silicon and subscript *2* to germanium. Thus, the neso molecules will be $n_1 = (\text{CH}_3)_2\text{SiCl}_2$ and $n_2 = (\text{CH}_3)_2\text{GeCl}_2$; the endgroups, $e_1 = (\text{CH}_3)_2\text{Si}(\text{O}_{1/2}-)\text{Cl}$ and $e_2 = (\text{CH}_3)_2\text{Ge}(\text{O}_{1/2}-)\text{Cl}$; and the middle groups, $m_1 = (\text{CH}_3)_2\text{Si}(\text{O}_{1/2}-)_2$ and $m_2 = (\text{CH}_3)_2\text{Ge}(\text{O}_{1/2}-)_2$. In these formulas $\text{O}_{1/2}-$ stands for half of an oxygen atom which bridges between two silicons, or a silicon and a germanium, or two germaniums. Also following prior usage,⁷ boldface type indicates which group bears the pair of methyl groups causing the observed resonance, and italics indicate the neighboring groups that affect the exact chemical shift of this resonance. For example, $e_2\mathbf{m}_1\mathbf{m}_1\mathbf{m}_2$ indicates that the resonance is attributable to the encircled hydrogens in the following assemblage of atoms:



Considering only nearest neighbors, it can readily be shown that there may be as many as four different endgroup resonances based on silicon ends, four on germanium ends, ten on silicon middles, and ten on germanium middles, corresponding to a total of 28 possible such structure fragments. The stoichiometry of the overall system bounded by the four compounds $(\text{CH}_3)_2\text{SiCl}_2$, $[(\text{CH}_3)_2\text{SiO}]$, $(\text{CH}_3)_2\text{GeCl}_2$, $[(\text{CH}_3)_2\text{GeO}]$ may be represented by two parameters. We have chosen as the two parameters the mole ratios $R \equiv [\text{Cl}]/([\text{Si}] + [\text{Ge}])$ and $R' \equiv [\text{Si}]/([\text{Si}] + [\text{Ge}])$; see Table I and Figures 2 and 3.

RESULTS AND INTERPRETATION

NMR Assignments

The initial tentative assignment of the various resonances observed in the spectra was carried out by comparison with the previously evaluated spectra on the all-neso system, in which chlorine atoms were scrambled with methoxyl groups between dimethylsilicon and dimethylgermanium moieties.⁸ The positions of these resonances, referred to tetramethylsilane, are shown as part B of Figure 1. In the families of compounds studied here the resonances appear as the two pertinent neso peaks plus three sets of

partially overlapping peaks. As shown in Figure 1, the set at -0.47 through -0.60 ppm consists of two overlapping groups of resonances. This was demonstrated by the fact (see experiments 1 to 13 in Table I) that this set first diminished nearly to zero and then went through a high maximum, as would be expected from two different sets of overlapping peaks. The assignment of these groupings of peaks was verified quantitatively by material-balance calculations, as shown by the comparison between the values of $R \equiv [Cl]/([Si] + [Ge])$ and of $R' \equiv [Si]/([Si] + [Ge])$ calculated from the ingredients and those calculated from the NMR spectra (second and third columns of Table I). It should be noted that the overlapping of the \mathbf{e}_1 and \mathbf{m}_2 resonances in the region of -0.47 to -0.60 ppm in the NMR spectra causes no problems, since these resonances never appear simultaneously.

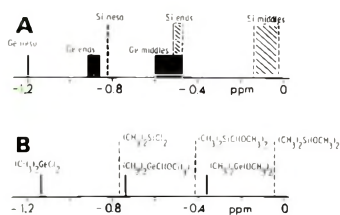


Fig. 1. The approximate NMR chemical shifts, in ppm from $(CH_3)_4Si$, for (A) the $(CH_3)_2SiCl_2-(CH_3)_2GeCl_2-[(CH_3)_2SiO]-[(CH_3)_2GeO]$ system and (B) the related all-*iso* system, in which methoxyl groups replace the bridging oxygen atoms.

The detailed assignment of the individual resonances making up each of the four groups \mathbf{e}_2 , \mathbf{m}_2 , \mathbf{e}_1 , and \mathbf{m}_1 could be approximately estimated on the assumption that a building unit having a resonance lying upfield (or downfield) would, as a nearest neighbor, tend to move the particular resonance proportionately upfield (or downfield). For example, from inspection of Figure 1 it would appear that the $\mathbf{e}_2\mathbf{e}_2$ resonance should be downfield of $\mathbf{e}_2\mathbf{m}_2$, which in turn should be downfield of $\mathbf{e}_2\mathbf{m}_1$. In most cases, the assignments of the individual resonances could be made by a comparison with the values calculated from the equilibrium constants (given in parentheses underneath the appropriate experimental values in Table I).

Equilibrium Constants

It has been shown that the molecular size distributions observed in the all-silicon³ and all-germanium⁴ families of compounds can be interpreted to a good approximation on the basis that the only equilibrium constants deviating from randomness are those dealing with the arrangement of nearest-neighbor groups about a given group. In other words, the reorganization heat order⁶ is unity. On this basis we shall assume that the same treatment may be applied to the mixed system described herein. Therefore, we should expect that the kinds and proportions of noncyclic

molecules would be described in terms of the following four equilibrium constants:

$$K_{Si} = [\text{Si neso}][\text{Si middles in chains}]/[\text{Si ends}]^2 \quad (2)$$

$$K_{Ge} = [\text{Ge neso}][\text{Ge middles in chains}]/[\text{Ge ends}]^2 \quad (3)$$

$$K_O = [\text{SiOSi}][\text{GeOGe}]/[\text{SiOGe}]^2 \quad (4)$$

$$K_I = [\text{Si middles}][\text{Ge neso}]/[\text{Si neso}][\text{Ge middles}] \quad (5)$$

The values of K_{Si} and K_{Ge} were taken, from our previous work,^{3,4} to be 0.110 and 0.020, respectively. It would be expected that these values will apply throughout the entire system being reported here. The value of K_O was shown to be 0.35 in the exchange of silicon with germanium about an oxygen atom in the bromine system⁹ analogous to the one reported here. A preliminary approximation of the value of K_I was given by a study in which chlorine atoms were exchanged with methoxyl groups instead of with bridging oxygen atoms between the dimethylsilicon and dimethylgermanium moieties. For this case, exchanging methoxyl with chlorine atoms, the value of K_I was found⁷ to be equal to 10^{13} .

Compositions Studied and Time for Equilibration

This complicated system was studied by taking three different cuts through it, as shown in Figure 2. Cut A corresponded to mixtures of various proportions of $(\text{CH}_3)_2\text{SiCl}_2$ and $[(\text{CH}_3)_2\text{GeO}]$; cut B, to various proportions of $(\text{CH}_3)_2\text{SiCl}_2$ plus $(\text{CH}_3)_2\text{GeCl}_2$ with $[(\text{CH}_3)_2\text{GeO}]$; and cut C, to various proportions of $(\text{CH}_3)_2\text{GeCl}_2$ with $[(\text{CH}_3)_2\text{SiO}]$. The various mixtures corresponding to cut A (experiments 1 to 7) showed noticeable heat evolution upon mixing, and the NMR pattern taken 5 min. after mixing corresponded to essentially stoichiometric transfer of the chlorine atoms to the germanium and of the oxygen atoms to the silicon. With Cut B (experiments 8 to 13) a similar rapid reaction was observed. On the other hand, the various mixtures corresponding to cut C showed no heat

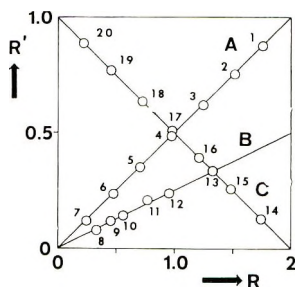


Fig. 2. Compositions in the $(\text{CH}_3)_2\text{SiCl}_2$ - $(\text{CH}_3)_2\text{GeCl}_2$ - $[(\text{CH}_3)_2\text{SiO}]$ - $[(\text{CH}_3)_2\text{GeO}]$ system for which experimental data were obtained in this study. The numbers accompanying the points are the experiment numbers of Table I, in which experiments 14 to 20 were not included for the reason given in the text. The axes of this plot are $R = [\text{Cl}]/([\text{Si}] + [\text{Ge}])$ and $R' = [\text{Si}]/([\text{Si}] + [\text{Ge}])$.

evolution and exhibited NMR patterns consisting of little more than the unchanged reagents even after either several weeks at 150°C. with 2% by weight of AlCl_3 as catalyst or several months at room temperature with or without catalyst. Equivalent results are to be expected with other Friedel-Crafts catalysts, such as FeCl_3 , ZnCl_2 , and similar compounds.

These findings show that the scrambling of chlorines with oxygen atoms between the dimethylsilicon and dimethylgermanium moieties is rapid and that there is strong preference of the chlorine atoms to be on the dimethylgermanium and of the oxygen atoms to be on the dimethylsilicon. This is in accord with the prior work on the all-neso system, in which the chlorine atoms were scrambled with methoxyl groups between dimethylsilicon and dimethylgermanium. Although the chlorine-oxygen exchange occurs rapidly at room temperature, this does not mean that the resulting molecules will represent an equilibrium distribution. Rather, complete equilibration is expected to take a considerably longer time, since it has generally been found^{10,11} that the exchange of a halogen with an oxygen is rapid compared with the exchange of one oxygen for a differently substituted oxygen. Because of this the equilibrium runs reported in Table I were all carried out at 120°C. with 2% AlCl_3 : for 12 days in the case of cut A, 7 days in the case of cut B, and 17 days in the case of cut C. Pilot samples held at temperature for twice these lengths of time showed no change in their NMR spectra. It should be noted that the exchange of chlorines with bridging oxygens on germanium is rapid at room temperature,⁴ so that the experimental data reported here must correspond to equilibrium of the silicon parts of the molecules at 120°C. and of the germanium parts at 25°C.

Evaluation of Experimental Data

The intersystem equilibrium constant K_I depends solely upon the areas of the NMR peaks corresponding to the silicon and germanium neso compounds and the total areas of middle-group peaks corresponding to silicon and germanium, respectively. A range of large positive values of K_I near the preliminary value (see above) of 10^{13} were tested, and it was found that the best fit with the experimental data resulted when K_I was set equal to 10^{10} . It should be noted that this value is completely independent of the value selected for K_O when K_O exhibits the random value of 0.25. The assumed value of $K_O = 0.35$ is sufficiently close that assumption of independence is probably applicable.

The experimental findings (except for the data of cut C) are summarized in Table I along with the calculated values (in parentheses) for the relative proportions of the various structural arrangements obtained from the best set of equilibrium constants: $K_{Si} = 0.11$ (at 120°C.), $K_{Ge} = 0.02$ (at 25°C.), $K_O = 0.35$ (at 120°C.), and $K_I = 1 \times 10^{10}$ (between 25 and 120°C.). Experiments 14 through 21 (cut C of Fig. 2) were omitted from Table I, since along this cut the products were essentially identical with the reactants. In Table I agreement between the theoretical and experimental values is

TABLE I
Relative Areas of the Major Sets of Proton NMR Peaks
in the System $(\text{CH}_3)_2\text{SiCl}_2-(\text{CH}_3)_2\text{GeCl}_2-[(\text{CH}_3)_2\text{SiO}]-[(\text{CH}_3)_2\text{GeO}]$ at Equilibrium

Expt. no.	$R \equiv [\text{Cl}]/$ $([\text{Si}] + [\text{Ge}])$		$R' \equiv [\text{Si}]/$ $([\text{Si}] + [\text{Ge}])$		Neso		Ends				Middles	
	R	R'	Si, n ₁	Ge, n ₂	e/e ₁	e/m ₁	e ₂ e ₂	e ₂ m ₁	e ₂ m ₂	e ₂ m ₁	Si, Σm_1	Ge, Σm_2
1	1.754 ^a (1.752) ^c	0.877 ^a (0.874) ^c	63.5 ^b (64.0) ^d	12.7 (12.3)	20. (21.1)	1.8 (1.7)	—	—	—	—	1.1 (0.9)	— (0.0)
2	1.509 (1.502)	0.755 (0.767)	33.8 (31.6)	22.4 (24.5)	31.4 (30.5)	6.4 (8.2)	—	—	—	—	5.1 (5.2)	— (0.0)
3	1.245 (1.230)	0.623 (0.608)	8.2 (6.9)	35.6 (37.7)	18.7 (16.6)	16.0 (18.8)	—	—	—	—	17.2 (20.1)	— (0.0)
4	0.978 (0.969)	0.489 (0.494)	— (0.0)	46.8 (46.6)	— (0.0)	— (0.1)	—	—	—	—	49.4 (48.8)	0.6 (0.0)
5	0.706 (0.715)	0.353 (0.343)	— (0.0)	12.2 (10.5)	— (0.0)	— (0.0)	—	—	—	—	34.3 (35.3)	6.5 (4.6)
6	0.471 (0.508)	0.235 (0.223)	— (0.0)	1.6 (1.3)	— (0.0)	— (0.0)	—	—	—	—	22.3 (23.5)	28.5 (30.7)

7	0.232 (0.259)	0.118 (0.118)	— (0.0)	0.3 (0.2)	4.3 (3.0)	←21.→ (17.0)	11.3 (11.8)	63.2 (65.2)
8	0.326 (0.347)	0.078 (0.083)	— (0.0)	0.6 (0.3)	6. (6.1)	26. (22.9)	8.3 (7.8)	57.6 (59.9)
9	0.452 (0.475)	0.120 (0.122)	— (0.0)	1.2 (0.9)	10.1 (12.3)	←35.→ (24.7)	12.2 (12.0)	41.6 (43.7)
10	0.550 (0.588)	0.144 (0.150)	— (0.0)	2.4 (1.7)	19. (19.3)	14. (23.2)	15.0 (14.4)	28.6 (31.4)
11	0.764 (0.774)	0.207 (0.204)	— (0.0)	9.7 (7.4)	25. (31.9)	17. (10.7)	20.4 (20.7)	11.9 (10.3)
12	0.956 (0.954)	0.240 (0.242)	— (0.0)	23.9 (22.0)	20.6 (27.3)	←27.→ (2.6)	24.2 (24.0)	4.3 (2.4)
13	1.322 (1.303)	0.334 (0.330)	— (0.0)	64.2 (65.3)	— (0.0)	2. (1.3)	33.0 (33.1)	0.8 (0.0)

^a Values calculated from mole proportions of ingredients.

^b Relative NMR areas.

^c Values in parentheses calculated from NMR areas.

^d Values in parentheses calculated from $K_{Si} = 0.15$, $K_{Co} = 0.02$, $K_I = 10^{+10}$, and $K_o = 0.35$.

gratifying and demonstrates the general correctness of the interpretation of the NMR spectra presented here. Considerably more detail was available in the NMR spectra than is shown in Table I. For example, in the spectrum of experiment 3 the $e_1m_1e_1$ and $e_1m_1m_1$ resonances were clearly distinguishable (they are combined in Table I as e_1m_1), as were $e_1m_1m_1e_1$ and $e_1m_1m_1m_1$. However, in other spectra (particularly experiment 6) the overlapping between the various Ge middle-group resonances or Si middle-group resonances was so extreme that even qualitative resolution into individual peaks was suspect. When resolution was good, the areas of the resolved peaks agreed quite well with the appropriate values calculated from the four equilibrium constants of eqs. (2)–(5).

In accord with the theory previously presented,⁶ one can now calculate the distribution of linear molecules for any stoichiometry within the system (corrected for the presence of any ring molecules). For values of R greater than about 0.2 the amount of cyclic molecules is small and can be ignored. The compositions for $R = 0$ have been considered in a related study,⁹ in which bromine, instead of chlorine, atoms were scrambled with bridging oxygens between dimethylsilicon and dimethylgermanium.

DISCUSSION

It is interesting to note that the literature^{12–14} dealing with inorganic polymers either implies or states that for oligomeric structures in which a number of different atoms can replace each other the replacement atoms will be found more or less randomly scattered throughout the molecule. This paper demonstrates that for at least one system this is not the case. Since the equilibrium favors the placement of chlorine on germanium and bridging oxygen on silicon, the germanium atoms will occur with a strong preference at the ends of the chain molecules. This preferential placement is attributable to thermodynamic causes, being due to the fact that the intersystem equilibrium constant K_I deviates by 10 orders of magnitude from its statistically random value of unity.

Such a large deviation from the random value of the equilibrium constant K_I , controlling the exchange of two kinds of substituents between two polyfunctional moieties based on different elements, is expected to be much more commonly occurring than the situation in which the constant K_I is not far from its random value. This follows from the fact that the free energy for the exchange of substituents Z and T between two different kinds of polyfunctional moieties, Q and M, must involve the difference between the sum of the bond energies of Q–Z plus M–T and the sum of the bond energies of Q–T plus M–Z, and it is likely that this difference corresponds to more than about 5 kcal.

In Figure 3 we have plotted the various arrangements of building units with their nearest neighbors as they exist in the overall system $(CH_3)_2SiCl_2-(CH_3)_2GeCl_2-[(CH_3)_2SiO]-[(CH_3)_2GeO]$, as calculated from the four equilibrium constants K_{Si} , K_{Ge} , K_O , and K_I (assuming no cyclic molecules, the presence of which will cause a small perturbation in the regions for $0 < R <$

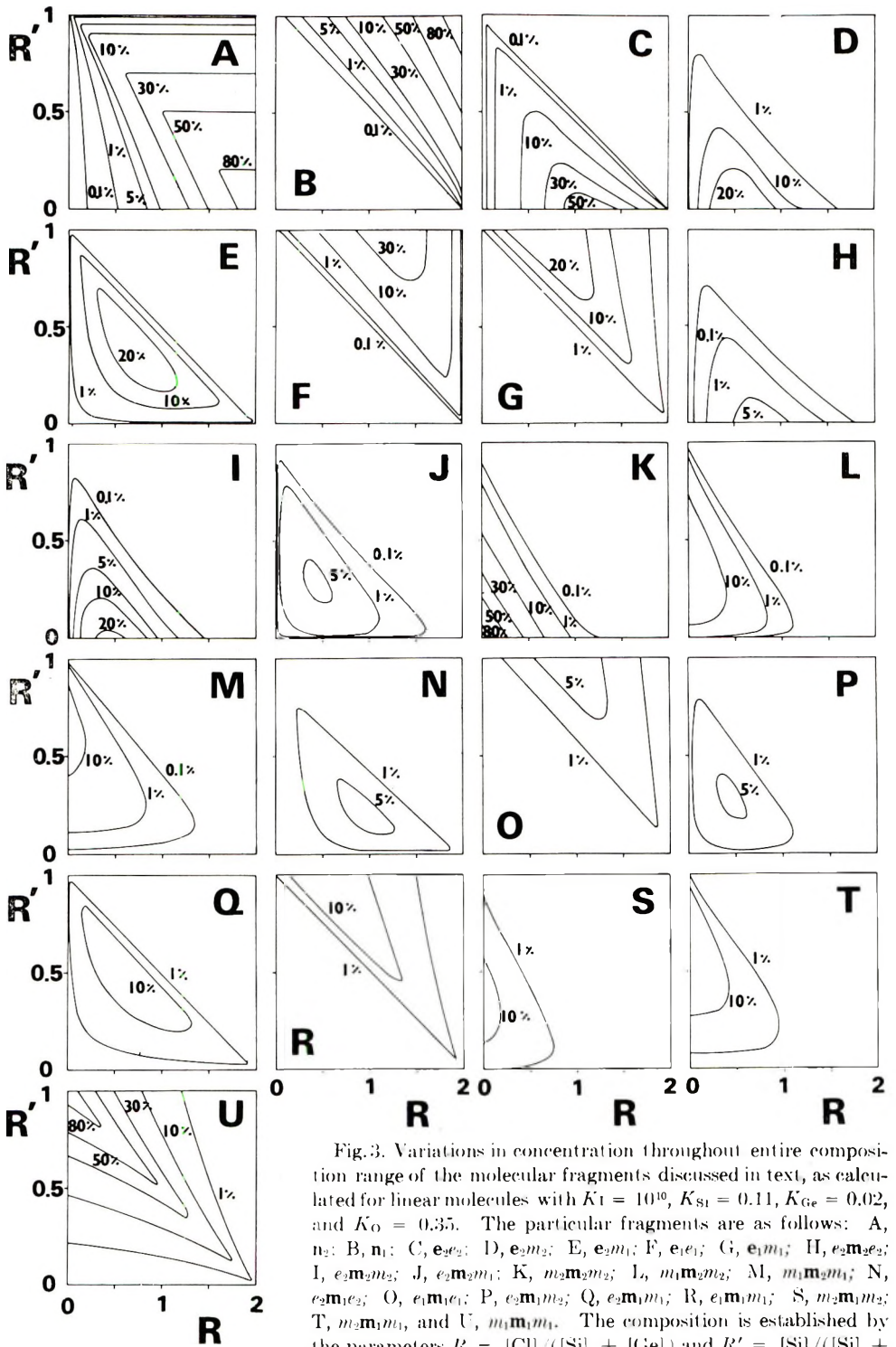


Fig. 3. Variations in concentration throughout entire composition range of the molecular fragments discussed in text, as calculated for linear molecules with $K_1 = 10^{10}$, $K_{S1} = 0.11$, $K_{Ge} = 0.02$, and $K_O = 0.35$. The particular fragments are as follows: A, n_2 ; B, n_1 ; C, e_2e_2 ; D, e_2m_2 ; E, e_2m_1 ; F, e_1e_1 ; G, e_1m_1 ; H, $e_2m_2e_2$; I, $e_2m_2m_2$; J, $e_2m_2m_1$; K, $m_2m_2m_2$; L, $m_1m_2m_2$; M, $m_1m_2m_1$; N, $e_2m_1e_2$; O, $e_1m_1e_1$; P, $e_2m_1m_2$; Q, $e_2m_1m_1$; R, $e_1m_1m_1$; S, $m_2m_1m_2$; T, $m_2m_1m_1$, and U, $m_1m_1m_1$. The composition is established by the parameters $R = [Cl]/([Si] + [Ge])$ and $R' = [Si]/([Si] + [Ge])$.

ca. 0.2 with an appreciable one for $R = 0$). It should be noted that certain of the 28 possible arrangements of building units with their nearest neighbors do not appear in appreciable concentration in any part of the overall system. These nonappearing arrangements are e_1e_2 , e_2e_1 , e_1m_2 , $e_2m_1e_1$, $e_2m_2e_1$, $e_1m_1m_2$, $e_1m_2m_2$, $e_1m_2e_1$, and $e_1m_2m_1$. Graph A of Figure 3, representing the neso compound $(\text{CH}_3)_2\text{GeCl}_2$, shows an abrupt change at the diagonal leading from $R = 0$ with $R' = 1$ to $R = 2$ with $R' = 0$. On the lower left side of this diagonal this compound is obviously in equilibrium with oligomeric and polymeric structures containing dimethylgermanium groups, whereas on the other side of the diagonal it is apparent that all the dimethylgermanium is to be found as the $(\text{CH}_3)_2\text{GeCl}_2$ molecule. Graph B shows that the silicon neso compound appears only above the diagonal, so that in the region below the diagonal, where we had inferred from graph A that germanium is involved in the larger molecules, there is no $(\text{CH}_3)_2\text{SiCl}_2$. Graphs C to E demonstrate that germanium end groups appear only below the diagonal. Likewise, graphs F and G show that the opposite is true of silicon end groups. From graphs H to M it is apparent that germanium middle groups are to be found only below the diagonal. On the other hand, graphs N to U show that silicon middle groups are found throughout the diagram.

The quantitative data given in Figure 3 may be summarized by pointing out that in the upper right-hand portion of the diagrams (above the diagonal) siloxane polymers are dissolved in dimethyldichlorogermane. This represents the situation in which the latter acts as an "inert" solvent, even though it is at equilibrium with respect to exchange of its chlorine atoms with either the chlorines or bridging oxygen atoms of the siloxanes. In the lower left-hand portion of the graphs mixed germoxane-siloxane molecules are to be found (see graphs E, J, L, M, N, P, Q, S, and T). The interesting behavior of this system, in which the diagonal line is a simple mixture of $(\text{CH}_3)_2\text{GeCl}_2$ and $[(\text{CH}_3)_2\text{SiO}]_n$ (see graphs A and U) is attributable to the very large positive value of the equilibrium constant K_T .

We wish to thank Raymond E. Miller for the NMR measurements and Leo C. D. Groenweghe and David W. Matula for the mathematical apparatus employed in this work.

References

1. K. A. Andrianov, *Metalorganic Polymers*, Interscience, New York, 1965.
2. J. I. Jones, in *Developments in Inorganic Polymer Chemistry*, M. F. Lappert and G. J. Leigh, Eds., Elsevier, 1962, Ch. 7 and 8, pp. 162-255.
3. K. Moedritzer and J. R. Van Wazer, *J. Am. Chem. Soc.*, **86**, 802 (1964).
4. K. Moedritzer and J. R. Van Wazer, *Inorg. Chem.*, **4**, 1753 (1965).
5. L. C. D. Groenweghe, private communication from the Monsanto Company.
6. D. W. Matula, L. C. D. Groenweghe, and J. R. Van Wazer, *J. Chem. Phys.*, **41**, 3105 (1964).
7. J. R. Van Wazer and K. Moedritzer, *Angew. Chem. Intern. Ed. Engl.*, **5**, 341 (1966).
8. J. R. Van Wazer, K. Moedritzer, and L. C. D. Groenweghe, *J. Organomet. Chem.*, **5**, 420 (1966).

9. K. Moedritzer and J. R. Van Wazer, *J. Am. Chem. Soc.*, in press.
10. K. Moedritzer and J. R. Van Wazer, *Inorg. Chem.*, **3**, 268 (1964).
11. J. R. Van Wazer and K. Moedritzer, *J. Inorg. Nucl. Chem.*, **26**, 737 (1964).
12. D. N. Hunter, *Inorganic Polymers*, Wiley, New York, 1963.
13. F. R. Gimblett, *Inorganic Polymer Chemistry*, Butterworths, London, 1963.
14. E. L. Geftter, *Organophosphorus Monomers and Polymers*, Associated Technical Services, Inc., Glen Ridge, N.J., 1962.

Received June 13, 1967

Revised August 9, 1967

Lithiation of Diene Polymers

YUJI MINOURA, KYO SHIINA, and HIROSHI HARADA,
*Department of Applied Chemistry, Faculty of Engineering,
Osaka City University, Kitaku, Osaka, Japan*

Synopsis

It was found that the metallation of diene polymers with *n*-butyllithium in *n*-heptane takes place in the presence of a tert amine, i.e. *N,N,N',N'*-tetramethylethylenediamine. Butyllithium was added to the diene polymer in *n*-heptane in the presence of an equimolar amount of the amine, and the mixture was allowed to react at 80°C. for 60 min. under nitrogen. As a result, 27% and 9% per monomer unit for polybutadiene and polyisoprene, respectively, were metallated. The effects of the concentrations of the diene polymer, butyllithium, and the amine on the reaction were studied at 80°C., and the reaction mechanism was discussed. The overall rate of metalation was proportional to the diene polymer concentration and to the square root of the butyllithium concentration. The overall activation energies of metalation were 6.6 and 8.4 kcal./mole for polybutadiene and polyisoprene, respectively. Many kinds of polymer derivative were obtained by treating the metallated polymers with various reagents, such as carbon dioxide, Michler's ketone, trimethylchlorosilane, triphenylchlorosilane, benzaldehyde, and pyridine.

INTRODUCTION

The reactions of vinyl polymers such as polystyrene and poly(vinyl chloride) have been widely investigated. As regards the metalation reactions of polymers, examples of polystyrene¹ and some others are known, which are used for synthesizing polymer derivatives. However, the reactions of polymers of the diene type are sometimes accompanied by undesirable secondary reactions, such as gelation, so that no extensive study has been made of these reactions. In particular, there has been no example of the metalation of diene polymers.

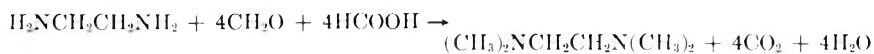
We have investigated the direct metalation of diene polymers, such as 1,4-*cis*-polybutadiene and 1,4-*cis*-polyisoprene, using an organolithium compound, *n*-butyllithium, and then producing polymer derivatives or anionic graft copolymers with vinyl monomers, using the lithiated diene polymers obtained. So far the metallation by *n*-butyllithium of hydrocarbons having nonconjugated double bonds, such as diene polymers, has been regarded as difficult. Recently, however, Eberhardt and Butle² reported that the metalation of hydrocarbons having an extremely weak acidity, such as toluene or benzene, was possible by making a strong Lewis base, such as a tertiary amine, coexist in *n*-butyllithium.

Knowing that tertiary amines are effective for the metallation of aromatic hydrocarbons, we investigated in this work the metallation of diene polymers, using *n*-butyllithium in the presence of a tertiary amine, i.e. *N,N,N',N'*-tetramethylethylenediamine. Then we tried synthesizing polymer derivatives by making the lithiated polymers thus obtained react with various reagents, such as carbon dioxide, Michler's ketone, trimethylchlorosilane, triphenylchlorosilane, benzaldehyde, and pyridine.

EXPERIMENTAL

Materials

1,4-*cis*-Polybutadiene (Phillips Cis4) and 1,4-*cis*-polyisoprene (Cariflex 305), which hereinafter are designated PB and PI, were used after reprecipitation and drying. Squalene was distilled under vacuum; b.p., 203°C. at 0.15 mm. Hg. Commercial butyllithium (BuLi) solution in *n*-hexane was used after the concentration had been determined by Gilman's double titration.³ *N,N,N',N'*-Tetramethylethylenediamine (TMEDA) was synthesized from ethylene diamine by the Eschweiler-Clarke reaction;⁴ b.p., 121°, $n_D^{20} = 1.4189$.



The solvent *n*-heptane was refluxed with sodium wire and distilled, after traces of aromatic hydrocarbons and olefins had been removed by nitration. Benzene was similarly dehydrated. For carbon dioxide, Dry Ice was used in the form of a slurry in tetrahydrofuran (THF).

Michler's ketone, trimethylchlorosilane, triphenylchlorosilane, benzaldehyde, pyridine, and other reagents were obtained from several commercial sources.

Reactions

Lithiation of Polymers. An *n*-heptane solution of the polymer and TMEDA were placed in a reaction tube, which had a nitrogen inlet, and which was cooled in a Dry Ice-methanol bath, and the inside of the tube was degassed and then filled with dry nitrogen. A given amount of BuLi was injected from a syringe during flushing with nitrogen, and the reaction was carried out in an oil bath at a constant temperature under a nitrogen atmosphere.

Several minutes after the start of the reaction the color turned from a light yellow to a red and then to a dark red and, as the lithiation progressed, part of the polymer was deposited. The reaction mixture was cooled with ice immediately after the reaction and thereafter subjected to the following reactions.

Carbonation of Lithiated Polymer. The reaction mixture was poured on to a slurry of Dry Ice and THF and agitated violently. The reaction polymer was dissolved or swelled in THF or water and hydrolyzed by formic

acid. The carbonated polymer was reprecipitated with a THF-water system and dried.

Lithiated PB and Michler's ketone. A 0.54 g. amount of PB (0.01 mole of monomer unit) was dissolved in 25 ml. of *n*-heptane in a 100 ml. three-necked flask, to which was added TMEDA (0.01 mole) and BuLi (0.01 mole) from a syringe during flushing with nitrogen. The reaction was carried out under a nitrogen atmosphere at 80°C. for 1 hr. After the reaction the temperature was reduced to room temperature, and a solution of Michler's ketone (0.01 mole) in benzene was added under stirring. After 90 min. it became a green, homogeneous solution, which was poured into methanol, and the product polymer was reprecipitated by means of a benzene-methanol system. The yield was 0.9 g. of a yellowish-brown powder. Then 0.12 g. of the reaction polymer was dissolved in chloroform, to which was added a chloroform solution of iodine, and immediately the characteristic malachite green developed. The dark-blue precipitate was filtered and washed repeatedly with water. The yield was 0.18 g.

Lithiated PB and Trimethylchlorosilane and Triphenylchlorosilane. Lithiated PB (0.01 mole) obtained under the same conditions as those mentioned above (2.2.3.) was allowed to react with 2 g. of trimethylchlorosilane (0.018 mole) and 5 g. of triphenylchlorosilane, respectively, each in 30 ml. of benzene. In each case the system turned from a dark red to a light yellow and became a homogeneous solution. After 2 hr. the reaction mixture was precipitated in methanol and filtered. The product polymers were dissolved in toluene and, after the small quantity of insoluble residue had been filtered off, were reprecipitated in methanol.

Lithiated PB and Benzaldehyde. A 1.6 g. amount of benzaldehyde (0.015 mole) in 20 ml. of benzene was allowed to react with the lithiated PB (0.01 mole) obtained under the same conditions as those mentioned above. The product polymer was hydrolyzed by water and then reprecipitated with a benzene-methanol system.

Lithiated PB and Pyridine. A 1.2 g. amount of pyridine (0.01 mole) in 20 ml. of benzene was permitted to react with lithiated PB (0.01 mole), obtained under the same conditions as those described above. The reaction product, which was precipitated in methanol, washed repeatedly and dried, was an insoluble light-yellow polymer.

Analysis Method

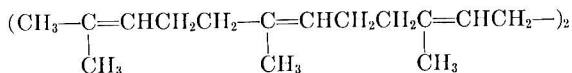
Degree of Lithiation. Since it is not possible to measure the degree of lithiation of lithiated diene polymers directly, the carboxylic group content of the polymers obtained by carbonation of the lithiated polymers was used for estimating the degree of lithiation. In the estimation 150 mg. of the carboxylic polymer was dissolved in 30 ml. of dry pyridine and titrated with 0.1*N* alcoholic KOH.⁵ Phenolphthalein was used as the indicator.

Degree of Unsaturation of Polymer. The double-bond content in the polymer was determined⁶ by means of the addition reaction of iodine monochloride.

RESULTS AND DISCUSSION

Lithiation of Squalene

To determine the mechanism of the lithiation of diene polymers by BuLi, a test on squalene, which is considered the model substance for diene polymers, was carried out. Squalene is a liquid having the following formula:



Squalene was dissolved in *n*-heptane, to which was added 6 eq. of BuLi and TMEDA (equivalent to the double bonds of squalene). The mixture was heated at 80°C. for 1 hr. under a nitrogen atmosphere. After the reaction part of the reaction mixture was hydrolyzed by ethanol, and the remainder was carbonated, and the infrared spectrum of each product was compared with the original squalene (Fig. 1). The unsaturations, molecular weights, and neutralization equivalents of the reaction products and squalene also were measured; the results are shown in Table I.

From Figure 1 it may be seen that the carbonated reaction product showed the strong characteristic absorptions of the carboxylic group at 2600, 1710, 1420, 1290, and 930 cm^{-1} , showing that squalene had been lithiated. However, the infrared spectrum of the hydrolysis product of the lithiated squalene was the same as that of the original squalene, the unsaturation showing little reduction and the molecular weight being unchanged. Therefore, it is considered that BuLi did not add to the double bond of squalene, but that the exchange reaction took place between lithium and the allylic hydrogen

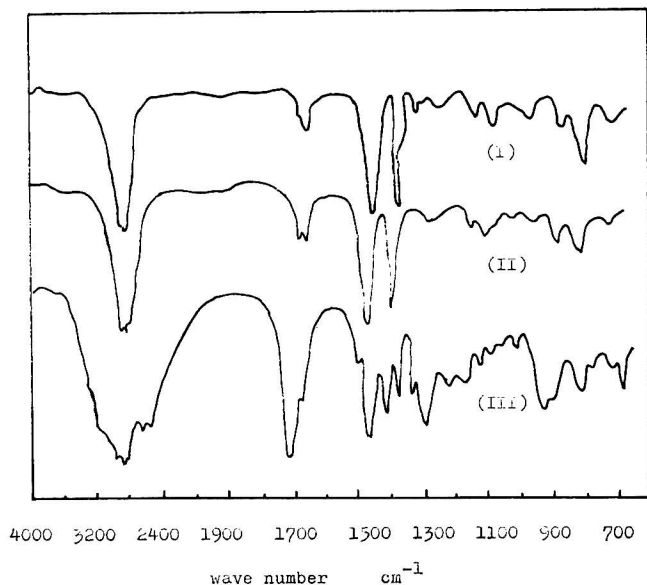


Fig. 1. Infrared spectra of products of reaction between squalene and BuLi: (I) original squalene; (II) hydrolyzed product; (III) carbonated product.

TABLE I
Analyses of Reaction Products of Squalene and BuLi^a

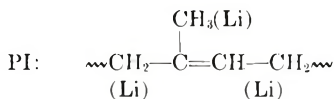
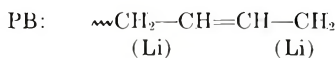
	Mol. wt. ^b	Unsaturation, %	Neutralization equiv.	Character
Original squalene	417	98	0	oil
Hydrolyzed product	416	93	0	oil
Carbonated product	—	—	174 ^c	wax

^a Reaction conditions: squalene, 0.01 mole; BuLi and TMEDA, 0.06 mole; solvent, *n*-heptane; temperature, 80°C.; time, 60 min.

^b Determined by the cryoscopic method in benzene.

^c 1.3 of COOH group per squalene molecule.

of the polymer. Thus, squalene was lithiated 1.3 per molecule of squalene. The same may be considered in the case of PB and PI:



Lithiation of Diene Polymers

Effect of Polymer Concentration. Reactions were carried out keeping the $[\text{BuLi}]_0$ and $[\text{TMEDA}]_0$ (initial concentrations of BuLi and TMEDA, respectively) constant and changing $[\text{PB}]_0$ (initial concentration of PB), at 80°C. Carbonation of the lithiated polymers was carried out after the required reaction time. The reaction degrees were determined from the COOH contents of the carbonated products, the results of which are shown in Figure 2.

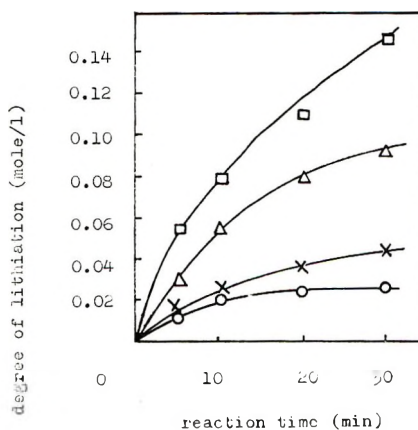


Fig. 2. Conversion of PB in lithiation as a function of time. Concentrations (moles per liter): $[\text{PB}]_0$, (○) 0.16; (×) 0.26, (Δ) 0.52 at 80°C., (□) 0.78; $[\text{BuLi}]_0$, 0.26; $[\text{TMEDA}]_0$, 0.26.

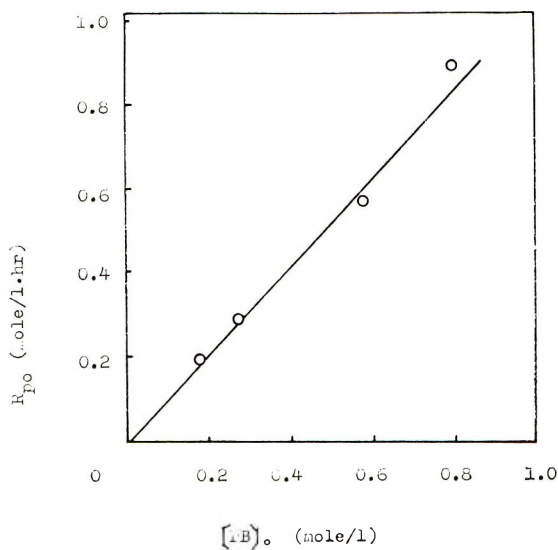


Fig. 3. Initial rate of lithiation versus initial concentration of PB at 80°C. Initial concentrations (moles per liter): $[BuLi]_0$, 0.26; $[TMEDA]_0$, 0.26.

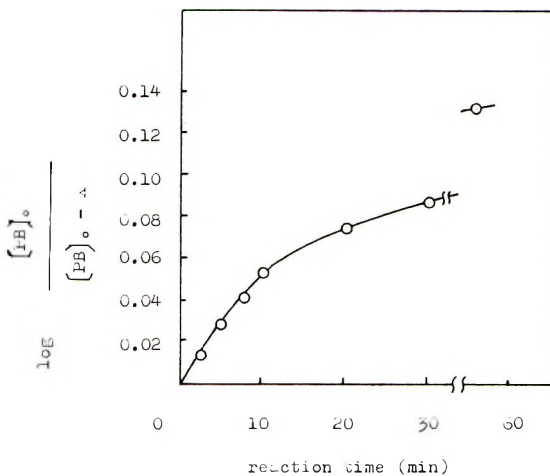


Fig. 4. First-order consumption plot of PB. Initial concentrations (moles per liter): $[PB]_0$, 0.26; $[BuLi]_0$, 0.26. Reaction temperature, 80°C.; X , concentration of lithiated PB.

The initial reaction velocity R_{p0} at each concentration was obtained from the tangential gradient at the origin in Figure 2, and by plotting R_{p0} against $[PB]_0$ Figure 3 was obtained. From Figure 3 it was found that R_{p0} was proportional to the first order of $[PB]_0$. Moreover, as is clear from the relation between the first-order consumption velocity of PB and the reaction time (Fig. 4), up to about 10 min. after the reaction started, or up to the lithiation of about 11% per monomer unit of PB, the first-order relation was maintained relative to $[PB]_0$, but thereafter a sudden deviation of this

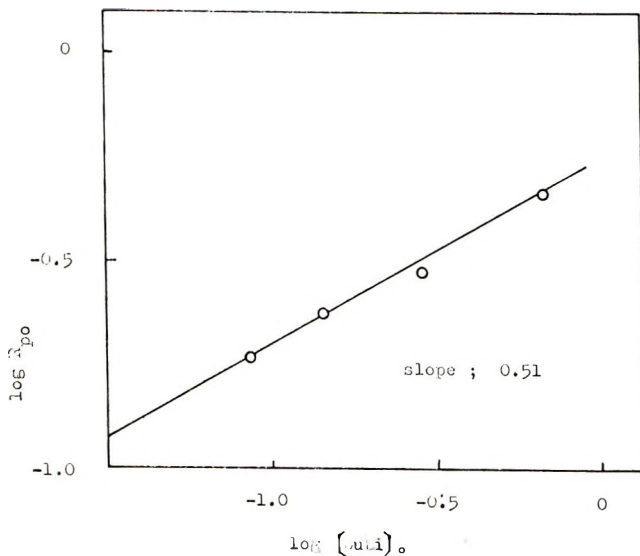


Fig. 5. Logarithmic plot of initial lithiation rate versus initial concentration of BuLi at 80°C. Initial concentrations (moles per liter): $[\text{PB}]_0$, 0.26; $[\text{TMEDA}]_0$, 0.26; $[\text{BuLi}]_0$, 0.078 and 0.52.

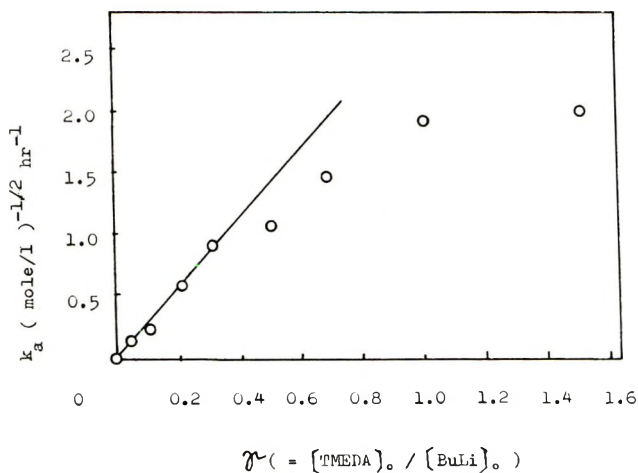


Fig. 6. Rate constant K_a of lithiation, versus initial concentration of $[\text{TMEDA}]_0$. Initial concentrations (moles per liter) at 80°C.: $[\text{PB}]_0$, 0.26; $[\text{BuLi}]_0$, 0.26.

relation was observed. This phenomenon agreed well with the time that the separation of lithiated PB started. Thus it is thought that this is caused by the polymer precipitation. As a result, after BuLi had been added to diene polymers in *n*-heptane in the presence of an equimolar amount of TMEDA, and the mixture had been allowed to react at 80°C. for 60 min. under nitrogen, it was found that 28 and 9% per monomer unit for PB and PI, respectively, were metalated.

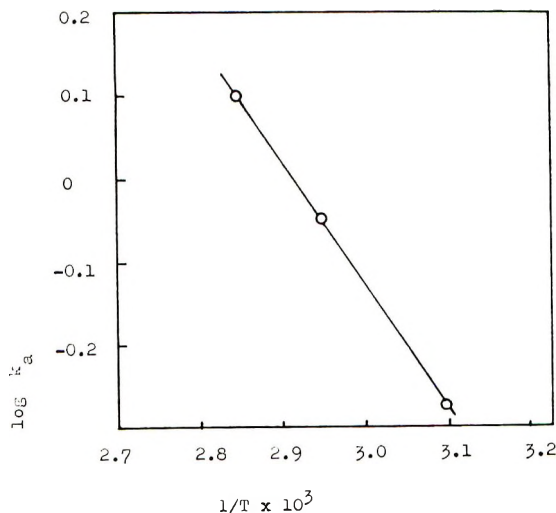


Fig. 7. Arrhenius plot for lithiation of PB. Initial concentrations (moles per liter): $[\text{PB}]_0$, 0.41; $[\text{BuLi}]_0$, 0.42; $[\text{TMEDA}]_0$, 0.42.

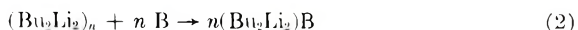
Effect of BuLi Concentration. The effect of the BuLi concentration on the lithiation when $[\text{PB}]_0$ and $[\text{TMEDA}]_0$ were maintained constant was investigated. Figure 5 shows $\log R_{p0}$ in relation to $\log [\text{BuLi}]_0$. It was found from the slope of the straight line obtained that R_{p0} is proportional to about a half-order of $[\text{BuLi}]_0$. As a result, the kinetic formula of this reaction is represented as follows:

$$R_p = K_a[\text{PB}][\text{BuLi}]^{1/2} \quad (1)$$

But k_a changes, depending upon the TMEDA concentration.

Effect of TMEDA Concentration. To determine the effect of the TMEDA concentration, the lithiation of PB was carried out with $[\text{PB}]_0$ and $[\text{BuLi}]_0$ constant and various $[\text{TMEDA}]_0$. The relation between k_a and $\gamma = [\text{TMEDA}]_0/[\text{BuLi}]_0$ is shown in Figure 6. From Figure 6 it was found that the relation between γ and k_a was a straight line passing through the origin. Therefore, it was confirmed that no lithiation took place with BuLi alone and that the amine definitely participated in the reaction.

Eastham and his co-workers⁷⁻⁹ and others explained that BuLi was dissociated into the solvated dimer in the presence of small quantities of a Lewis base as (amine or ether) and associated to hexamer in hydrocarbon solution:



where B is a Lewis base and n is equal to 3. Further, they confirmed that in the case of a diamine, such as triethylene diamine (TED), a complex with alkyllithium, $(\text{R}_2\text{Li}_2\text{-TED-R}_2\text{Li}_2)$ was produced quantitatively.¹⁰

The fact that R_p is proportional to the square root of the BuLi concentration in the lithiation of diene polymer is explained by the existence of BuLi

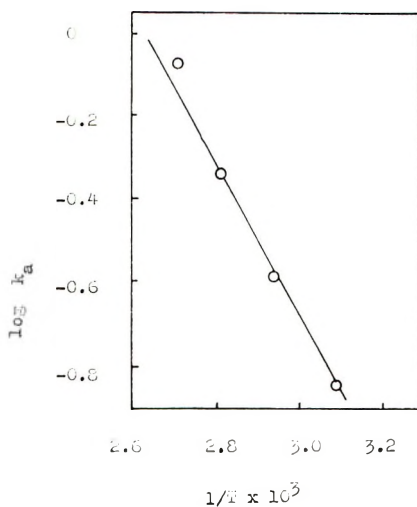
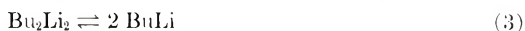


Fig. 8. Arrhenius plot for lithiation of PI. Initial concentrations (moles per liter): $[\text{PI}]_0$, 0.38; $[\text{BuLi}]_0$, 0.38; $[\text{TMEDA}]_0$, 0.38.

as the dimer in the presence of TMEDA and of the equilibrium between the dimer and monomeric BuLi, which attacks the diene polymers, as follows



In this case it is not clear how TMEDA is coordinated to $(\text{BuLi})_2$, but since the deviation of k_a from the straight line became large at the place where γ was in the range 0.2 to 0.3, it is considered that, as in the case of TED, the TMEDA and BuLi form a 1:4 complex.

Effect of Reaction Temperature. The lithiation velocities of PB and PI at various temperatures were investigated. When $\log k_a$ was plotted against $1/T$, a straight line was obtained (Figs. 7 and 8), and from each gradient the overall activation energy of lithiation was calculated. As a result, 6.6 and 8.4 kcal./mole for PB and PI, respectively, were obtained.

Characterization of Hydrolyzed Product of Lithiated Polymers

Lithiated PB and PI were hydrolyzed by ethanol, and the products were compared with the original polymers. Tables II and III show the changes

TABLE II
Hydrolyzed Product of Lithiated PB^a

Reaction time, ^b min.	Lithiation, %	Unsaturation, %	$[\eta]$ at 30°C. in toluene
0	0	97.8	2.4
10	12	96.3	0.5
30	18	95.7	0.2
60	27	92.3	0.1

^a Initial concentrations (moles/l.): $[\text{PB}]_0$, 0.26; $[\text{BuLi}]_0$, 0.26; $[\text{TMEDA}]_0$, 0.26.

^b Reaction at 80°C.

TABLE III
Hydrolyzed Product of Lithiated PI^a

Reaction time, ^b min.	Lithiation, %	Unsaturation, %	[η] at 30°C. in toluene
0	0	98.2	4.10
10	3.0	97.0	1.1
30	5.9	97.5	0.55
60	8.9	95.0	0.68
120	12.5	95.0	0.50

^a Initial concentrations: $[PI]_0 = [BuLi]_0 = [TMEDA]_0 = 0.18$ mole/l.^b Reaction at 80°C.

of lithiation degree, unsaturation percentage, and intrinsic viscosity with reaction time for PB and PI, respectively. In this case there was no change in the infrared spectrum of the hydrolyzed polymer. It was found that in all the cases the changes in unsaturation percentage were small. From the decrease of unsaturated bond it was considered that a reaction of the double bond with BuLi took place slightly, too. The intrinsic viscosity decreased with the progress of the lithiation, and the chain scission of PB was more than that of PI. This phenomenon was especially noticeable, but the reason for the chain scission was not clear.

Characterization of Carbonated Polymers

It is thought that the carboxylic polymers obtained by the carbonation of the lithiated PB have the construction shown by (I) below:

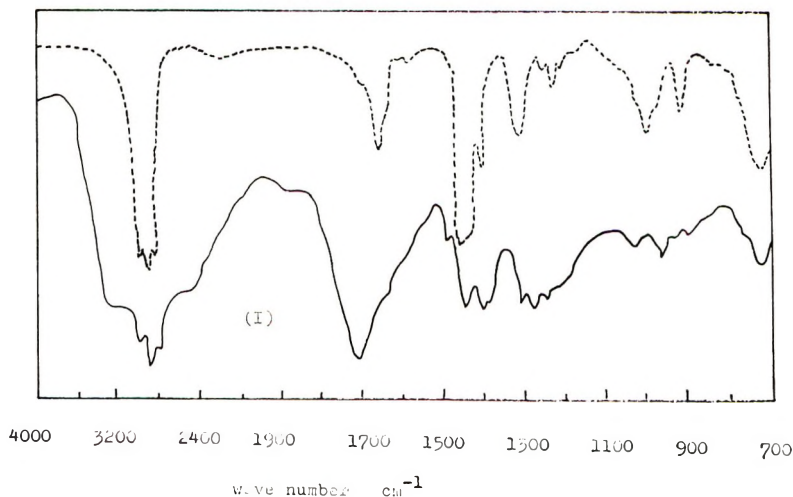
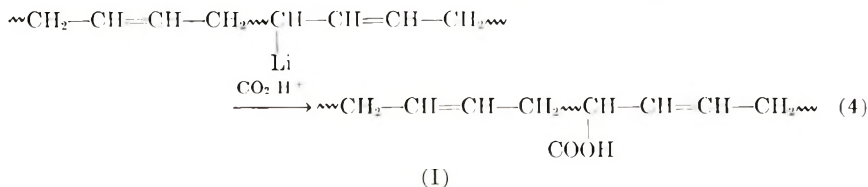


Fig. 9. Infrared spectra of carboxylic polymer: (---) original PB; (I) carboxylic polymer.

TABLE IV
Characterization of Carboxylic PB

COOH content, %	Solvent ^a				Character	$[\eta]$ in THF at 30°C.
	Benzene	Pyridine or THF	DMF	aq. NaOH		
7.2	sol.	sol.	ins.	ins.	rubberlike	—
19.2		sol.	sol.	sol.	mass	—
28.6		sol.	sol.	sol.	powder	0.1

^a Sol., soluble; insol., insoluble.

The infrared spectrum of the carboxylic polymer shown in Figure 9 showed bands characteristic of the carboxylic group in the neighborhood of 3400, 2600, 1710, 1290, and 930 cm^{-1} . The properties of the carboxylic polymer obtained are given in Table IV. As the COOH content increased, the polymers changed from a viscous rubber to a thermoplastic powder. The solubility of the polymer also changed according to the COOH group content. Thus, the polymer having a low COOH content was soluble in benzene and chloroform, but the polymer having a high COOH content was insoluble in benzene and soluble in THF, pyridine, dimethylformamide, and aqueous alkali.

Characterization of Reaction Product with Michler's Ketone

The deep-green color (malachite green) obtained from the reaction with Michler's ketone, followed by the oxidation of the derived *tert*-carbinol with iodine, is a most useful and familiar means of identifying organoalkali com-

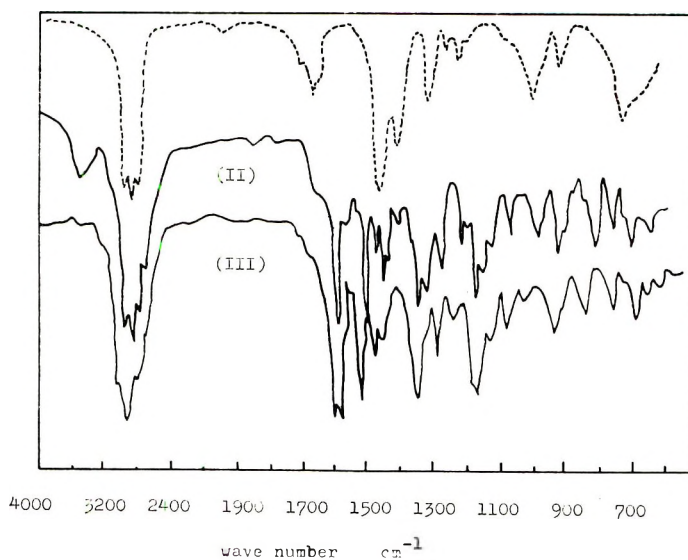


Fig. 10. Infrared spectra of reaction products with Michler's ketone: (---) original polymer; (II) *tert*-carbinol polymer; (III) malachite green polymer.

pounds. A light-yellow powdery polymer was obtained from the reaction of Michler's ketone with lithiated PB, which was changed to a deep-green or deep-blue powder by iodine. These results afford evidence of the existence in the reaction mixture of a polymeric lithium component, by which Michler's ketone was attacked, as shown in eq. (5):

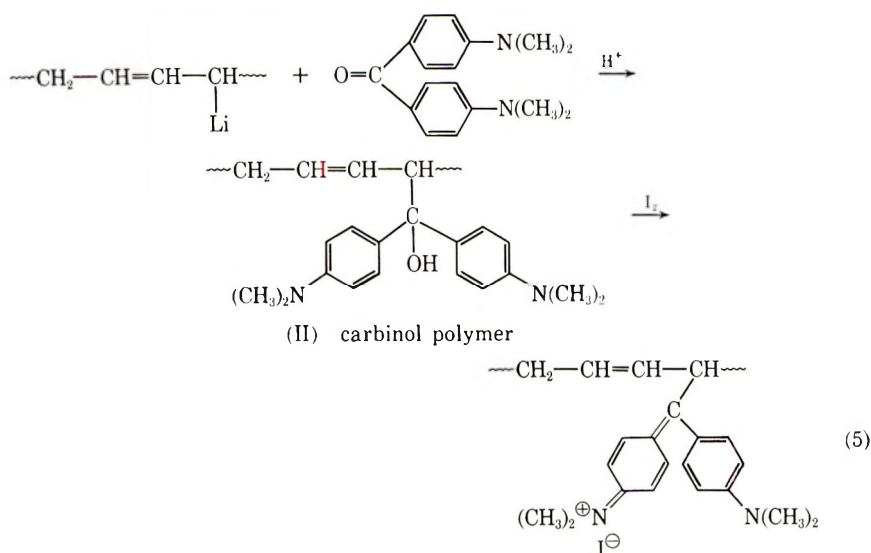


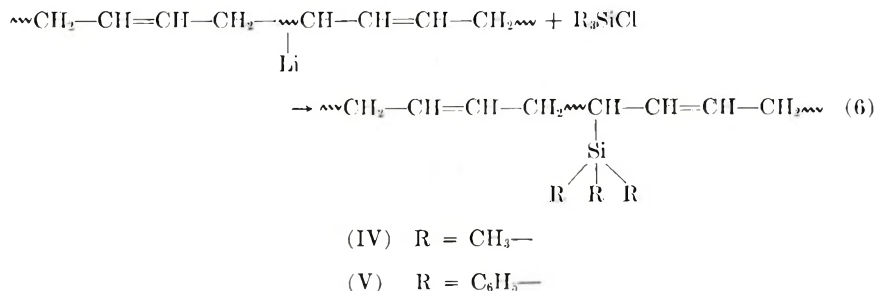
Figure 10 shows the infrared spectra of (II) and (III). In (II) a band characteristic of OH at 3500 cm.^{-1} , aromatic ring absorption at 1610 , 1520 , and 810 cm.^{-1} , and $\text{N}=\text{CH}_3$ absorption at 1290 cm.^{-1} were observed. Moreover in (III) a strong band due to $\text{C}=\text{N}^+$ was observed at 1580 cm.^{-1} . The reaction conditions and results of the analyses for (II) and (III) are given in Table V. The carbinol polymer (II) had a nitrogen content of 5.83% , which corresponded to 25.6 units of malachite green per 100 monomer units of PB. This value coincided well with the COOH content (27.0) of the carboxylic polymer obtained by lithiation under the same conditions. Product (II) was soluble in benzene and chloroform, but (III) was insoluble in nonpolar solvents, owing to its salt construction, and soluble in a THF-methanol system. However, this polymer was insoluble in water, which is a very good solvent for malachite green.

TABLE V
Results of Reaction Between Lithiated PB and Michler's Ketone

	Analyses of polymer, %			$[\eta]$ toluene 30°C.	Appearance
	C	H	N		
II	80.6	7.31	5.83	0.1	light-yellow powder
III	76.6	5.55	2.93	—	dark-blue powder, dark green in solution

Characterization of Reaction Products Between Lithiated PB and Trimethylchlorosilane and Triphenylchlorosilane

It is known that organolithium compounds react with organosilicon compounds of the type R_3SiCl and produce condensation products. When trimethylchlorosilane and triphenylchlorosilane, respectively, were allowed to react with lithiated PB, polymers having the constructions (IV) and (V) in eq. (6), respectively, were expected:



Infrared spectral studies of (IV) showed absorptions of $\text{Si}=\text{CH}_3$ at 1259 and 840 cm^{-1} , and studies of (V) showed absorptions of $\text{Si}=\text{C}_6\text{H}_5$ at 1780 to

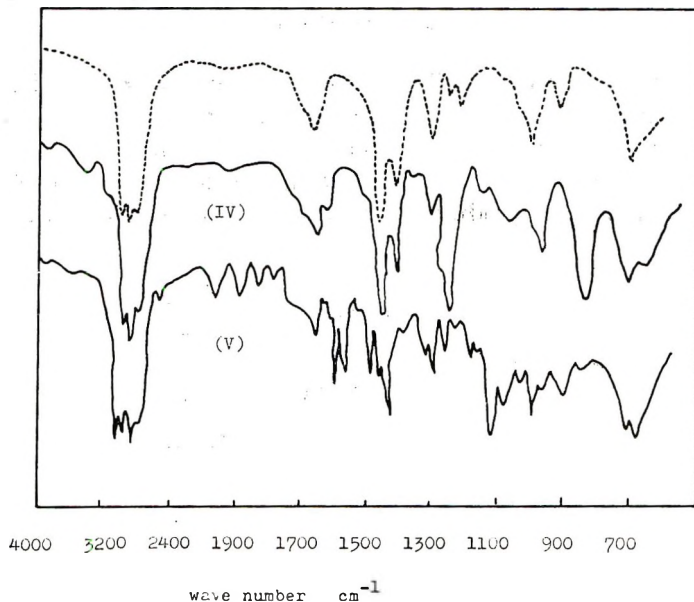


Fig. 11. Infrared spectra of reaction products with (IV) trimethylchlorosilane and (V) triphenylchlorosilane; (---) original PB.

1970, 1592, 1120, and 700 cm^{-1} ; see Figure 11. Substance (IV) was a light-yellow viscous polymer, and (V) was a yellowish-brown polymer. They were both soluble in benzene and chloroform.

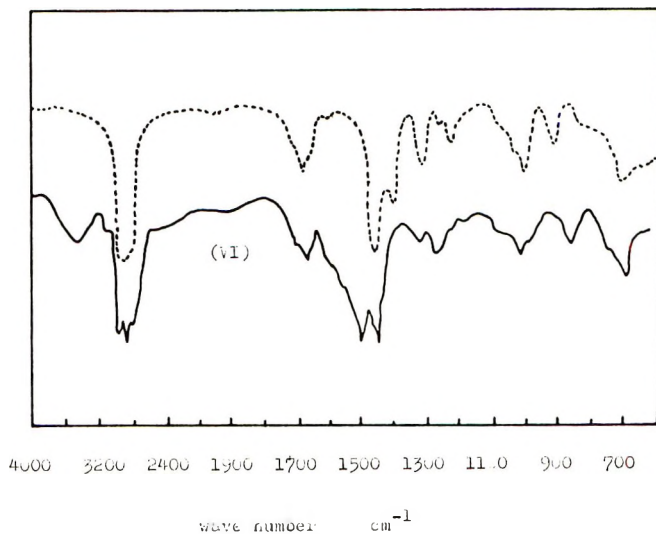
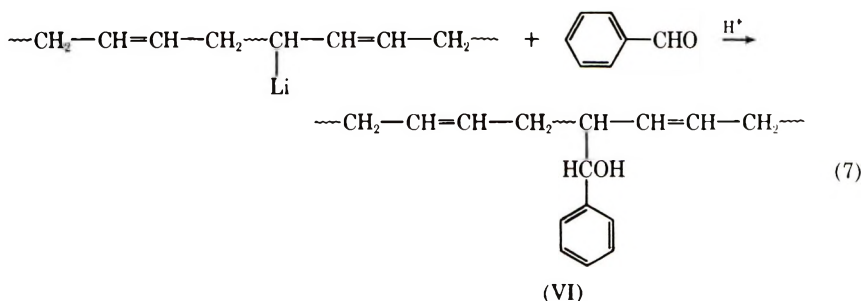


Fig. 12. Infrared spectrum of reaction product with (VI) benzaldehyde; (---) original PB.

Characterization of Reaction Product Between Lithiated PB and Benzaldehyde

When lithiated PB was allowed to react with benzaldehyde, it was thought that the polymer having the construction (VI) in eq. (7) was obtained. The infrared spectrum of (VI), shown in Figure 12, showed an OH absorption at 3500 cm.^{-1} and aromatic ring absorptions at 1603, 1495, 830, and 700 cm.^{-1} . The product polymer was brown and viscous.



Characterization of Reaction Product Between Lithiated PB and Pyridine

The reaction product between lithiated PB and pyridine was a light brown and was a crosslinked polymer insoluble in organic solvents. The analysis of this polymer showed a nitrogen content of 2.3%.

References

1. D. Braun, *Makromol. Chem.*, **30**, 85 (1959).
2. G. G. Eberhardt and W. A. Butle, *J. Org. Chem.*, **29**, 2928 (1964).
3. H. Gilman and A. H. Hanbein, *J. Am. Chem. Soc.*, **66**, 1515 (1944).
4. H. F. Clarke and H. B. Gillespie, *J. Am. Chem. Soc.*, **55**, 4571 (1933).
5. H. P. Brown, *Rubber Chem. Technol.*, **30**, 1347 (1957).
6. T. Lee, *J. Polymer Sci.*, **3**, 66 (1948).
7. J. F. Eastham and G. W. Gibson, *J. Am. Chem. Soc.*, **85**, 2171 (1963).
8. Z. K. Cheema, G. W. Gibson, and J. F. Eastham, *J. Am. Chem. Soc.*, **85**, 3517 (1963).
9. F. A. Settle, M. Haggerty, and J. F. Eastham, *J. Am. Chem. Soc.*, **86**, 2076 (1964).
10. C. G. Screttas and J. F. Eastham, *J. Am. Chem. Soc.*, **87**, 3276 (1965).

Received July 3, 1967

Revised August 17, 1967

Chain Transfer for Vinyl Monomers Polymerized in *N*-Allylstearamide

EDMUND F. JORDAN, JR., BOHDAN ARTYMYSHYN, and
A. N. WRIGLEY, *Eastern Regional Research Laboratory, Eastern Utilization
Research and Development Division, Agricultural Research Service,
U.S. Department of Agriculture, Philadelphia, Pennsylvania 19118*

Synopsis

Apparent transfer constants have been determined for styrene, methyl methacrylate vinyl acetate, and diethyl maleate polymerized in *N*-allylstearamide at 90°C. Regression coefficients for transfer were: methyl methacrylate, 0.301×10^{-3} ; styrene, with no added initiator, 0.582×10^{-3} ; styrene, initiated with benzoyl peroxide, 0.830×10^{-3} ; vinyl acetate, 62.01×10^{-3} ; and diethyl maleate, 2.24×10^{-3} . Rates of polymerization were retarded for both styrene and methyl methacrylate. Vinyl monomer and comonomer disappearance followed an increasing exponential dependence on both initiator and monomer concentration. Although degradative chain transfer probably caused most of the retardation, the cross-termination effect was not eliminated as a contributing factor. Rates for the vinyl acetate copolymerization were somewhat retarded, even though initiator consumption was large because of induced decomposition. The kinetic and transfer data indicated that the reactive monomers added radicals readily, but that rates were lowered by degradative chain transfer. Growing chains were terminated at only moderate rates of transfer. Unreactive monomers added radicals less easily, producing reactive radicals, which transferred rapidly, so that molecular weights were lowered precipitously. Although induced initiator decomposition occurred, rates were still retarded by degradative chain transfer. A simple empirical relation was found between the reciprocal number-average degree of polymerization, $1/\bar{X}_{n1}$ and the mole fraction of allylic comonomer entering the copolymer F_2 , which permitted estimation of the molecular weight of copolymers of vinyl monomers with allylic comonomers. This equation should be applicable when monomer transfer constants for each homopolymer are known and when osmometric molecular weights of one or two copolymers of low allylic content have been determined.

INTRODUCTION

It has been known for a long time that copolymers of vinyl monomers with allylic comonomers generally have substantially lower molecular weights than entirely vinyl copolymers of the same molar composition. This is a consequence of the ease of hydrogen abstraction from allylic monomers by chain radicals,¹ which terminates their growth, and lowers the molecular weights of the copolymers. Rates of copolymerization are also abnormally lowered because of degradative destruction of the resonance-stabilized allylic radicals. Qualitative demonstrations of these

effects were found in copolymerization studies of styrene and allyl chloride,² acrylonitrile and allyl alcohol,³ maleic anhydride and allyl acetate,⁴ and ethyl acrylate and allyl chloride.⁵ In examples from the patent literature, allylic comonomers were used to control molecular weight in copolymers^{6,7} and to produce telomers.^{8,9} Using a more quantitative approach to allylic transfer, several authors have determined transfer constants for selected vinyl monomers in the presence of allyl monomers considered as solvents. In this way, vinyl acetate was studied in allyl chloride, allyl acetate, and methallyl chloride;¹⁰ and ethylene,¹¹ methyl methacrylate,¹² and styrene¹³ in 1-olefins. In general, the magnitude of the constants increased with vinyl radical reactivity.

As part of a general investigation of the use of long-chain vinyl monomers in homopolymerization and copolymerization, apparent transfer constants were determined for several vinyl monomers using *N*-allylstearamide as the solvent. *N*-Allylstearamide was selected because its homopolymerization characteristics¹⁴ and copolymerization parameters¹⁵ were known, and because of its ease of preparation.¹⁶ Four vinyl monomers, namely, styrene, methyl methacrylate, vinyl acetate, and diethyl maleate, were chosen because of their large differences in reactivity in vinyl copolymerization. Each occupies one of the four quadrants of the Price-Alfrey *Q* and *e* map.¹⁷ Calculated^{15,18a} instant copolymer compositions and reactivity ratios for each system investigated (Fig. 1) illustrate the reactivity differences. Since *N*-allylstearamide melts at 85°C., all polymerizations were conducted at 90°C. A useful and general empirical expression was derived which provides an estimation of molecular weight of copolymers containing allylic comonomers based on knowledge of the reactivity ratios for the system and the molecular weight of one or two copolymers of known allylic content.

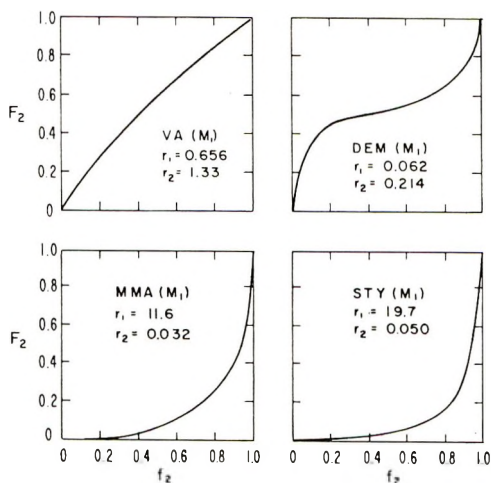


Fig. 1. Plots of mole fraction amide in the feed (f_2) vs. the initial mole fraction of amide in the copolymer (F_2) for vinyl acetate (VA), diethyl maleate (DEM), methyl methacrylate (MMA), and styrene (STY).

EXPERIMENTAL

Monomer Preparation and Purification

N-Allylstearamide was prepared from 99% pure methyl stearate. The amide was made in batches from 174 g. portions of ester. The reactions were run in crown-capped bottles at 70°C. for 24 hr. by using the procedure of experiment 2, previously described.¹⁶ The crude reaction product was isolated as in the reference procedure and crystallized from acetone (10 ml./g.) at 0°C. The yield was 80.69% of a product with m.p. 84.0–85.0°C.

ANAL. Calcd.: C, 77.95%; H, 12.77%; N, 4.33%. Found: C, 78.21%; H, 12.84%; N, 4.30%. The amide was 99% pure by gas-liquid chromatography.

All of the vinyl monomers were of the purest grades available commercially and were distilled before use, usually at reduced pressure, through an efficient column in a nitrogen atmosphere.

Copolymerization and Kinetic Procedure

N-Allylstearamide was charged by use of a long-stem funnel and weighed analytically into either a 25- or 50-ml. round-bottomed flask having a long neck (neck length 25.5 cm., I.D. 10 mm.). The vinyl monomer was introduced by use of a nitrogen-filled syringe fitted with a long needle and was weighed analytically. In general, 4 g. of vinyl monomers and 3–25 g. of *N*-allylstearamide were used for each series. The initiator, when used, was weighed into a small glass cup (length 15 mm., O.D. 9 mm.) and placed in the flask neck on a Teflon-coated bar magnet, held by a similar magnet strapped to the outside neck of the flask. The "elevator" so formed was lowered to the bottom of the neck, the flask was out-gassed five times at –80°C. and at reduced pressure, and sealed after filling with nitrogen. The elevator was then raised to the top of the neck while the amide was allowed to dissolve in the vinyl monomer at 90°C. At equilibrium, the outer bar magnet was removed, permitting the initiator cup to fall into the flask, thus initiating the polymerization. This time was noted as t_0 . During the solution and equilibrium period (30 min.) some thermal homopolymerization of styrene and methyl methacrylate occurred, but was experimentally determined to be negligible (<0.5% conversion). Some precipitation of polymer occurred with styrene and methyl methacrylate, but the vinyl acetate and diethyl maleate systems were homogeneous. Polymerizations were stopped at approximately 10% conversion in most instances (see Table I); the polymers were isolated by precipitation in excess hot methanol, extracted free of amide with hot methanol (except for vinyl acetate, with which petroleum ether, b.p. 63–70°C., was used), and were dried in a vacuum oven at 50°C. to constant weight. Rates were computed by assuming a linear relation for the conversion-time curve between t_0 and t . Quantities in grams were converted to moles per liter by determining, in separate experiments, density at 90°C. as a function of mole fraction for styrene, and methyl methacrylate, at

TABLE I
 Molecular Weights and Compositions of the Copolymers

Experiment No.	\bar{M}_n	$1/\bar{X}_n \times 10^4$	$\frac{[S]}{[M]}$	Amide in	Amide in		Conversion, %	
				feed f_2	copolymer		Homo-	Copoly-
					F_2	Found ^a	polymer ^b	mer ^c
Styrene, no added initiator								
1	1,230,000	0.847	0	0	0	0	4.78	4.78
2	348,300	3.07	0.234	0.190	0.013	0.017	5.36	3.24
3	286,400	3.84	0.534	0.348	0.027	0.032	4.17	1.69
4	173,300	6.58	0.930	0.482	0.045	0.025	3.15	0.93
5	99,800	13.27	2.49	0.713	0.121	0.026	5.32	0.87
6	56,250	25.14	3.96	0.798	0.170		2.79	0.33
Styrene, initiated with benzoyl peroxide ^d								
7	128,200	8.12	0	0	0	0	12.24	12.24
8	100,000	10.74	0.250	0.200	0.015	0.020	12.81	7.44
9	74,850	14.79	0.537	0.349	0.030	0.030	12.26	5.07
10	71,500	16.10	0.981	0.495	0.050	0.046	14.52	4.17
11	51,200	24.84	2.16	0.684	0.105	0.041	9.78	1.73
12	34,700	40.11	3.69	0.787	0.160		5.14	0.66
Methyl methacrylate, initiated with benzoyl peroxide								
13 ^e	5,555,000	0.18	0	0	0	0	10.53	10.53
14	2,640,000	0.38	0	0	0	0	11.57	11.57
15	777,500	1.35	0.250	0.199	0.021	0.012	10.89	6.01
16 ^e	433,200	2.44	0.252	0.201	0.026	0.020	10.10	6.04
17	282,300	3.87	0.520	0.342	0.042	0.024	8.07	3.42
18 ^e	374,150	2.93	0.536	0.349	0.043	0.011	6.21	2.58
19	270,500	4.31	0.982	0.496	0.075	0.025	9.33	2.71
20 ^e	322,350	3.62	0.989	0.492	0.075	0.031	4.76	1.52
21	179,500	7.39	2.19	0.687	0.146	0.033	8.19	1.59
22 ^e	179,850	7.41	2.18	0.686	0.149	0.087	9.26	1.84
Vinyl acetate, initiated with benzoyl peroxide ^d								
23	244,500	3.52	0	0	0	0		14.95
24	53,600	17.49	0.022	0.021	0.032	0.020		11.59
25	32,600	30.74	0.042	0.040	0.060	0.034		11.01
26	24,500	43.60	0.063	0.060	0.087	0.046		10.92
27	21,150	54.20	0.086	0.079	0.121	0.060		10.93
28	17,050	69.00	0.102	0.093	0.133	0.079		18.58
Diethyl maleate, initiated with bisazoisobutyronitrile ^d								
29	9,875	248.3	0.344	0.256	0.482	0.403		2.42
30	9,430	262.8	0.495	0.331	0.500	0.405		3.76
31	9,605	260.4	0.658	0.397	0.515	0.393		4.23
32	9,390	269.6	0.993	0.498	0.535	0.440		4.42
33	9,325	273.9	1.34	0.573	0.550	0.454		3.69
34	8,995	287.9	1.87	0.651	0.573	0.433		3.23

^a From % nitrogen determinations on the copolymer.

^b Calculated as $[\text{g. polymer} - (\text{g. polymer} \times \text{weight fraction of amide in polymer})] \times 100 / \text{initial weight of vinyl monomer}$.

^c Calculated as $\text{g. polymer} / \text{g. total monomer} \times 100$.

^d $[\text{Initiator}] / [\text{styrene}] = 3.50 \times 10^{-4}$; $[\text{initiator}] / [\text{diethyl maleate}] = 5.0 \times 10^{-3}$.

^e No added initiator.

^f Initiator amount necessary to yield 10% conversion calculated by use of constants of eq. (3).

several amide concentrations. Densities were read off of the smooth curve. During the density measurements, added hydroquinone (0.1 wt.-%) was experimentally determined to inhibit polymerization. Monomer and initiator (benzoyl peroxide) concentrations used for the vinyl acetate (Table I) experiments were $[VAc] = 10.82, 9.96, 9.20, 8.52, 7.91,$ and 7.36 mole/l. and $[I] = 0.196, 0.951, 2.19, 4.42, 7.35,$ and 18.96 mmole/l. for experiments 23, 24, 25, 26, 27, and 28, respectively. The rate of polymerization and $R_p/[M]^2$ for experiment 23 were 17.97×10^{-4} mole/l.-sec. and 15.34×10^{-6} l./mole-sec.; the rate of copolymerization and of $R_p/[M]^2$ for experiment 27 were 4.30×10^{-4} mole/l.-sec. and 5.82×10^{-6} l./mole-sec. The rate of copolymerization for experiment 32 of the diethyl maleate series was 0.14×10^{-4} mole/l.-sec. The comonomer concentration was 3.6 mole/l.

Solution Properties

Osmometric molecular weights were determined with a Mechrolab membrane osmometer, Model Number 501, and Schleicher and Schuell type 0-S membranes. Duplicate determinations were made at 37°C. in toluene at four concentrations; when diffusion was noticed, extrapolation to zero time was attempted. The instrument was frequently checked on N.B.S. polystyrene #705, and only membranes yielding values within 3% of the standard were used.

Statistical Analysis

Regression coefficients, intercepts, and the mean deviation, s , of the regression coefficients for the data fitting eqs. (3), (4), and (5) were obtained on an IBM 1130 computer by using program designation IBM POLRG.

TABLE II
Mean Deviations at the Slopes

Monomer	Equation no.	$s \times 10^3$
Vinyl acetate	3	± 130
Styrene, thermal	4	± 0.037
Styrene, initiated	4	± 0.43
Methyl methacrylate	4	± 0.28
Diethyl maleate	4	± 0.32
Vinyl acetate	4	± 2.01
Styrene, thermal	5	± 1.3
Styrene, initiated	5	± 1.4
Vinyl acetate	5	± 0.28
Diethyl maleate	5	± 5.0

In all cases the data did not deviate significantly from a one degree polynomial, so that a linear regression was allowed. The mean deviations s at the slopes are listed in Table II.

RESULTS AND DISCUSSION

Experimental Results and Rate Data

Experimental results are listed in Table I. Because copolymerization occurred together with transfer, the table lists the monomer feed composition as mole fraction of amide f_2 , and the initial copolymer composition as mole fraction of amide in the copolymer F_2 , together with the *N*-allylamide to monomer mole ratio, $[S]/[M]$. Conversions reflect both vinyl monomer and comonomer disappearance. The amide content of the copolymers F_2 was computed from the reactivity ratios (Fig. 1), which were estimated from Q and e parameters determined for three copolymer systems.¹⁵

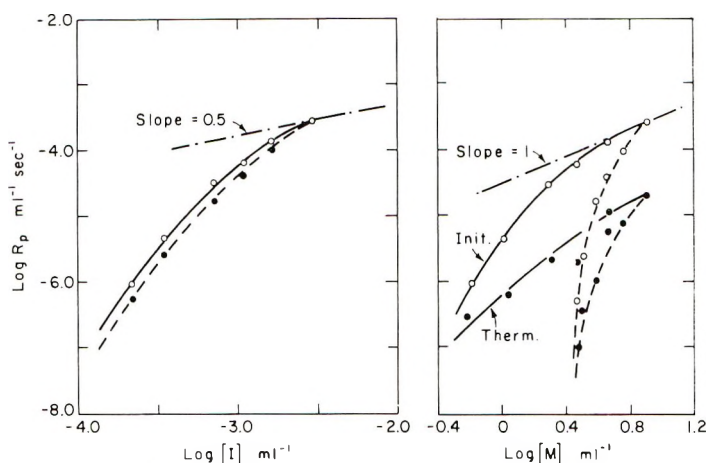


Fig. 2. Plots of $\log R_p$ vs. $\log [I]$ and $\log [M]$ for styrene polymerized in *N*-allylstearamide at 90°C: (—) as rates of styrene homopolymerization in amide "solvent" and (---) as rate of styrene-amide copolymerization. Peroxide initiated (Init.) and thermally initiated (Therm.) data included. Allyl amide content increases from right to left.

These values were considered to be more reliable than the values found by nitrogen analysis (column 7, Table I) because of the very low nitrogen content of *N*-allylstearamide (4%) and its low incidence in some of the copolymers studied. In any case, the found value tended to support the calculated values, although they were generally lower. Molecular weights \bar{M}_n declined rapidly with increase in allylamide content, the effect being most pronounced with vinyl acetate. Relatively constant composition and low molecular weight were found for the diethyl maleate system regardless of feed composition.

Rate data are shown in Table III for both styrene and methyl methacrylate, with and without added initiator. Both homopolymerization and copolymerization rates are given. In these two systems, where little amide enters the copolymer even at high dilution, rates of homopolymerization might be expected to resemble rates in simple solvents. However, the ratio $R_p/[M]^2$ tended to rise and then fall to low values for homopolymer-

ization and to rapidly drop for copolymerization. This ratio, should be constant with dilution in thermal polymerization and in initiated polymerizations^{19a} when the initiator to monomer ratio is constant. It would appear that complex kinetics accompanied by marked rate retardation characterized these two systems.

In the absence of retardation, rates of vinyl homopolymerization are often proportional to the 0.5 power of the initiator concentration and to the first power of the monomer concentration:

$$R_p = K[I]^{0.5} \quad (1)$$

$$R_p = K'[M] \quad (2)$$

In Figure 2, $\log R_p$ for homopolymerization and copolymerization (Table III) is plotted as a function of $\log [I]$ and $\log [M]$ for the styrene system. As the concentration of *N*-allylstearamide increases, a continuous rise in the exponential dependence of both initiator and monomer concentration can be seen by comparison with the 0.5 and 1.0 power slope indicated in

TABLE III
Rates of Homopolymerization and Copolymerization for Styrene
and Methyl Methacrylate in *N*-Allylstearamide at 90°C.

Experiment No.	Concentration, mole/l.		Initiator concn. $\times 10^3$, mole/l.	$R_p \times 10^4$, mole/l.-sec.		$R_p/[M]^2 \times 10^6$, l./mole-sec.	
	Vinyl mono- mer	Comono- mer		Homo- polymer- ization	Copoly- meriza- tion	Homopoly- merization	Copolymer- ization
Styrene, no added initiator							
1	8.09	8.09	0	0.215	0.215	0.328	0.328
2	4.64	5.73	"	0.126	0.094	0.584	0.286
3	2.99	4.60	"	0.020	0.078	0.225	0.368
4	2.04	3.95	"	0.021	0.012	0.504	0.077
5	0.91	3.17	"	0.0067	0.004	0.810	0.038
6	0.60	2.96	"	0.0031	0.001	0.870	0.012
Styrene, initiated with benzoyl peroxide							
7	8.09	8.09	2.87	2.75	2.75	4.20	4.20
8	4.51	5.63	1.61	1.38	1.00	6.78	3.16
9	2.99	4.59	1.07	0.661	0.420	7.40	1.99
10	1.96	3.89	0.701	0.309	0.176	8.03	1.16
11	1.03	3.25	0.348	0.046	0.026	4.34	0.246
12	0.64	2.99	0.215	0.009	0.005	2.20	0.056
Methyl methacrylate, initiated with benzoyl peroxide							
13 ^a	8.59	8.59	0	5.02	5.02	6.80	6.80
14	8.59	8.59	0.070	5.52	5.52	7.48	7.48
15	4.30	5.48	0.393	2.23	1.57	12.1	5.23
16 ^a	4.18	5.23	0	0.469	0.351	2.69	1.28
17	3.12	4.75	0.251	0.140	0.902	14.4	4.00
18 ^a	3.07	4.71	0	0.264	0.169	2.81	0.76
19	1.99	3.95	0.424	1.55	0.891	39.0	5.72
20 ^a	2.11	4.19	0	0.186	0.118	4.18	0.67

^a No added initiator.

the figure. In the methyl methacrylate system, initiator was varied somewhat, so that a similar comparison could not be made for the initiator concentration. Similar results, however, were obtained for the thermally initiated polymerization with respect to the monomer concentration. These data indicate that rates fall off rapidly as amide content increases. Both thermal and initiated data are moving toward very low rates as *N*-allylstearamide homopolymerization is approached with dilution. It would seem that degradative chain transfer is effectively controlling rate in these systems by removing active centers. However, a cross-termination effect^{19b} is not excluded. It is pertinent that rates of copolymerization of styrene and vinyl stearate were observed in this laboratory to be extremely low. Here degradative effects are excluded.

In contrast to the two previous copolymerizations, initiator consumption was very large in the vinyl acetate system, implying that rates were high because of induced peroxide decomposition.¹⁴ Actually, the limited rate data given in the experimental section for the vinyl acetate system indicate that the rates of copolymerization had been somewhat lowered. The derivative of monomer to peroxide consumption, dM/dP ,²⁰ declined rapidly as the amide concentration increased. The variation of dM/dP as a function of mole fraction of amide in the copolymer was observed to follow the empirical relation

$$dM/dP = (dM/dP)_{\text{amide}} (F_2)^{-a} \quad (3)$$

where F_2 is the mole fraction of amide entering the instant copolymer, $(dM/dP)_{\text{amide}}$ is the derivative for the *N*-allylstearamide homopolymer, and a is a constant. A plot of $\log dM/dP$ as a function of $\log F_2$ was linear (Fig. 3), yielding the parameter, $a = -1.89$, as the slope and $(dM/dP)_{\text{amide}} = 2.02$, as the intercept. dM/dP for the homopolymer had previously¹⁴ been found to be about 2.0, in close agreement with the extrapolated value of eq. (3). Use was made of eq. (3) to calculate the initiator needed to obtain a 10% conversion at reaction times exceeding the whole life of the peroxide (17 hr.). These initiator concentrations are given in the experimental section. The initiator dependence for diethyl maleate was much less than for vinyl acetate but was still considerable (Table I).

The difference in rates and in initiator dependence between styrene and methyl methacrylate on one hand, and between vinyl acetate and diethyl maleate on the other, is probably related to differences in vinyl monomer reactivity. The reactive monomers, styrene and methyl methacrylate, add radicals from the peroxide rapidly to initiate chains, while degradative chain transfer lowers both rates of copolymerization and the degree of polymerization. In contrast, the relatively unreactive monomer vinyl acetate is reluctant to add radicals, thus encouraging induced decomposition of the peroxide by amide "solvent" radicals.¹⁴ Although rates are apparently still lowered, considerable wastage of peroxide occurs. Hence, decreasing values of dM/dP were found as amide content was increased.

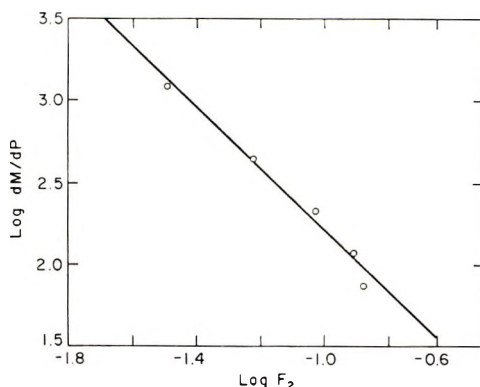


Fig. 3. Relation between $\log dM/dP$ and the log of the mole fraction of amide entering the copolymer (F_2) with vinyl acetate.

Induced peroxide decomposition and initiator wastage were particularly severe in the homopolymerization of *N*-allylstearamide.¹⁴ Results with diethyl maleate are a little surprising. Olefins 1,2-disubstituted by electron-withdrawing groups, when copolymerized with allylic monomers, characteristically display high rates and induced peroxide decomposition.⁴ Rates for the present system seem a little low on the basis of very limited data (see the Experimental section).

Determination of the Apparent Transfer Constants

Apparent transfer constants were determined for all four vinyl monomers by using the relation of Mayo:²¹

$$1/\bar{X}_n = 1/\bar{X}_{n_0} + C_S[S]/[M] \quad (4)$$

where $[S]$ is the *N*-allylstearamide concentration, $[M]$ the vinyl monomer concentration, \bar{X}_n the degree of copolymerization, \bar{X}_{n_0} the degree of polymerization of the vinyl comonomer, and C_S the transfer constant. Because of the variation found in $R_p/[M]^2$ and the marked lowering of rates already discussed, as well as the complications caused by the entrance of amide "solvent" into the polymer chain, values of C_S are considered to be only apparent values and are designated by primes. This follows a modification of the usage employed by Clark.¹⁰ A plot of $1/\bar{X}_n$ versus $[S]/[M]$ is shown in Figure 4 for all of the systems studied, and the regression coefficients and the intercepts are listed in Table IV. The transfer coefficients increased in the order: methyl methacrylate < styrene < diethyl maleate < vinyl acetate, which is the approximate order of decreasing monomer reactivity. This general order had previously been observed for monomers of similar reactivity.^{10,12,13} However diethyl maleate, which has nearly the same reactivity as vinyl acetate, has a much lower transfer constant. The lower slope together with the large extrapolated intercept found for this monomer (Fig. 4) are seen to reflect the small variation in copolymer composition caused by the alternation characteristic of ethylenes 1,2-disub-

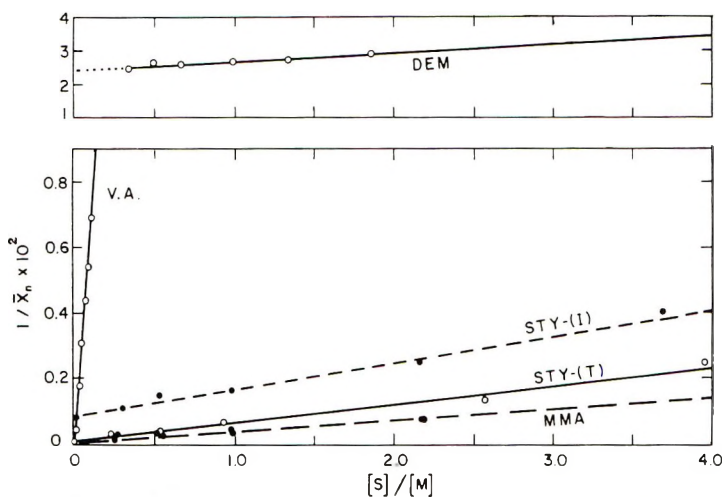


Fig. 4. Plots of $1/\bar{X}_n$ against $[S]/[M]$ for (MMA) methyl methacrylate, (STY-T) thermally polymerized styrene, (STY-I) styrene initiated by benzoyl peroxide, (VA) vinyl acetate, and (DEM) diethyl maleate in *N*-allylstearamide at 90°C .

stituted by electron-withdrawing groups when copolymerized with allyl monomers. Because C_M for diethyl maleate is unknown, the real curve for the relation between $1/\bar{X}_n$ and $[S]/[M]$ for 1,2-disubstituted olefins cannot be drawn. However, it is of interest that a literature value⁴ of \bar{X}_n for a 1:1 maleic anhydride-allyl acetate copolymer was 54, as determined in water, close enough to the value of 37 found in this work at the same composition to suggest a common relation for the two systems.

An increase was found in the value of C_s' for styrene initiated by benzoyl peroxide over the value obtained by thermal copolymerization (Table IV; Fig. 4). This is frequently observed in transfer studies.²² Corrections for initiated systems, such as used by Palit,²² could not be used here because of the variable dependence of rate on the monomer and initiator concentra-

TABLE IV
Regression Coefficients for Transfer of the Vinyl Monomers in
N-Allylstearamide at 90°C .^a

Comonomer	$C_s' \times 10^{3b}$	$(1/\bar{X}_{n0}) \times 10^{3c}$	$(1/\bar{X}_{n1}) \times 10^{3d}$	$K_1 \times 10^2$	$K_2 \times 10^2$
Styrene, no initiator	0.582	0.090	0.056	1.32	8.67
Styrene, peroxide initiated	0.830	0.857	0.768	1.91	8.01
Methyl methacrylate	0.301	0.101	0.074	0.46	9.53
Vinyl acetate	62.01	0.389	0.291	4.65	5.32
Diethyl maleate	2.24	24.6	6.28	3.89	5.48

^a Mean deviations of the slopes are listed in Table II.

^b The degree of polymerization (\bar{X}_n) estimated from the copolymer composition based on P_2 of Table I.

^c Intercept of the Mayo equation, eq. (4).

^d Intercept of eq. (5).

tion. In contrast, the methyl methacrylate data were apparently insensitive to initiator concentration because the regression line fitted both the thermal and initiated experiments equally well.

Although increasing and rather substantial amounts of initiator (see the experimental section) had to be used in the vinyl acetate copolymerization to obtain a 10% conversion, curvature was not observed in the transfer regression line (Fig. 4). It appears that chain transfer in this instance terminates all chains because chain length was dependent on the amide concentration only, and was independent of initiator concentration. This resembles allylic homopolymerization,^{1,20} where \bar{X}_n is independent of initiator concentration.

Estimation of the Degree of Polymerization of Allylic Copolymers

When the reciprocal number-average degree of polymerization ($1/\bar{X}_n$, Table I) was plotted as a function of the mole fraction of amide entering the copolymer F_2 for all five systems, the relation was found to be linear:

$$1/\bar{X}_n = 1/\bar{X}_{n1} + K_1 F_2 \quad (5)$$

where $1/\bar{X}_{n1}$ is the reciprocal degree of polymerization for the vinyl comonomer $1/\bar{X}_{n0}$ of the Mayo equation, eq. (4), and K_1 is a constant. This equation is therefore related to the copolymerization equation, since

$$F_2 = 1 - F_1 = 1 - (r_1 f_1^2 + f_1 f_2) / (r_1 f_1^2 + 2f_1 f_2 + r_2 f_2^2) \quad (6)$$

When eq. (5) was extrapolated to the limit $F_2 = 1$, the reciprocal number-average degree of polymerization for *N*-allylstearamide ($1/\bar{X}_{n2} = 0.1$) was not obtained in any experiment.¹⁴ Values were always considerably less than the true value and varied with the vinyl monomer. An empirical equation was derived which extended the relationship of eq. (5) to the limit of unity in F_2 . This was done by adding a term of higher degree in F_2 modified by a coefficient representing the difference between the value of the linear regression through F_2 , $(1/\bar{X}_{n2} - 1/\bar{X}_{n1})$, and the experimental value of K_1 , to give

$$1/\bar{X}_n = 1/\bar{X}_{n1} + K_1 F_2 + K_2 (F_2)^3 \quad (7)$$

where K_1 and $1/\bar{X}_{n1}$ are the coefficient and intercept, respectively, of eq. (5) and $K_2 = [(1/\bar{X}_{n2}) - (1/\bar{X}_{n1})] - K_1$. The regression coefficients for K_1 and values of K_2 and $1/\bar{X}_{n1}$ are given in Table IV for all five systems, while the mean deviations are given in Table II. Plots of eq. (7) for three of the systems studied are shown in Figure 5. The solid lines representing the experimental slopes, K_1 of eq. (5), are extended beyond the experimentally determined portion of the abscissa F_2 , to clarify the calculated curves. The dashed lines define the calculated curves and can be seen to fit the experimental data fairly well. The curvature required by eq. (7) was fixed by the available experimental data; terms of higher degree in F_2 would, of course, lower the slope. Because data were not available at higher values of F_2 to more clearly define the

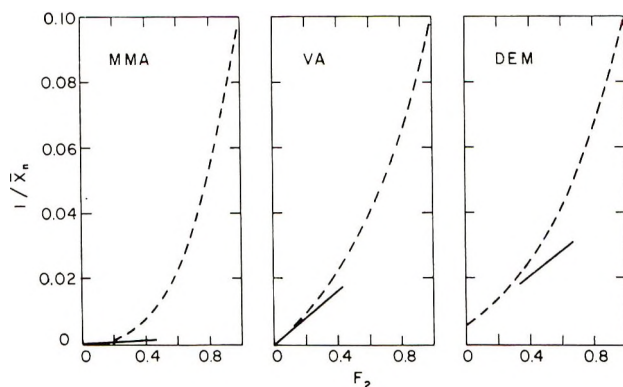


Fig. 5. Empirical relation between $1/\bar{X}_n$ and F_2 [eq. (7)], dashed line, compared with the initial slope [K_1 of eq. (5)] for (MMA) methyl methacrylate, (VA) vinyl acetate, and (DEM) diethyl maleate in *N*-allylstearamide at 90°C.

curvature, eq. (7) represents an upper limit for the rate of decrease in molecular weight resulting from allylic copolymerization. The intercepts $1/\bar{X}_{n1}$ and $1/\bar{X}_{n0}$ (Table IV) are significantly different, suggesting that curvature actually present in eq. (5) distorted the fitted linear regression line and

TABLE V
Transfer Constants from the Literature for Vinyl Monomers in Allyl Monomers

Vinyl monomer	Allylic monomer	Polymerization temp., °C.	$C'_s \times 10^3$	$(1/\bar{X}_n) \times 10^3$	$K_1 \times 10^2$	$K_2 \times 10^{2a}$	Reference
Styrene	Allyl chloride		1.51 ^b	0.75	5.45	6.07	2
Ethyl acrylate	Allyl chloride	30	0.15 ^b	0.05	0.37	11.23	5
Acrylonitrile	Allyl alcohol	30	0.595 ^b	0.15 ^c	0.16	19.82	3
Vinyl acetate	Allyl chloride	60	310.0	0.25 ^c	15.1	-3.54	10
Vinyl acetate	Allyl acetate	60	90.0	0.25 ^c	12.7	-7.73	10
Vinyl acetate	Methallyl chloride	60	40.0	0.25 ^c	1.50	8.48	10
Styrene	<i>n</i> -Hexene-1	60	0.25	0.25 ^b	0.76	9.22	13
Methyl methacrylate	<i>n</i> -Butene-1		0.51	0.10 ^d	1.58	8.40	12

^a $1/\bar{X}_{n2}$ of allyl chloride = 0.116²⁶; of allyl alcohol = 0.23³; of allyl acetate = 0.05²⁰; for other monomers, a value of 0.1 was assigned.

^b Estimated from the experimental data given in the reference.

^c $C_M = 1/\bar{X}_{n1}$ assumed from the reference data.

^d Assumed to be the same as $1/\bar{X}_{n0}$ of Table IV.

caused a lowering of the intercept, $1/\bar{X}_{n1}$. The parabola expressed by eq. (7) probably does not describe the true slope of the theoretical curve for the diethyl maleate systems. This might be expected to be sigmoidal for $0 < F_2 < 1.0$ in analogy with the slope of the instant copolymer-composition curve (Fig. 1). However, because only copolymers between $F_2 = 0.4$ and 0.6 can usually be made with olefins 1,2-disubstituted by electron-withdrawing groups, the parabolic expression comes fairly close to predicting experimental values even in this limiting case.

Literature data were used to estimate the parameters C'_s , K_1 , K_2 , and $1/\bar{X}_{n1}$ for several vinyl monomers copolymerized with various allylic comonomers. Data are shown in Table V. The parameters K_1 were calculated from given values of C'_s and $1/\bar{X}_{n1}$ and low values of F_2 (< 0.1). Allylic content F_2 was computed from reactivity ratios derived from the respective Q and e parameters.^{18a} When C'_s was not available, this constant was estimated from \bar{X}_n taken from experimental intrinsic viscosities (by using an appropriate Mark-Houwink relation^{18b}) and the polymer-composition data provided in the paper. While these can be considered to be only rough estimates, the agreement with the data in Table IV is fairly good, if the parameters for vinyl monomers of similar reactivity are compared. When transfer constants are particularly large, K_1 exceeds $[(1/\bar{X}_{n2}) - (1/\bar{X}_{n1})]$, and K_2 is then negative. This occurred for allyl acetate and allyl chloride in this series.

Equation (7) can be used for estimating the molecular weight of an allylic copolymer, when the reactivity ratios and C_{M1} and C_{M2} are known and when molecular weights of one or two copolymers of low allylic content are available. Because the copolymerization equation [eq. (6)] holds only for chains of fairly high degree of polymerization,²³ both this equation [and eq. (7)] may fail at high F_2 , where the degree of polymerization is low. Mixtures containing homo-oligomers might result from attempts at copolymerization, especially where monomer reactivity differences are great.

The authors express their appreciation to Dr. C. Roland Eddy of the Mathematical Evaluation Section for the computer evaluation of some of the data.

References

1. R. C. Laible, in *Encyclopedia of Polymer Science and Technology*, Interscience, New York, 1964, Vol. 1, pp. 750-759.
2. T. Alfrey and J. G. Harrison, Jr., *J. Am. Chem. Soc.*, **68**, 299 (1946).
3. G. Oster and Y. Mizutani, *J. Polymer Sci.*, **22**, 173 (1956).
4. P. D. Bartlett and K. Nozaki, *J. Am. Chem. Soc.*, **68**, 1495 (1946).
5. T. L. Dawson and R. D. Lundberg, *J. Polymer Sci. A*, **3**, 1801 (1965).
6. M. Matsumoto, M. Maeda, and T. Osugi, U.S. Pat. 2,909,502 (1959).
7. E. C. Chapin and R. F. Smith, U.S. Pat. 2,817,651 (1957).
8. E. C. Shokal and P. A. Devlin, U.S. Pat. 2,588,890 (1952).
9. R. H. Reinhard and J. E. Fox, U.S. Pat. 2,951,831 (1960).
10. J. T. Clarke, R. O. Howard, and W. H. Stockmayer, *Makromol. Chem.*, **44-46**, 427 (1961).

11. I. Boghetich, G. A. Mortimer, and G. W. Daves, *J. Polymer Sci.*, **61**, 3 (1962).
12. T. Otsu, A. Shimizu, and M. Imoto, *J. Polymer Sci. B*, **2**, 973 (1964).
13. A. P. Titov and I. A. Livshits, *J. Gen. Chem. USSR*, **29**, 1578 (1959).
14. E. F. Jordan, Jr. and A. N. Wrigley, *J. Polymer Sci. A*, **2**, 3909 (1964).
15. E. F. Jordan, Jr. and A. N. Wrigley, *J. Appl. Polymer Sci.*, **8**, 527 (1964).
16. E. F. Jordan, Jr., B. Artymyshyn, C. R. Eddy, and A. N. Wrigley, *J. Am. Oil Chemists' Soc.*, **43**, 75 (1966).
17. C. C. Price, *J. Polymer Sci.*, **3**, 772 (1948).
18. J. Brandrup and E. H. Immergut, *Polymer Handbook*, Interscience, New York, 1966, (a) II-352 to II-362; (b) IV-7 to IV-28.
19. P. J. Flory, *Principles of Polymer Chemistry*, Cornell Univ. Press, Ithaca, N.Y., 1953, (a) pp. 132-144; (b) pp. 199-203.
20. M. Litt and F. R. Eirich, *J. Polymer Sci.*, **45**, 379 (1960).
21. F. R. Mayo, *J. Am. Chem. Soc.*, **65**, 2324 (1943).
22. S. R. Palit, S. R. Chatterjee, and A. R. Mukherjee, in *Encyclopedia of Polymer Science and Technology*, Interscience, New York, 1966, Vol. 3, pp. 575-610.
23. D. Prevorsek, *J. Polymer Sci. B*, **1**, 229 (1963).
24. N. G. Gaylord, *J. Polymer Sci.*, **22**, 71 (1956).

Received August 2, 1967

Photochemical Crosslinking of Polypropylene

C. KUJIRAI, S. HASHIYA, H. FURUNO, and N. TERADA, *Textile Research Institute, Faculty of Engineering, Fukui University, Fukui Japan*

Synopsis

A study was carried to determine experimentally the crosslinking of irradiated polypropylene by ultraviolet rays *in vacuo*. Three methods of detecting crosslinking were used: measuring the degree of swelling in decalin at room temperature, measuring the gel fraction in a tetrachloroethylene solution of the irradiated sample, and comparing the infrared spectra before and after irradiation. It was found that as the time of irradiation increases, the degree of swelling decreases, whereas the gel fraction in tetrachloroethylene solution increases. This shows that the crosslinking reaction proceeds with time. On the other hand, the infrared spectra of the irradiated sample remained almost unchanged, which shows that different bond species can hardly be formed by irradiation *in vacuo*. From these facts it may be concluded that the measurements amply confirm the hypothesis. Furthermore, it is demonstrated that ash residue in polypropylene plays an important role in photocrosslinking; that is, the photochemical primary process of the reaction is the absorption of light by the ash residue.

It has been reported that unmodified polypropylene may be crosslinked by ultraviolet rays or radiation sources only in the presence of some sensitizer and with the use of an appropriate bridging molecule.¹ Contrary to this report, we have confirmed experimentally that *in vacuo* polypropylene can be directly crosslinked without a bridging molecule by ultraviolet irradiation. The experimental methods and results are given below.

Experimental

Unmodified polypropylene was prepared by using a modified Ziegler-Natta method on a laboratory scale. The sample was supplied in pellet form by Asahi Chemical Industry Co. Ltd., Takatsuki, Osaka, Japan. Most of the experiments were carried out with the polymer in powder form. The powder was prepared by precipitation from 1% hot xylene solution by gentle cooling, filtering, drying, and screening to uniform size (0.3-0.5 mm.) with standard sieves. As occasion demanded, the sample was used in the form of a film of 20 μ thickness, which was prepared by solvent (tetrachloroethylene) casting over mercury. The tacticity of the polypropylene was estimated at about 81% by Luongo's infrared absorption method.²

Our previous studies³ have shown that the photodegradation of polypropylene is a photosensitization reaction caused by the ash remaining from the Ziegler-Natta catalyst. The same effect of ash could be expected in this case. To perform the experiment for confirmation of this point, samples containing various contents of ash were prepared by extraction with methanol for different periods of time, which removed the ash to various degrees. TiO_2 , one of the main constituents of ash, was intentionally added to the hot xylene solution, and the polymer was precipitated. The ash content was determined by gravimetric analysis; see Table I.

TABLE I
Ash Contents of Samples

Sample ^a	Ash content, ppm
1	422
2	512
3	1580

^a Sample 1, methanol extraction for 300 hr.; sample 2, original sample; sample 3, TiO_2 added to sample.

The apparatus for exposure consisted of a light source, light filter, reaction vessel, and light thermostat. The light source was a low vapor-pressure quartz mercury lamp (10 w.). The filter was a Toshiba UV25, which can cut the wavelength to less than 2100 Å. The reaction vessel was of quartz in tubular form, 40 mm. in diameter and 6 cm. long; it was set horizontally in the light thermostat so that half of its diameter was immersed in the water of the bath, and it was rotated at the rate of 100 rpm. Thus special regard was paid to mixing and uniform illumination of the powder sample as well as to keeping the temperature constant (30°C.) during exposure.

The film sample was irradiated in the same reaction vessel, in which it was wound around the inner surface of the wall.

The light source was of tubular form and had almost same diameter and length as the reaction vessel. The distance between the center of the source and that of the reaction vessel was about 6 cm.

Two measurements of the degree of crosslinking were used: one was the gel fraction, and the other was the degree of swelling.

For determining the gel fraction a powder sample was used because of the difficulty of obtaining films having uniform thickness. A film sample may be used, however, for determining the degree of swelling, since observations may be made over the whole sample.

The gel fraction of the irradiated sample was determined in the following way. The irradiated sample was first extracted in tetrachloroethylene at 100°C. for 30 min. Then the solution was filtered free from the gel fraction with a glass filter, and the filtrate, which contained uncrosslinked polymer, was subjected to infrared absorption analysis. In this case the 2915 cm.^{-1} band was used as the analytical line, being transparent to the

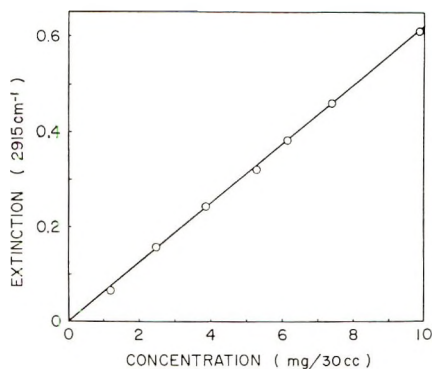


Fig. 1. Calibration curve for determining weight of uncrosslinked polypropylene in filtrate.

quartz cell and the solvent (tetrachloroethylene). A calibration curve of the extinction at 2915 cm.^{-1} versus the concentration of polypropylene in 30 cm.^3 of tetrachloroethylene was constructed as shown in Figure 1. Then from the measurement of the extinction at 2915 cm.^{-1} of the filtrate of the partially crosslinked sample solution the weight of uncrosslinked polymer in 30 cm.^3 of solvent was easily determined. The gel fraction, then, is given by

$$\text{gel fraction (\%)} = (W_0 - W)/W_0 \times 100$$

where W_0 is the total weight of the partially crosslinked sample, and W is the weight of uncrosslinked polypropylene dissolved out in tetrachloroethylene.

The degree of swelling was determined by measuring under a low-power microscope the change in length of the polypropylene film on immersion in decalin for 20 hr. at room temperature. The degree of swelling may be obtained from

$$\text{degree of swelling (\%)} = (l - l_0)/l_0 \times 100$$

where l_0 and l are the lengths of the film before and after swelling, respectively.

These two measurements were made at various times of exposure.

The infrared spectra were taken by a Shimadzu Infrared Spectrophotometer, type RI-27.

Results and Discussion

As shown in Figure 2, the degree of swelling in decalin decreases with time of irradiation, suggesting that the crosslinking reaction proceeds with the time of exposure. On the other hand, the gel fraction of the sample extracted in tetrachloroethylene increases with time of exposure, as shown in Figure 3. These two experimental facts emphasize that polypropylene is crosslinked by exposure to ultraviolet rays *in vacuo*.

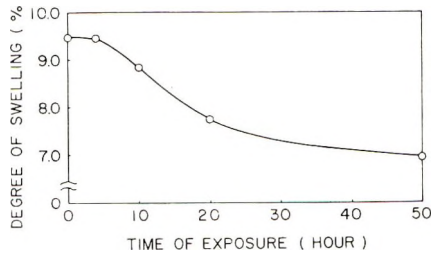


Fig. 2. Relation between degree of swelling and time of exposure.

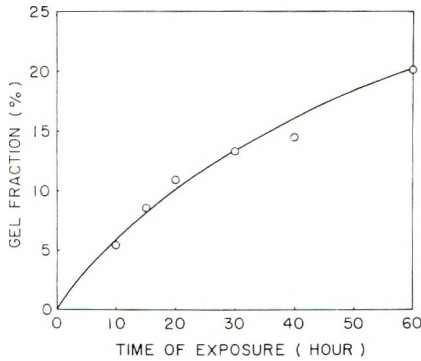


Fig. 3. Relation between gel fraction and time of exposure.

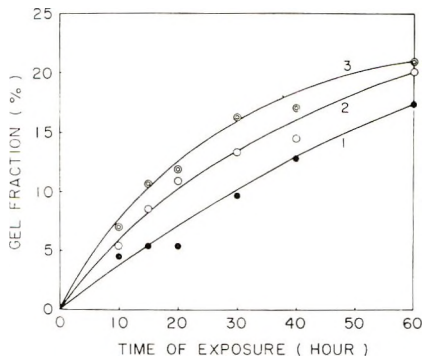


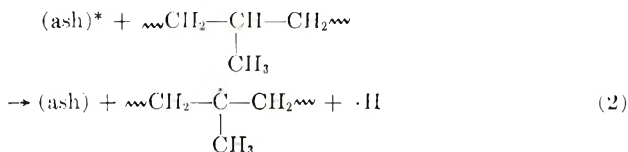
Fig. 4. Effect of ash content on photochemical crosslinking. Curve numbers correspond to sample numbers given in Table I.

It is necessary to recollect what the light absorber is in this photochemical crosslinking. Polypropylene itself is transparent to light of a wavelength longer than 2000 Å.³ An interesting fact, which may be pertinent here, is that ash accelerates photochemical crosslinking, as shown in Figure 4. Now, the main components of the ash probably are TiO_2 and Al_2O_3 . Examination of the absorption spectra of these compounds shows that TiO_2 absorbs at wavelengths shorter than 4000 Å. and Al_2O_3 at wavelengths shorter than 3000 Å.⁴ Therefore the primary process of photochemical

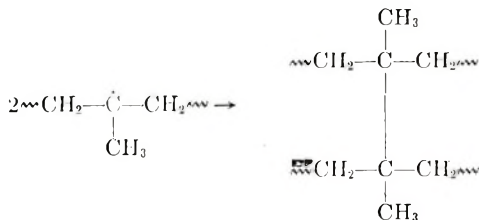
crosslinking by means of ultraviolet rays is mainly the absorption by ash, which contains these inorganic compounds:



The resulting excited ash collides with the polypropylene molecules and so possibly drives the hydrogen atom attached to tertiary carbon out of the molecule:



If two such polypropylene radicals collide with each other, there may be formed one crosslink:



Experimental evidence that supports this reaction mechanism is the infrared absorption spectra. The difference between the spectra of polypropylene film before and after irradiation *in vacuo* could not be detected qualitatively. This fact suggests that different bond species cannot be formed by irradiation, and this seems to support eq. (2).

It is still necessary that the mechanism described above be experimentally examined more precisely. Furthermore, the physical and chemical (especially the photochemical) properties of photochemically cross-linked polypropylene are very interesting, and studies of them are now in progress and will be published.

The authors wish to express their thanks to Asahi Chemical Industry Co., Ltd. for kindly supplying the sample for this study.

References

1. J. R. Hutton, J. B. Jackson, and R. G. J. Miller, *Polymer*, **8**, 411 (1967).
2. J. P. Luongo, *J. Appl. Polymer Sci.*, **3**, 302 (1960).
3. C. Kujirai, S. Hashiya, K. Shibuya, and K. Nishio, *Kobunshi Kagaku*, in press.
4. C. F. Goodeve and J. A. Kitchner, *Trans. Faraday Soc.*, **34**, 902 (1938).

Received August 7, 1967
 Revised October 12, 1967

Direct Determination of Crosslinking and Chain Scission in Polymers

D. I. C. KELLS, M. KOIKE,* and J. E. GUILLET, *Department of Chemistry, University of Toronto, Toronto, Canada*

Synopsis

A direct method has been developed for determining $G(\text{crosslinks})$ for irradiated polymers using the analytical ultracentrifuge. The sedimentation velocity technique is employed to follow changes in the molecular weight of a narrow distribution polystyrene sample irradiated in vacuum with ^{60}Co γ -rays. It is shown that $G(\text{crosslinks})$ can be determined at low doses before significant structural changes have occurred in the polymer. At about one-fifth of the gel dose $G(\text{crosslinks})$ was found to be 0.019 compared to a value of 0.040 obtained from gel-sol fraction measurements. It is concluded that $G(\text{crosslinks})$ may increase with dose due to processes such as the addition of radicals to double bonds formed during the irradiation.

Introduction

When hydrocarbon polymers are subjected to high-energy radiation, two reactions occur which cause considerable change in the physical properties of the polymers. These reactions are crosslinking and chain scission.

In the past, estimation of the extent of reaction has been made by measurement of solution viscosity, gel-sol fraction, swelling ratio, etc. With these procedures high doses of radiation usually must be used in order to obtain a measurable effect. Consequently, the material undergoes significant structural changes during the irradiation, and determination of the radiation sensitivity of the original material is difficult. The development of improved techniques for studying molecular weight distributions has made it possible to determine crosslinking and chain scission by direct measurement on samples that have received only low radiation doses and hence have not undergone substantial structural change.

We wish to report some preliminary studies made on irradiated "mono-disperse" ($\bar{M}_w/\bar{M}_n \sim 1.01$) polystyrene which illustrate the simplicity and precision with which such measurements can be made, using the analytical ultracentrifuge to follow changes in molecular weight.

Experimental

Polystyrene samples were irradiated in solid chip form under high vacuum by using a ^{60}Co γ -ray source (0.8 Mrad/hr.). Sedimentation velocity ex-

* Present address: Reactor Chemistry Laboratory, Japan Atomic Energy Research Institute, Tokai, Japan.

periments were performed on cyclohexane solutions of the polymer at 34.5°C. in a Spinco Model E ultracentrifuge at 60,000 rpm. Figures 1, 2, and 3 show representative Schlieren photographs of the starting material (I), material irradiated to low dose (12.7 Mrad) (II), and material irradiated to a higher dose (25.1 Mrad) (III), respectively.

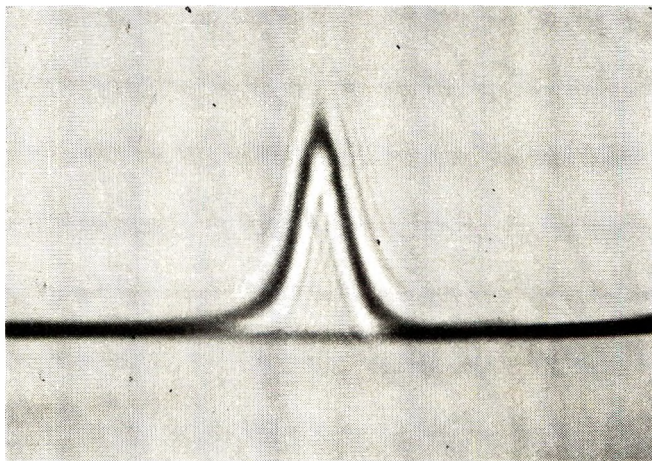


Fig. 1. Schlieren photograph of starting material (I).

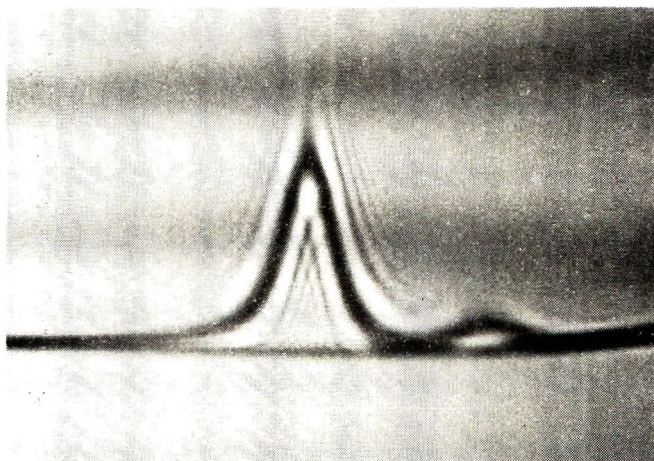


Fig. 2. Schlieren photograph of material irradiated to 12.7 Mrad (II).

Computer programs based on the methods proposed by Uede et al.¹ were used to determine the integral molecular weight distributions of the starting material (I) and the material irradiated to low dose (II). Figure 4 shows these results.

In order to use a simple calculation procedure proposed by Flory² to calculate $G(\text{crosslinks})$ it was necessary to assume that the starting material was strictly monodisperse. $G(\text{crosslinks})$ can then be determined from a

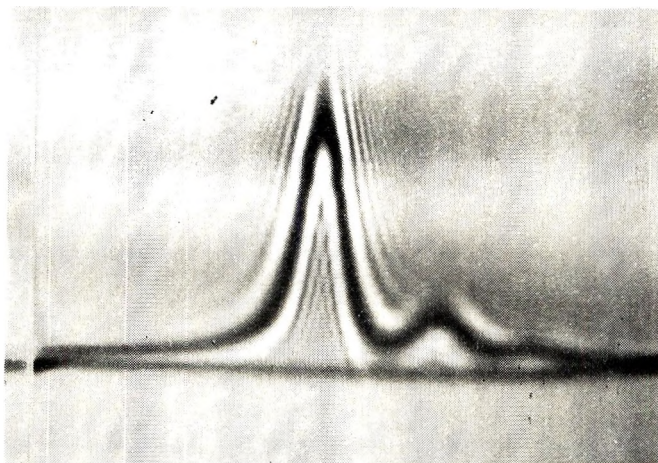


Fig. 3. Schlieren photograph of material irradiated to 25.1 Mrad (III).

measurement of the weight fraction of material uncrosslinked in the irradiated sample. That is:

$$W_1 = e^{-qu_1} \quad (1)$$

where W_1 is the weight fraction of uncrosslinked material, q is the proportion of units crosslinked in the sample, u_1 is the degree of polymerization of the starting material.

$$G(\text{crosslinks}) = 0.48 \times 10^6 (1/Mr) \ln (1/W_1) \quad (2)$$

Here M is the molecular weight of the starting material and r is the radiation dose in megarads.

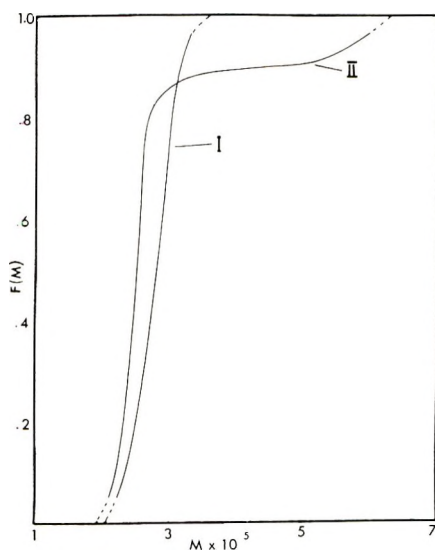


Fig. 4. Integral molecular weight distributions of materials I and II.

The weight fraction of uncrosslinked material was determined from the same set of ultracentrifuge results by three procedures.

Method 1. Inspection of the calculated integral molecular weight distributions shows that there is no material in the starting sample having a molecular weight greater than 363,000. Hence material in the irradiated sample with molecular weight greater than this must have been formed by crosslinking. From Figure 4 the weight fraction of uncrosslinked material is 0.88. This result yields $G(\text{crosslinks}) = 0.017$ for a number-average molecular weight of 278,000 as the molecular weight of the starting sample.

Method 2. It is assumed that all material under the large peak in Figure 2 is uncrosslinked while the smaller peak contains only crosslinked material. Hence the leading edge of the main peak can be extrapolated to the solvent baseline, and the weight fraction of uncrosslinked material can be determined from the relation:³

$$W_1 = \frac{\int_{r_1}^{r_{p1}} r^2 \partial n / \partial r dr}{\int_r^{r_{p1}} r^2 \partial n / \partial r dr + \int_{r_2}^{r_{p2}} r^2 \partial n / \partial r dr} \quad (3)$$

where r_i is the radial distance from the axis of rotation to the start of the i th peak, r_{p_i} is the radial distance from the axis of rotation to the end of the i th peak, $\partial n / \partial r$ is the refractive index gradient (i.e., the curve height in the Schlieren photographs).

The integrals in eq. (3) were evaluated numerically by using a computer program.

The results obtained from a series of six different concentrations, each having a time sequence series of five Schlieren photographs, are summarized in Table I.

TABLE I
 $G(\text{crosslinks})$ by Numerical Integration of Schlieren Peaks

Concentration of solution (w/v), %	Weight fraction of main peak (W_1) ^a	$G(\text{crosslinks})/100$ e.v.
0.226	0.847	0.023
0.293	0.849	0.022
0.426	0.860	0.020
0.517	0.891	0.016
0.617	0.878	0.018
0.750	0.871	0.018
	Mean	0.019
	σ	0.003

^a Average of five Schlieren patterns for each concentration.

Method 3. The Schlieren peaks obtained from the five photographs made at a single concentration (0.750%) were magnified ten times on a Nikon Shadowgraph and traced onto sheets of ordinary graph paper. The traced

TABLE II
 $G(\text{crosslinks})$ by Weighing of Schlieren Peaks

Total weight of both peaks, g.	Weight of main peak, g.	Weight fraction of main peak (W_1)	$G(\text{crosslinks})$
0.1466	0.1266	0.86 ₃	0.019
0.1490	0.1289	0.86 ₅	0.019
0.1495	0.1306	0.87 ₄	0.018
0.1373	0.1217	0.88 ₆	0.018
0.1472	0.1284	0.87 ₂	0.018
		Mean	0.018

curves were then cut out and weighed to determine the weight fraction of uncrosslinked material. Table II summarizes the results of this experiment.

Gel-Sol Fraction Measurements

$G(\text{crosslinks})$ was also determined by the conventional method from measurements of the sol fraction for a sample which had been irradiated beyond the gel dose. From these measurements $G(\text{crosslinks})$ was found to be 0.040, which is in good agreement with the results of Wall and Brown⁴ and Charlesby.⁵

Measurement of Chain Scission

The extent of chain scission can be determined in a similar manner by inspection of the low end of the molecular weight distributions. From Figure 4 it can be seen that there is very little irradiated material having molecular weight less than 204,000 (the lowest molecular weight material found in the starting sample). Further direct evidence for the small amount of chain scission in irradiated solid polystyrene can be seen by comparing Figures 1 and 2. These two Schlieren photographs were taken at the same sedimentation time for approximately equal concentrations of materials I and II. The two main peaks can be superimposed, indicating that very little chain scission has occurred.

Comparison with GPC Measurements

Samples of material II and III were analyzed on a Waters gel permeation chromatograph with the use of tetrahydrofuran as solvent by Mr. J. Duerksen of McMaster University, Hamilton. The GPC trace for material III is shown in Figure 5. The resolution of the GPC is not satisfactory for branched samples, as expected from theoretical considerations.

Discussion

The integral molecular weight distribution curves (Fig. 4) clearly show that the material in the crosslinked peak can be characterized by an approximate median molecular weight of 570,000. The median molecular weight of the starting material is 283,000. Hence the crosslinked molecules

must be essentially "dimers" of the original starting material. Similarly, the three peaks in Figure 3 for the higher dose sample can be attributed to starting material or "monomer," "dimer," and "trimer," respectively.

Our studies confirm that the principal structural change which occurs on irradiation of solid polystyrene is crosslinking, with very little chain scission. Using the direct method described in this paper, a G value of 0.019 is obtained, whereas methods involving irradiation above the gel dose, both with our polymer and from the data of Wall and Brown⁴ and Charlesby⁵ give values about twice as high. We conclude from this that the G value for crosslinking may increase with dose due to processes such as the addition of radicals to the double bonds formed in the polymer by the hydrogen

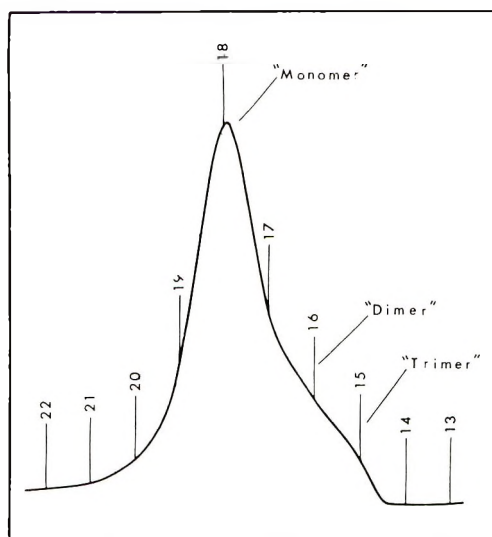


Fig. 5. GPC trace of material irradiated to 25.1 Mrad (III).

abstraction reaction which is taking place concurrently. If this proves to be the case, our method should give a more reliable estimate of the G value for crosslinking of the unchanged polystyrene molecule.

Benoit et al.⁶ have demonstrated that the GPC technique separates molecules on the basis of their hydrodynamic volume rather than on the basis of chain length or molecular weight. Thus in spite of an increase in molecular weight by crosslinking the actual volume of such branched molecules in solution may be quite similar to that of the linear parent molecules. Separation of these crosslinked and linear molecules on the basis of hydrodynamic volume is then impossible. The ultracentrifuge separates components on the basis of molecular mass and density. Since the solution density of a branched molecule will be greater than that of a linear molecule, the sedimentation rate is increased for these components, thus improving the resolution of the branched components.

We wish to thank the Polymer Corporation Ltd., Sarnia, Ontario, for furnishing us with the polystyrene used in this investigation. The financial assistance of Polymer Corporation, the National Research Council of Canada, and the Province of Ontario is gratefully acknowledged.

References

1. T. Homma, K. Kawahara, H. Fujita, and M. Uede, *Makromol. Chem.*, **67**, 132 (1963).
2. P. J. Flory, *J. Am. Chem. Soc.*, **63**, 3096 (1941).
3. H. Fujita, *Mathematical Theory of Sedimentation Analysis*, Academic Press, New York, 1962.
4. L. A. Wall and D. W. Brown, *J. Phys. Chem.*, **61**, 129 (1957).
5. A. Charlesby, *J. Polymer Sci.*, **11**, 513, 521 (1953).
6. H. Benoit, Z. Grubisic, P. Rempp, D. Decker, and J. Zilliox, paper presented at Third International Seminar on Gel Permeation Chromatography, Geneva, Switzerland, 1966.

Received March 16, 1967

Revised June 26, 1967

Liquid Carbon Dioxide as a Solvent for the Radiation Polymerization of Ethylene

MIYUKI HAGIWARA, HIROSHI MITSUI, SUEO MACHI, and
TSUTOMU KAGIYA, *Japan Atomic Energy Research Institute,
Takasaki Radiation Chemistry Research Establishment,
Takasaki, Gunma, Japan*

Synopsis

The usefulness of liquid carbon dioxide as a solvent for polymerization of ethylene was studied. The effect of liquid carbon dioxide on the polymerization was investigated under conditions of the pressure of 400 kg./cm.² over the temperature range 20–45°C. by using γ -radiation and AIBN as initiators. The infrared spectrum of the polymers showed that carbon dioxide had little effect on the polymer structure. The polymers contained no combined carbon dioxide and only small amounts of vinylidene unsaturation. The methyl content of the polymers was 0.5–4.0 CH₃/1000C. The polymer yield and molecular weight were found to be decreased by the addition of carbon dioxide in both polymerization by γ -radiation and AIBN. The number of polymer molecules formed per unit time increased with the content of carbon dioxide in the γ -ray polymerization, and was constant in the case of AIBN. The advantages of the use of liquid carbon dioxide as a solvent in this polymerization were also considered from the viewpoints of the continuous process, the separation of polymer, the stability of carbon dioxide to radiation, and commercial applications.

INTRODUCTION

The γ -ray-induced polymerization of ethylene has been widely investigated with the use of various organic solvents.^{1–3} Liquid carbon dioxide is expected to be a suitable solvent in the radiation process because of its high stability to ionizing radiation. However, no investigation on the ethylene polymerization in liquid carbon dioxide has been reported.

This is the first of a series of papers on the radiation polymerization of ethylene in the presence of carbon dioxide, and the purpose of this note is to investigate the usefulness of liquid carbon dioxide as a solvent.

EXPERIMENTAL

The reaction vessel was a stainless-steel autoclave of 100 ml. capacity. The ethylene monomer used was 99.9% pure (free of CO and H₂S) and contained less than 5 ppm of O₂. Carbon dioxide was 99.99% pure and its major impurities were H₂O (37 ppm), CH₄ (20 ppm), and O₂ (2 ppm). Before starting an experiment, the system was evacuated and flushed

three times with carbon dioxide. A definite amount of carbon dioxide was charged into the vessel, which was cooled in a methanol–Dry Ice bath. Ethylene was then fed to the reaction pressure. The reaction temperature was maintained constant within $\pm 0.5^\circ\text{C}$. during the course of the reaction. Cobalt-60 (5000 curies) was used as the γ -ray source. The radical initiator, azobisisobutyronitrile (AIBN) was purified by recrystallization from acetone. The amount of monomer polymerized was determined by direct weighing. The molecular weight was calculated by Tung's equation⁴ from the measured solution viscosity in tetralin at 130°C . The density was determined by the gradient-tube method at 25°C ., with the use of a water–methanol solution, and the degree of crystallinity X was calculated from the density d by using the equation:

$$d = 2.0 \times 10^{-3}X + 0.803$$

The methyl content in the polymer was determined by the method of Bryant and Voter,⁶ and the unsaturation according to Cross⁷ and Cernia.⁸

RESULTS AND DISCUSSION

Effect of Carbon Dioxide on Polymer Structure

In order to investigate the effect of carbon dioxide on polymer structure, the infrared spectra were obtained for the polymers formed under three different conditions; these are shown in Figure 1. The polymer giving

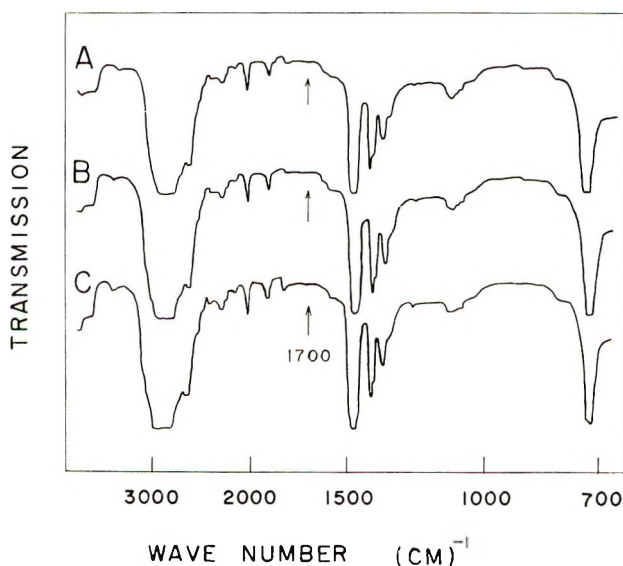


Fig. 1. Infrared spectra of polymers: (A) $\text{CO}_2/\text{C}_2\text{H}_4$ (molar ratio) = 0.31, pressure = 400 kg./cm.², temperature = 20°C ., dose rate = 2.5×10^4 rad/hr., time = 2.0 hr.; (B) $\text{CO}_2/\text{C}_2\text{H}_4$ = 0.31, pressure = 400 kg./cm.²; temperature = 45°C ., [AIBN] = 4.3 mmole/l., time, 8.0 hr.; (C) CO_2 free, pressure = 400 kg./cm.²; temperature = 20°C .; dose rate = 2.5×10^4 rad/hr., time = 1.0 hr.

spectrum *A* was obtained by using γ -rays and that giving *B* by AIBN in liquid carbon dioxide; that giving spectrum *C* was obtained with γ -rays in the absence of carbon dioxide. No marked difference is observed among these spectra. The absence of the peaks near 1700–1750 cm^{-1} ascribed to carbonyl group in the polymers formed in liquid carbon dioxide indicates that the polymers have no combined carbon dioxide. Also, as can be seen in Table I, in which the number of short chain branches and various types of unsaturation of these polymers are summarized, there are no essential differences among the structures of three polymers. The methyl content in the polymers is 0.5–4.0 $\text{CH}_3/1000\text{C}$, and the polymers have only small amounts of vinylidene unsaturation.

TABLE I
Molecular Structure of Polyethylene^a

Polymer	Molecular weight	Density, g./cc.	Crystal- linity %	Methyl content, $\text{CH}_3/1000\text{C}$	Double bonds/1000C		
					RRC= CH_2	RCH= CHR	RCH= CH_2
A	204,000	0.934	66	2.0	0.051	0	0
B	198,000	0.932	65	4.0	0.060	0	0
C	360,000	0.946	72	0.5	0.031	0	0

^a Polymerization conditions: A: $\text{CO}_2/\text{C}_2\text{H}_4$ (molar ratio), 0.31; pressure, 400 kg./cm^2 ; temperature, 20°C.; dose rate, 2.5×10^4 rad/hr.; time, 2.0 hr. B: $\text{CO}_2/\text{C}_2\text{H}_4$, 0.31; pressure, 400 kg./cm^2 ; temperature, 45°C.; AIBN, 4.3 mmole/l.; time, 8.0 hr. C: CO_2 free; pressure, 400 kg./cm^2 ; temperature, 20°C.; dose rate, 2.5×10^4 rad/hr.; time, 1.0 hr.

In view of these results, it is concluded that liquid carbon dioxide has little effect on polymer structure.

Effect of Carbon Dioxide on the Rate of Polymerization and the Molecular Weight of Polymer

Figure 2 shows the variation of the rate of polymerization and the molecular weight of polymer with respect to the molar ratio of carbon dioxide to ethylene monomer. The rate of polymerization in liquid carbon dioxide solution is lower than that in bulk polymerization. This decrease in rate may be caused by a decrease in the rate of initiation and/or propagation or an increase in the rate of termination. On the other hand, the polymer molecular weight is depressed by the addition of carbon dioxide. However, a polymer of high molecular weight is obtained even in the presence of a large amount of carbon dioxide. This may indicate that carbon dioxide does not terminate the growing radicals. By using the experimental results given in Figure 2, the rate of formation of the polymer molecule, defined as the ratio of the amount of polymerized monomer to the degree of polymerization in unit time, is shown in Figure 3. It can be seen that the rate is independent of the amount of carbon dioxide in the polymeriza-

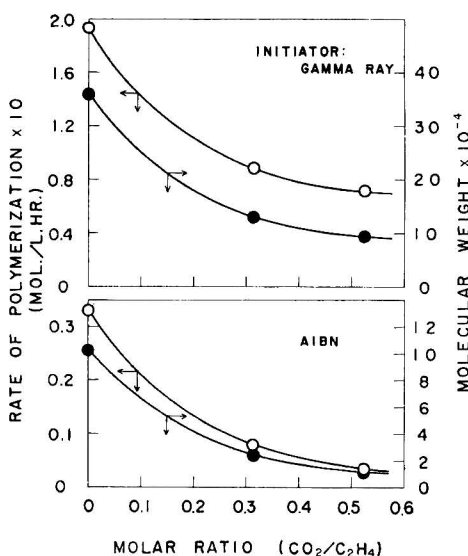


Fig. 2. Rate of polymerization and polymer molecular weight vs. molar ratio of carbon dioxide to ethylene. Conditions for γ -radiation polymerization: pressure = 400 kg./cm.², temperature = 20°C., dose rate = 2.5×10^4 rad/hr., time = 1.0 hr. Conditions for AIBN-initiated polymerization: pressure = 400 kg./cm.²; temperature = 45°C.; [AIBN] = 4.3 mmole/l.; time = 1.0 hr.

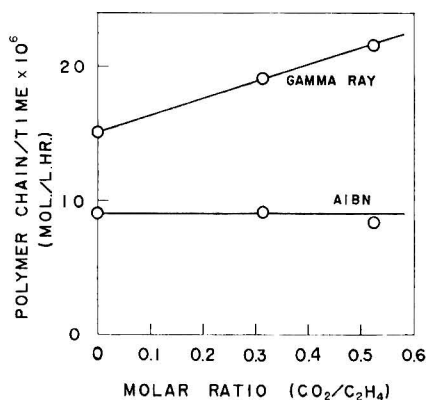


Fig. 3. Rate of formation of polymer molecule vs. molar ratio of carbon dioxide to ethylene. Polymerization conditions are the same as given for Fig. 2.

tion by AIBN. This fact and the absence of carbonyl groups in the polymer indicate that carbon dioxide does not act as a transfer agent and has no effect on the initiation in the polymerization by AIBN. However, the increase in the rate of formation of polymer molecule with carbon dioxide in the radiation polymerization suggests that carbon dioxide has an effect on the initiation and/or transfer reactions in this process. However, the absence of transfer to carbon dioxide with the use of AIBN leads to the consideration that the increase in the rate of formation of polymer mole-

cules may be due to an increase in initiation rather than in transfer. For $\text{CO}_2/\text{C}_2\text{H}_4$ molar ratios of 0, 0.314, and 0.524, the electron densities of the mixtures are calculated as 520, 605, and 665 mole/l., respectively, and the rates of formation of polymer molecules are determined to be 15.1, 19.1, and 21.6 $\mu\text{mole/l.-hr.}$, respectively. The change in the calculated electron densities is shown to coincide well with the increase in the rates of formation of polymer molecule. Therefore, the main role of carbon dioxide in the initiation reaction may be to increase the rate of energy absorption of the irradiated mixture.

On the basis of these considerations, the decrease in both the rate of polymerization and the polymer molecular weight on addition of carbon dioxide is thought to be due mainly to a decrease in the propagation rate owing to a decrease in the fugacity of ethylene with increasing content of carbon dioxide in the mixture. A detailed study on the reaction kinetics is being carried out and will be reported in a subsequent paper.

Advantages of Carbon Dioxide as a Solvent

By using the specially designed stainless-steel autoclave with a quartz window,⁹ we were able to observe the appearance of the polyethylene in a reaction medium under a pressure of 400 kg./cm.² In the bulk polymerization at normal temperature, the polymer separates from the monomer as a white powder which aggregates and forms a continuous layer on the wall of the reaction vessel. This polymer layer sticks to the wall and swells to some extent in the monomer. The polymer can be separated from the wall only when the vessel is violently vibrated and then sticks to the wall again. This behavior is not desirable for a continuous process to produce powdery polyethylene. Thus, the polymer is not well transported by the flow of gaseous ethylene. The polymer accumulates on the reactor wall, making decreasing the reaction zone and clogging the pipeline.

On the other hand, in solution polymerization with an organic solvent, the behavior of the polymer is quite different. The polyethylene formed is suspended in the mixture as a fine powder when the solvent used is the precipitant for the polymer. This powdery polymer does not aggregate and not stick to the wall of the vessel. Such conditions are favorable for a continuous process. In general, the solvent process with organic materials has, however, some disadvantages, i.e., the instability of the solvent to radiation, the decrease in the rate of polymerization and the polymer molecular weight, the change in polymer structure resulting from the participation by the solvent in the polymerization reaction, and the difficulty of the separation of the solvent from polymer.

The polymerization in liquid carbon dioxide obviates these difficulties. It was observed that the mixture of ethylene and carbon dioxide exists in a homogeneous phase, and that the polymer forms as slightly swollen particles and precipitates continuously in the bottom of the vessel during the course of the reaction. These polymer particles have little tendency to stick together and are easily broken to smaller particles by vibration of the vessel.

Further, in the flow system, they are well transported in the reaction mixture. The liquid carbon dioxide process has other advantageous features, namely, the polymer is easily separated from the reaction mixture by simple degassing, and carbon dioxide is quite stable even in the radiation field. No increase in O₂ and CO which might be produced by the radiolysis of carbon dioxide was observed in the residual gas.

From the commercial point of view, carbon dioxide has an additional advantage because it can easily be obtained in a highly pure form as a by-product in several industrial processes.

References

1. E. J. Henley and C. Chong Ng, *J. Polymer Sci.*, **36**, 511 (1959).
2. S. S. Medvedev, A. D. Abkin, P. M. Khomikovskii, G. N. Gerasimov, V. F. Gromov, Yu. A. Chikin, V. A. Tsingister, A. L. Auer, M. K. Yalovleva, L. P. Mezhirova, A. V. Matveeva, and Z. G. Bezzubuk, *Polymer Sci. USSR*, **2**, 457 (1961).
3. R. H. Wiley, N. T. Lipscomb, C. F. Parrish, and J. E. Guillet, *J. Polymer Sci. A*, **2**, 2503 (1964).
4. L. H. Tung, *J. Polymer Sci.*, **24**, 333 (1957).
5. S. Machi, T. Tamura, S. Fujioka, M. Hagiwara, M. Gotoda, and T. Kagiya, *J. Appl. Polymer Sci.*, **9**, 2537 (1965).
6. W. M. D. Bryant and R. C. Voter, *J. Am. Chem. Soc.*, **75**, 6113 (1953).
7. L. H. Cross, R. B. Richards, and H. A. Willis, *Discussions Faraday Soc.*, **9**, 235 (1950).
8. E. Cernia, C. Mancini, and G. Montaudo, *J. Polymer Sci. B*, **1**, 371 (1963).
9. S. Machi, M. Hagiwara, and T. Kagiya, *J. Polymer Sci. B*, **4**, 1019 (1966).

Received March 9, 1967

Revised June 13, 1967

Kinetics of the γ -Radiation-Induced Polymerization of Ethylene in Liquid Carbon Dioxide

MIYUKI HAGIWARA, HIROSHI MITSUI, SUEO MACHI,
and TSUTOMU KAGIYA, *Japan Atomic Energy Research Institute,
Takasaki Radiation Chemistry Research Establishment,
Takasaki, Gunma, Japan*

Synopsis

The γ -radiation-induced polymerization of ethylene with the use of liquid carbon dioxide as a solvent, was studied from the viewpoint of kinetics. The polymerization was carried out at conversions less than 10% under the pressures ranging from 100 to 400 kg./cm.², dose rates 1.3×10^4 – 1.6×10^6 rad/hr., and temperatures of 20–90°C. The concentration of carbon dioxide varied up to 84.1 mole-%. The polymerization rate and the polymer molecular weight were observed to increase with reaction time. This observation, however, becomes less pronounced with increasing concentration of carbon dioxide and with rising temperature. The exponents of the pressure and the dose rate were determined to be 2.3 and 0.85 for the rate, and 2.0 and –0.20 for the molecular weight, respectively. From the kinetic considerations for these results, the effect of carbon dioxide on the initiation and termination reaction in the polymerization was evaluated.

INTRODUCTION

In the previous paper¹ of this series, the effects of carbon dioxide on the polymer structure, the rate of polymerization, and the molecular weight of polymer were investigated. Carbon dioxide was found to have many advantages as a solvent for the radiation polymerization of ethylene.

The purpose of this paper is to determine the effects of reaction conditions such as irradiation time, pressure, dose rate, and temperature on the polymerization, and to discuss the role of carbon dioxide from the viewpoint of kinetics.

EXPERIMENTAL

The reaction vessel, materials (ethylene monomer, carbon dioxide), irradiation facilities, and experimental procedure have already been described.¹ In all experiments, the reaction pressure remained essentially constant during the course of the reaction, since the polymerization was carried out to low conversion (less than 10%).

RESULTS AND DISCUSSION

Effects of Irradiation Time

Polymer yield and molecular weight at various concentrations of carbon dioxide are summarized in Table I, and, in Figure 1, the polymer yield is plotted against reaction time. It is clear that the rate of polymerization is accelerated, since the polymer yield increases rapidly with the time in all series of experiments, and that the yield decreases with increasing concentration of carbon dioxide in whole period of the reaction. Another effect of the time is observed in molecular weight of polymer. As can be seen in Figure 2, the molecular weight increases with the time and reaches a high value (over 10^5). These observations are very similar to those in the bulk polymerization at normal temperature with the use of γ -radiation^{2,3} or azobisisobutyronitrile.⁴ It should be noted, however, that the rate acceleration and the increase in the molecular weight with the time become less pronounced at higher concentrations of carbon dioxide.

TABLE I
Effect of Reaction Time on Polymer Yield
and Molecular Weight^a

Concentration of carbon dioxide, mole-%	Reaction time, hr.	Polymer yield, g.	Molecular weight $\times 10^{-1}$
0	0.50	0.140	19.0
	1.0	0.537	36.0
	1.5	1.245	53.2
5.7	0.50	0.106	14.0
	1.0	0.349	26.0
	2.0	1.283	38.5
23.9	0.67	0.131	10.6
	1.0	0.248	13.0
	1.3	0.394	16.7
	2.0	0.686	20.4
	3.0	1.346	24.6
34.2	1.0	0.201	9.2
	2.0	0.420	10.1
	3.0	0.790	12.6
	4.0	1.120	13.1
	5.0	1.602	15.1
57.3	5.0	0.576	5.1
84.1	8.0	0.074	0.31

^a Reaction pressure, 400 kg./cm.²; temperature, 20°C.; dose rate, 2.5×10^4 rad/hr.; reactor volume, 100 ml.

To show the extent of the time dependency of the polymer yield and the molecular weight, the time-yield and time-molecular weight relations in Figures 1 and 2, respectively, are plotted in logarithmic scale in Figures 3 and 4, respectively. From the slopes of the lines, the time exponents at carbon dioxide concentrations of 0, 5.7, 23.9, and 34.2 mole-% are

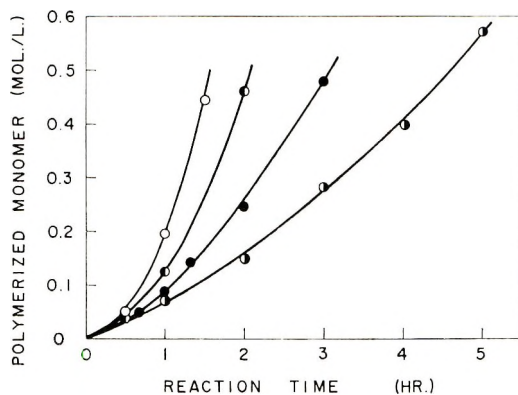


Fig. 1. Polymer yield vs. reaction time at various concentrations of carbon dioxide: (O) 0; (◐) 5.7 mole-%; (●) 23.9 mole-%; (◑) 34.2 mole-%. Reaction pressure, 400 kg./cm.²; temperature, 20°C.; dose rate, 2.5×10^4 rad/hr.

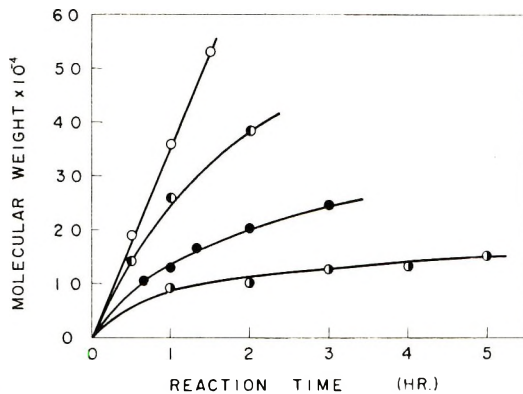


Fig. 2. Molecular weight vs. reaction time. Reaction conditions and symbols are the same as in Fig. 1.

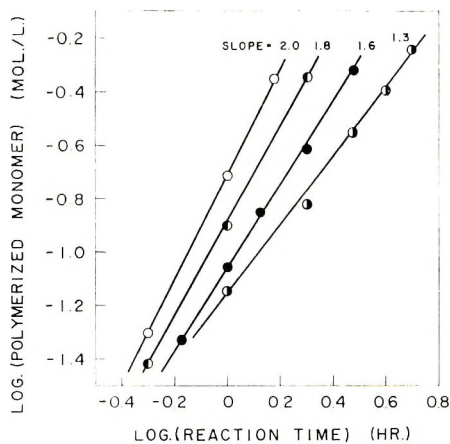


Fig. 3. Logarithmic plot of polymer yield vs. reaction time. Reaction conditions and symbols are the same as in Fig. 1.

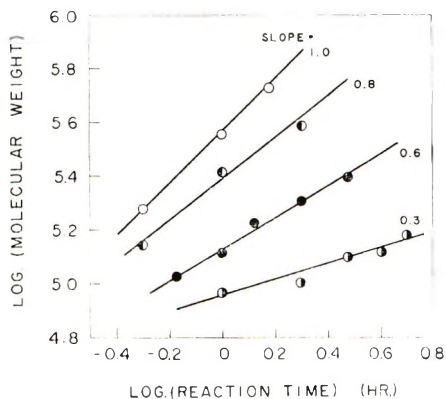


Fig. 4. Logarithmic plot of molecular weight vs. reaction time. Reaction conditions and symbols are the same as in Fig. 1.

found to be 2.0, 1.8, 1.6, and 1.3 for the yield and 1.0, 0.8, 0.6, and 0.3 for the molecular weight, respectively. The significance of these results will be fully discussed below from the viewpoint of kinetics.

Effects of Reaction Pressure, Dose Rate, and Temperature

In order to elucidate the effects of the reaction pressure on the polymer yield and the polymer molecular weight, the polymerization was carried out under various pressures at constant concentration of carbon dioxide of 23.9 mole-%; the results are given in Table II. Figure 5 shows the plot of the yield and the molecular weight against the pressure, where all values were normalized to unit reaction time by using the time exponents of 1.6 for the yield and 0.6 for the molecular weight, respectively. It can be seen that both the yield and the molecular weight increase rapidly with the pressure. From the logarithmic plot, the exponents of the pressure are found to be 2.3 for the yield and 2.0 for the molecular weight, respectively.

Table III contains the results of the experiments run at different dose rates. The yield and the molecular weight normalized to unit time are plotted on a logarithmic scale against the dose rate in Figure 6. From the

TABLE II
Effect of Reaction Pressure on Polymer Yield and Molecular Weight^a

Reaction pressure, kg./cm. ²	Reaction time, hr.	Polymer yield, g.	Molecular weight $\times 10^{-4}$
100	22.0	1.792	4.7
150	22.0	2.831	9.4
200	7.0	1.414	13.0
300	4.0	0.942	11.5

^a Reaction temperature, 20°C.; dose rate, 2.5×10^3 rad/hr.; concentration of carbon dioxide, 23.9 mole-%; reactor volume, 100 ml.

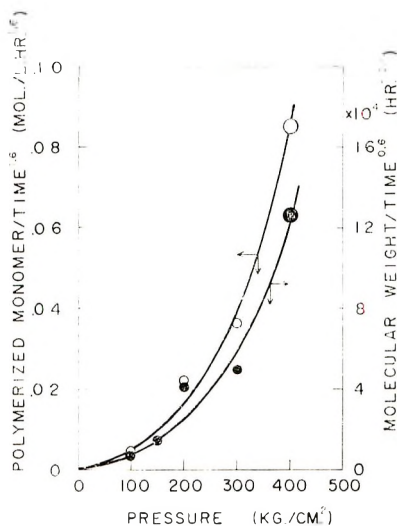


Fig. 5. Effect of reaction pressure on (O) polymer yield and (●) molecular weight. Reaction temperature, 20°C.; dose rate, 2.5×10^4 rad/hr.; concentration of carbon dioxide, 23.9 mole-%. Large circles show mean values at different reaction times.

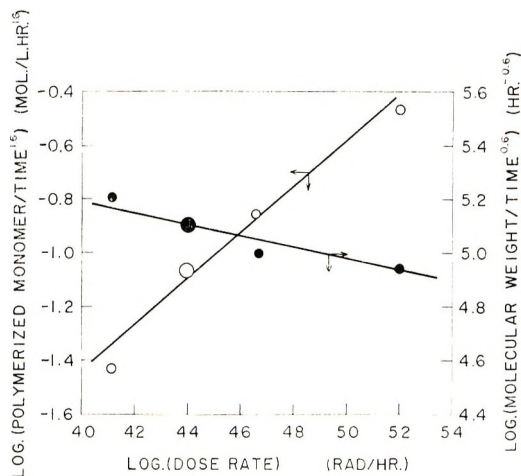


Fig. 6. Effect of dose rate on (O) polymer yield and (●) molecular weight. Reaction pressure, 400 kg./cm.²; temperature, 20°C.; concentration of carbon dioxide, 23.9 mole-%. Large circles show mean values at different reaction time.

slopes of the lines, the dose rate exponents are obtained as 0.85 for the yield and -0.20 for the molecular weight, respectively; these values do not follow the square-root law for a stationary-state polymerization with bimolecular termination.

In Table IV, the yield and the molecular weight are summarized for the polymerization at various temperatures. The time-yield and the time-molecular weight curves are shown in Figures 7 and 8. It can be seen

TABLE III
 Effect of Dose Rate on Polymer Yield and Molecular Weight^a

Dose rate, rad/hr.	Reaction time, hr.	Polymer yield, g.	Molecular weight $\times 10^{-4}$
1.6×10^5	1.0	0.959	8.8
4.5×10^4	1.0	0.390	9.7
1.3×10^4	2.0	0.312	24.5

^a Reaction pressure, 400 kg./cm.²; temperature, 20°C.; concentration of carbon dioxide, 23.9 mole-%; reactor volume, 100 ml.

 TABLE IV
 Effect of Reaction Temperature on Polymer Yield and Molecular Weight^a

Reaction temperature, °C.	Reaction time, hr.	Polymer yield, g.	Molecular weight $\times 10^{-4}$
45	1.0	0.247	13.6
	2.0	0.679	20.7
	3.0	1.577	25.8
60	1.5	0.164	6.4
	3.0	0.388	8.4
	5.0	0.725	9.5
90	1.5	0.159	2.1
	3.0	0.314	1.8
	5.0	0.576	1.4

^a Reaction pressure, 400 kg./cm.²; dose rate, 2.5×10^4 rad/hr.; concentration of carbon dioxide, 23.9 mole-%; reactor volume, 100 ml.

that the acceleration in the rate of polymerization and the increase in the molecular weight with the time become less pronounced with rising temperature; namely, the polymerizations at 20 and 45°C. are characterized

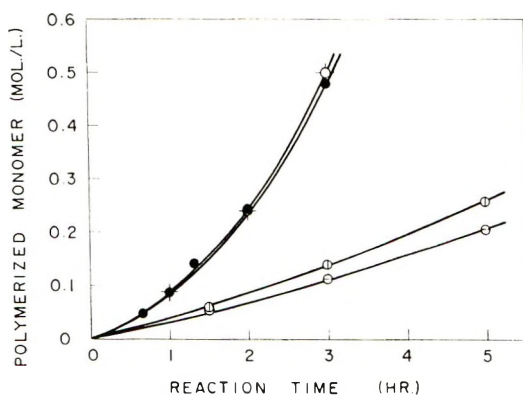


Fig. 7. Polymer yield vs. reaction time at various temperatures: (●) 20°C.; (- -) 45°C.; (○) 60°C.; (⊖) 90°C. Reaction pressure, 400 kg./cm.²; dose rate, 2.5×10^4 rad/hr.; concentration of carbon dioxide, 23.9 mole-%.

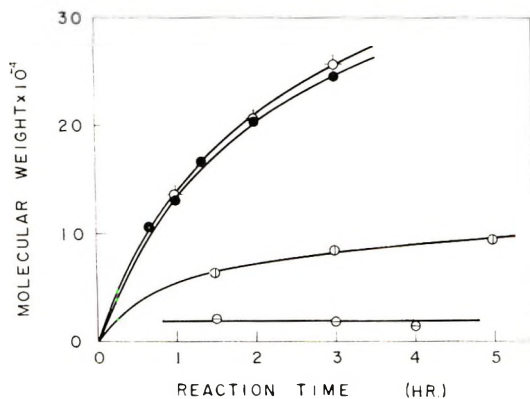


Fig. 8. Molecular weight vs. reaction time. Reaction conditions and symbols are the same as in Fig. 7.

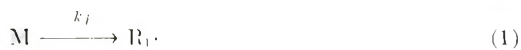
by a rapid increase in rate and in molecular weight with the time, while, in the polymerization at higher temperature ($90^{\circ}\text{C}.$), the rate is only slightly accelerated, and the molecular weight is almost independent of the time.

In these observations of the effects of the pressure, dose rate, and temperature on the yield and the molecular weight, there is no marked difference between the polymerization in liquid carbon dioxide and in the bulk polymerization^{3,5} where the yield and the molecular weight increase rapidly with pressure, and the dose rate exponents are 0.9 for the yield and almost zero for the molecular weight.

Kinetic Considerations on the Role of Carbon Dioxide

Rate of Polymerization. Since the kinetic features similar to the bulk polymerization were observed in the polymerization in liquid carbon dioxide, the reaction mechanism given in eqs. (1)-(5) which was proposed by us for the bulk polymerization³ is also assumed for this polymerization.

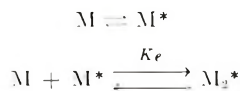
Initiation:



with

$$R_i = k_i \rho_M I$$

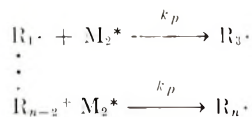
Ethylene excitation



with

$$f_{\text{M}_2^*} = K_e f_{\text{M}}^2 \quad (2)$$

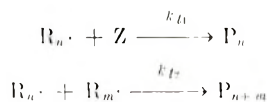
Propagation:



with

$$R_p = k_p [R \cdot] f_{M_2^*} \quad (3)$$

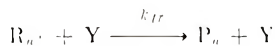
Termination:



with

$$R_t = k_{t1} [Z] [R \cdot] + k_{t2} [R \cdot]^2 \quad (4)$$

Transfer:



with

$$R_{tr} = k_{tr} [R \cdot] [Y] \quad (5)$$

Here M represents the ethylene monomer; $[R \cdot]$, the total concentration of all the active polymer chains, irrespective of size (i.e., $\sum_{n=1}^{\infty} [R_n \cdot]$); M^* is the excited ethylene monomer; M_2^* is the excited ethylene dimer; Y , the substance to which the activity of $R_n \cdot$ is transferred; Z the substance by which $R_n \cdot$ is deactivated; P_n , a dead polymer composed of n monomers; R_i, R_p, R_{tr} , and R_t , the rates of initiation, propagation, transfer, and termination, respectively; k_i, k_p, k_{tr} , and k_t , the rate constants of these reactions; ρ_M , the density of ethylene; I , the dose rate; f_M , the fugacity of ethylene; $f_{M_2^*}$, the fugacity of the excited ethylene dimer, and K_e , the equilibrium constants of the reaction between the ethylene monomer and excited one to form the excited dimer.

Continuous increase in the polymerization rate and molecular weight with the time indicates that nonstationary-state kinetics should be applied for the polymerization. The overall rate of polymerization R with no termination is given by:³

$$R = dM_p/dt \simeq R_p = k_p k_i K_e \rho_M f_M^2 I t \quad (6)$$

By integrating, the polymer yield M_p is:

$$M_p = (1/2) k_p k_i K_e \rho_M f_M^2 I t^2 \quad (7)$$

Equation (7) shows that M_p should increase proportionally with the square of the time. As shown in Figure 9, where M_p is plotted against t^2 , this requirement is realized in the absence of carbon dioxide. When carbon

dioxide is added, however, the plots deviate from this proportionality, and the deviation becomes marked at higher concentrations of carbon dioxide. This fact and similar features in the molecular weight (Fig. 2) indicate that the termination reaction is brought about by the addition of carbon dioxide.

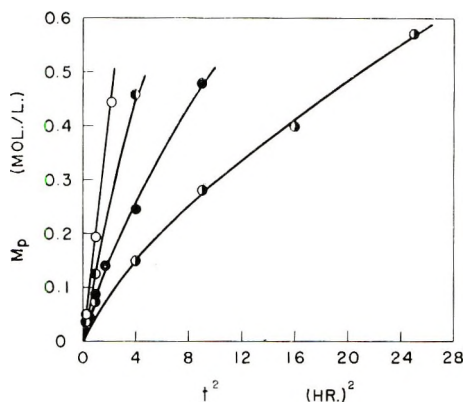


Fig. 9. M_p vs. t^2 . Reaction conditions and symbols are the same as in Fig. 1.

In order to determine the rate of termination, the following graphical method⁶ was used for the polymerization. The concentration of growing radical $[R \cdot]$ at time t is given as the difference between the total number of radicals produced and the number of radicals disappearing as a result of termination.

$$[R \cdot] = \int_0^t R_i dt - \int_0^t R_t dt \tag{8}$$

Since the termination by recombination of growing radicals is thought from the high dose rate exponent of the polymer yield to be negligible, the rate of termination can be represented by:

$$R_t = k_t[Z][R \cdot] \tag{9}$$

where $[Z]$ is the concentration of a terminating agent (which may be carbon dioxide or its radiolysis products).

From eqs. (1), (9), and the relation, $M_p \simeq \int_0^t R_p dt$, eq. (8) becomes:

$$[R \cdot] = k_i \rho_M I t - \{k_t[Z]/k_p K_e f_M^2\} M_p \tag{10}$$

where $[Z]$ is assumed to be independent of the time. By combination of eqs. (3) and (10), the rate of polymerization is given as:

$$R \simeq R_p = k_i k_p K_e \rho_M f_M^2 I t - k_t [Z] M_p \tag{11}$$

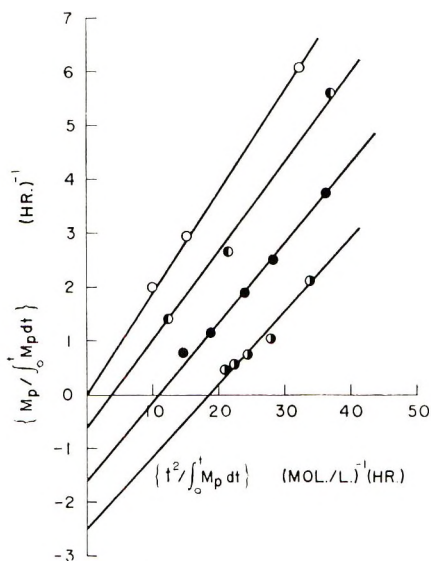


Fig. 10. $\left\{M_p / \int_0^t M_p dt\right\}$ vs. $\left\{t^2 / \int_0^t M_p dt\right\}$. Reaction conditions and symbols are the same as in Fig. 1.

Hence, both sides of eq. (11) is integrated with respect to the time and rearranged to give:

$$\left\{M_p / \int_0^t M_p dt\right\} = (1/2)k_t k_p K_c \rho_M f M^2 I \left\{t^2 / \int_0^t M_p dt\right\} - k_t [Z] \quad (12)$$

Consequently, the plots of $\left\{M_p / \int_0^t M_p dt\right\}$ versus $\left\{t^2 / \int_0^t M_p dt\right\}$ give a straight line, and an apparent first-order termination rate constant, $k_t [Z]$, can be obtained from the intercept on the ordinate.

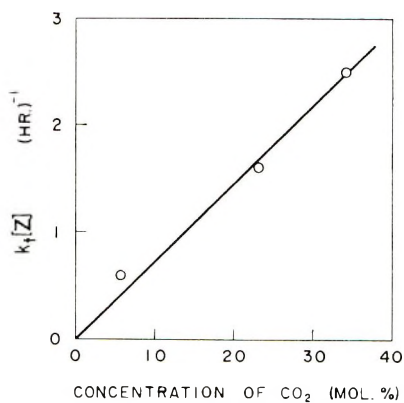


Fig. 11. $k_t [Z]$ vs. concentration of carbon dioxide. Reaction pressure, 400 kg./cm.²; temperature, 20°C.; dose rate, 2.5×10^4 rad/hr.

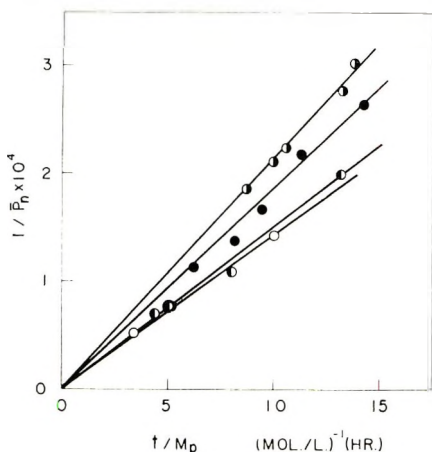


Fig. 12. $1/\bar{P}_n$ vs. t/M_p . Reaction conditions and symbols are the same as in Fig. 1.

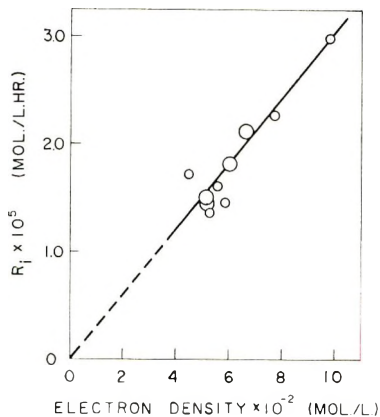


Fig. 13. R_i vs. electron density. Reaction pressure, 100–400 kg./cm.²; temperature, 20°C.; dose rate, 2.5×10^4 rad/hr.; concentration of carbon dioxide, 0–84.1 mole-%. Large circles show mean values at different reaction times.

According to the above procedure, the plots are made in Figure 10, and the values of $k_t [Z]$ are then determined for the various concentrations of carbon dioxide as listed in Table V. Further, in Figure 11, they are

TABLE V
Effect of the Concentration of Carbon Dioxide on the Apparent First-Order Termination Rate Constant^a

Concentration of carbon dioxide, mole-%	$k_t(Z)$, hr. ⁻¹
0	0
5.7	0.6
23.9	1.6
34.2	2.5

^a Reaction pressure, 400 kg./cm.²; temperature, 20°C.; dose rate, 2.5×10^4 rad/hr.

plotted as a function of the concentration of carbon dioxide. The fact that the value of $k_t [Z]$ increases proportionally with the concentration of carbon dioxide leads to the conclusion that carbon dioxide participates in the termination reaction.

Degree of Polymerization. The reciprocal degree of polymerization, $1/\bar{P}_n$, is given by eq. (13) for the polymerization without bimolecular termination.³

$$1/\bar{P}_n = k_i \rho_M I \{t/M_p\} + k_{tr} [Y] / k_p K e f_M^2 \quad (13)$$

By plotting $1/\bar{P}_n$ against t/M_p according to eq. (13), linear relations were obtained for various concentrations of carbon dioxide, as shown in Figure 12. From the fact that all lines go through origin, it is concluded that the transfer reaction does not take place in this system. In addition, the slope of the line ($k_i \rho_M I$) slightly increases with the concentration of carbon dioxide. This indicates that the rate of initiation is increased by the addition of carbon dioxide.

Since the termination by recombination of growing radicals and the transfer reaction are absent, the increase in number of polymer molecules is due solely to the initiation reaction. The rate of initiation, therefore, is calculated by using eqs. (14) and (15),⁷

$$R_i = dN_p/dt \quad (14)$$

$$R_i = d(M_p/\bar{P}_n)/dt \quad (15)$$

where N_p is the number of moles of polymer chain per unit volume. For various concentrations of carbon dioxide, the rates of initiation are calculated as listed in Table VI. This shows that the rate of initiation increases with the concentration of carbon dioxide as well as the electron density of the reaction mixture. As can be seen in Figure 13, the increase in the rate of initiation is proportional to the electron density of the mixture.

TABLE VI
Rate of Initiation^a

Reaction pressure, kg./cm. ²	Concentration of carbon dioxide, mole-%	Electron density $\times 10^{-2}$, mole/l.	Rate of initiation $\times 10^5$, mole/l.-hr.
100	23.9	4.50	1.73
150	23.9	5.30	1.37
200	23.9	5.60	1.62
300	23.9	5.90	1.46
400	0	5.20	1.43
400	5.7	5.14	1.51
400	23.9	6.05	1.82
400	34.2	6.65	2.15
400	57.3	7.79	2.26
400	84.1	9.80	2.98

^a Reaction temperature, 20°C.; dose rate, 2.5×10^4 rad/hr.

Effect of Temperature. The rates of initiation and the apparent termination rate constants were determined at various temperatures ranging from 20 to 60°C., by the above procedure and by using eqs. (13) and (12); the results are listed in Table VII. It is found that the activation energy of the initiation reaction is zero since the rate of initiation normalized to unit electron density (R_i/ρ_{Elec}) is almost independent of temperature. Further, the fact that all the values of R_i/ρ_{Elec} are almost same irrespective of the presence of carbon dioxide shows that the radiation energy absorbed by carbon dioxide is also effective in initiation of the polymerization, as is the energy absorbed by ethylene monomer.

TABLE VII
Effect of Reaction Temperature on the
Rates of Initiation and Termination^a

Reaction temperature, °C.	$R_i/\rho_{\text{Elec}}, \text{hr.}^{-1}$		$k_t/[Z], \text{hr.}^{-1}$	
	No CO ₂	23.9 mole-%	No CO ₂	23.9 mole-%
		CO ₂		CO ₂
20	2.75	3.01	0	1.6
45	—	3.09	—	1.6
60	3.41 ^b	3.09	1.5 ^b	2.8

^a Reaction pressure, 400 kg./cm.²; dose rate, 2.5×10^4 rad/hr.

^b From the literature data⁵ at 58°C.

The apparent termination rate constants of the polymerization in liquid carbon dioxide are found to be larger than those in the bulk polymerization at every temperature investigated, and they increase in both cases. This means that the contribution of carbon dioxide to the termination reaction is significant. The role of carbon dioxide in the initiation and termination reaction is not clear, but radiolysis products of carbon dioxide such as carbon monoxide and oxygen may play an important role in these reactions.

References

1. M. Hagiwara, H. Mitsui, S. Machi, and T. Kagiya, *J. Polymer Sci. A-1*, **6**, 605 (1968).
2. S. Machi, M. Hagiwara, M. Gotoda, and T. Kagiya, *J. Polymer Sci. B*, **2**, 765 (1964).
3. S. Machi, M. Hagiwara, M. Gotoda, and T. Kagiya, *Bull. Chem. Soc. Japan*, **39**, 675 (1966).
4. S. Machi, T. Sakai, T. Tamura, M. Gotoda, and T. Kagiya, *J. Polymer Sci. B*, **3**, 709 (1965).
5. S. Machi, M. Hagiwara, M. Gotoda, and T. Kagiya, *Bull. Chem. Soc. Japan*, **39**, 2696 (1966).
6. T. Kagiya, M. Izu, K. Fukui, and S. Machi, paper presented at the 14th Polymer Symposium, Kyoto, Japan, October 5-7, 1965.
7. S. Machi, M. Hagiwara, M. Gotoda, and T. Kagiya, *J. Polymer Sci. A-1*, **4**, 1517 (1966).

Received March 9, 1967

Emulsion Polymerization. I. Recalculation and Extension of the Smith-Ewart Theory

J. L. GARDON, *Rohm and Haas Company,
Spring House, Pennsylvania 19477*

Synopsis

The most important assumptions underlying the Smith-Ewart theory are that the locus of chain propagation is the monomer-swollen latex particle, polymeric chains are initiated by radicals entering from the water phase into the particles, chain termination is an instantaneous reaction between two radicals within one particle, and particles are nucleated by radicals absorbed into monomer-swollen soap micelles. Right or wrong, these and other assumptions used by Smith and Ewart are retained in this paper. The newly derived and experimentally verifiable equations contain only such parameters which can be determined by experiments not involving emulsion polymerization. The proportionality constant between the particle number and the appropriate powers of soap and initiator concentrations is defined in terms of these independent parameters. Absolute rate equations are presented for the intervals before and after the completion of particle nucleation. To calculate these rates it is not necessary to have prior knowledge of the experimental particle number. The conversion at which particle nucleation is complete is calculated. The molecular weight is defined in terms of independent parameters. Predictions are made for the particle size distribution. It is shown that the validity of the theory is confined to specifiable intervals of conversion, to a certain range of monomer/water ratio, and to soap concentrations whose upper and lower limits are given.

INTRODUCTION

It is convenient to distinguish three intervals in isothermal, single-charge emulsion homopolymerization. All particles are formed in interval I. In the absence of aggregation, the number of particles is constant in intervals II and III. In intervals I and II the reaction mixture consists of three phases: monomer-swollen latex particles, droplets of monomer, and the aqueous phase. When the conversion has proceeded far enough, the monomer droplets disappear, and the reaction mixture becomes a two-phase system of monomer-swollen latex particles and aqueous phase in interval III. In other words, the particle number is increasing and monomer droplets are present in interval I, the particle number is constant and monomer droplets are present in interval II, and the particle number is constant but there are no monomer droplets present in interval III. This distinction among the three intervals will be justified by theory and experiment in this series of papers.¹⁻⁵

In a mathematical theory of homogeneous polymerization, the rates of at least three processes have to be specified: initiation, propagation, and termination of polymeric chains. For heterogeneous emulsion polymerization a fourth process must be specified, the nucleation of particles. The simplest available mathematical theory is that of Smith and Ewart,⁶ which provides a complete description of intervals I and II.

In their paper, Smith and Ewart provided only two experimentally verifiable equations. They predicted that the final particle number should be proportional to the 0.4 power of the initiator concentration and to the 0.6 power of the soap concentration. The proportionality constant, μ in their theory, is not defined in terms of independent parameters. The other experimentally verifiable equation gives the absolute reaction rate during interval II in terms of the particle number, the propagation rate constant, and the monomer concentration in the particles.

One possible limitation of the Smith-Ewart theory is that the basic assumptions are not applicable to all monomers and to all experimental conditions. This paper will not take issue with the basic assumptions, though some will be replaced in subsequent papers (Parts III, IV and V).²⁻⁴ The present paper will establish the limits of validity of the Smith-Ewart model and derive new, experimentally verifiable formulae. Right or wrong, the Smith-Ewart assumptions are the basis of all derivations presented here although the mathematical approach followed is different from that of Smith and Ewart.

CALCULATION OF THE FINAL NUMBER OF PARTICLES

Derivation of the Differential Equation of Particle Nucleation

To illustrate the problem let us assume a monomer/water ratio of 40/60 and about 0.75% sodium lauryl sulfate (SLS) on monomer. If there are about 50 soap molecules in a micelle, the initial charge contains about 2×10^{17} micelles/cc. of water. When the polymerization is complete, 10^{14} to 10^{12} latex particles are usually found in 1 cc. of water. It is evident that not every micelle becomes a latex particle, although it is the general experience that the particle number increases and the particle size decreases with increasing soap level.

In the initial charge the monomer can be found in three loci: in the micelles, whose diameter is about 25-50 Å., in the monomer droplets whose diameter is much larger, 10^4 - 10^5 Å., and dissolved in water. The total surface of the micelles is very large, being perhaps 100 times larger than that of the droplets though they contain only a small fraction of the monomer. As polymerization proceeds, many new particles are formed whose total surface soon becomes much larger than that of the droplets. The primary radicals are formed only in the aqueous phase and are all irreversibly absorbed into the monomer swollen micelles and particles. Only a small fraction of the radicals are absorbed into the droplets so that poly-

merization in droplets is negligible. Even if some initiator radicals combine with monomers dissolved in the aqueous phase, the thus formed oligomeric radicals never grow large enough to precipitate out from the aqueous phase; they became absorbed in micelles or particles and continue to grow there. This matter is further discussed in the Appendix.

The number of radicals produced in 1 cc. of water per second is R (equal to ρ in the original Smith-Ewart theory). Its value can be calculated from k_d , the decomposition rate constant of initiator, $[I]$, the initiator concentration in water, and N_A , the Avogadro number:

$$R = 2N_A k_d [I] \quad (1)$$

For persulfates it is justifiable to assume a constant value of R because the half-life of such initiators is long. The data of Kolthoff and Miller⁷ give half-life values of 41 days to 2.4 hr. at pH 4 and temperatures of 40 and 80°C. At pH 1 the half-lives are shorter at these temperatures, 3.9 days and 0.8 hr., respectively.

As a particle grows, its surface remains saturated with soap and the area per soap molecule is the same on the micelle and particle surfaces. It follows that as long as there is micellar soap available, the total oil phase (micelle + particle)/water interfacial area is constant. This constant area is introduced into the theory by the parameter S , the square centimeters surface area of soap molecules present in 1 cc. of water. It can be calculated from A_s , the area of a soap molecule, $[S]$, the soap concentration in water, and N_A , the Avogadro number:

$$S = N_A A_s [S] \quad (2)$$

In the Smith-Ewart paper $a_s S$ stands for the symbol S used here. To be exact, $[S]$ should stand for the difference between actual soap concentration and CMC, the critical micelle concentration. However, in most experiments $[S] \gg \text{CMC}$.

It is shown in the Appendix that each particle absorbs radicals at a rate proportional to its surface, $4\pi r_i^2$. If n_i is the number of particles per cubic centimeter of water whose radius is r_i , $4\pi \sum n_i r_i^2$ is the total surface of all particles at any given instant. The radicals entering into particles do not nucleate particles, the rest of the radicals enter into micelles and thus nucleate new particles. If N_t is the number of particles per cubic centimeter of water at time t , the differential equation of particle nucleation is:

$$\Delta N_i / \Delta t = dN_i / dt = R [1 - (4\pi/S)(\sum n_i r_i^2)_t] \quad (4)$$

It is assumed here that micellar soap is consumed by two mechanisms: either it is absorbed onto growing polymeric particles, or it becomes "nonmicellar" when a micelle absorbs a radical to become a particle. When the micelles disappear because all soap is absorbed onto the particles, particle nucleation stops. Thus the validity limit of eq. (4) is $S \geq 4\pi \sum n_i r_i^2$.

Rate of Growth of a Single Particle

Since polymerization in the aqueous phase and in monomer droplets is negligible, the sole loci for chain propagation are the monomer swollen particles. There is no polymerization in micelles because a micelle stung by a radical is considered to be a particle.

The radical in a particle continues to grow, and the particle absorbs more monomer to keep the particle growing and also to keep the polymer in the particle swollen. The water phase is saturated with monomer, so that the monomer flux into the particles originates from the monomer droplets and perhaps from other micelles. Thus the monomer droplets act as an inert reservoir of monomer. The chain propagation in the particles can be described by the laws of bulk polymerization; in other words the growth rate of the particle depends on the propagation rate constant k_p and upon the monomer concentration in the particle. The diffusion of monomer into the particle is extremely fast, so that even while the particle grows, the amount of monomer in the particle corresponds to a thermodynamic equilibrium. It is assumed that this equilibrium monomer concentration in the particle is not a sensitive function of particle size. Thus the monomer concentration in the growing particles is about constant and independent of conversion.

The bulk and solution polymerization kinetics depend upon the monomer and radical concentrations:

$$-d[M]/dt = k_p[M][R] \quad (5)$$

To apply this equation for emulsion polymerization, it must be transformed. We define: Ω as the number of converted moles of monomer in the system, V as the volume of the system, q as the number of radicals in the container, ϕ_m as the monomer volume fraction, V_m as the molar volume of monomer; N_A is Avogadro's number.

$$d\Omega/dt = -Vd[M]/dt \quad (6a)$$

$$q = N_A V [R] \quad (6b)$$

$$\phi_m = V_m [M] \quad (6c)$$

Substitution into eq. (5) gives:

$$d\Omega/dt = (k_p/N_A V_m)\phi_m q \quad (7)$$

This equation is equally valid for solution (bulk) polymerization where V , the solution volume, is constant and for polymerization in an emulsion particle where V , the volume of particle, changes with time.

The molar volume of a converted monomer unit is $V_m d_m/d_p$, where d_m , d_p are densities of monomer and polymer, respectively. The volume of polymer in the particle is:

$$\Omega V_m d_m/d_p = V(1 - \phi_m) = (4\pi/3)r^3(1 - \phi_m)$$

Differentiation and substitution into eq. (7) gives the rate of volume growth:

$$d(r^3)/dt = (d\Omega/dt)(3/4\pi)V_m d_m/d_p(1 - \phi_m) = \\ (3/4\pi)(k_p/N_A)(d_m/d_p)q\phi_m/(1 - \phi_m)$$

It is assumed that in interval I each particle grows as if it contained one radical only; $q = 1$. Furthermore, ϕ_m is constant. A new constant, K , is defined:

$$d(r^3)/dt = K \\ K = (3/4\pi)(k_p/N_A)(d_m/d_p)\phi_m(1 - \phi_m) \quad (8)$$

The parameter μ of the Smith-Ewart paper is equal to $4\pi K/3$. Equation (8) is consistent with an analogous equation presented by Flory.⁸

A particle is nucleated at time τ after the polymerization starts and is assumed to have zero radius at τ . Its cubed or squared radius at time t ($t > \tau$) will be:

$$r^3 = K(t - \tau) \quad (9)$$

$$r^2 = K^{2/3}(t - \tau)^{2/3} \quad (10)$$

Variation of Total Particle Surface with Time in Interval I

At time τ the number of particles nucleated during $\Delta\tau$ is ΔN_τ . Each of these particles will have a value of r^2 equal to $K^{2/3}(t - \tau)^{2/3}$ at time t . At a fixed t the total area of all particles divided by 4π is:

$$(\sum n_i r_i^2)_t = \sum_{\tau=0}^{\tau=t} K^{2/3}(t - \tau)^{2/3} \Delta N_\tau$$

Substitution from eq. (4) gives:

$$(\sum n_i r_i^2)_t = K^{2/3} R \sum_{\tau=0}^{\tau=t} [1 - (4\pi/S)(\sum n_i r_i^2)_\tau] (t - \tau)^{2/3} \Delta\tau \\ = K^{2/3} R \int_0^t [1 - (4\pi/S)(\sum n_i r_i^2)_\tau] (t - \tau)^{2/3} d\tau \quad (11)$$

The validity of these equations is limited to the interval $0 \leq 4\pi(\sum n_i r_i^2) \leq S$. When $4\pi\sum n_i r_i^2 = S$, particle nucleation stops and there are no more micelles.

New variables, the dimensionless total surface y , the dimensionless times x and ξ , are now introduced and substituted into eq. (11).

$$y = (4/S)(\sum n_i r_i^2) \quad (12)$$

$$x/t = \xi/\tau = (12\pi/5)^{3/8} K^{2/8} (R/S)^{3/8} \quad (13)$$

$$y_x = (5/3) \int_0^x [(1/\pi) - y_\xi](x - \xi)^{2/3} d\xi \quad (14)$$

The limits of validity of this equation are $0 \leq y \leq (1/\pi)$. Particle nucleation stops when $y = (1/\pi)$.

This integral equation belongs to the class of the Volterra equations. It was solved by using a Bendix B-15 computer by the conventional numerical methods⁹ and by the conventional series expansion method.¹⁰ These two independent calculations give the same results as the very simple way of solving this equation, outlined below.

If $F(\xi) = \int_a^b f(\xi) d\xi$, the definite integral between limits a and b is given by the Simpson rule:

$$F(a) - F(b) = \int_b^a f(\xi) d\xi = \frac{a-b}{6} \left[f(a) + 4f\left(\frac{a+b}{2}\right) + f(b) \right]$$

This rule gives an exact solution if $f(\xi)$ is of third order or less. To apply this rule to eq. (14), we set $f(\xi) = (5/3) [(1/\pi) - y(\xi)] (x - \xi)^{2/3}$, $F(a) = y(x)$, $F(b) = y(0) = 0$, $f(x) = 0$, $f(0) = 5x^{2/3}/3\pi$, and $f(x/2) = (5/3) [(1/\pi) - y(x/2)](x/2)^{2/3}$.

Substitution and rearrangement gives the following recursion formula:

$$y(x) = 0.318x^{5/3} - 0.701x^{5/3}y(x/2) \quad (15)$$

To start the calculation, one chooses a sufficiently low value of $x = x_1$ so that the second term on the right-hand side is negligibly small. If one aims for better than 1% accuracy, $x_1 \leq 0.1$ satisfies this requirement. For the first step one calculates $y(2x_1) = 0.318(2x_1)^{5/3} - 0.701(2x_1)^{5/3}y(x_1)$. The values of $y(4x_1)$, $y(8x_1)$, etc. are calculated in analogous manner.

An important result of these calculations is that nucleation stops ($y = 1/\pi$) when $x = x_{cr}$ and $t = t_{cr}$, where the subscript cr refers the quantity to the point when particle nucleation is just complete.

$$x_{cr} = 1.232 \quad (16)$$

$$t_{cr} = 0.365(S/R)^{0.6}/K^{0.4} \quad (17)$$

As will be shown in Part II,¹ the theoretical and experimental values of t_{cr} are about few minutes.

Solution of the Differential Equation of Particle Nucleation

The integral form of eq. (4) is:

$$N_t = R \int_0^t [1 - 4\pi(\sum n_i v_i^2)_\tau / S] d\tau \quad (18)$$

The new dimensionless variable ν for the number of particles is defined:

$$\nu_x = 4(5/12\pi)^{2/3} S^{-3/4} (K/R)^{2/3} N_t \quad (19)$$

Combination of eqs. (12), (13), (18), and (19) gives:

$$\nu_x = (5/3) \int_0^x (1/\pi - y_\xi) d\xi \quad (20)$$

Conventional numerical integration⁸ with the aid of computer and the recursion formula obtained with the aid of the Simpson rule give the same values of ν_x . The Simpson rule solution is given below and should be handled in a manner discussed in conjunction with eqs. (14) and (15).

$$\nu_x = 0.279x[1.91 - y(x) - y(x/2)] \quad (21)$$

Particle nucleation stops when $x = 1.232$ according to eq. (16). At this point $\nu = \nu_{cr}$ and $N_t = N$, where N is the final number of particles in 1 cc. of water.

$$\nu_{cr} = 0.3717 \quad (22)$$

$$N = 0.208S^{0.6}(R/K)^{0.4} \quad (23)$$

This is the exact mathematical equivalent of the corresponding Smith-Ewart solution.* As will be shown in Part II,¹ this equation predicts 10^{12} – 10^{15} particles/cc. of water, in good agreement with experimental findings.

VARIATION OF CONVERSION WITH TIME IN INTERVAL I

The amount of polymer formed is proportional to the total volume of the particles, or to $\sum n_i r_i^3$. A particle nucleated at time τ has a cubed radius of $K(t - \tau)$ at time t , in accordance with the previous assumptions. The number of particles nucleated in $\Delta\tau$ at time τ is ΔN_τ , and the total volume divided by $4\pi/3$ is

$$(\sum n_i r_i^3)_t = \sum_{\tau=0}^{\tau=t} K(t - \tau) \Delta N_\tau \quad (24)$$

Substitution from eq. (4) and replacement of summation by integration yields:

$$(\sum n_i r_i^3)_t = RK \int_0^t [1 - 4\pi/S(\sum n_i r_i^2)_\tau](t - \tau) d\tau \quad (25)$$

The new dimensionless volume z is now introduced:

$$z_x = 4(12\pi/5)^{1/2} S^{-6/5} (R/K)^{1/2} (\sum n_i r_i^3)_t \quad (26)$$

Combination of eqs. (12), (13), (25), and (26) gives:

$$z_x = (5/3) \int_0^x (1/\pi - y_\xi)(x - \xi) d\xi \quad (27)$$

The conventional numerical and the Simpson rule solutions of this integral equation can be fitted with the following analytical formula with better than 1% accuracy within the validity range $0 \leq x \leq 1.232$:

$$z = 0.265x^2 - 0.047x^{3.55} \quad (28)$$

* Equation (26a) of the Smith-Ewart paper reads: $N = 0.37(a_s S)^{0.6}(\rho/\mu)^{0.4}$.

When particle nucleation stops, $x = 1.232$ and $z = z_{cr}$:

$$z_{cr} = 0.3016 \quad (29)$$

It is convenient for the analysis of experimental data, and also for the new mathematical derivations of Part III,² to express the amount of converted monomer in terms of volume of polymer per unit volume of water. The symbol P is assigned to this quantity.

$$P = (1 - \phi_m)(4\pi/3)(\sum n_i \bar{v}_i^3) \quad (30)$$

Combination of eqs. (13), (26), (28), and (30) gives the variation of conversion with time in interval I.

$$P = 1.47(1 - \phi_m)KRt^2[1 - 1.65K^{0.62}(R/S)^{0.93}t^{1.55}] \quad (31)$$

For very short times, $t \leq 0.18(S/R)^{0.6}K^{-0.4} = 0.5t_{cr}$, the second term in the bracket is much less than unity. Substitution from eq. (8) gives the initial part of the conversion-time curve:

$$P = 0.351(k_p/N_A)(d_m/d_p) \phi_m Rt^2 \quad (32)$$

It follows that for a very short initial time, while particles become nucleated, the conversion is proportional to the initiator concentration and to t^2 and is independent of the soap concentration. Initial proportionality between conversion and t^2 was also predicted by Bakker.¹¹

Particle nucleation stops at $P = P_{cr}$, at a value corresponding to z_{cr} :

$$P_{cr} = 0.209S^{1.2}(K/R)^{0.2} (1 - \phi_m) \quad (33)$$

It is likely that one of the reasons for the occasional deviations from the Smith-Ewart predictions is that in the experiments either the soap concentration was too high or the monomer/water ratio was too low, so that no well defined transition from interval I to interval II was obtained, and the reaction entered interval III directly from interval I without an intermediate interval II stage.

The quantity P_{cr} is not a fractional conversion, but an absolute value. It will be shown in Part II⁴ that its value is about 0.05–0.1 cc. polymer/cc. water. On the other hand, the transition between intervals II and III, P_{II-III} , is defined by a fractional conversion, and its value depends upon the monomer/water weight ratio (m/w) in the initial charge. The equilibrium weight fraction of the polymer in the monomer swollen latex particles is equal to the critical fractional conversion at which transition between intervals II and III takes place. It follows that:

$$P_{II-III} = (m/w)(1 - \phi_m)d_{\text{water}}/d_p [1 - \phi_m + (d_m/d_p) \phi_m] \quad (34)$$

where d_{water} is density of water.

This equation is valid only if the monomer solubility in water is negligible.

GROWTH HISTORY OF INDIVIDUAL PARTICLES DURING INTERVAL I

Number of Radicals Absorbed by Latex Particles During Interval I

In interval I the interfacial area between oil and water phase is constant and equal to S square centimeters per cubic centimeter of water. The number of radicals entering into this interface is R per second. The surface of a particle is $4\pi r^2$, and the number of radicals entering it per second is:

$$d\omega/d^*t = 4\pi r^2 R/S$$

where ω is the number of radicals captured by a particle.

For sake of simplicity it is assumed that a newly nucleated particle has zero initial radius and the particle age *t is measured from the point of nucleation. At time *t the radius of the particle is $(K^*t)^{1/3}$ by eq. (9). It follows that:

$$\begin{aligned} d\omega/d^*t &= 4\pi(R/S) (K^*t)^{2/3} \\ \omega &= 4\pi K^{2/3} (R/S) \int_0^{^*t} ^*t^{2/3} d^*t = (12\pi/5)K^{2/3} (R/S) ^*t^{5/3} \end{aligned}$$

We define *t_1 , the average time needed for a single radical to enter a particle which contains only one growing polymer chain, and obtain this value by setting $\omega = 1$ in the defining equation. In eq. (35) *t_1 is compared to t_{cr} , the time when particle nucleation stops [cf. eq. (17)].

$$^*t_1 = (5/12\pi)^{3/5} (S/R)^{0.6} / K^{0.4} = 0.81t_{cr} \quad (35)$$

As can be seen, the dimensionless time scale x in eq. (13) was so chosen that $x = 1$ at *t_1 .

Actually *t_1 is overestimated here because the proper lower boundary condition for integration should express the fact that at $^*t = 0$ the radius of the particle is not zero but equal to the radius of a micelle. This error is ignored at present.

All particles nucleated within the interval from $(t_{cr} - ^*t_1)$ to t_{cr} are hit within interval I only by those radicals which nucleated them. The number of these particles can be calculated from eq. (21) and is 67.3% of the final number of particles.

It is now assumed that when a radical enters into a particle containing a growing chain, it terminates growth instantaneously. The average radius of particles containing a single terminated chain is $(K^*t_1)^{1/3}$. These "dead" particles do not grow till a third radical enters them. The rate of radical entry into such "dead" particles is:

$$d\omega/d^*t = \Delta\omega/\Delta^*t = 4\pi (R/S)(K^*t_1)^{2/3}$$

From $\Delta\omega = 1$, *t_2 , the average length of time while the particle is "dead" is obtained:

$$^*t_2 = 0.486t_{cr} \quad (36)$$

It is evident that $(*t_1 + *t_2) > t_{cr}$. On the average, within interval I none of the particles is hit by more than one radical in addition to the one that nucleated it. Only 32.7% of the particles are hit by such a second radical and are "dead" when particle nucleation stops. In this context it is of interest to establish a material balance for radicals. The number of particles which absorbed only one radical in interval I is $0.673N$, and the number which absorbed two radicals is $0.327N$. The total number of radicals absorbed is calculable from eq. (23):

$$(0.673 + 2 \times 0.327)N = 1.327N = 0.275S^{0.6} (R/K)^{0.4}$$

The total number of radicals formed in interval I can be calculated from eq. (17):

$$Rt_{cr} = 0.365S^{0.6}(R/K)^{0.4}$$

There is a 25% discrepancy in these numbers; this is the maximum error in N and is due to ignoring the effect of second radical entry upon particle growth rate in the derivation of eq. (23).

It also follows from these calculations that at the completion of particle nucleation the average number of radicals per particle is 0.673.

Initial Molecular Weight

The initial molecular weight is calculated from the average volume of a particle with one terminated chain in it, $(4\pi/3)K*t_1$. The number-average molecular weight of the "dead" chain is obtained by multiplying this volume by the volume fraction of the polymer in the particle $(1 - \phi_m)$, polymer density, d_p , and Avogadro's number, N_A . It is convenient to present the result of this multiplication after rearranging it in terms of eqs. (8), (23), and (35).

$$M_{\text{initial}} = 1.44 k_p \phi_m d_m N/R \quad (37)$$

As will be shown this value is 44% higher than calculated for interval II. However, it is not likely that in reality the initial molecular weight is higher than the interval II value. The error in $*t_1$ used to calculate M_{initial} can be quite serious. It makes a difference whether a particle grows from initial zero size or initial micellar size. It can only be said that according to the theory the initial molecular weight should not differ significantly from the interval II molecular weight.

DESCRIPTION OF INTERVAL II

Conversion Rate in Interval II

In eq. (7) the value of Ω , the number of moles of converted monomer per particle, is given. From it the total volume of polymer present in 1 cc. of water P can be calculated:

$$P = \Omega V_m N d_m / d_p \quad (38)$$

To obtain the overall conversion rate, eqs. (7) and (38) are combined and q , the actual number of radicals per particle, is replaced by Q , the average number of radicals per particle.

$$dP/dt = (k_p/N_A)(d_m/d_p)N\phi_m Q \quad (39)$$

The validity of this equation rests only on the one assumption that the monomer swollen latex particles are the sole loci of chain propagation. To make better use of this equation N , ϕ_m , and Q must be specified.

By restricting to $P > P_{cr}$ [cf. eq. (33)] N is constant. This implies, following the interval I assumptions, that all radicals originating in the aqueous phase are now absorbed into the monomer-swollen latex particles. If they were not, new particles would be nucleated.

As in interval I, ϕ_m is assumed to stay constant. At this point, this arbitrary sounding approximation requires explanation. Even if the monomer and the polymer are miscible in all proportions in bulk, i.e., even if the monomer is a good solvent for the polymer, only a limited amount of monomer can enter a latex particle from the monomer saturated aqueous phase. This is equally true for a polymerizing or for a "dead" latex particle. The reason was given by Morton et al.¹² The free energy of mixing would favor the entry of monomer into the particles without limitation as long as the water is kept saturated with monomer from an external reservoir. However, the specific surface of the tiny particles is very large; on swelling, the surface of the particles increases, and the total surface energy change obtained when these tiny particles swell has the same order of magnitude as the free energy of mixing but of opposite sign. Thus each particle can swell only to the extent where the free energy of mixing and the surface energy change on swelling exactly compensate each other and there is a well-defined swelling equilibrium analogous to the swelling equilibrium obtainable with crosslinked polymers. The theory predicts that, for a given monomer-polymer system, the swelling, i.e., ϕ_m , should increase with increasing particle size and with decreasing interfacial tension between particles and water.

This matter will be analyzed in detail in Part VI.⁵ It should suffice to say now that according to the theory ϕ_m is a relatively insensitive function of particle size in the particle size range encountered during emulsion polymerization. While this in itself favors the approximation of constant ϕ_m in interval II, additional factors make this approximation plausible.

The surface of the particles is saturated with soap only during interval I. In interval II the total surface of monomer-swollen particles present in 1 cc. of water becomes larger than S and increases with conversion. Thus the water-particle interface becomes less and less completely covered by soap molecules; the interfacial tension rises and this, by itself, would depress ϕ_m . This effect may just about compensate the effect of increasing particle size which by itself, at constant interfacial tension, would cause an increase in ϕ_m .

For ϕ_m to be actually independent of conversion during the reaction it is necessary that the monomer diffusion into the particle from the monomer saturated water phase should be much faster than its consumption in the particle by polymerization so that the ϕ_m corresponding to thermodynamic equilibrium should be maintained. Experimental evidence to be reviewed in Part VI³ indicates that this is indeed so.

It is evident that ϕ_m can be maintained at the saturation equilibrium value only as long as there is enough unconverted monomer present in the reaction mixture to saturate the aqueous phase and the latex particles. This requirement is satisfied by the criterion $P < P_{II-III}$ [cf. eq. (34)].

To determine the value of Q , the termination rate has to be specified. Here we restrict ourselves to the Smith-Ewart case 2 and assume infinitely fast termination. Accordingly, no two radicals can coexist in a particle. If a radical enters a growing particle, it immediately terminates the growth of the chain. The particle is "dead" till hit by another radical which starts new chain growth. The average interval between radical entries is N/R , assumed to be constant. Thus each particle contains one radical half of the time, no radical the other half of the time. Since the process is random, at any time only half of the particles contain radicals and throughout interval II Q is constant, equal to half, and independent of conversion. It will be shown in Parts III and IV^{2,3} that this assumption holds only as a limiting case for latexes of very small particle size made at low initiation rates. In such small particles two radicals can meet very fast for cross-termination, and the interval between radical entries, N/R , is much larger than the time needed for cross-termination. Restriction of the validity of the instantaneous termination assumption to such systems is also consistent with the Stockmayer¹³ theory.

Since $Q = 0.5$ and since N and ϕ_m are also independent of conversion, the conversion rate in interval II given by eq. (39) is constant. This constant rate in interval II will be called the "Smith-Ewart rate" and the symbol B is assigned to it:*

$$B = 0.5 (k_p/N_A) (d_m/d_p) \phi_m N = dP/dt \quad (40)$$

This equation is not explicit in k_p and ϕ_m since N is a function of these parameters. Combination of eqs. (8), (23), and (40) gives:

$$B = 0.185(k_p\phi_m S d_m/d_p N_A)^{0.6} [R(1-\phi_m)]^{0.4} \quad (41a)$$

or

$$B = 0.435(1 - \phi_m)(KS)^{0.6} R^{0.4} \quad (41b)$$

Equation (40) can be written in terms of the dimensionless variables [cf. eqs. (8), (13), (22), (26), and (30)].

$$dz/dx = 0.5\nu_{cr} = 0.186 \quad (42)$$

*Equation (40) is equivalent to eq. (15) of the Smith-Ewart paper.

The conversion rate in interval I can be calculated by differentiating eq. (28). At the completion of particle nucleation ($x = 1.232$), $dz/dx = 0.373$ is obtained. This would be the conversion rate just before and at the transition between intervals I and II if all particles contained one growing radical, as was assumed in deriving eq. (28). If the steady-state termination were reached after the second radical entry, so that the average number of radicals per particle should become half at $t \leq t_{cr}$, the interval I kinetics [eq. (28)] would predict exactly the same conversion rate at $t = t_{cr}$ as given in eq. (42). If, as shown in the previous section, the average number of radicals per particle is 0.623 at $t = t_{cr}$, the conversion rate may temporarily exceed the Smith-Ewart interval II rate by 26% at $t = t_{cr}$ but this would probably be unnoticeable experimentally.

Thus the combined interval I and interval II models [eqs. (28), (31), (40), and (42)] predict the conversion rate to rise from zero at $t = 0$ to about the value of B at $t = t_{cr}$. From here on the rate is predicted to be constant and equal to B within interval II.

The variation of conversion with time in interval II has to satisfy the boundary condition $P = P_{cr}$ when $t = t_{cr}$. It follows that:

$$P = Bt + (P_{cr} - Bt_{cr}) \quad (43)$$

The value of the extrapolated intercept of the conversion-time plot of interval II is calculable from eqs. (17), (33), and (41):

$$P_{cr} - Bt_{cr} = (0.051 + 0.158\phi_m) (K/R)^{0.2} S^{1.2} \quad (44)$$

Thus the linear portion of the conversion-time curve should not extrapolate exactly to the origin. However, the intercept on the conversion axis is very small; this can be ascertained by putting into eq. (44) experimental K , R , and S values given in Part II.¹ It is likely that this intercept is too small to be experimentally observable.

Molecular Weight in Interval II

The volume of polymer produced in one second in a single growing particle is $2B/N$; the factor 2 is here to take into account that only half of the particles are growing at a given time. The interval between the entry of two radicals into the particle, N/R , is the growth time of a single polymer chain, assuming instantaneous termination. It follows that the number-average molecular weight in interval II is:

$$M_{SE} = (2B/N) (N/R) N_A d_p = 2BN_A d_p / R \quad (45)$$

This value will be referred to as the Smith-Ewart molecular weight. By substituting from eqs. (8), (23), and (40) alternate expressions for M_{SE} are obtained:

$$M_{SE} = k_p \phi_m N d_m / R \quad (46)$$

$$M_{SE} = 0.318 [N_A d_p (1 - \phi_m)]^{0.4} (d_m k_p \phi_m S / R)^{0.6} \quad (47)$$

These equations predict molecular weights in the several million range, consistent with experiments. It is noteworthy that M_{SE} is proportional to the 0.6 power of soap concentration and is inversely proportional to the 0.6 power of initiator concentration by eqs. (1), (2), and (47). An equation analogous to eq. (46) was also presented by Vanderhoff et al.¹⁴

PARTICLE SIZE DISTRIBUTION

It is customary to determine the particle size distribution of latexes only at full conversion. It is evident that no prediction can be made concerning the size distribution of a fully converted latex based on the Smith-Ewart model since this model is valid only for intervals I and II. For example, about the last 55% of styrene emulsion polymerization lies outside the validity limits of the Smith-Ewart model, i.e., within interval III. In interval III the monomer concentration within the particles decreases. Termination is known to be a diffusion-controlled process so that the termination rate constant must decrease with increasing conversion during interval III; this is due to the Trommsdorff gel effect.¹⁵ It would follow that the Smith-Ewart assumption of instantaneous termination becomes a very questionable approximation for interval III, even for small particle sized latexes with low initiation rates. Part III² will show that slow termination rates lead to an accumulation of radicals in the particles and to a broadening of size distribution. These limitations should be borne in mind in the interpretation of experimental particle size distribution data.

The Smith-Ewart model predicts that with increasing conversion the particle size distribution should broaden in interval I and should become progressively narrow in interval II. The mathematics leading to this conclusion are presented below.

In interval I a broad particle size distribution might be obtained for two reasons. One reason is that the growth of particles is often terminated earlier or later than the average by a second radical entry and that "dead" particles are often reinitiated earlier or later than the average by the entry of a third radical. Thus the $*t_1$ and $*t_2$ values of eqs. (35) and (36) are averages only, the actual times of second and third radical entries are distributed around $*t_1$ and $*t_2$ by the Poisson distribution. This effect is ignored here and the degree of polydispersity is underestimated.

The second reason for polydispersity is that particles nucleated at different times have different growth times and the particles nucleated earlier are expected to be larger in size. The value of $\sum n_i r_i^4$ and $\sum n_i r_i^4$ at $t = t_{cr}$ is needed to calculate the effect on polydispersity. Two new dimensionless variables are defined:

$$\rho = 4(5/12\pi)^{1/6}(K/R)^{1/6}S^{-4/6} \sum n_i r_i^4 \quad (48)$$

$$u = 4(12\pi/5)^{2/6}(R/K)^{2/6}S^{-7/6} \sum n_i r_i^4 \quad (49)$$

The derivation and solution of the integral equations which describe the time dependence of these quantities during interval I is analogous to the

treatments involving eqs. (14), (18), and (27). The integral equations to solve are:

$$\rho = (5/3) \int_0^x (1/\pi - y_\xi) (x - \xi)^{1/2} d\xi \quad (50)$$

$$u = (5/3) \int_0^x (1/\pi - y_\xi) (x - \xi)^{3/2} d\xi \quad (51)$$

The solution of these equations at the completion of particle nucleation is:

$$\rho_{cr} = 0.3429 \quad (52)$$

$$u_{cr} = 0.2898 \quad (53)$$

Polydispersity at the completion of particle nucleation is measured by the ratios of the appropriate averages of particle sizes: r_n , the number-average radius; r_w , the weight-average radius; and r_{sv} , the surface to volume-average radius. The dimensionless variables, y , v , and z defined and evaluated in eqs. (12), (19), (22), (26), and (29) are also used:

$$r_n = \sum n_i r_i / N = (5/12\pi)^{1/2} (KS/R)^{1/2} \rho / v \quad (54)$$

$$r_{sv} = \sum n_i r_i^3 / \sum n_i r_i^2 = (5/12\pi)^{1/2} (KS/R)^{1/2} z / y \quad (55)$$

$$r_w = \sum n_i r_i^4 / \sum n_i r_i^3 = (5/12\pi)^{1/2} (KS/R)^{1/2} u / z \quad (56)$$

From the critical values of the dimensionless variables the following ratios of the radius averages at the completion of particle nucleation are obtained:

$$(r_w/r_n)_{cr} = u_{cr} v_{cr} / z_{cr} \rho_{cr} = 1.04 \quad (57)$$

$$(r_{sv}/r_n)_{cr} = z_{cr} v_{cr} / y_{cr} \rho_{cr} = 1.03 \quad (58)$$

$$(r_w/r_{sv})_{cr} = u_{cr} y_{cr} / (z_{cr})^2 = 1.01 \quad (59)$$

The polydispersity which would be due solely to differences in particle growth times, is independent of the monomer properties, of the methods of initiation, and of the nature soap. The ratios of different radius averages are quite close to unity; it follows that the particle size distribution at the completion of particle nucleation would be quite narrow if only differences in growth times contributed to polydispersity. Part IV³ will show that the experimental $(r_w/r_n)_{cr}$ is about 1.2, higher than predicted in eq. (57). This is not unexpected, since in the theory the effect of random entry of radicals into particles was neglected.

As to interval II, the theory predicts that the rate of volume growth of each particle should be independent of its size. This should hold even if radicals did not always enter the particles at intervals equal to N/R , but instead at intervals having a Poisson distribution with N/R as average. If each particle undergoes a sufficiently large number of cycles of initiation and termination within interval II, the average growth rate of each should be about equal. It follows from the model that:

$$dV^3/dt = 3V^2 dV/dt = 0.5K = \text{constant} \quad (60)$$

Thus the rate of increase in the particle radius is inversely proportional to the radius squared. The rate of relative increase in radius, dr/r , is inversely proportional to the radius and the relative growth of the larger particles is slower than that of the smaller particles. It follows that, according to the model, the distribution should sharpen during interval II.

APPENDIX

The assumption that during interval I particles absorb radicals at a rate proportional to their surface will be justified here. A criterion will be established for the validity of the assumption that all radicals are absorbed from the aqueous into the organic phase.

It is assumed that not all radicals are absorbed into the organic phase. Radicals which cross-terminate without initiating or terminating a polymeric chain are ignored. The radicals which do not absorb into the organic phase initiate monomers dissolved in the aqueous phase. When the oligomeric radicals reach a critical size, they precipitate and become new latex particles. They then absorb more monomer and grow indistinguishably from particles nucleated by radical absorption into monomer swollen micelles.

A radical is assumed to reach the critical size for precipitation in a well defined time, t_{prec} . During t_{prec} it moves, by Brownian motion, from its origin to an average distance L , which can be calculated from the mean diffusive displacement with the aid of the diffusion coefficient D .

$$L = (2Dt_{\text{prec}})^{0.5} \quad (61)$$

It may be of interest to estimate the order of magnitude of L . Priest¹⁶ found that poly(vinyl acetate) began to precipitate at a degree of polymerization equal to 53.5 when a 0.27*M* aqueous vinyl acetate solution was polymerized at 51°C. For a value for 2.76×10^6 cm.³/mole-sec. as propagation constant,¹⁷ t_{prec} is estimated to be 0.07 sec. A diffusion coefficient of 10^{-6} cm.²/sec. is assumed and gives by eq. (61) $L = 3.7 \times 10^{-4}$ cm.

If there is no particle or monomer swollen micelle within the distance L from the origin of a radical, this radical must precipitate and nucleate a new particle. On the other hand, if a radical originates within the distance L from the surface of some spherical oil-phase unit (micelle or particle), it may or may not collide with this unit. It is assumed that if the radical collides with the sphere, it becomes irreversibly absorbed into it. The probability of collision, $p(r, \lambda)$, is a function of sphere radius and of the distance λ of the site of radical origin to the sphere surface.

For calculating the probability we assume that if the radical moves within the conelike space whose cross section is shaded in Figure 1, it collides with the sphere; if it moves outside the conelike space, it does not.

The length of the tangent drawn to the sphere from the site of the origin of the radical is θ . Two cases are distinguished: case A with $0 < \theta < L$ and case B with $\theta > L$ but $\lambda < L$.

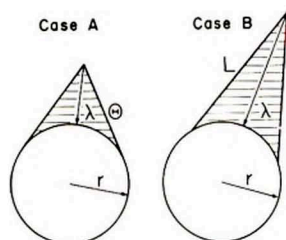


Fig. 1. Cross-sections of geometrical models to calculate the probability that a radical formed at a distance λ from the particle will hit it. The particle radius is r , L is the free mean pass, θ is the length of tangent from the point where the radical originates. In case A $\lambda < \theta < L$; in case B $\theta > L$; but $\lambda < L$. The shaded figure is the cross-section of the volume which divided by the volume of a sphere either with radius θ in case A or with radius L in case B gives the probability.

It is easy to show that for case A

$$\theta^2 = 2r\lambda + \lambda^2$$

and that the volume of the conelike space is

$$V_A = (\pi/3)\lambda^2 r^2 / (r + \lambda)$$

The probability of collision in case A is

$$p_A(r, \lambda) = V_A / [(4\pi/3)\theta^3]$$

The validity limit of case A is when $L = \theta$; here $\lambda = \lambda_c$.

$$\lambda_c = -r + (r^2 + L^2)^{0.5}$$

For case B the volume of the conelike space and the probability of hit are:

$$V_B = (\pi/3) [(L^2 - r^2)\lambda r / (\lambda + r) - (L^2 - \lambda^2)^2 / 4(\lambda + r)]$$

$$P_B(r, \lambda) = V_B / [(4\pi/3)L^3]$$

To calculate the rate of radical entry, $d\omega/dt$, into an isolated particle a spherical shell at distance λ from the sphere surface is considered. The volume of this shell is $4\pi(r + \lambda)^2 d\lambda$. Since R is the number of radicals produced unit volume of water per second, the number of radicals produced within the shell per second is $4\pi(r + \lambda)^2 R d\lambda$. The probability that any of these radicals will hit the particles is $p(r, \lambda)$. It follows that the total number of radicals entering into the particle per second is:

$$d\omega/dt = 4\pi R \int_0^{\lambda_c} p_A(r, \lambda)(r + \lambda)^2 d\lambda + 4\pi R \int_{\lambda_c}^L p_B(r, \lambda)(r + \lambda)^2 d\lambda$$

The result of this integration is:

$$(d\omega/dt) / (\pi r^2 LR) = 2 [(1 + L^2/r^2)^{0.5} - 1] r^2/L^2 + 2 [(1 + L^2/r^2)^{3/2} - 1] r^4/3L^3 - r^2/L^2 + 1 - 2 (r/L) \ln [(L/r) + (L^2/r^2 + 1)^{0.5}]$$

It can be shown that this equation is approximated by the following simple function with better than 1% accuracy over the whole range of interest, i.e., $0 < L/r < \infty$:

$$d\omega/dt = \pi r^2 LR \{ [2.5 + (L/r)] / [10 + (L/r)] \}$$

It follows that

$$0.25 \leq (d\omega/dt) / (\pi r^2 LR) \leq 1$$

Since the particles and micelles in interval I are very small, we can assume that $L > r$. For this case we have:

$$d\omega/dt = \pi r^2 LR = 0.25 (\text{particle surface}) LR \quad (62)$$

According to the Smith-Ewart assumptions, the total surface of all particles plus all micelles stays constant during interval I. This surface equals S square centimeters per cubic centimeter of water. The rate at which radicals are absorbed by the micelles and particles present in 1 cc. of water is, according to eq. (62), equal to $0.25SLR$. Since it is impossible to absorb more radicals than the number of radicals formed, all radicals formed in the aqueous phase must be absorbed into the oil phase if:

$$0.25SL \geq 1$$

For the Smith-Ewart model to be valid, it is not enough that the soap should be present at a concentration above the critical micelle concentration. It is also required that the value of S should be equal to or larger than $4/L$ at this concentration. For the case where these conditions are not fulfilled, all the equations based on the Smith-Ewart model can be validated by replacing S in them by $4/L$.

It is likely that the order of magnitude of L is influenced by the soap present. By solubilizing monomer into the homogeneous aqueous phase, the soap can decrease L . This would happen if the monomer at higher concentration polymerizes faster and reaches its critical size for precipitation faster. Alternately, by solubilizing the growing oligomeric radicals themselves, the soap present may cause the critical precipitation size of the oligomeric radicals to increase so that L should increase.

The calculations on the computer were carried out by Mr. L. DeFonso.

References

1. J. L. Gardon, *J. Polymer Sci. A-1*, **6**, 643 (1968) (Part II).
2. J. L. Gardon, *J. Polymer Sci. A-1*, **6**, 665 (1968) (Part III).
3. J. L. Gardon, *J. Polymer Sci. A-1*, **6**, 687 (1968) (Part IV).
4. J. L. Gardon, in preparation (Part V).
5. J. L. Gardon, in preparation (Part VI).
6. M. V. Smith and R. H. Ewart, *J. Phys. Chem.*, **16**, 592 (1948).
7. I. M. Kolthoff and I. K. Miller, *J. Am. Chem. Soc.*, **73**, 3055 (1951).
8. P. J. Flory, *Principles of Polymer Chemistry*, Cornell Univ. Press, Ithaca, N. Y., 1953, p. 213.
9. R. A. Buckingham, *Numerical Methods*, Pitman, London, 1957, pp. 362-367.

10. H. Morgenau and G. M. Murphy, *The Mathematics of Physics and Chemistry*, Van Nostrand, Princeton, N. J., 1956, pp. 521-531.
11. J. Bakker, Ph.D. Thesis, Utrecht University, Netherlands, 1952; *Phillips Res. Rep.*, **7**, 344 (1952); quoted by B. M. E. Van der Hoff, *Polymerization and Polycondensation Processes*, *Adv. Chem. Series*, No. **34**; American Chemical Society, 1962, pp. 6-31.
12. M. Morton, S. Kaizerman, and M. W. Altier, *J. Colloid Sci.*, **9**, 300 (1954).
13. W. H. Stockmayer, *J. Polymer Sci.*, **24**, 314 (1957).
14. J. W. Vanderhoff, E. B. Bradford, H. L. Tarkowsky, and W. B. Wilkinson, *J. Polymer Sci.*, **50**, 265 (1961).
15. E. Trommsdorff, H. Kohle, and P. Legally, *Makromol. Chem.*, **1**, 169 (1947).
16. W. J. Priest, *J. Phys. Chem.*, **56**, 1077 (1952).
17. M. S. Matheson, E. E. Auer, E. B. Bevilacqua, and E. J. Hart, *J. Am. Chem. Soc.*, **71**, 2610 (1949).

Received May 24, 1967

Revised July 3, 1967

Emulsion Polymerization. II. Review of Experimental Data in the Context of the Revised Smith-Ewart Theory

J. L. GARDON, *Rohm and Haas Company,
Spring House, Pennsylvania 19477*

Synopsis

Tables are presented for convenient calculation of the basic parameters of the revised Smith-Ewart theory. For the methyl methacrylate (MMA)/sodium lauryl sulfate (SLS)/ $K_2S_2O_8$, and for the styrene/SLS/ $K_2S_2O_8$ reaction mixtures parameters are presented from which the absolute values of the following quantities can be conveniently calculated for any temperature, soap, and initiator concentration: particle number, particle radius, conversion where particle nucleation stops, rate and molecular weight in interval II, the interval after completion of particle nucleation and before the disappearance of monomer droplets. The theoretical predictions are compared to new experimental data and to those from the literature. The available data confirm the theoretical prediction that particle nucleation stops after a very small amount of polymer is formed, of the order of 0.01 cc. polymer/cc. water in most recipes. The theory and experiments are in good qualitative agreement for the conversion rate prior to completion of particle formation: the conversion rate rises with time and, when particle nucleation stops, it levels off. Excellent quantitative agreement can be obtained between theoretical and experimental particle size values. In the experiments of this laboratory the SLS concentration was varied 60-fold, the $K_2S_2O_8$ concentration was varied 140-fold and the difference between theoretical and experimental poly(MMA) particle radii was always less than about 20%. Similar good agreement was obtained for polystyrene over the temperature range 30–90°C. Some polystyrene data from the literature with carboxylic soaps give just as good fit as the data with SLS of this laboratory. The predicted proportionality between particle number and the product of 0.6 power of soap concentration and of 0.4 power of initiator concentration was observed for several monomers. The theoretical predictions for the rate and molecular weight obtained in interval II are valid only for relatively low initiator and high soap recipes. For recipes for MMA and styrene the rate data are in good agreement with those calculated from the theory. The theory also correctly predicts the order of magnitude of the experimental molecular weights. For several monomers the rate and molecular weight vary with initiator and soap concentrations in a manner close to theoretical predictions.

INTRODUCTION

In the first paper of this series (Part I),¹ new experimentally verifiable equations were derived based on the Smith-Ewart model² and the validity limits of this model were established. It was also found convenient to define three intervals of emulsion polymerization. In Interval I the particles are nucleated and there is monomer present in excess to that needed

to saturate latex particles and water. In intervals II and III the particle number is constant but in interval II there is still a separate monomer phase present while in interval III the conversion proceeded far enough so that unconverted monomer is present only dissolved in latex particles and in water.

Most of the experimental data reviewed below is relevant to interval I. Experimental data for intervals II and III obtained in this laboratory will be described in Part IV.³

EXPERIMENTAL VALUES OF THE PARAMETERS

The Initiator Parameter

The influence of the initiator upon the outcome of the polymerization can be expressed by the single parameter R , the number of radicals produced in 1 cc. of water per second. Its value can be calculated from the mole/cc. concentration $[I]$, the decomposition rate constant k_d , and the Avogadro number N_A :

$$R = 2k_d N_A [I] \quad (1)$$

The factor 2 takes into account the fact that two radicals are formed from a single initiator molecule. The parameter R is in units of reciprocal cubic centimeter-seconds.

For the commonly used persulfate initiators, k_d was determined by Kolthoff and Miller.⁴ They found it to increase with soap concentration and with decreasing pH. As will be shown, satisfactory agreement between theory and experiment is obtained without taking into account the effect of soap upon initiator decomposition. This effect is small during emulsion polymerization or there are compensating errors in the calculations. In using eq. (1) 100% initiator utilization efficiency was assumed. Perhaps the initiator decomposes faster than calculated without taking the soap effect into account but it is not 100% efficient.

Above pH 4 the value of k_d is independent of pH, but it increases with decreasing pH below pH 4. If the experiment is started neutral, the effect of pH can be ignored initially. However, persulfates have acidic decomposition products and the pH of the reaction mixture decreases with increasing time.

TABLE I
Values of the Parameter R of $K_2S_2O_8$ Solutions at pH 3.5 and at Concentration C_I

Temperature, °C.	$(R/C_I) \times 10^{-12}$
40	1.14
45	2.67
50	5.8
55	12.5
60	24.5
65	62.5

It is convenient to make a small deliberate error concerning the pH dependence of k_d and use a single R value for describing the whole conversion process. To minimize the error at the beginning and at the end, the R values are calculated for pH 3.5. These are shown in Table I in a way to be easily calculable for any per cent concentration C_l based on water.

The Soap Parameter

The soap effects can be expressed by the single parameter S , the area at an oil-water interface occupied by a monolayer the soap molecules present in 1 cc. of water. Its value is calculable in units of reciprocal centimeters from A_s , the area per soap molecule and $[S]$, the concentration in moles/cubic centimeter.

$$S = N_A A_s [S] \quad (2)$$

The S values of several soaps are given in Table II in a way that they should be easily calculable from the per cent soap concentration in water, C_s . Since it is customary to formulate reaction mixtures on a per cent basis, the effectiveness of soaps in reducing the particle size is greatest if their surface area per gram is large. The S/C_s values of Table II measure of this efficiency. It may be noted that an extensive tabulation of A_s values and critical micelle concentrations is given by Gerrens.¹¹

The data of Table II are based on A_s values determined either by x-ray measurements or by applying Gibbs adsorption isotherm to the dependence of interfacial tension on $[S]$, or by soap titration of latex samples. The last method involves addition of small increments of soap to a latex of known particle size. At the point where the surface tension of the latex starts to drop, the latex particles are covered by soap. These methods give reliable A_s values which are relevant to emulsion polymerization. It should be noted that A_s determined for the air-water interface from the variation of surface tension with concentration can differ significantly from that determined for the oil-water interface.

TABLE II
Values of the Parameter S for Aqueous Soap
Evaluations at C_s Per Cent Concentration

	$S/C_s \times 10^{-5}$	Ref. for A_s
Na lauryl sulfate	1.25	5, 6
K laurate	1.26	7
Na laurate	1.06	8
Na myristate	0.77	8, 9
Na palmitate	0.53	8
Na oleate	0.50	8
Na stearate	0.46	8
Na decylbenzene sulfonate	0.59	10
OPE ₁₀ ^a	0.18	5

^a Adduct of octylphenol and 40 ethylene oxide units.

TABLE III
Monomer Parameters

Monomer ^a	d_{m1} g./cm ³	d_{m2} g./cm ³	ϕ_m	$k_p \times 10^{-5}$, cm. ³ /mole-sec.							Ref.
				25°C.	30°C.	35°C.	40°C.	50°C.	60°C.		
St	0.905	1.06	0.6	0.46	0.55	—	0.83	1.24	1.76	15	
MMA	0.939	1.19	0.73	1.23	1.42	—	1.95	2.70	3.6	16	
VAc	0.934	1.19	0.85	10.1	12.4	—	19.7	26.4	37.0	17	
MA	0.95	1.22	0.85	—	7.2	—	—	—	21.0	18	
nBA	0.894	—	0.65	0.22,	—	0.31	—	—	—	19	
				0.13	—	or 0.15	—	—	—		
nPMA	—	—	—	—	4.67	—	—	—	—	20	
nBMA	0.889	1.06	0.60	—	3.62	—	—	—	—	21	
OMA	—	—	—	—	0.98	—	—	—	—	22	
GMA	—	—	—	—	5.34	—	—	—	9.75	23	
MN	0.80	1.10	—	0.26	—	0.39	—	—	—	24	
VCl	0.919	1.40	0.30	19.0	—	—	—	100.0	—	25, 26	

^a Monomers: St, styrene; MMA, methyl methacrylate; VAc, vinyl acetate; MA, methyl acrylate; nBA, *n*-butyl acrylate; nPMA, *n*-propyl methacrylate; nBMA, *n*-butyl methacrylate; OMA, octyl methacrylate; GMA, glycidyl methacrylate; MN, methacrylonitrile; VCl, vinyl chloride.

When using the S values of Table II, which are determined at room temperature, one must assume that A_s is independent of temperature. This assumption is probably an adequate approximation. Crook et al.¹² found only up to 20% increase in the A_s of octylphenol-ethylene oxide adducts at the air-water interface when the temperature was increased from 25°C. to 100°C.

The Monomer Parameters

To predict the outcome of an experiment, the monomer and polymer densities, d_m and d_p , the propagation constant k_p , and the monomer volume fraction in the particles ϕ_m have to be known. These values are shown for several monomers in Table III. For some calculations it is also convenient to combine these into a single parameter, the volume growth rate constant K , defined as the rate of increase in the cubed radius of a particle containing one radical.

$$K = (3/4\pi)(d_m/d_p)(k_p/N_A)\phi_m/(1 - \phi_m) \quad (3)$$

It should be noted that the units of d_m and d_p and of k_p are so chosen that the units of all parameters are internally consistent. The densities of Table III are taken either from a handbook¹³ or from Schildeknecht.¹⁴ Table IV gives the numerical values of K for styrene (St) and methyl methacrylate (MMA).

The values of ϕ_m are known to depend on particle size and soap concentration. Nevertheless, it is an insensitive function of these variables because latexes polymerized at high soap levels have small particle sizes. The high soap levels cause decrease in the particle-water interfacial tension. In terms of the theory of Morton et al.,²⁷ lower interfacial tension increases ϕ_m . A low particle size at a given interfacial tension causes reduction in ϕ_m . Thus the effects of the soap used at polymerization upon ϕ_m are partially self-compensating. Similarly, the effect of temperature upon ϕ_m is also relatively small; this was demonstrated by Van der Hoff²⁸ and Gerrens²⁹ for styrene/polystyrene. Part VI³⁰ will show that it is justifiable to assign the typical ϕ_m values to each monomer-polymer system of Table III. Using these values, one hardly commits more than

TABLE IV
Values of $K \times 10^{20}$ at Different Temperatures

Temperature, °C.	$K \times 10^{20}$, cm. ³ /sec.	
	St	MMA
40	4.2	16.4
45	5.17	19.4
50	6.3	22.8
55	7.5	26.5
60	8.84	30.8
65	10.6	34.1

20% error. At this point it should be mentioned that ϕ_m is usually determined either from the equilibrium swelling of nonpolymerizing latex samples with their monomers or from the conversion where the monomer droplets disappear during polymerization. The agreement between these two methods is usually very good.

The values of k_p shown in Table III were all determined by homogeneous photopolymerization; no k_p determined by emulsion polymerization is presented in this table.

The kinetic equations derived in Part I¹ are all independent of the monomer concentration in water, so long as the monomer is in sufficient excess to saturate water and the latex particles. When the excess monomer is used up, the reaction enters interval III in which the theory is no longer valid. This upper validity limit is reached when the fractional weight conversion γ becomes equal to the equilibrium weight fraction of polymer in the monomer saturated particles. At this point γ is equal to γ_{II-III} . This value can be calculated if the solubility of monomer in water is assumed to be negligible:

$$\gamma_{II-III} = (1 - \phi_m) / [1 - \phi_m + (d_m/d_p)\phi_m] \quad (4)$$

For styrene, 100 γ_{II-III} is about 45%, and for MMA it is about 25%.

The conversion in the kinetic equations of Part I¹ is measured by P , the volume of polymer present per unit volume of water. This is related to the fractional weight conversion with the aid of the monomer/water weight ratio in the charge, m/w , and the water density, $d_w \sim 1$:

$$P = (m/w)(d_w/d_p)\gamma \quad (5)$$

Specifically, at the transition between intervals II and III the value of P is:

$$P_{II-III} = (m/w)(d_w/d_p) \gamma_{II-III} \quad (6)$$

CONVERSION UP TO COMPLETION OF PARTICLE NUCLEATION

Definition of the Critical Conversion

This value is reached when the total surface of all monomer-swollen latex particles present in 1 cc. of water becomes equal to S so that formation of new particles is completed. At this point the volume of polymer per unit volume of water is P_{cr} .

$$P_{cr} = 0.209S^{1.2} (K/R)^{1.2}(1 - \phi_m) \quad (7)$$

For recipes with sodium lauryl sulfate (SLS), $K_2S_2O_8$, and styrene or MMA, the values of P_{cr} can easily be calculated from the values in the first two rows of Table V. This table also gives the corresponding values of per cent conversion, 100 γ_{cr} , for $m/w = 40/60$. Experimental γ_{cr} data can be interpreted only if m/w is known.

TABLE V
Particle Size, Conversion, and Molecular Weight Calculated for
the Systems MMA/SLS/K₂S₂O₈ and St/SLS/K₂S₂O₈^a

	40°C.	45°C.	50°C.	55°C.	60°C.	65°C.
$(P_{cr}C_I^{0.2}/C_S^{1.2}) \times 10^2$						
MMA	3.02	2.60	2.32	2.02	1.85	1.56
St	3.62	3.70	2.86	2.54	2.35	1.93
$(100\gamma_{cr}C_I^{0.2}/C_S^{1.2})$						
MMA	5.37	4.64	4.14	3.60	3.29	2.78
St	5.75	5.08	4.54	4.03	3.73	3.06
$(N/C_S^{0.6}C_I^{0.4}) \times 10^{-15}$						
MMA	1.27	1.71	2.18	2.88	3.43	4.74
St	2.23	2.90	3.64	4.62	5.56	7.62
$(rC_S^{0.2}C_I^{0.133}) \times 10^6$						
MMA	4.74	4.28	3.84	3.60	3.40	3.05
St	4.16	3.80	3.53	3.25	3.07	2.45
$(B/C_S^{0.6}C_I^{0.4}) \times 10^5$						
MMA	11.2	17.3	26.0	39.9	55.4	85.5
St	7.85	12.5	19.1	28.6	41.0	67.5
$(b/C_S^{0.6}C_I^{0.4})$						
MMA	1.20	1.85	2.79	4.27	5.83	9.15
St	0.75	1.19	1.82	2.75	3.82	6.45
$(M_{SE}C_I^{0.6}/C_S^{0.6}) \times 10^{-6}$						
MMA	11.8	7.8	5.4	3.73	2.72	1.76
St	8.3	5.62	3.96	2.77	2.02	1.30

^a C_S (%) is concentration of SLS in water; C_I (%) is concentration of K₂S₂O₈ in water; P_{cr} is volume of polymer (cc.) per cc. of water when particle nucleation stops, calculated from eq. (7); $100\gamma_{cr}$ (%) is fractional conversion, where particle nucleation stops calculated from P_{cr} by eqs. (5) and (7) assuming a monomer/water (m/w) weight ratio of 40/60; N (cm.⁻³) is number of particles per cc. of water calculated from eq. (11); r (cm.) is root-mean-cube particle radius at $m/w = 40/60$ and 100% conversion calculated from eq. (12); B (sec.⁻¹) is interval II rate in cc. of polymer produced in 1 cc. of water per sec. calculated from eq. (16); b (%/min.) is interval II rate at $m/w = 40/60$ calculated from B ; M_{SE} (g./mole) is interval II molecular weight calculated from eq. (18).

It is evident that P_{cr} is very insensitive to the monomer properties and to the initiation method since the monomer and initiator parameters, R and K , enter into eq. (7) by a very low power. The effect of temperature on P_{cr} is also expected to be small, because in eq. (7) only K and R are temperature-sensitive. The value of P_{cr} is sensitive to the soap concentration. In most practical recipes the SLS concentration is less than 1% or the concentration of other soaps is so chosen to give $S < 10^5$ cm.⁻¹ (cf. Table II). In such recipes P_{cr} should have very low value, in the order of 0.01. This would correspond to a low fractional conversion at technically used m/w values. The experimental data, reviewed below, are consistent with this prediction.

Variation of Particle Number and Particle Size with Conversion

The most obvious way to determine P_{cr} is to monitor the particle number as a function of conversion. The data of Van der Hoff²⁸ for styrene suggest $P_{cr} \sim 0.1$ but this investigator used an oil-soluble peroxide initiator so that

the present theoretical model is not strictly applicable to his results. Peggion's³¹ vinyl chloride data indicate $P_{cr} \sim 0.04$. The results obtained with vinyl acetate by French³² show $P_{cr} \sim 0.08$ at low soap concentrations. As the soap concentration is increased, P_{cr} rises to about 0.25. Finally, Morris et al.³³ found very low P_{cr} (<0.003) for methyl acrylate in the absence of soap.

The particle number per cubic centimeter of water, N , cannot be determined directly. Some average of the particle radii is measured instead, from which N is calculated. It has to be realized that the calculated value of N should depend strongly on the nature of the average used if the particle size distribution is broad. Since N refers to the subdivision of the total polymer volume present in unit volume of water, it cannot be related to the number-average radius, but to the number-average volume. Thus the correct radius average to use for calculating N is the root-mean-cube average:

$$r_{\text{rnc}} = (\sum n_i r_i^3 / \sum n_i)^{1/3} \quad (8)$$

TABLE VI
Variation of Particle Size with the Conversion of MMA^a

100 γ , %	$r_n \times 10^6$, cm.	$r_{\text{rnc}} \times$ 10^6 cm.	r_{rnc} $\gamma^{1/3}$	Average of $r_{\text{rnc}}/\gamma^{1/3}$ $\times 10^6$, cm. ^b	Standard devia- tion \times 10^6 , cm.	95% Confi- dence limits $\times 10^6$, cm. ^b	Theoretical $r_{\text{rnc}}/\gamma^{1/3}$ $\times 10^6$, cm. ^c
2.57	2.17	2.30	8.40				
5.25	2.26	2.56	6.85				
12.75	2.76	2.95	5.87	5.95	0.91	± 2.33	6.25
19.10	2.92	3.26	5.76				
36.05	4.21	4.40	6.15				
45.65	4.66	4.84	6.3				
93.60	5.18	5.37	6.12				
98.60	5.24	5.49	5.52				

^a Procedure: MMA/water = 40/60, 55°C., 0.242% SLS, 0.164% K₂S₂O₈ on water. The reaction was in a three-necked flask, under nitrogen blanket. Mild stirring was used. At different conversions aliquots of latex were removed, poured into a mixture of ice water, hexane, and hydroquinone, and extracted cold with hexane to remove unreacted monomer. After about 95% conversion the latex was treated at 80°C. for 0.5 hr. to stabilize it. The thus treated latex samples were submitted for electronmicrography.

^b Only samples with conversion higher than 12.75% are taken in calculating this average because above this conversion there is no significant trend in the $r_{\text{rnc}}/\gamma^{1/3}$ values. The confidence limits are calculated with Student's t for five degrees of freedom. It follows from this analysis that particle nucleation continues at a 95% probability level if $r_{\text{rnc}}/\gamma^{1/3}$ exceeds $(5.95 + 2.33) \times 10^{-6} = 8.28 \times 10^{-6}$ cm. Thus at 2.56% conversion particle nucleation still takes place. It is uncertain whether at 5.25% conversion there is particle nucleation or not. The $r_{\text{rnc}}/\gamma^{1/3}$ at this conversion is about one standard deviation higher than the mean.

^c See Table V.

Here n_i is the number of particles counted whose radius is r_i . The value of r_{rnc} is larger than the customarily used number-average value r_n :

$$r_n = \Sigma n_i r_i / \Sigma n_i \quad (9)$$

It is evident that the volume of each particle is proportional to the fractional conversion γ if N is constant. A criterion for the constancy of N is the constancy of the ratio $r_{\text{rnc}}/\gamma^{1/3}$. Such data are shown for MMA in Table VI and suggest $\gamma_{cr} < 0.05$ corresponding to $P_{cr} < 0.03$; the theoretical value of P_{cr} is 0.006. Considering the experimental uncertainties in determining very low particle sizes, the agreement between theory and experiment is acceptable.

Variation of the Conversion Rate with Conversion

A second method to determine P_{cr} is the measurement of the variation of conversion rate (the time derivative of conversion) with time or conversion. A consequence of the model is that the conversion rate, dP/dt , should initially increase sharply with time and then should, at $P = P_{cr}$, reach a value approximately equal to dP/dt in interval II. The calculated interval I conversion rate is

$$dP/dt = 2.94 (1 - \phi_m) KRt - 6.44 (1 - \phi_m) K^{1.62} R^{1.93} S^{-0.93} t^{2.55} \quad (10)$$

This equation has not yet been quantitatively verified because it is difficult to obtain precise data at very low conversions. However, the reported conversion rate data of Van der Hoff,²⁸ Gerrens et al.³⁴⁻³⁶ and Hummel et al.³⁷ show sharp rise in dP/dt at low conversions and leveling off in the value of dP/dt at intermediate conversions, as predicted by the theory. The conversion values, where Hummel et al. observed this transition, define $P_{cr} \sim 0.005$ for styrene and 0.02 for MMA.

Variation of Surface Tension with Conversion

The soap micelles should disappear at the end of particle nucleation. Consequently, the surface tension of the latex should increase sharply at $P \sim P_{cr}$. Indeed, Gerrens et al.³⁵ observed a sharp rise in surface tension which coincided with the break in the conversion rate-time curve. Thus a third experimental method to determine P_{cr} is to observe the fractional conversion at which a sharp increase in surface tension occurs. Such isoprene-styrene copolymerization data, obtained by Harkins,³⁸ suggest $P_{cr} \sim 0.06$. Yeliseyeva et al.³⁹ found that the excess soap disappeared at very low conversion in methyl acrylate-butyl acrylate-acrylic acid copolymerization and that the particle number was constant in the measured ranges of conversion.

FINAL NUMBER AND RADIUS OF PARTICLES

Absolute Values of N and of Final Particle Radius

The most important consequence of the model is that N , the final number of particles per cubic centimeter of water, can be calculated from the independent parameters R , S , and K . The derived equation is:

$$N = 0.208S^{0.6} (R/K)^{0.4} \quad (11)$$

The value of N is independent of the monomer/water ratio as long as $P_{cr} \leq P_{II-III}$ [cf. eqs. (6) and (7)]. The final particle radius is a function of m/w , since the volume of each particle at 100% conversion and at constant N is proportional to m/w . The theoretical root-mean-cube radius at 100% conversion is:

$$r_{\text{rme}} = 1.05 (m/w)^{0.333} (d_w/d_p)^{0.333} S^{-0.2} (K/R)^{0.133} \quad (12)$$

It is evident that according to this theory N is proportional to $C_S^{0.6}C_I^{0.4}$ and that r is inversely proportional to the cube root of this product. Table V presents parameters from which the theoretical N and r_{rme} values can be

TABLE VII
Final Particle Size Values Obtained with MMA^a

Theory	$r \times 10^6$, cm.		Concentration in water, %		
	Electron	Light	C_S	C_I	$C_{Na_2SO_4}$
	microscopy	scattering			
2.4	3.2	—	4.88	1.54	0
2.8	3.6	—	3.44	0.905	0
3.6	4.3	—	2.00	0.035	0
5.2	5.1	—	0.514	0.206	0
6.2	7.35	—	0.323	0.107	0
6.2	5.2	—	0.302	0.117	0
6.2	5.25	6.8	0.242	0.164	0
7.85	6.3	7.9	0.256	0.029	0
7.85	7.1	8.7	0.256	0.029	0.05
7.85	—	8.6	0.256	0.029	0.15
7.85	8.25	9.9	0.256	0.029	0.30
7.85	8.8	—	0.192	0.044	0
7.85	8.15	—	0.158	0.059	0
7.85	8.5	—	0.128	0.081	0
9.9	8.85	—	0.203	0.0065	0.05
9.9	8.65	9.5	0.152	0.010	0
9.9	—	9.6	0.152	0.010	0.025
9.9	8.75	10.3	0.152	0.010	0.05
9.9	9.55	—	0.100	0.0184	0
12.42	10.05	—	0.12	0.0023	0.05
12.42	12.0	—	0.08	0.0042	0.05

^a Procedure: soap, SLS; initiator, $K_2S_2O_8$; $m/w = 40/60$. Salt (Na_2SO_4) was added to low initiator recipes to reduce viscosity. All experiments were run in three-necked flasks, with gentle stirring, under nitrogen at 40°C.

conveniently calculated at any temperature or SLS and $K_2S_2O_8$ concentration for MMA and styrene. If the values of these parameters outside the temperature range of Table V are needed, it is convenient to obtain them by extrapolation from an Arrhenius type plot.

In interpreting experimental results it is important to use the correct average of radii. Strictly speaking, only r_{rme} [cf. eq. (8)] should be used in the context of this theory; other averages are applicable only if the particle size distribution is narrow. The most convenient average calculable from electron micrographs is the number-average, r_n , defined in eq. (9); this average is reported in Tables VII and VIII. It was obtained by counting at least 300, but often as many as 900 particles. The value of r_{rme} is quite close to r_n and is also calculable from the electron micrographs. In the literature occasionally averages higher than r_{rme} are used in calculating N , and this might cause some deviations from the Smith-Ewart predictions. The tables also present some data obtained by dissymmetry light scatter. This method gives a very high average radius, defined below:

$$r_{ls} = (\sum n_i r_i^8 / \sum n_i r_i^6)^{0.5} \quad (13)$$

Tables VI, VII, and VIII demonstrate that, for methyl methacrylate, the theoretical predictions and data agree within experimental error when SLS is the soap and $K_2S_2O_8$ is the initiator. Table VII is of particular interest because it demonstrates that if the initiator concentration is increased and the soap concentration is decreased so that $C_s^{0.6} C_I^{0.4}$ remains constant, the particle size also remains constant within experimental error. Constancy in the $C_s^{0.6} C_I^{0.4}$ product is indicated in this table by the constancy of the theoretical radius values. In this table the theory is proven to be correct when the soap concentration is varied 60-fold, the initiator concentration is varied 140-fold, the particle radius is varied 5-fold and the particle number is varied 125-fold. Table VIII shows that the theory is valid at 40 and 55°C. for MMA.

In Table IX experimental and theoretical radius values for polystyrene are compared. This table includes experimental data obtained by Smith⁴⁰ with carboxylic soaps. The agreement is again within experimental error. It is noteworthy that these data cover the temperature range from 30 to 90°C., two different soaps, a tenfold change in initiator concentration, a threefold change in radius, and a 27-fold change in particle number.

Smith⁴¹ estimated the volume growth rate constant from interval II data and calculated N with the aid of this estimate. He obtained excellent agreement with the experimental data, just like in the present study where the volume growth rate constant was taken from independent parameters.

Unfortunately not all available data which can be interpreted quantitatively give such good agreement. Gerrens has extensive data on polystyrene³⁵ and poly(methyl methacrylate)⁴² obtained with $K_2S_2O_8$ initiator and a sulfonated C_{18} olefin soap. This soap has $S/C_s = 6.4 \times 10^4 \text{ cm.}^{-1}/\%$.⁴³ If one calculates the particle numbers using this characteristic surface area of the soap, the theoretical values are consistently two to three times larger

TABLE VIII
Final Particle Sizes and Molecular Weights Obtained with MMA at Two Different Temperatures^a

Temperature, °C.	<i>m/w</i>	<i>C_s</i> , %	<i>C_I</i> , %	<i>r</i> × 10 ⁶ , cm.				<i>M_{SE}</i> × 10 ⁻⁶
				Theory	Electron microscopy	Light scattering	Final MW × 10 ⁻⁶ (expl.)	
40 ^b	40/60	0.66	0.23	6.3	7.2	—	—	—
40	35/65	0.63	0.23	5.75	7.8	7.9	8.76	27.8
40	35/65	0.305	0.73	—	—	—	7.2	7.0
40	35/65	2.58	0.23	4.6	5.2	6.1	11.7	51.0
40	38/62	1.47	0.142	5.2	4.7	—	10.7	48.0
55	36/64	0.305	0.117	6.4	—	6.7	7.9	6.5
55 ^b	40/60	0.242	0.164	6.2	5.25	6.8	4.11	4.73

^a Procedure; except as noted, the experiments were run in a dilatometer under N₂. Gentle stirring was used.

^b Experiments run in a three-necked flask.

TABLE IX
Final Particle Sizes and Molecular Weights Obtained with Styrene

Temperature, °C.	<i>m/w</i>	<i>C_S</i> , %	<i>C_T</i> , %	<i>r</i> × 10 ⁶ , cm.		MW × 10 ⁻⁶		
				Electron microscopy	Theory	Expt.	Theory	
Experiments in This Laboratory ^a								
40	40/60	0.63	1.39	3.0 ^b	4.3	4.02	5.20	
40	40/60	0.66	0.23	4.8	5.45	3.2	15.6	
60	10/90	0.66	0.25	2.2	3.38	2.0	3.8	
60	40/60	0.66	0.23	4.2	4.22	2.35	3.8	
60	40/60	0.66	0.23	4.3	4.22	3.54	3.8	
60	40/60	0.67	0.24	4.64	4.22	3.78	3.8	
80	20/80	0.125	0.125	3.7	3.32	—	—	
80	20/80	0.5	0.125	2.50	2.50	—	—	
Experimental Results Published ¹⁰ by Smith ^c								
30.5	37/63	0.5	0.165	7.90	8.31	23	20	
50	37/63	0.5		to	5.80	5.84	4.4	6.2
70	37/63	0.5			4.82	4.12	1.1	1.4
90	37/63	0.5	0.172	4.20	3.70	0.32	0.27	
70	37/63	2.0		0.511	3.6	2.80	2.1	4.5
70	37/63	0.5	to		4.53	3.78	0.53	0.57
				0.516				

^a Run in three-necked flasks, under nitrogen, with SLS and K₂S₂O₈.

^b This value of *r* was determined by soap titration, not by electron microscopy.

^c With SF flakes and K₂S₂O₈. The reaction mixtures were shaken under nitrogen in closed test tubes. The SF flakes are known to be a mixture of sodium stearate, oleate, and palmitate. For this soap *S/C*s = 5 × 10⁴ cm.⁻¹/% was taken in calculating the presented theoretical values.

than the experimental values. In other words, the theory underestimates the particle radii by 25 to 45%. A similar discrepancy was also observed by Van der Hoff⁴⁴ for a styrene-K₂S₂O₈-potassium laurate system. This author, like Smith,⁴¹ estimated the value of the particle volume growth rate from interval II data and calculated N with the aid of this estimate. Van der Hoff's theoretical values of N were up to three times higher than the experimental values. Van der Hoff thought that this discrepancy was caused by inefficiency in radical utilization. Perhaps the possibility of estimating the absolute particle size to 40% accuracy from completely independent parameters is in itself quite satisfactory and indicates that the model is a reasonably good approximation of the truth. However, the data of Tables VI-IX show that the theory can give much more accurate predictions; indeed the agreement between theory and experiment shown in these tables cannot be fortuitous.

Variation of N with Soap and Initiator Concentration

While the most stringent test for the validity of the theory involves the prediction of absolute particle sizes, it is of interest to test its other implications. The most obvious aspect of the theory is the prediction that N is proportional to $C_S^{0.6}$ and $C_I^{0.4}$. Approximately correct values for either or both power exponents were obtained for styrene by Gerrens et al.,³⁵ Smith,⁴¹ and Manyasek et al.;⁴⁵ for MMA by Gerrens;⁴² for chloroprene by Manyasek et al.;⁴⁵ for vinylidene chloride by Wiener⁴⁶ and Hay et al.;⁴⁷ for vinyl caproate by Okumara et al.;⁴⁸ for butadiene by Morton et al.;⁴⁹ and for vinyl acetate by Dunn et al.⁵⁰

There is also a large body of data indicating power exponents for the C_S and C_I dependence of N which differ significantly from those of the Smith-Ewart theory. An interesting case is vinyl chloride, which gives N independent of C_I and proportional to $C_S^{0.6}$ according to Gerrens et al.³⁶ Peggion et al.⁵¹ also found an exponent of 0.6 for C_S for vinyl chloride with some soaps, and higher than 0.6 with other soaps. Power exponents for C_S less than 0.6 were found for acrolein by Chedron et al.;^{51,52} for acrylonitrile by Chedron⁵¹ and Thomas et al.;⁵³ and for vinyl acetate by Okumara et al.⁵⁴ Finally power exponents for C_I in the 0.7-3 range, usually coupled with power exponents for C_S less than 0.4, were found for vinyltoluene and vinylxylene by Gerrens;²⁹ for ethylene by Stryker et al.;⁵⁵ for vinyl acetate by French;³² for styrene by Ewart et al.⁵⁶ and Vanderhoff et al.;⁵⁷ and for MMA and butyl methacrylate by Brodnyan et al.⁵⁸ Some of these data can probably be dismissed as being irrelevant because either particle aggregation in intervals II and III was not taken into account, or the data do not fall within the validity limits of the theory or they are based upon the wrong averages of radius values. It should be remembered here that for the applicability of eq. (11) it is important that P_{cr} should be smaller than P_{II-III} , that the soap should be in micellar form over the whole range of

measurement, and that S should be larger than $4/L$, as defined in the Appendix of Part I,¹ where L is the free mean path of a radical growing in water. If particles do not form by radical absorption into monomer-swollen micelles but by precipitation of radicals growing in the aqueous phase, L is the mean distance from their origin through which these radicals move by Brownian motion before they precipitate. It is possible that, in some of these experiments, particles were nucleated by precipitation of growing radicals, and the power exponent for C_S reflects the effect of soap upon L . Finally, some of the experiments indicating deviations from the Smith-Ewart interval I model can be explained only by admitting that this model is not applicable to the investigated systems. There can be many causes for this. For very polar monomers, such as acrylonitrile, the soap is likely not to adsorb well on the newly formed particles. Some soaps may adsorb well at equilibrium but not adsorb fast enough to comply with the Smith-Ewart model. In some systems there may be a barrier to free radical absorption into particles or micelles. Some soaps may not satisfy the criterion of having the same area per soap molecule on the micelle and on the particle surfaces. In some systems the solubility of monomer in particles is too low, so that the polymerization locus is not inside the particles but at their surface. Any of these phenomena can cause significant deviations from the predictions of eq. (11). It should be emphasized that, while the Smith-Ewart interval I model gives excellent quantitative predictions for some monomer-soap-initiator systems, it is not valid for every system.

Temperature Dependence of N

The only temperature sensitive parameters in eq. (11) are R and K , proportional to k_t and k_p , respectively. For an activation energy of initiator-decomposition of about 32 kcal./mole by the data of Table I and an activation energy of monomer propagation of about 8 kcal./mole by the data of Table III, the apparent activation energy of particle formation can be calculated to be about $0.4(32-8) = 9.6$ kcal./mole, by eq. (11). Smith⁴¹ found that at identical recipe composition the N of polystyrene was 2.4 times larger at 50°C. than at 30°C. This corresponds to the predicted 9.6 kcal./mole apparent activation energy. A similar apparent activation energy is defined by the particle radius data of Table IX obtained at 60°C. and 40°C.

An interesting case is initiation by high-energy irradiation. In this case the effective value of R is independent of temperature, and the temperature dependence of N is determined solely by that of K . In this case N would be associated with a negative activation energy about equal to $0.4 \times 8 = 3.2$ kcal./mole. Vanderhoff et al.⁵⁷ found that, with increasing temperature, N increased at $K_2S_2O_8$ initiation and decreased at initiation by irradiation.

CONVERSION RATE IN INTERVAL II

Relationship Between Particle Number and Rate

In the conversion range $P_{cr} \leq P \leq P_{II-III}$ the conversion rate is predicted to have the following constant value:

$$dP/dt = 0.5 (k_p/N_A) (d_m/d_p) N \phi_m \quad (14)$$

Here N is the final, time-independent value, and ϕ_m is the time-independent value corresponding to the swelling equilibrium. The validity of eq. (14) does not depend upon the validity of the Smith-Ewart interval I model; the final number of particles need not be identical to that given in eq. (11).

An equivalent form of this equation is often quoted in the literature. It expresses the rate in terms of $[M]$, the molar concentration of monomers in the particles at swelling equilibrium:

$$\begin{aligned} \text{moles of converted monomer per cubic centimeter of water per second} = \\ 0.5 (k_p/N_A) N [M] \end{aligned} \quad (15)$$

There are numerous reports in the literature indicating that in interval II the conversion is not linear with time as these equations predict. The conversion-time curve is often convex to the time axis. There are also numerous reports showing that if the particle number is reduced by reducing the soap level, the rate per particle, $(dP/dt)/N$, increases and does not remain constant. These matters will not be discussed here further, they are the subject of Parts III and IV of this series.^{3,59}

For low particle size systems at low initiation rates, the conversion in interval II is indeed found to be linear with time and the rate per particle is found to be independent of N . With such data the theory can be put to a very stringent test. One determines the linear rate, the particle number, and monomer concentration in the particles and calculates from these the propagation constant which should be identical to that value determined by homogeneous photopolymerization. Reasonably satisfactory agreement was obtained for MMA by Gerrens⁴² and for styrene by Van der Hoff,²⁸ Smith,⁴¹ Manyasek et al.,⁴⁵ Gerrens et al.,^{29,35} Burnet et al.,^{60,61} Pastiga et al.,⁶² Morton et al.,⁶³ and Paoletti and Billmeyer.⁶⁴ Some of these data gave k_p values up to threefold higher than those of homogeneous photopolymerization. This discrepancy will be explained in Parts III and IV.^{3,59}

Equations (14) and (15) give a very convenient method for determining unknown propagation constants by emulsion polymerization from the experimental particle number, the monomer concentration in particle and the linear rate. As will be shown in Parts III and IV,^{3,59} this procedure can lead to some error if the rate per particle is not constant when the particle number is varied. Data obtained with seven monomers are presented in Table X; they are not very reliable because no proper checks for the validity of eq. (14) and (15) were made. It can be concluded only that the k_p values and activation energies obtained appear to have the right order of

TABLE X
Propagation Constants Calculated from Particle Number, Monomer Concentration in
Particles, and Linear Interval II Rate of Emulsion Polymerization

Monomer	Temp. for k_p , °C.	$k_p \times 10^{-5}$, cm. ³ /mole sec.	Activation energy for k_p , kcal./mole	Reference
Butadiene	60	1.0	9.3	49
Dimethylbutadiene	60	1.2	9.0	65
Isoprene	60	5.0	9.8	63
Vinyltoluene	60	3.36	13.4	64
<i>o</i> -Methylstyrene	60	1.38	13.9	64
<i>p</i> -Methylstyrene	60	2.18	7.66	64
Chloroprene	40	2.20	—	45

magnitude so that the Smith-Ewart interval II model cannot be grossly in error for these monomers.

The Absolute Value of Rate in Interval II

Assuming that both interval I and interval II models are valid, eqs. (3), (11) and (14) can be combined to obtain the interval II rate in terms of independent parameters:

$$dP/dt = B = 0.185 [(k_p/N_A) (d_m/d_p) (1 - \phi_m)S]^{0.6} (R \phi_m)^{0.4} \quad (16)$$

The constant B is defined as the Smith-Ewart rate. In Table V some parameters are presented allowing convenient calculation of B for MMA and styrene when the soap is SLS and the initiator is $K_2S_2O_8$. This table also gives the corresponding rate, b , in per cent per minute. As can be seen, the predicted values of b are a few per cent per minute, i.e., of the order of magnitude generally found in experiments.

The parameter B will be used in Part IV of this series.³ Almost all conversion-time curves of interval II were convex to time axis in the experiments conducted in this laboratory. Thus, these data are not suited for testing eq. (14) or eq. (16). However, a linear conversion-time plot was obtained with methyl methacrylate in the experiment described in the first line of Table VIII. The slope of this line defined an experimental value of B equal to 4.65×10^{-5} sec.⁻¹. The theoretical value is 4.8×10^{-5} sec.⁻¹.

Effect of Soap, Initiator, and Temperature upon Interval II Rate

If both interval I and interval II models are correct, the interval II rate should be proportional to $C_S^{0.6}$ and $C_I^{0.4}$. Approximately theoretical power exponents (+ 0.1) for either C_S or C_I were obtained for styrene by Gerrens et al.,³⁵ Bovey et al.,⁶⁶ Price et al.,⁶⁷ Kolthoff et al.,⁶⁸ Okumara et al.,⁶⁹ and Medvedev et al.;^{70,71} for MMA by Gerrens et al.,⁴² Brodnyan et al.,⁵⁸ and Medvedev et al.;⁷² for vinylidene chloride by Wiener;⁴⁶ for butadiene by Morton and Salatiello;⁷³ and for the copolymerization of butadiene

and styrene by Kolthoff and Medalia.⁷⁴ Again, there are numerous data in the literature with quite different power exponents. The theory of Part III⁵⁹ will explain why the rate is often more sensitive to initiator concentration and is less sensitive to soap concentration than predicted by eqs. (1), (2), and (16).

In eq. (16) the temperature-sensitive parameters are k_p and R , the former to the 0.6 power the latter to the 0.4 power. As for calculating the temperature dependence on N , activation energies equal to 8 and 32 kcal./mole for k_p and R , respectively are assumed. The predicted activation energy for the overall interval II conversion is $(0.6 \times 8) + (0.4 \times 32) = 17.6$ kcal./mole. For styrene Medvedev⁶⁶ found 14 kcal./mole. Data on vinyltoluene and vinylxylene obtained by Gerrens et al.²⁹ also show about 14–15 kcal./mole for the overall activation energy.

MOLECULAR WEIGHT

If termination is an instantaneous reaction between a long molecular chain and a primary or an oligomeric radical, the distinction between termination by disproportionation and termination by combination can be disregarded. Even if termination occurred between a long chain and an oligomeric radical by disproportionation, the oligomeric terminated molecule would be lost in the purification process.

The interval II molecular weight calculable from the Smith-Ewart model is M_{SE} :

$$M_{SE} = k_p \phi_m N d_m / R \quad (17)$$

If both interval I and interval II models are valid, substitution from eqs. (3) and (11) gives M_{SE} in terms of independent parameters:

$$M_{SE} = 0.318 d_p N_A (1 - \phi_m)^{0.4} (d_m k_p \phi_m S / R)^{0.6} \quad (18)$$

Since S is proportional to the soap concentration and R is proportional to the initiator concentration, $M_{SE}(C_I/C_S)^{0.6}$ is constant for a given monomer-soap-initiator system at a given temperature. This quantity is tabulated in Table V for MMA, styrene, SLS, and $K_2S_2O_8$.

Due to chain transfer to monomer, there is a theoretical upper limit for the molecular weight. If the above equation predicts molecular weights higher than about 10 million, it is not likely that the experimental facts will correspond to theory. The chain transfer coefficients to monomer are about 10^{-5} for MMA⁷⁵⁻⁸³ and St.⁸⁴⁻⁸⁶ This means 1 out of 10^5 double bond reactions will not be monomer addition to a growing chain but rather radical transfer to the monomer. The highest possible molecular weight would be about 10^5 times the monomer molecular weight, or about 10 million.

Tables VIII and IX present the final (high conversion) experimental molecular weights and the interval II theoretical molecular weights for MMA and styrene. The agreement is very good for all cases in which the

theoretical molecular weight is lower than 10 million. This good agreement is unexpected because the final molecular weight includes the molecular weight of the polymer formed in interval III for which the Smith-Ewart model does not make predictions. As will be shown in Part IV,³ the good agreement between M_{SE} and the final experimental molecular weight is due to two compensating factors. In reality the interval II molecular weight is higher than M_{SE} and the molecular weight of the polymer produced at the end of the interval III is lower than M_{SE} . The reason for higher molecular weight in interval II is slow termination. The reason for low molecular weight in interval III is that the monomer concentration in the particles is low, resulting in slow propagation rates. These two effects happen to compensate in these experiments so that the final molecular weight is about equal to M_{SE} . It should be noted that according to the theory the interval I molecular weight is about the same as M_{SE} .

Schulz et al.⁸⁷ found excellent quantitative agreement between the theoretical molecular weight of eq. (17) and the experimental value obtained with styrene up to 39% conversion, i.e., within intervals I and II. The final molecular weights were lower than M_{SE} . Part IV will show final molecular weights higher than M_{SE} for poly(butyl methacrylate). Similarly, Vanderhoff et al.⁵⁷ found final molecular weights higher than M_{SE} for polystyrene.

The Smith-Ewart model gives a number-average molecular weight but the data of Tables VIII and IX are viscosity averages. The poly(methyl methacrylate) molecular weights were calculated from the intrinsic viscosities in acetone by the equation, $[\eta] = \beta (MW)^\alpha$, where $\beta = 7.7 \times 10^{-5}$ and $\alpha = 0.70$, given by Fox et al.⁸⁸ For polystyrene the $[\eta]$ values were determined in benzene and Green's parameters⁸⁹ of $\beta = 11.2 \times 10^{-5}$ and $\alpha = 0.73$ were used. The experimental molecular weights taken from Smith in Table IX are those reported by this author. The theoretical values are newly calculated by eq. (18).

It is well known that in solution and bulk polymerization an increase in the initiator concentration causes reduction in the molecular weight. The present theory and the available experimental data^{35,40,42,70,71,90-92} indicate that this is also true for emulsion polymerization.

The present theory predicts that the molecular weight should increase with the soap concentration in isothermal, single-charge recipes because N increases with $C_s^{0.6}$ and M_{SE} is proportional to N/R . This expectation is confirmed for methyl acrylate by Hummel;³⁷ for MMA by Gerrens;⁴² and for styrene by Gerrens et al.,³⁵ by Smith,⁴⁰ by Vanderhoff et al.,⁵⁷ by Medvedev et al.,^{70,71} by Mateo et al.,⁹³ and by Hummel.⁹⁴

If termination is instantaneous, the molecular weight should remain constant throughout interval II. Such data for styrene were obtained by Medvedev et al.⁷² and by Price et al.⁹¹ However, there is a large body of data, including results obtained in this laboratory, which show an increase in molecular weight with conversion during interval II. These data will be discussed in Part IV of this series.³

The polymerization experiments were carried out by Mr. C. Killmeier and Mr. E. M. Young. Dr. R. Wilkins made the electron micrographs. Mr. H. Mason and Mrs. E. Ginsberg carried out the dissymmetry light-scattering and intrinsic viscosity determinations. The polystyrene data obtained at 80°C., shown in Table IX, were supplied by Dr. N. Shachat.

References

1. J. L. Gardon, *J. Polymer Sci. A-1*, **6**, 623 (1968) (Part I).
2. W. V. Smith and R. H. Ewart, *J. Chem. Phys.*, **16**, 592 (1948).
3. J. L. Gardon, *J. Polymer Sci. A-1*, **6**, 687 (1968) (Part IV).
4. I. M. Koltzoff and I. K. Miller, *J. Am. Chem. Soc.*, **73**, 3055 (1951); *ibid.*, **73**, 5118 (1951).
5. J. G. Brodnyan and G. L. Brown, *J. Colloid Sci.*, **15**, 76 (1960).
6. W. M. Sawyer and S. H. Rehfeld, *J. Phys. Chem.*, **67**, 1973 (1965).
7. Z. Pelzbauer, V. Hynkova, M. Bezdek, and F. Hrabak, in *International Symposium on Macromolecular Chemistry, Prague, 1965* (*J. Polymer Sci. C*, **16**), O. Wichterle and B. Sedláček, Chairmen, Interscience, New York, 1966, pp. 507-514.
8. S. H. Maron, M. E. Elder, and I. N. Ulevich, *J. Colloid Sci.*, **9**, 89 (1954).
9. H. B. Klevens, *J. Colloid Sci.*, **2**, 365 (1947).
10. M. Morton, P. P. Satatiello, and M. W. Altier, *J. Polymer Sci.*, **19**, 457 (1956).
11. H. Gerrens, in *Polymer Handbook*, J. Brandrup and E. H. Immergut, Eds., Interscience, New York, 1966, pp. II-399 to II-419.
12. E. H. Crooks, G. F. Trebbi, and D. B. Fordyce, *J. Phys. Chem.*, **68**, 3592 (1964).
13. *Handbook of Chemistry and Physics*, Chemical Rubber Publishing Co., Cleveland, Ohio, 43rd Ed., 1961-1962, p. 1564.
14. C. E. Schildknecht, *Vinyl and Related Polymers*, Wiley, New York, 1952.
15. M. S. Matheson, E. E. Auer, B. B. Bevilacqua, and E. J. Hart, *J. Am. Chem. Soc.*, **73**, 1700 (1951).
16. M. S. Matheson, E. E. Auer, B. B. Bevilacqua, and E. J. Hart, *J. Am. Chem. Soc.*, **71**, 497 (1949).
17. M. S. Matheson, E. E. Auer, B. B. Bevilacqua, and E. J. Hart, *J. Am. Chem. Soc.*, **71**, 2610 (1949).
18. M. S. Matheson, E. E. Auer, B. B. Bevilacqua, and E. J. Hart, *J. Am. Chem. Soc.*, **73**, 5395 (1951).
19. H. W. Melville and A. F. Bickel, *Trans. Faraday Soc.*, **45**, 1049 (1949).
20. G. M. Burnett, P. Evans, and H. M. Melville, *Trans. Faraday Soc.*, **49**, 1105 (1952).
21. G. M. Burnett, P. Evans, and H. M. Melville, *Trans. Faraday Soc.*, **49**, 1096 (1953).
22. P. Hardy, K. Nytray, N. Fedorova, and G. Kovacs, *Vysokomolekul. Soedin.*, **4**, 1872 (1962).
23. I. M. Kochnov and M. F. Sorokin, *Vysokomolekul. Soedin.*, **6**, 791 (1964).
24. N. Gassie and E. Vance, *Trans. Faraday Soc.*, **52**, 727 (1956).
25. W. I. Bengough and R. A. M. Thomson, *Trans. Faraday Soc.*, **61**, 1735 (1965).
26. G. M. Burnett and W. W. Wright, *Proc. Roy. Soc. (London)*, **A221**, 28 (1954).
27. M. Morton, S. Kaizerman, and M. W. Altier, *J. Colloid Sci.*, **9**, 300 (1954).
28. B. M. E. Van der Hoff, *Advan. Chem. Ser.*, **34**, 6 (1964).
29. H. Gerrens and E. Köhnlein, *Z. Elektrochem.*, **64**, 1199 (1960).
30. J. L. Gardon, in preparation (Part VI).
31. E. Peggion, F. Testa, and G. Talamini, *Makromol. Chem.*, **71**, 137 (1964).
32. D. M. French, *J. Polymer Sci.*, **32**, 396 (1958).
33. C. E. M. Morris, A. E. Alexander, and A. G. Parks, *J. Polymer Sci. A-1*, **4**, 985 (1966).
34. H. Gerrens, *Fortschr. Hochpolymer. Forsch.*, **1**, 234 (1959).
35. E. Bartholome, H. Gerrens, R. Herbeck, and H. M. Weitz, *Z. Elektrochem.*, **60**, 334 (1956).

36. H. Gerrens, W. Fink, and E. Köhnlein, in *Macromolecular Chemistry, Prague, 1965* (*J. Polymer Sci. C*, **16**), O. Wichterle and B. Sedláček, Chairmen, Interscience, New York, 1967, p. 2781.
37. D. Hummel, G. Ley, and C. Schneider, *Advan. Chem. Ser.*, **34**, 60 (1962).
38. W. D. Harkins, *J. Am. Chem. Soc.*, **69**, 1428 (1947).
39. V. I. Yeliseyeva, P. I. Zubov, and V. F. Malofeyevskaya, *Vysokomolekul. Soedin.*, **7**, 1348 (1965).
40. W. V. Smith, *J. Am. Chem. Soc.*, **71**, 4077 (1949).
41. W. V. Smith, *J. Am. Chem. Soc.*, **70**, 3695 (1948).
42. H. Gerrens, *Ber. Bunsenges. Physik. Chem.*, **67**, 741 (1963).
43. H. Gerrens, private communication.
44. B. M. E. Van der Hoff, *J. Polymer Sci.*, **44**, 241 (1960).
45. Z. Manyasek and A. Rezabek, *J. Polymer Sci.*, **56**, 47 (1962).
46. H. Wiener, *J. Polymer Sci.*, **7**, 1 (1951).
47. P. M. Hay, J. C. Light, L. Marker, R. W. Murray, A. T. Santonicola, O. J. Sweeting, and J. C. Wepsic, *J. Appl. Polymer Sci.*, **5**, 23 (1961).
48. S. Okumara and T. Motoyama, *Kogyo Kagaku Zasshi*, **61**, 384 (1958).
49. M. Morton, P. P. Salatiello, and H. Landfield, *J. Polymer Sci.*, **8**, 111 (1952).
50. A. S. Dunn and P. A. Taylor, *Makromol. Chem.*, **83**, 207 (1965).
51. H. Chedron, *Kunststoffe*, **50**, 568 (1960).
52. H. Chedron, R. C. Schulz, and W. Kern, *Makromol. Chem.*, **32**, 197 (1959).
53. W. M. Thomas, E. H. Gleason, and G. Mino, *J. Polymer Sci.*, **24**, 43 (1957).
54. S. Okumara and T. Motoyama, paper presented at International Symposium on Macromolecular Chemistry, Montreal, 1962; *J. Polymer Sci.*, **58**, 221 (1962).
55. H. K. Stryker, A. F. Helin, and G. J. Mantell, *J. Appl. Polymer Sci.*, **9**, 1807 (1965).
56. R. H. Ewart and C. I. Carr, *J. Phys. Chem.*, **58**, 640 (1954).
57. J. W. Vanderhoff, E. B. Bradford, H. L. Tarkowsky, and B. W. Wilkinson, *J. Polymer Sci.*, **50**, 265 (1961).
58. J. G. Brodnyan, J. A. Cala, T. Konen, and E. L. Kelley, *J. Colloid Sci.*, **18**, 73 (1963).
59. J. L. Gardon, *J. Polymer Sci. A-1*, **6**, 685 (1968)(Part III).
60. G. M. Burnett and R. S. Lehrle, *Proc. Royal Soc. (London)*, **A253**, 331 (1959).
61. G. M. Burnett, R. S. Lehrle, D. W. Ovenall, and F. W. Peaker, *J. Polymer Sci.*, **29**, 417 (1958).
62. R. Pastiga, M. Litt, and V. Stannett, *J. Phys. Chem.*, **64**, 801 (1960).
63. M. Morton, P. P. Salatiello, and H. Landfield, *J. Polymer Sci.*, **8**, 279 (1955).
64. K. P. Paoletti and F. W. Billmeyer, *J. Polymer Sci. A*, **1**, 2679 (1963).
65. M. Morton and W. E. Gibbs, *J. Polymer Sci. A*, **2**, 2049 (1964).
66. F. A. Bovey, I. M. Kolthoff, A. I. Medalia, and E. J. Meehan, *Emulsion Polymerization*, Interscience, New York, 1955, pp. 196, 201.
67. C. C. Price and C. E. Adams, *J. Am. Chem. Soc.*, **67**, 1674 (1950).
68. I. M. Kolthoff and W. J. Dale, *J. Am. Chem. Soc.*, **69**, 441 (1947).
69. S. Okumara and T. Motoyama, *J. Polymer Sci.*, **58**, 221 (1962).
70. G. D. Berezhnoi, P. M. Khomikovskii, and S. S. Medvedev, *Vysokomolekul. Soedin.*, **2**, 141 (1960).
71. G. D. Berezhnoi, P. M. Khomikovskii, and S. S. Medvedev, *Vysokomolekul. Soedin.*, **3**, 1839 (1961).
72. T. Krishan, M. F. Margaritova, and S. S. Medvedev, *Vysokomolekul. Soedin.*, **5**, 535 (1963).
73. M. Morton and P. P. Salatiello, *J. Polymer Sci.*, **8**, 215 (1952).
74. I. M. Kolthoff and A. I. Medalia, *J. Polymer Sci.*, **5**, 391 (1950).
75. S. R. Palit, U. S. Nandi, and N. G. Saha, *J. Polymer Sci.*, **14**, 295 (1954).
76. U. S. Nandi and S. R. Palit, *J. Polymer Sci.*, **17**, 65 (1955).
77. N. G. Saha, U. S. Nandi, and S. R. Palit, *J. Chem. Soc.*, **1956**, 427.

78. U. S. Nandi, *J. Colloid Sci.*, **12**, 321 (1957).
79. T. E. Ferrington and A. V. Tobolsky, *J. Colloid Sci.*, **10**, 536 (1955).
80. B. Baysal and A. V. Tobolsky, *J. Polymer Sci.*, **8**, 529 (1952).
81. S. C. Baiton, R. A. Binda, and K. E. Russell, *Can. J. Chem.*, **41**, 2737 (1963).
82. J. L. O'Brien and F. Gornick, *J. Am. Chem. Soc.*, **77**, 4757 (1955).
83. G. V. Schulz and G. Harbroth, *Makromol. Chem.*, **1**, 106 (1947).
84. C. H. Bamford and M. J. S. Dewar, *Discussions Faraday Soc.*, **2**, 310 (1947).
85. M. Imoto, T. Ofsu, and T. Ofa, *Makromol. Chem.*, **16**, 10 (1955).
86. F. R. Mayo, R. A. Gregg, and M. S. Matheson, *J. Am. Chem. Soc.*, **73**, 1691 (1951).
87. S. Jovanovic, J. Romatowski, and G. V. Schulz, *Makromol. Chem.*, **85**, 187 (1965).
88. T. G. Fox, J. B. Kinsinger, H. F. Mason, and E. M. Schuele, *Polymer*, **3**, 71 (1962).
89. J. H. S. Green, *J. Polymer Sci.*, **34**, 514 (1959).
90. T. Guha and S. R. Palit, *J. Polymer Sci. A*, **1**, 877 (1963).
91. C. C. Price and C. E. Adams, *J. Am. Chem. Soc.*, **67**, 1674 (1945).
92. G. S. Whitby, M. D. Gross, J. R. Miller, and A. J. Constaza, *J. Polymer Sci.*, **16**, 549 (1955).
93. J. L. Mateo and I. Cohen, *J. Polymer Sci. A*, **2**, 711 (1964).
94. D. Hummel, *Angew. Chem.*, **75**, 330 (1963).

Received May 24, 1967

Revised July 3, 1967

Emulsion Polymerization. III. Theoretical Prediction of the Effects of Slow Termination Rate within Latex Particles

J. L. GARDON, *Rohm and Haas Company,
Spring House, Pennsylvania 19477*

Synopsis

The Smith-Ewart theory predicts that there is an interval during an isothermal homopolymerization when the conversion varies linearly with time. This prediction rests on the assumptions that, during this interval II, the particle number is constant, the monomer concentration in the particles is constant, and the termination rate within the particles is instantaneous, so that the average number of radicals per particle Q is half. In this paper this latter assumption is abandoned. If the termination rate is slow, two or more radicals can coexist in a particle. The termination rate within a particle becomes a function of the particle size because of the decreased probability that two radicals meet for termination in a given time when the volume in which these radicals are located increases. It follows that with increasing conversion the termination rate decreases. Stockmayer's calculations based on this model neglected the variation of particle volume with time, and it was assumed that a steady state of radical concentration in particles exists. In the present calculations these restrictive assumptions were not used. Stockmayer calculated only how Q should vary with conversion. In the present paper several experimentally verifiable consequences of the model are shown. The new calculations show that the interval II conversion-time curve can be represented by the formula $At^2 + Bt$, where B is the Smith-Ewart rate and is proportional to the particle number and the parameter A is independent of the particle number and depends mainly on initiation and termination rates. From A and B and propagation and termination rate constants can be calculated. With the aid of parameters A and B the conversion dependence of molecular weight and of Q can also be predicted for interval II. In the theoretical calculations the distribution of radicals among particles is established. It is shown that for a given value of Q this distribution is unique, independent of the experimental conditions leading to this Q . This distribution was derived solely from kinetic considerations and is analogous to the statistical Poisson distribution. With increasing Q , i.e., with increasing conversion, this distribution broadens. Since each particle grows proportionally to the number of radicals in it, particles must grow at greatly varying rates if there is broad distribution of radicals among them. It follows that the particle size distribution has to broaden with increasing conversion, contrary to predictions based upon the Smith-Ewart model. At present it is not yet possible to predict quantitatively the shape of the conversion-time curve in interval III, the interval following the disappearance of monomer droplets. The reason for this is that the functional dependence of the termination rate constant upon monomer concentration in the particles is not known. However, once the conversion-time curve is experimentally determined, it is possible to calculate from it the interval III values of Q and of molecular weight.

INTRODUCTION

A crucial assumption of the Smith-Ewart model¹ is that termination is an instantaneous reaction between two radicals in the particle. It follows from this assumption that after steady state is reached, only half of the particles can contain a radical at a given time, the other half of the particle is "dead" and the average number of radicals per particle is half.

The present paper retains all assumptions of the Smith-Ewart model except that concerning instantaneous termination. This change in the model has no significant effect upon what happens in the interval in which particle nucleation takes place. Within this interval I few particles absorb radicals in addition to the one that started their growth. Since particle nucleation is completed at relatively low conversion, few termination events can take place during interval I; this was shown in the first paper of this series,² referred to hereafter as Part I.

In all but the last section of this paper the so-called interval II will be discussed. The particle number is constant in interval II and monomer is present in excess of that needed for saturating water and the particles. It is assumed that particle swelling by monomer is independent of particle size throughout this interval; that the polymerization locus is exclusively in the monomer-swollen particles; that the propagation step can be described in terms of the propagation constant of homogeneous polymerization; that radicals form in the aqueous phase at a constant rate and are irreversibly absorbed into the particles. All these assumptions also underlie the Smith-Ewart interval II model. This model is presently modified by assuming that the termination of radicals in the particles proceeds at a finite rate. It follows that polymerization in the particles is not an "on-off" process. In their case 2, Smith and Ewart stated that when a particle containing a growing radical absorbs an additional radical, the two radicals immediately terminate and the particle contains no growing chain till an additional single radical enters it. If, as now assumed, termination between the two radicals proceeds at a finite rate, two radicals do not necessarily cross-terminate before a third radical enters the particle. Thus particles can contain any number of radicals and the average number of radicals per particle is not equal to half but can be larger than half and is a function of time.

Right or wrong, it is also assumed that radicals are completely trapped in particles. There is no chain transfer taking place from the particles to aqueous phase and there are no means available for exchanging radicals between particles.

RECAPITULATION OF SOME OF THE RESULTS OF PART I²

Conversion Rate

The classical rate equation for homogeneous polymerization gives the rate in terms of monomer and radical concentrations ($[M]$, $[R]$) and the propagation k_p :

$$-d[M]/dt = k_p [M] [R] \quad (1)$$

The equivalent equation for emulsion polymerization for the case where the polymerization locus is exclusively in the monomer-swollen particles is:

$$dP/dt = (k_p/N_A)(d_m/d_p) \phi_m N Q \quad (2)$$

Here P is volume of polymer per unit volume of water, t is time, k_p is the propagation constant, N_A is the Avogadro number, d_m and d_p are monomer and polymer densities, respectively, ϕ_m is the monomer volume fraction in the particles, N is the number of particles per cubic centimeter of water, and Q is the average number of radicals per particle.

It is assumed that ϕ_m and N are independent of conversion and that ϕ_m corresponds to the saturation swelling of the particles by monomer. Under these conditions the conversion rate is equal to B , to the Smith-Ewart rate, if the termination is instantaneous resulting in $Q = 0.5$. If Q is not equal to 0.5, then

$$dP/dt = 2QB \quad (3)$$

The Smith-Ewart rate is defined as:

$$B = 0.5(k_p/N_A)(d_m/d_p) \phi_m N \quad (4)$$

For the purposes of this paper it is not necessary to assume the validity of the Smith-Ewart interval I model so that in eqs. (2) and (4) N can be any constant number of particles. If N is that predicted by the Smith-Ewart interval I model, it is calculable from the parameters K , R , and S . Here K is the volume growth rate constant and equals the increase in cubic centimeters per second of the cubed radius of a particle which contains only one radical:

$$K = (3/4\pi) (k_p/N_A) (d_m/d_p) \phi_m / (1 - \phi_m) \quad (5)$$

The parameter R is the number of radicals produced per cubic centimeter of water per second and is calculable from the decomposition rate constant k_d and the concentration of the initiator in water $[I]$:

$$R = 2k_d N_A [I] \quad (6)$$

Finally, the parameter S is the area which the soap molecules present in 1 cc. of water would occupy at an oil-water interface. It is defined by the area per molecule A_s and the soap concentration in water $[S]$:

$$S = A_s N_A [S] \quad (7)$$

The Smith-Ewart interval I model gives:

$$N = 0.208 S^{0.6} (R/K)^{0.4} \quad (8)$$

Substitution into eq. (4) gives:

$$B = 0.435(1 - \phi_m)(KS)^{0.6} R^{0.4} \quad (9)$$

$$= 0.185(k_p \phi_m S d_m/d_p N_A)^{0.6} [R(1 - \phi_m)]^{0.4} \quad (10)$$

The Limits of Interval II

According to the Smith-Ewart interval I model particle nucleation stops at time t_{cr} when the conversion corresponds to P_{cr} :

$$t_{cr} = 0.365(S/R)^{0.6}/K^{0.4} \quad (11)$$

$$P_{cr} = 0.209 S^{1.2}(K/R)^{0.2} (1 - \phi_m) \quad (12)$$

Evidently, $P = P_{cr}$ is the lower validity limit of equations describing interval II. The upper validity limit is where the monomer droplets disappear, P_{II-III} . If it is justifiable to assume that the solubility of monomer in water is negligibly low, P_{II-III} is calculable from the monomer/water weight ratio m/w and from the weight fraction of polymer in the particles corresponding to ϕ_m :

$$P_{II-III} = (m/w) (1 - \phi_m) d_{\text{water}}/d_p [1 - \phi_m + (d_m/d_p) \phi_m] \quad (13)$$

Dimensionless Variables

In Part I most of the calculations were carried out with dimensionless variables; two of these, z , the dimensionless conversion, and x , the dimensionless time will be used here. In the definitions below, n_i is the number of monomer swollen particles per cubic centimeter of water whose radius is r_i .

$$z = 5.98S^{-1.2} (R/K)^{0.2} \sum n_i r_i^3 \quad (14)$$

Since

$$(4\pi/3) \sum n_i r_i^3 = P/(1 - \phi_m)$$

substitution from eqs. (8) and (9) provides this dimensionless variable in a form useful in this paper:

$$z = 0.1297 (R/NB)P \quad (15)$$

Another convenient form of z gives it in terms of the average volume of the monomer-swollen particle \bar{V} :

$$\bar{V} = P/N(1 - \phi_m) \quad (16)$$

$$z = 0.2594 (R/N) (N_A/k_p) (d_p/d_m) [(1 - \phi_m)/\phi_m] \bar{V} \quad (17)$$

The dimensionless time was defined in Part I;

$$x = 3.36K^{0.4}(R/S)^{0.6}t \quad (18)$$

Substitution from eq. (8) gives:

$$x = 0.698(R/N)t \quad (19)$$

The conversion rate in dimensionless variables is obtained from eqs. (3), (15) and (18):

$$dz/dx = 0.372Q \quad (20)$$

The values of z and x at the point where particle nucleation stops were given in Part I:²

$$z_{cr} = 0.3016 \quad (21)$$

$$x_{cr} = 1.232 \quad (22)$$

SPECIFICATION OF THE TERMINATION RATE

In homogeneous polymerization the following equation holds for the radical concentration:

$$d[\text{R}]/dt = 2k_d[\text{I}] - k_t[\text{R}]^2 \quad (23)$$

The present paper retains the phenomenological significance of the termination rate constant k_t . It must be emphasized that k_t of emulsion polymerization differs in its numerical value from that of bulk or solution polymerization. The termination process is diffusion-controlled, and k_t depends upon the viscosity of the medium. The particles contain at high concentration a very high molecular weight polymer and the viscosity in them is much larger than is encountered at low conversions in kinetic experiments involving solution or bulk polymerization.

In the interval II of emulsion polymerization ϕ_m is constant, hence the viscosity in the particle is independent of conversion. It follows that throughout interval II k_t is a conversion-independent constant. Because its value is not the same as in other polymerization processes, k_t is not an independent parameter; it can be determined only by analyzing emulsion polymerization data.

It is convenient to express termination rates in terms of the number of radicals per particle, q :

$$q = VN_A[\text{R}] \quad (24)$$

Here V is the volume of the monomer swollen particle. Since each radical can only react with $(q - 1)$ radicals, the termination rate is not proportional to q^2 , as predicted by the second term on the right-hand side of eq. (23) but is proportional to $q(q - 1)$. To define the first term on the right-hand side of eq. (23), the present model assumes that radicals are generated outside the particles. The average rate of entry of radicals into a given particle is R/N . Thus the equation for emulsion polymerization, which is equivalent to eq. (23), has the following form:

$$dq/dt = R/N - (k_t/VN_A)q(q - 1) \quad (25)$$

The termination rate, given in the second term above, decreases as the particle volume increases. This is not due to the Trommsdorff effect³ of homogeneous polymerization because in interval II there is no change in k_t with time. The decreasing termination rate with increasing conversion is solely due to the increase in particle volume.

STEADY-STATE SOLUTION

It is convenient to calculate N_q , the number of particles containing q radicals. It is evident that:

$$N = \sum N_q \quad (26)$$

$$Q = \sum qN_q/N \quad (27)$$

Particles containing q radicals are created when particles containing $(q - 1)$ radicals absorb a radical and when termination takes place in particles containing $(q + 2)$ radicals. The rate of the former process is $(R/N)N_{q-1}$ and the rate of the latter process, by eq. (25), is $(k_t/VN_A)(q + 2)(q + 1)N_{q+2}$. Similarly, particles with q radicals are destroyed by radical absorption at a rate of $(R/N)N_q$ and by termination at a rate of $(k_t/VN_A)q(q - 1)N_q$. It follows that:

$$\begin{aligned} dN_q/dt = (R/N)(N_{q-1} - N_q) + (k_t/N_A\bar{V}) \\ \times [N_{q+2}(q + 2)(q + 1) - N_q q(q - 1)] \quad (28) \end{aligned}$$

The fact that larger particles may absorb radicals at a rate greater than the average rate, R/N , is ignored. Differences in the size of particles are also ignored, so that instead of the true particle volume V the average volume \bar{V} is used.

Haward⁴ and Smith and Ewart¹ assumed a steady state of equal termination and initiation rates so that for each q value dN_q/dt should be zero. They also ignored the variation of \bar{V} with time. These assumptions lead to the following recursion formula:

$$(q + 2)(q + 1)N_{(q+2)} + \alpha N_{q-1} = N_q[q(q - 1) + \alpha] \quad (29)$$

$$\alpha = (R/N)(N_A\bar{V}/k_t) \quad (30)$$

Smith, Ewart, and Haward solved this recursion formula only for the limiting case when $\alpha = 0$, i.e., when either $\bar{V} \sim 0$ or $k_t \sim \infty$. They found that $N_0 = N_1 = 0.5N$ and that $Q = 0.5$. It was shown in Part I that this is an obvious result if very fast termination is assumed.

A general solution of eq. (29) has been provided by Stockmayer⁵ and by O'Toole.⁶ Stockmayer's solution is:

$$a^2 = 8\alpha \quad (31)$$

$$Q = (a/4)I_0(a)/I_1(a) \quad (32)$$

where $I_0(a)$ and $I_1(a)$ are Bessel functions of first kind and of zeroth and first order. This is the final form of the steady-state theory presented in the literature. Its theoretical implications upon the shape of the conversion-time curve, the molecular weight-conversion curve and the variation of particle size distribution with conversion were not explored.

The authors^{1,4-6} dealing with the steady-state solution also considered radical desorption into the aqueous phase. Equations (29)–(32) represent

the case of interest from the standpoint of the present paper where the radical desorption is assumed to be negligible.

It is of interest to represent eq. (32) in a form comparable to the non-steady-state solution of the present paper. The dimensionless termination parameter Ψ is introduced.

$$\Psi = (k_t/k_p)(d_p/d_m)(1 - \phi_m)/\phi_m \quad (33)$$

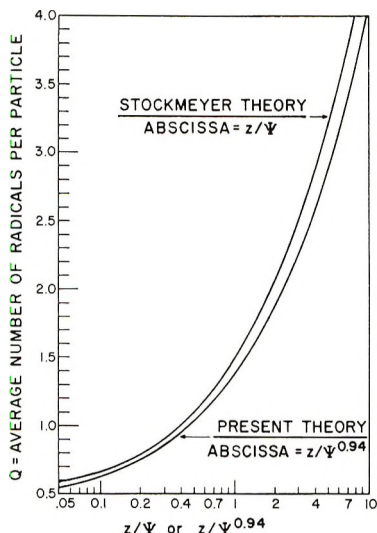


Fig. 1. Variation of the average number of radicals per particle with number-average particle volume or conversion in interval II; either of these two variables is proportional to z . The parameter Ψ defines the termination rate.

and eqs. (30), (31), (33), and (17) are combined:

$$a = 5.52(z/\Psi)^{0.5} \quad (34)$$

Stockmayer's solution in terms of the dimensionless conversion, z , is shown in Figure 1. This curve is obtained by combining eqs. (32) and (34).

SET OF EQUATIONS DESCRIBING THE NON STEADY STATE

It is desirable to recalculate this model for estimation of the error involved in assuming a steady state and in ignoring the variation of \bar{V} with time. More importantly, it is also desirable to deduce some experimentally verifiable implications from the model by deriving explicit expressions for the variation of conversion and molecular weight with time. Finally, the implications of the model upon particle size distributions should also be explored.

It is acknowledged that dN_o/dt is not zero and that \bar{V} is a function of time. It is expedient to eliminate the variables t and \bar{V} from eq. (28) with the aid of eqs. (3) and (16):

$$(2Q)(dN_q/dP) = (R/NB)(N_{q-1} - N_q) + [k_t N(1 - \phi_m)/N_A BP] \\ \times [N_{q+2}(q+2)(q+1) - N_q q(q-1)] \quad (35)$$

Equations (35), (27), (26), and (3) completely define the system. For solving this set of equations, it is convenient to change to dimensionless variables in terms of the dimensionless time x , the dimensionless conversion z , and the dimensionless termination parameter Ψ , defined in eqs. (19), (15), and (33), respectively. A new variable f_q the fraction of particles containing q radicals is:

$$f_q = N_q/N \quad (36)$$

After these substitutions, the variation of Q with z is defined by the following set of equations:

$$Qdf_0/dz = 3.81(-f_0) + (\Psi/z)(2f_2)$$

$$Qdf_1/dz = 3.81(f_0 - d_1) + (\Psi/z)(6f_3)$$

$$Qdf_2/dz = 3.81(f_1 - f_2) + (\Psi/z)(12f_4 - 2f_2)$$

.

.

.

$$Qdf_q/dz = 3.81(f_{q-1} - f_q) + \\ (\Psi/z)[(q+2)(q+1)f_{q+2} - q(q-1)f_q] \quad (37)$$

$$\sum f_q = 1 \quad (38)$$

$$Q = \sum qf_q = f_1 + 2f_2 + 3f_3 + 4f_4 + \dots \quad (39)$$

If the particle size was very small, termination would be instantaneous and all f_q values with $q \geq 2$ would be zero. Thus half of the particles would be terminated and would contain no radical and half would contain one growing radical.

It follows that the boundary conditions for solving combined eqs. (37), (38) and (39) are:

$$z = 0$$

$$f_0 = 0.5$$

$$f_1 = 0.5$$

$$Q = 0.5$$

$$f_2 = f_3 = f_4 = f_5 = \dots = 0$$

These boundary conditions express only the mathematical properties of the functions; they have no physical significance since the lower limit of the physical validity of these equations is $z = 0.3016$ by eq. (21).

The numerical solution of eqs. (37), (38), and (39) gives Q as a function of conversion, z . The conversion-time curve can be obtained by substituting the calculated Q values into the dimensionless conversion rate equation:

$$dz/dx = 0.372Q \quad (20)$$

For solving this equation, the boundary conditions defined by eqs. (21) and (22), i.e., $z = 0.3016$ when $x = 1.232$, are used. The value of Q at this boundary depends on the value of the parameter Ψ and is defined by the solution of eqs. (37), (38), and (39).

The numerical integration by the point-slope formula⁷ was carried out with an IBM 1620 computer with Ψ having values 1, 4, 10, 40, or 100 and with $0 < z < 100$. It can be shown that it is very unlikely that $z > 100$ would be needed to evaluate experimental data.

After the numerical solutions were tabulated, analytical equations were fitted to them by trial and error. These equations represent the true solutions with a precision that can be estimated. Subsequently, dimensionless variables in these analytical equations were changed to experimentally meaningful variables and parameters.

SOLUTION OF THE NON STEADY-STATE SOLUTION

Variation of Conversion with Time

The results of the numerical solution of combined eqs. (37), (38), (39), and (20) are shown in Figure 2. The first three columns of Table I give excerpts of the computer results for the variations of z with x . The follow-

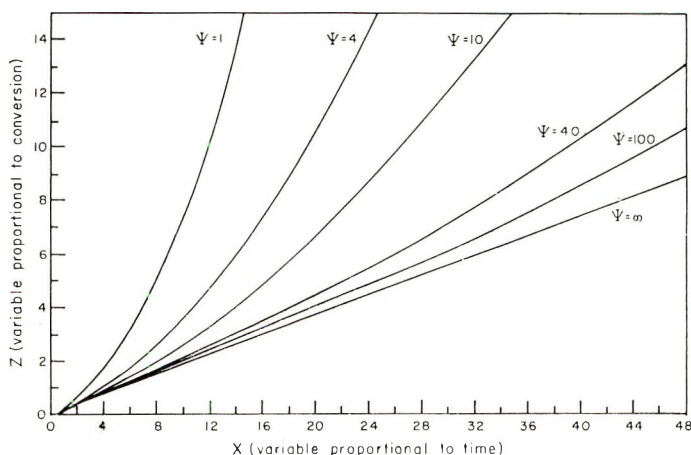


Fig. 2. Shape of conversion-time curves. Here ψ is a parameter having the same order of magnitude as the ratio between termination and propagation rate constants. The curve with $\Psi = \infty$ corresponds to the Smith-Ewart interval II theory.

ing equation was found to fit these results with better than -8 and $+0.5\%$ accuracy:

$$z = (0.05464/\Psi^{0.94})x^2 + 0.186x + 0.0721(1 - 1.14/\Psi^{0.94}) \quad (40)$$

The z values calculated from this equation are shown in the last column of Table I.

TABLE I
Precision of the Approximate Equations for the Interdependence of z , Q , and x

Ψ	Results of the numerical integration			Approximate equations ^a	
	z	x	Q	Q , eq. (46)	z , eq. (40)
1	0.3016	1.2320	0.8543	0.851	0.3117
	1.000	2.9239	1.3669	1.352	1.002
	3.000	5.8914	2.2554	2.230	2.984
	10.00	11.8931	4.0146	4.000	9.933
	30.00	21.7024	6.8703	6.890	29.78
	100.0	41.1812	12.4526	12.53	100.3
4	0.3016	1.2320	0.6238	0.615	0.2957
	1.000	3.7793	0.8524	0.822	0.9198
	3.000	8.7621	1.3064	1.238	2.777
	10.00	10.3409	2.2491	2.130	9.152
	30.00	37.1268	3.7932	3.620	27.42
	100.0	72.5959	6.8180	6.560	91.77
10	0.3016	1.2320	0.5540	0.587	0.3012
	1.000	4.3144	0.6660	0.657	1.000
	3.000	11.0968	0.9217	0.890	2.901
	10.00	26.5892	1.5076	1.432	9.545
	30.00	53.4337	2.4951	2.380	27.92
	100.0	107.6950	4.439	4.260	92.85
40	0.3016	1.2320	0.5141	0.514	0.3013
	1.000	4.7779	0.5459	0.546	0.9971
	3.000	13.9311	0.6302	0.630	2.992
	10.00	39.0499	0.8708	0.862	9.983
	30.00	87.6240	1.3420	1.330	29.21
	100.0	190.5193	2.3127	2.278	97.51
100	0.3016	1.232	0.5057	0.505	0.3102
	1.000	4.9009	0.5187	0.521	0.9990
	3.000	14.9261	0.5549	0.558	3.008
	10.00	45.6966	0.6697	0.676	10.07
	30.00	112.9968	0.9305	0.935	30.28
	100.0	266.0760	1.5269	1.529	100.4

^a The value of Q by eq. (46) was calculated from z values shown in the second column of this table. The value of z by eq. (40) was calculated from the x values shown in the third column.

Equations (4), (15), (19), and (33) are used to change from dimensionless variables to experimental variables and parameters. The following conversion-time relationship corresponds to eq. (40):

$$P = At^2 + Bt + C \quad (41)$$

Here B is the Smith-Ewart rate defined in the equivalent expressions of eqs. (4), (9), and (10). The parameters A and C are defined in eqs. (42) and (43):

$$A = 0.102(k_p^{1.94}/k_t^{0.94})(d_m/d_p N_A)[\phi_m^{1.94}/(1 - \phi_m)^{0.94}]R \quad (42)$$

$$C = 0.0503(1 - 1.14/\Psi^{0.94})(1 - \phi_m)S^{1.2}(K/R)^{0.2} \quad (43)$$

From the parameters given in Part II,⁸ the value of C can be estimated. For most practical recipes it is of the order of 10^{-2} cc. polymer/cc. water. This means that it can be safely disregarded at the interpretation of experimental data. Thus the following equation represents the theory with adequate accuracy:

$$P = At^2 + Bt \quad (44)$$

It is of interest that steady-state homogeneous polymerization rate is proportional to $(k_p^2 k_d/k_t)^{0.5}$. The corresponding term in eq. (42) is $(k_p^{1.94} k_d/k_t^{0.94})$. The power exponents 1.94 and 0.94 came from the curve fitting and are sufficiently close to 2 and 1 to indicate analogy. The At^2 term of eq. (44) is analogous to homogeneous polymerization while the Bt term comes from the classical Smith-Ewart model of emulsion polymerization. It is important that the theory predicts a conversion-time curve convex to the time axis. In general, there is therefore no rate independent of conversion and time in emulsion polymerization. It should be emphasized that the validity limit of eq. (44) is $P_c < P < P_{II-III}$ by eqs. (12) and (13).

From the experimental B , N and ϕ_m data, k_p can be calculated by eq. (4). The same parameters combined with the experimental A and R values define k_t through the following equation:

$$k_t/k_p = 0.158(RB/AN)^{1.062}\phi_m/(1 - \phi_m)$$

The Average Number of Radicals per Particle

The numerical solution of combined eqs. (37), (38), and (39) gives the variation of Q with z . Excerpts of the computer results are shown in the first, second, and fourth columns of Table I. The following equation fits the numerical solutions with better than 8% accuracy:

$$Q = 0.5(1 + 6.3z/\Psi^{0.94})^{0.5}$$

Values of Q calculated from this equation are shown in the fifth column of Table I. This equation is also plotted in Figure 1. It can be easily ascertained that it gives results very close to Stockmayer's steady-state solution to which, for all practical purposes, it is equivalent. It follows that the mathematical approximations involved in the steady state solution are justifiable as long as it is realized that the results of the steady-state solution are inconsistent with the assumptions on which it is based. Since at steady state N_q of eq. (28) is assumed to be independent of time, Q should also be independent of time, by eq. (27). This is true only as long

as the change in the average particle volume is negligible. However, with increasing time the particle volume increases, and Q also must increase so that the steady-state exists only momentarily, not over the time interval of an actual experiment. In homogeneous polymerization there can be a steady state of equal initiation and termination rates for extended times so that a linear conversion-time relationship can be obtained. By contrast, steady state exists only momentarily in emulsion polymerization and the number of live radicals increases with time even before the onset of the Trommsdorff effect. The only possibility for a steady state in emulsion polymerization occurs when termination is instantaneous, so that $Q = 0.5$ and is independent of conversion. At finite termination rates Q increases with conversion during interval II.

The value of Q can be calculated from the experimental variable P and the parameters A and B . The appropriate equation is obtained by substituting from eqs. (15), (33), and (42) into eq. (46).

$$Q = 0.5[1 + (4A/B^2)P]^{0.5} \quad (47)$$

This equation defines the validity limit of the Smith-Ewart interval II theory: $4AP/B^2 \ll 1$. Since A is proportional to R and B is proportional to N , the Smith-Ewart interval II theory is valid if the latex particle size is small and the initiation rate is low.

Distribution of Radicals among Particles

This distribution is defined by the values of f_q , the fraction of particles which contain q radicals. Inspection of the numerical solution of eqs. (37)–(39) revealed that this distribution depends solely on Q , and therefore only on the ratio of $z/\Psi^{0.94}$ or on the ratio of AP/B^2 .

Typical distributions are shown in Figure 3. As can be seen, the distribution broadens with increasing Q , or in terms of eq. (47), with increasing conversion. Since each particle grows proportionally to q , this distribution also defines the distribution of growth rates. In principle, from this growth rate distribution the particle size distribution could be calculated but this was not attempted. Here we confine ourselves to qualitative interpretation. It is clear that, with increasing conversion, more and more particles will be found which grow much slower or much faster than the average. The particle size distribution must therefore broaden with increasing conversion. It also follows from the curves of Figure 3 that the particle size distribution should become skew: with increasing conversion the population contains few very small particles and many large particles.

It is likely that the calculated breadth in the distribution of growth rates is too low. In the derivation it was assumed that the average rate of radical entry into each particle is R/N . As the particle size distribution broadens because of slow termination, the broadening is further enhanced by the fact that the larger particles capture radicals at a rate larger than the average, while the smaller ones capture radicals at a rate lower than the average. Furthermore, in the derivation all particles were assumed

TABLE II
Comparison Between the Theoretical Radical Distribution among Particles and the
Modified Poisson Distribution

	$Q = 1.0100$		$Q = 2.0274$		$Q = 4.0146$		$Q = 7.9158$	
	Theory ^a	Modified Poisson ^b	Theory ^a	Modified Poisson ^b	Theory ^a	Modified Poisson ^b	Theory ^a	Modified Poisson ^b
f_0	0.2901	0.3128	0.0903	0.0970	0.0092	0.0099	0.0000	0.0001
f_1	0.4596	0.4172	0.2664	0.2754	0.0519	0.0533	0.0010	0.0011
f_2	0.2056	0.2114	0.3192	0.3264	0.1337	0.1339	0.0058	0.0059
f_3	0.0401	0.0479	0.2090	0.2216	0.2096	0.2092	0.0195	0.0197
f_4	0.0042	0.0041	0.0835	0.0943	0.2257	0.2276	0.0473	0.0470
f_5	0.0002	0.0001	0.0237	0.0258	0.1787	0.1829	0.0876	0.0867
f_6	—	—	0.0047	0.0045	0.1048	0.1124	0.1296	0.1284
f_7	—	—	0.0007	0.0005	0.0524	0.0538	0.1574	0.1569
f_8	—	—	—	—	0.0205	0.0203	0.1605	0.1613
f_9	—	—	—	—	0.0066	0.0061	0.1397	0.1414
f_{10}	—	—	—	—	0.0018	0.0014	0.1051	0.1068
f_{11}	—	—	—	—	0.0004	0.0003	0.0691	0.0701
f_{12}	—	—	—	—	—	—	0.0401	0.0402

^a Result of the numerical solution of eqs. (37), (38), and (39).

^b Calculated from eq. (50). At low Q values the fit between the theoretical and the modified Poisson distribution would be improved if the variance would be calculated from eq. (49) without neglecting the second term in this equation.

to have average volume. In particles with larger than average volume the termination is slower than average, and in smaller particles it is faster. These effects are disregarded here.

One would intuitively expect that the distribution of the radicals among particles should follow the Poisson distribution, in which the average and the variance are equal. The variance of computer solutions of eqs. (37)–(39) was calculated from eq. (48):

$$\text{variance} = \sum q^2 f_q - Q^2 \quad (48)$$

This variance was found to be exactly $0.75Q$ at $Q \geq 4$ and exactly $0.5Q$ at $Q = 0.5$. The variance over the whole range of Q values fits the following approximate formula:

$$\text{variance} = 0.75 Q - 0.051/Q^{1.28} \quad (49)$$

Distributions analogous to the Poisson type but with a variance unequal to the mean, were described by Greenwood and Yule.^{9–11} A Greenwood-Yule distribution with a mean equal to Q and a variance equal to $0.75Q$ is defined for $0 < q < 4Q + 1$ by eq. (50):

$$\begin{aligned} f_0 &= (0.75)^{4Q} \\ f_1 &= 1.333 f_0 Q \\ f_2 &= f_1 (4Q - 1)/6 \\ f_3 &= f_2 (4Q - 2)/9 \\ &\cdot \\ &\cdot \\ &\cdot \\ f(q + 1) &= f_q (4Q - q + 1)/3q \end{aligned} \quad (50)$$

Table II shows that this Greenwood-Yule distribution gives an excellent fit to the numerical solution of eqs. (37)–(39). Thus these kinetic equations define a statistical distribution whose significance is known. The Poisson distribution would give the f_q values if the expected mean of any sample taken from the population was independent of the sampling method. The Greenwood-Yule modification of the Poisson distribution gives the f_q values when the expected sample mean depends on sampling, and thus Q is not the expected average of any sample population; it is the grand average of the total population. The present theory predicts that the particle size distribution broadens with increasing conversion. If only the largest particles were sampled, the expected average number of radicals per particle in this sample would be larger than Q . Conversely, a sample of smallest particles would contain on the average fewer number of radicals than Q . Since the expected sample average of q values can be influenced by the method of sampling, the distribution of radicals among particles

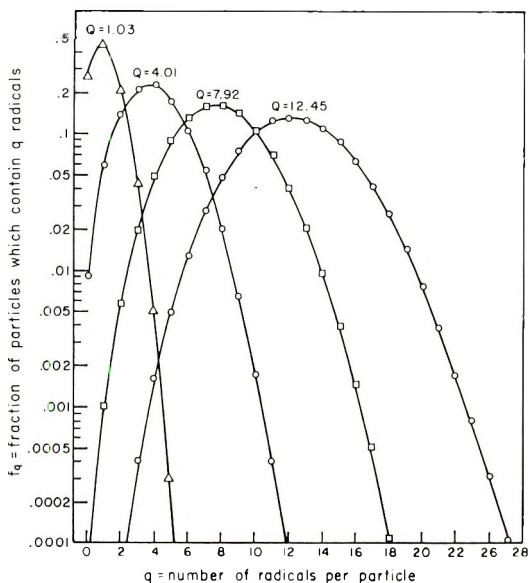


Fig. 3. Distribution of radicals among particles at different average number of radicals per particle Q . Since the growth rate of each particle is proportional to q , each of curve also gives the distribution of growth rates per particle.

cannot be of the Poisson type, it must be of the Greenwood-Yule type. While this explains why eqs. (37)–(39) give a distribution which is almost identical to that of Greenwood and Yule, it does not explain why it is narrower than the Poisson distribution. The likely reason for this is that with increasing conversion the distribution is generated from a very narrow one. In solving eq. (37)–(39) the boundary condition of $f_0 = f_1 = 0.5$ was assumed at zero conversion.

Molecular Weight

It is assumed that termination is by combination of two radicals. If Λ is the average number of terminated polymer molecules per particle, 2Λ is the number of radicals absorbed from the aqueous phase which were used to create this number of terminated chains. At time t , on the average, $(R/N)t$ radicals were absorbed by a particle. It follows that:

$$(R/N)t = 2\Lambda + Q \quad (51)$$

It is easy to show that in all practical cases $Rt \gg NQ$. Thus the following approximation is justifiable:

$$\Lambda = 0.5(R/N)t \quad (52)$$

Since the average volume of polymer per particle is P/N , the number-average molecular weight of all terminated chains in a single particle is:

$$\bar{M}_n = (P/N) N_A d_p / \Lambda \quad (53)$$

Combination of eqs. (52) and (53) gives the interdependence of the three variables P , t and \bar{M}_n :

$$\bar{M}_n = (2d_p N_A/R)(P/t) \quad (54)$$

The validity of this equation is not confined to interval II, it is also valid for interval III. For interval II the time as a variable can be readily eliminated by combining eqs. (54) and (44):

$$\bar{M}_n = (4AN_A d_p/BR) P / \{ [1 + (4A/B^2) P]^{0.5} - 1 \} \quad (55)$$

This equation gives \bar{M}_n as a unique function of P in terms of the independent parameters A , B , d_p , and R and thus can be experimentally tested.

Another molecular weight value of interest is that of the polymer formed at any given instant, M_{inst} . The following relationships hold by definition:

$$\bar{M}_n = (1/t) \int_0^t M_{\text{inst}} dt \quad (56)$$

$$(\partial \bar{M}_n / \partial t)t + \bar{M}_n = M_{\text{inst}} \quad (57)$$

Combination of eqs. (57), (54), (47), and (3) gives:

$$M_{\text{inst}} = (2 d_p N_A B/R) [1 + (4A/B^2)P]^{0.5} \quad (58)$$

Equations (54), (55), and (58) are valid even if the radicals enter into larger particles faster and into smaller particles slower than the average radical entry rate R/N , and even if the actual time lapse between the entry of two radicals into a particle is not the average value, N/R , but is sometimes shorter or longer. These deviations from the assumed model would have no effect upon the number-average value of the molecular weight. In calculating any other average, these effects could cause some error. In calculating an average which should be close to the viscosity average we choose to ignore these effects.

Since in practical emulsion polymerization the molecular weights obtained are in the million range, the intrinsic viscosity is the most convenient method of molecular weight determination; the number-average molecular weight is very difficult to determine. The viscosity-average molecular weight is between the number average and weight average. We can approximate its value by averaging the instantaneous number-average molecular weights by weight:

$$\bar{M}_v = (1/P) \int_0^P M_{\text{inst}} dP \quad (58)$$

$$\bar{M}_v = (B^3 N_A d_p / 3AR) \{ [1 + (4A/B^2) P]^{1.5} - 1 \} / P \quad (59)$$

It is of interest that if the approximations used in deriving eq. (59) are correct, we have:

$$1 \leq \bar{M}_v / \bar{M}_n \leq 1.333$$

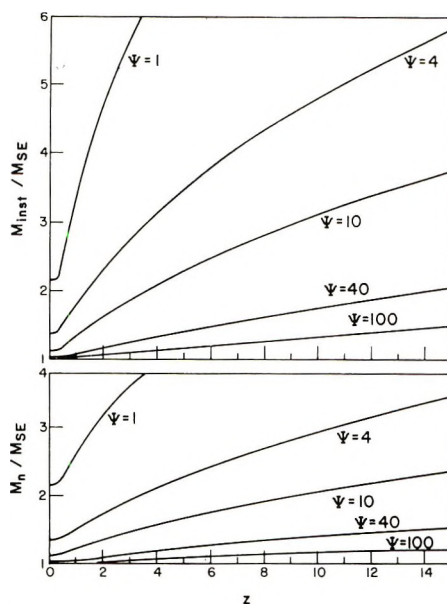


Fig. 4. Variation of the number-average molecular weight with conversion in intervals I and II. M_{inst} is the molecular weight of the polymer formed at the instant when z reaches a specified value, M_n is the molecular weight averaged over the interval 0 to z . M_{SE} is the molecular weight that would be obtained with $\psi = \infty$ in interval II. The variable z is proportional to particle volume or conversion. The parameter ψ defines the termination rate.

The upper limit of this ratio would be reached at infinitely slow termination. It follows that the viscosity-average and number-average molecular weights in emulsion polymerization can be quite close.

In Part I² instantaneous termination was assumed. A consequence of this assumption was that the molecular weight in interval II should be independent of conversion and be equal to M_{SE} , the Smith-Ewart molecular weight.

$$\begin{aligned} M_{\text{SE}} &= 2 d_p N_A B / R \\ &= k_p d_m \phi_m N / R \end{aligned} \quad (60)$$

Universal molecular weight-conversion curves giving $\bar{M}_n / M_{\text{SE}}$ and $M_{\text{inst}} / M_{\text{SE}}$ as functions of the dimensionless variable z and of the dimensionless termination constant Ψ are given in Figure 4. As can be seen, the actual interval II molecular weights can be much higher than that of the Smith-Ewart model. In drawing the curves of Figure 4, it was assumed that the molecular weight does not change with conversion in interval I and equals that obtained from the interval II theory at $P = P_{cr}$.

Effect of Post-Added Initiator

If the Smith-Ewart assumption of instantaneous termination was valid, post-addition of initiator during interval II would have no effect upon the

rate since Q would remain equal to 0.5. Experimental data to be reviewed in Part IV¹² show that the rate is increased when the initiator level is increased after completion of particle nucleation.

For calculating this effect, the parameter ϵ , the ratio between initiator concentrations after and before post-addition is introduced. It follows that after post-addition the radical production rate is ϵR . By replacing R in eq. (35) with ϵR , the new experimental conditions are described.

The calculations were carried out in terms of the dimensionless variables z and x . In eq. (37) the term $3.81(f_{q-1} - f_q)$ was replaced with the term $3.81\epsilon(f_{q-1} - f_q)$ and the thus modified equation was combined with eqs. (38), (39), and (20).

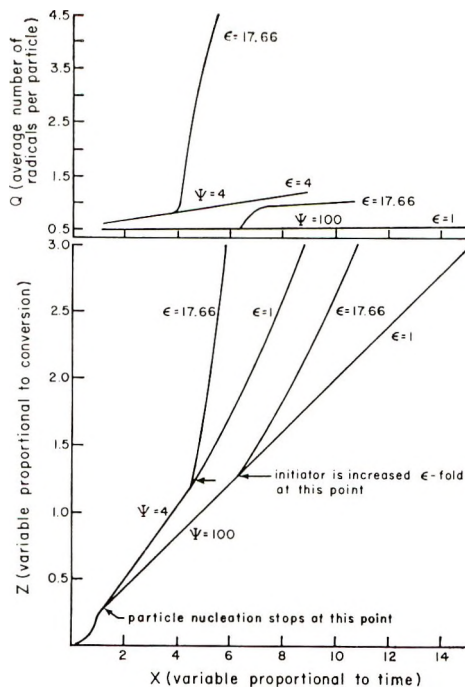


Fig. 5. Effect of post-added initiator.

The new set of equations contains two parameters, Ψ and ϵ . As earlier Ψ was taken to be 4, 10, 40, and 100. The parameter ϵ was used at two values: 17.66 and 5, so that the solutions should be useful in analyzing some of the experimental results obtained by Gerrens and Kohnlein.¹³ To fit these experimental results with reasonably good accuracy, it was assumed that the initiator concentration was increased at a conversion corresponding to $z = 1.25$.

Typical results of the numerical solutions are shown in Figure 5. According to these calculations the distribution of radicals among particles is the same unique function of Q as determined earlier for $\epsilon = 1$.

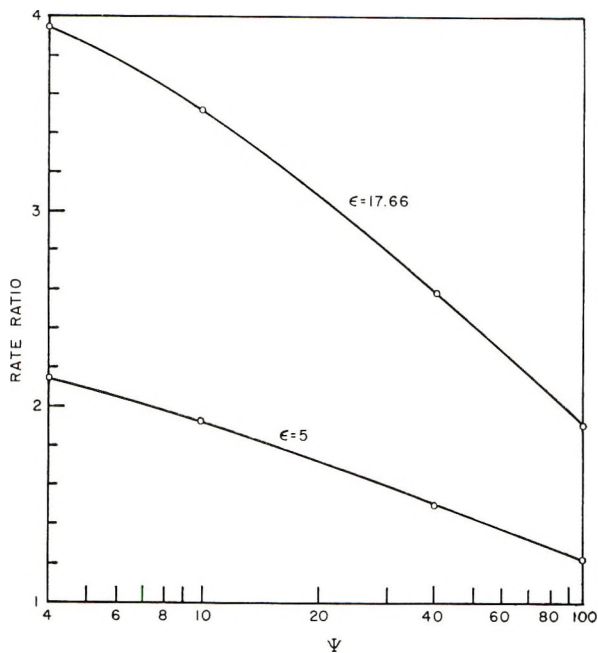


Fig. 6. Calculated ratio of apparent linear interval II rates obtained after and before post-addition of initiator. The initiator level is assumed to be increased 5 or 17.66-fold at a conversion corresponding to $z = 1.25$. Interval II is assumed to span to $z = 3$. Note that $\psi = (k_t/k_p)(d_p/\dot{a}_m)(1 - \phi_m)/\phi_m$.

In their experiments, Gerrens and Köhnlein¹³ did not take into account the curvature in the conversion-time curves and reported the ratio of rates before and after initiator post-addition. For the purpose of reanalyzing these data, the same rate ratios can be calculated from the numerical solutions of the present equations. The average slope of the z versus x plots was determined in the range $z = z_{cr} = 0.3016$ to $z = 1.25$ with $\epsilon = 1$ and Ψ varied. In addition, the average slopes were determined in the range $1.25 < z < 3$ for the same Ψ values but with ϵ equal to either 5 or 17.66. The results of these calculations are shown in Figure 6.

In Part IV¹² Figure 6 will be used for determining the k_t/k_p ratio. The experimentally found ratio of rates at a given experimental ϵ value is indicated on the ordinate. The corresponding Ψ value defines k_t/k_p by eq. (33). It will be shown that the k_t/k_p ratios thus determined are of the same order of magnitude as the values determined from A , B , R , ϕ_m , and N values [cf. eq. (45)] taken from independent experiments in which no initiator was post-added.

DESCRIPTION OF INTERVAL III

After the monomer droplets disappear at P_{II-III} conversion [cf. eq. (13)], most of the unconverted monomer is present in the monomer-swollen latex particles, and a small fraction of it may also be dissolved in water. During

interval II the conversion proceeds at an approximately constant monomer concentration in the particles and the particle volumes increase with time. In interval III the conversion proceeds at the expense of monomer concentration in particles and the monomer-swollen particle volume may actually shrink due to contraction at polymerization.

It is justifiable to assume that k_p is independent of conversion because propagation is generally not a diffusion-controlled process. However, as the monomer concentration in the particles decreases with increasing conversion in interval III, the viscosity within the particles increases and the value of k_t is bound to decrease, as predicted by Trommsdorff et al.³ Thus the shape of the interval III conversion-time curve is determined by two processes whose effects oppose each other. If the value of k_t stayed constant, the conversion rate and the molecular weight would have to decrease uniformly with increasing conversion because the propagation rate is proportional to the decreasing monomer concentration in the particles. However, with increasing conversion, the termination rate decreases and this, by itself, would cause an increase in rate and in molecular weight by the Trommsdorff gel effect.

It was shown earlier that in interval II the value of dP/dt should increase with conversion, not because of the Trommsdorff effect, but because of the retardation of the termination rate caused by increasing particle volume. In interval III the value of dP/dt may continue to increase for a short time after P_{II-III} , if the Trommsdorff effect is more important than the effect of the decreasing rate of propagation. At high conversion, however, dP/dt and the molecular weight is bound to decrease with increasing conversion because here the slow propagation can be expected to predominate. It is of interest in this context that, as will be shown in Part V,¹⁴ there is a theoretical limit to the lowest possible value of the k_t/k_p ratio.

At present the functional relationship between k_t and the monomer concentration in the particles is not known. For this reason it is not possible to develop a predictive, quantitative theory for interval III. In this work it was assumed that k_t decreases either linearly or quadratically with the monomer concentration and that the shrinkage at polymerization is negligible, so that the particle volume in interval III remains constant. With the aid of these assumptions, equations in many respects analogous to eqs. (37) and (20) were derived and solved numerically. The only interesting result of these calculations is that the distribution of radicals among particles was found to be the same unique function of Q as the one found for interval II. It would follow that if the experimental data suggest an increase in Q with increasing conversion, the particle size distribution is bound to broaden with increasing conversion.

While at present it is not yet possible to predict the shape of the conversion-time curve in interval III, it is possible to calculate from the experimentally determined curve the variation of Q and of molecular weight with conversion. The equation for molecular weight was presented earlier, it is eq. (54). As to Q , it is noted that dP/dt equals B if $Q = 0.5$ and if the

effective volume fraction of monomer in the particles, ϕ_{eff} , equals the equilibrium value, ϕ_m . The more general relationship is given in eq. (61):

$$dP/dt = (2B/\phi_m) \phi_{\text{eff}} Q \quad (61)$$

For determining ϕ_{eff} , it is convenient to assume that the solubility of monomer in water is negligible. Thus all unconverted monomer is present in the latex particles during interval III and the weight fraction of polymer in the particles equals the fractional conversion γ . It follows that:

$$\phi_{\text{eff}} = (1 - \gamma) / \{1 - \gamma[1 - (d_m/d_p)]\} \quad (62)$$

From the experimental interval II parameters, B and ϕ_m , and from the absolute value of the conversion rate and the fractional conversion, the value of Q in interval III can be calculated in terms of these equations.

The author is greatly indebted to Mr. L. DeFonso for finding a method to solve the combined eqs. (37), (38), (39), and (20) and for carrying out the calculations on the computer.

References

1. W. V. Smith and R. H. Ewart, *J. Chem. Phys.*, **16**, 592 (1948).
2. J. L. Gardon, *J. Polymer Sci. A-1*, **6**, 623 (1968) (Part I).
3. E. Trommsdorff, H. Kohle, and P. Legally, *Makromol. Chem.*, **1**, 169 (1947).
4. R. N. Haward, *J. Polymer Sci.*, **4**, 273 (1949).
5. W. H. Stockmayer, *J. Polymer Sci.*, **24**, 314 (1957).
6. J. T. O'Toole, *J. Appl. Polymer Sci.*, **9**, 1291 (1965).
7. W. Milne, *Numerical Solution of Differential Equations*, Wiley, New York, 1953, pp. 19-24.
8. J. L. Gardon, *J. Polymer Sci. A-1*, **6**, 643 (1969) (Part II).
9. M. Greenwood and G. U. Yule, *J. Royal Statist. Soc.*, **83**, 255 (1920).
10. M. J. Moroney, *Facts from Figures*, Penguin Books Ltd., Hammondsworth, Middlesex, England, 1954, pp. 96-107.
11. M. G. Kendall, *The Advanced Theory of Statistics*, Hafner, New York, 5th Ed., 1952, Vol I, pp. 124-125.
12. J. L. Gardon, *J. Polymer Sci. A-1*, **6**, 687 (1968) (Part IV).
13. H. Gerrens and E. Kohnlein, *Z. Elektroche.*, **64**, 1199 (1960).
14. J. L. Gardon, in preparation (Part V).

Received May 24, 1967

Revised July 3, 1967

Emulsion Polymerization. IV. Experimental Verification of the Theory Based on Slow Termination Rate within Latex Particles

J. L. GARDON, *Rohm and Haas Company,
Spring House, Pennsylvania 19477*

Synopsis

A large body of data shows that the time dependence of conversion fits the equation $P = At^2 + Et$ in the interval where, according to the Smith-Ewart model, the relationship should be linear. For latexes of very small particle size the Smith-Ewart linear relationship ($P = Bt$) is often observed, and for latexes of very large particle size the conversion was found to be proportional to t^2 . The experimental value of parameter B was in good agreement with independent theoretical predictions. From A and B the ratio between termination and propagation constants was calculated and was in the 5-200 range. Independent estimates of this ratio give the same order of magnitude. These independent estimates are from the literature and are obtained from the increase in conversion rate at catalyst post-addition during emulsion polymerization or from emulsion polymerization initiated by intermittent irradiation or from homogeneous polymerization in the presence of inert polymers of high viscosity. The conversion-time curves describing the whole conversion process generally have sigmoid shape. The molecular weight is often found to pass through a maximum as the conversion increases. In one experiment this maximum coincided with the calculated maximum in the average number of radicals per particle Q . The variation of experimental molecular weights with conversion accurately followed the theoretical predictions. The deviation from the Smith-Ewart model was often significant. The value of Q was not 0.5, as the Smith-Ewart model requires it to be, but often reached values much larger, as large as 10. The particle size distribution broadened with increasing conversion and became increasingly skew. Numerous data taken from the literature are in good quantitative or qualitative agreement with the theory proposed in Part III and for these data the observed deviations from the Smith-Ewart theory are readily explainable. The new data obtained with styrene, *n*-butyl methacrylate, and methyl methacrylate are also in quantitative agreement with the new theory. One experiment involving methyl methacrylate is analyzed in great detail. The variation of time, of Q , of molecular weight, of average particle size, and of particle size distribution with conversion are reported. The molecular weight distribution is also calculated from the conversion dependence of molecular weight.

INTRODUCTION

One of the basic assumptions advanced by Smith and Ewart¹ is that in emulsion polymerization the sole loci of chain propagation are the monomer-swollen latex particles, and that the diffusion of monomer to these loci is not rate-controlling. If the monomer cannot swell the latex particles because it is a poor solvent for the polymer, because stirring is inadequate,

or because the monomer is gradually added during the reaction, the Smith-Ewart theory cannot apply. Under such conditions the locus of propagation could be the particle surface, and the propagation could be diffusion controlled, as advocated by Medvedev.^{2,3} This possibility was disregarded in the preceding theoretical papers of this series, Parts I and III.^{4,5} The evidence reviewed in Part II⁶ and in the present paper suggests that experimental deviations from the Smith-Ewart model are not due to diffusion-controlled propagation when the monomers are good solvents for their polymers, all monomer is charged to the reactor at the beginning of the reaction, and stirring is adequate. It follows that under such conditions the propagation rate is proportional to the monomer concentration in the particles and to the propagation constant, k_p .

For describing what happens after the particle nucleation is complete, Smith and Ewart in their case 2 assumed that termination is an instantaneous reaction of two radicals in the particles and showed that, as a consequence of this assumption, the average number of radicals per particle Q should be half. One can visualize either negative or positive deviations from this prediction.

If the predominant mode of chain termination is chain transfer from the particles to the aqueous phase or crosstermination of radicals located in different particles, Q could be significantly lower than 0.5. Several authors⁷⁻¹⁰ consider that this can occur, but since no mathematical theory has yet been advanced for quantitative experimental test of this assumption, the available evidence for its validity is at best circumstantial. Actually, it is quite possible, and even likely, that radicals can desorb from particles. However, as will be shown in this paper, many experimental data obtained with persulfate initiators can be explained with adequate accuracy by the theoretical model of Part III,⁵ where radical desorption was assumed to be negligible. Termination by radical desorption may be important in radiation-initiated reactions.⁷⁻⁹

Part III assumed that termination takes place solely within the particles and proceeds at a finite rate. A consequence of this assumption is a positive deviation from the Smith-Ewart model in that Q can assume values larger than half. Several other consequences of this assumption were derived for interval II. In this interval the particle number is constant, there are monomer droplets present and the monomer concentration in the particles is approximately constant. The predictions made in Part III are as follows: (a) the interval II conversion-time curve is convex to the time axis; (b) even if the conversion-time curve appears to be linear, the conversion rate is not proportional to the particle number; (c) when initiator is post-added during interval II, the conversion rate increases; (d) the molecular weight in interval II increases with conversion; (e) the particle size distribution broadens with increasing conversion.

These predictions are contrary to the Smith-Ewart interval II model. Experimental verification of these predictions is described in the present paper.

EQUATIONS DESCRIBING AN EMULSION POLYMERIZATION EXPERIMENT

The effects of initiator and soap are introduced into the theory by the parameters R and S , respectively. The number of radicals produced per cubic centimeter of water per second is R ; S is the area at the oil-water interface occupied by the soap molecules present in 1 cc. of water. These quantities are calculable from the decomposition rate constant and molar concentration of the initiator, k_d and $[I]$, the area per soap molecule and molar concentration of soap, A_s and $[S]$, and Avogadro number, N_A :

$$R = 2k_d N_A [I] \quad (1)$$

$$S = A_s N_A [S] \quad (2)$$

It is often convenient to measure the initiator and soap concentrations in per cent based on water and the symbols C_I and C_S will be used for them. In Part II the values of R/C_I at various temperatures are tabulated for persulfate initiators and the values of S/C_S are tabulated for various soaps.⁶

The most important parameters describing the monomer are the monomer volume fraction in a monomer-saturated latex particle ϕ_m , the propagation constant k_p , and d_m and d_p , monomer and polymer density, respectively. These values are tabulated for numerous monomers in Part II. In Part II the parameter K , the volume growth rate constant, is also tabulated for styrene and methyl methacrylate (MMA) at various temperatures. This parameter is defined in eq. (3):

$$K = (3/4\pi)(k_p/N_A)(d_m/d_p)\phi_m/(1 - \phi_m) \quad (3)$$

From these parameters it is possible to calculate the final number of particles N , the volume of polymer P_{cr} formed in 1 cc. of water when particle nucleation stops, and the Smith-Ewart rate B , which would be equal to the polymer volume production per second in 1 cc. of water during interval II if termination were instantaneous.

$$N = 0.208S^{0.6}(R/K)^{0.4} \quad (4)$$

$$P_{cr} = 0.209S^{1.2}(K/R)^{0.2}(1 - \phi_m) \quad (5)$$

$$B = 0.5(k_p/N_A)(d_m/d_p)\phi_m N \quad (6)$$

$$= 0.185(k_p\phi_m S d_m/d_p N_A)^{0.6} [R(1 - \phi_m)]^{0.4} \quad (7)$$

The theoretical values of the quantities $N/C_S^{0.6} C_I^{0.4}$, $P_{cr} C_I^{0.2}/C_S^{1.2}$, and $B/C_S^{0.6} C_I^{0.4}$ are tabulated in Part II for styrene and MMA monomers, persulfate initiator, sodium lauryl sulfate (SLS) soap, and various temperatures.

The root-mean-cube average radius at 100% conversion can be calculated from the monomer/water weight ratio, m/w , in the initial charge:

$$r_{rnc} = 1.05 [(m/w)(d_{water}/d_p)]^{0.333} S^{-0.2} (K/R)^{0.133} \quad (8)$$

The theoretical values of $r_{\text{rmc}} C_S^{0.2} C_I^{0.133}$ for the system styrene, MMA-SLS-K₂S₂O₈, $m/w = 40/60$ are tabulated in Part II.⁶

The conversion is conveniently expressed in terms of P , the volume of polymer present per unit volume of water. Interval II is defined to span in the conversion range $P_{cr} \leq P \leq P_{\text{II-III}}$. At the conversion corresponding to $P_{\text{II-III}}$ the monomer droplets disappear.

$$P_{\text{II-III}} = (m/w)(1 - \phi_m) d_{\text{water}}/d_p [1 - \phi_m + (d_m/d_p) \phi_m] \quad (9)$$

In interval II the monomer concentration in the particles is about constant, and it is justifiable to use a single, conversion-independent termination rate constant k_t , for describing the interval II kinetics. This constant is introduced into the theory via the parameter A , defined below:

$$A = 0.102 (k_p^{1.94}/k_t^{0.94})(d_m/d_p N_A) [\phi_m^{1.94}/(1 - \phi_m)^{0.94}]R \quad (10)$$

The variation of conversion with time during interval II is predicted to fit the equation:

$$P = At^2 + Bt \quad (11)$$

Since k_t is dependent upon the monomer concentration at the polymerization locus, its value cannot equal that of homogeneous polymerization at high dilution. It follows that A cannot be predicted from independent parameters. However, from the experimental values of A , B , N , and R the value of k_t can be calculated:

$$k_t/k_p = 0.158(RB/AN)^{1.062} \phi_m/(1 - \phi_m) \quad (12)$$

With the aid of parameter A one can predict the variation of molecular weight with conversion during interval II. Below, \bar{M}_n is the number-average molecular weight and \bar{M}_v is an average close to the viscosity-average:

$$\bar{M}_n = (4AN_A d_p/BR)P/\{[1 + (4A/B^2)P]^{0.5} - 1\} \quad (13)$$

$$\bar{M}_v = (B^3N_A d_p/3AR) \{[1 + (4A/B^2)P]^{1.5} - 1\}/P \quad (14)$$

The variation of the average number of radicals per particle Q with conversion during interval II is given by eq. (15):

$$Q = 0.5 [1 + (4A/B^2)P]^{0.5} \quad (15)$$

This equation measures the deviation from the Smith-Ewart model. If $1 \gg (4A/B^2)P$, the Smith-Ewart interval II model is valid, and the number-average interval II molecular weight is:

$$M_{SE} = k_p \phi_m N d_m/R \quad (16)$$

$$= 0.318 [d_p N_A (1 - \phi_m)]^{0.4} (d_m k_p \phi_m S/R)^{0.6} \quad (17)$$

In interval III, when $P > P_{\text{II-III}}$, it is possible to calculate the variation of Q and \bar{M}_n with conversion from the shape of the conversion-time curve. If the monomer solubility in water is negligible, the monomer

volume fraction in the particles after the monomer droplets disappeared, ϕ_{eff} , is calculable from the fractional conversion, γ :

$$\phi_{\text{eff}} = (1 - \gamma) / \{1 - \gamma[1 - (d_m/d_p)]\} \quad (18)$$

The variation of Q and \bar{M}_n with conversion in interval III is:

$$Q = (dP/dt) \phi_m / 2 \phi_{\text{eff}} B \quad (19)$$

$$\bar{M}_n = (2d_p N_A / R) (P/t) \quad (20)$$

In using the last equation, t should be measured from the start of the reaction.

These equations are valid only for isothermal, single-charge homopolymerization in the presence of water soluble initiators and micelle forming soaps. Equations (1)–(9) and (16) and (17) were derived in Part I,⁴ while eqs. (10)–(15) and (17)–(20) in Part III.⁵ The molecular weights given in eqs. (13), (14), (16), (17), and (20) are valid only if termination is by combination of two radicals in the absence of chain transfer.

EXPERIMENTAL METHODS

Some of the experiments were run in three-necked flasks under nitrogen blanket and good stirring. For determining the variation of conversion with time, aliquots of the reaction mixture were weighed into a methanolic hydroquinone solution. The thus inhibited dispersion was dried, and the amount of polymer was determined by weighing. The molecular weight of this polymer was also determined in some instances.

In one experiment the conversion dependence of particle size distribution was also determined. A small fraction of the reaction mixture was poured over ice and hydroquinone to stop the reaction. This slurry was extracted with ice-cold hexane to remove the monomer and then allowed to come to room temperature to obtain a stable nonpolymerizing latex which could be handled by the conventional techniques of electron microscopy.

On several occasions the conversion–time curve was determined in automatic, self-recording dilatometers. The reaction chamber was of about 100 cc. in size, of oblate spheroid shape, and equipped with a magnetic stirrer. It was connected through a water-filled capillary to one leg of a U-tube containing mercury. On contraction in the reaction chamber, the mercury in the open end of the U-tube was pulled downwards and a pencil lead electrode immersed in the mercury became increasingly exposed. A constant current of 0.4 ma. was passed through the pencil lead electrode into the mercury. In this arrangement, only the exposed part of the pencil lead electrode contributed to the electrical resistance of the circuit. The current intensity was continuously recorded on the chart of a voltmeter. The increase in voltage was found to be exactly proportional to the distance through which the mercury meniscus moved and hence to the conversion. The whole dilatometer assembly was immersed in a constant temperature bath. The connecting glass joints in this assembly

contained Teflon gaskets. Teflon stopcocks were used so that the reaction mixture was not in touch with stopcock grease. The mixture of monomer, water, and soap was allowed to come to thermal equilibrium before the initiator was added in concentrated solution. Prior to its introduction to the reaction chamber by a syringe, the initiator solution was brought to reaction temperature. The arrangement was such that measurement could be started in less than 1 min. after the introduction of the initiator. Though only boiled water and purified monomers were used, the induction times were found to be longer than that, ranging from several minutes to a quarter of an hour. In spite of careful initial degassing, gas bubbles may develop during the reaction. To prevent this, in all experiments the dilatometer was put under 14 psi pressure, applied through the open end of the mercury-containing U-tube.

One problem in dilatometric measurements is that the monomer/water ratio continuously changes as more water is sucked into the reaction chamber. To minimize this error, the reported C_s , C_I , and m/w values are based upon the average water content of the reaction chamber during the reaction. For example, if the chamber was 105 cc. and 40 cc. of monomer was charged to it, it initially contained 65 cc. of water. If the monomer contracted on reaction by 20%, i.e., by 8 cc., at the end of the reaction 73 cc. of water was in the chamber. Under these conditions C_s , C_I , and m/w were based on 69 cc. of water.

To determine the interval II parameters A and B , measurements obtained below 45% conversion for styrene, 25% conversion for methyl methacrylate, and 30% conversion for *n*-butyl methacrylate were used. For each of these monomers P_{cr} was also calculated by eq. (5) and only data at conversions higher than this were used. In this interval, at least ten pairs of conversion-time data were obtained in experiments involving three-necked flasks. In dilatometer experiments more numerous data points were read from the voltmeter charts.

It is convenient to measure conversion in per cent and time in minutes. We define γ to be fractional conversion, 100γ to be per cent conversion, and T to be time in minutes. The time is measured from an arbitrary point during the induction period. From this point to the start of the reaction, the time elapsed is T_0 , so that the total experimentally determined time is the sum of the reaction time, T , and this T_0 , whose exact value is calculable. The interval II data are fitted to the following equation by the least-square method:

$$100\gamma = a^*(T + T_0)^2 + b^*(T + T_0) - c^* \quad (21)$$

If eq. (11) is valid, the following relationship has to hold:

$$100\gamma = aT^2 + bT \quad (22)$$

It is easy to show that:

$$a = a^* \quad (23)$$

$$b = (b^{*2} + 4a^*c^*)^{0.5} \quad (24)$$

The units of a and b are per cent per minute squared and per cent per minute, respectively. From these parameters A and B in reciprocal square second and reciprocal second are calculated by eqs. (25) and (26):

$$A = 2.778 \times 10^{-6} (m/w) (d_{\text{water}}/d_p) a \quad (25)$$

$$B = 1.667 \times 10^{-4} (m/w) (d_{\text{water}}/d_p) b \quad (26)$$

The molecular weights were calculated from the intrinsic viscosities by the equation:

$$[\eta] = \beta \bar{M}_v^\alpha \quad (27)$$

The intrinsic viscosities were determined for polymer samples purified by several reprecipitations. The solvent for polystyrene was benzene, with $\beta = 11.5 \times 10^{-5}$ and $\alpha = 0.73$, given by Green.¹¹ Later in this paper data given by Smith¹² will also be discussed. The presented polystyrene molecular weights were calculated from Smith's published $[\eta]$ values obtained in benzene. The $[\eta]$ values of poly(methyl methacrylate) were determined in acetone and of poly(*n*-butyl methacrylate) in methyl ethyl ketone. Values of $\beta = 7.7 \times 10^{-5}$ and $\alpha = 0.70$ were used for the former, $\beta = 1.56 \times 10^{-5}$ and $\alpha = 0.81$ were used for the latter; these values were determined in the laboratories of the Rohm and Haas Co.

DEPENDENCE OF CONVERSION UPON TIME

Shape of the Conversion-Time Curve in Interval II

The conversion-time curve is usually not linear in interval II and it is not justifiable to assign a constant rate to emulsion polymerization. Linear conversion-time curves are obtained only for latexes of small particle size at low initiator rates; in this limiting case the Bt term is much larger than the At^2 term of eq. (11). This limiting case was already discussed in Part II.⁶ In the more general case, the conversion-time curve is convex to the time axis by eq. (11). If not enough data points are obtained, or if the conversion range investigated is too narrow, the curvature in the conversion-time relationship may be overlooked and the data can fit a linear relationship. However, the thus determined apparent rates may not equal the Smith-Ewart rate, B , because the At^2 term also influences the results. Since this term is independent of particle size, the rate per particle, $(dP/dt)/N$, is often found to increase with particle size when the soap concentration is reduced in single-charge recipes, or when the particle size is increased in seeded recipes. Such results are inconsistent with the Smith-Ewart interval II model and have been reported for styrene,¹²⁻¹⁶ methyl methacrylate,¹⁶⁻¹⁸ *n*-butyl methacrylate,¹⁸ vinyltoluene,¹⁹ vinylxylene,¹⁹ vinyl chloride,²⁰ chloroprene,¹⁶ and vinyl acetate.¹⁶

Conversion-time curves convex to the time axis in interval II are shown in Figures 1 and 2. Such curves fit well the $P = At^2 + Bt$ equation, as indicated by the A and B parameters shown in Tables I, II, and III and

TABLE I
 Kinetic Data Obtained with Methyl Methacrylate^a

Reaction conditions	40°C.	40°C. ^b	40°C.	40°C.	55°C. ^c	55°C.	55°C. ^d
m/w	35/65	35/65	35/65	38/62	36/64	40/60	40/60
C_s of SiS_2 , %	0.63	0.305	2.58	1.47	0.305	0.244	0.244
C_t of $\text{K}_2\text{S}_2\text{O}_8$, %	0.23	0.73	0.23	0.142	0.117	0.165	0.165
$r \times 10^6$ at full conversion, cm.	7.8	—	5.2	4.9	6.7	7.6	5.25
Experimental (elec. micr.)	5.75	5.75	4.6	5.2	6.4	6.2	6.2
Theory [eq. (8)]							
$B \times 10^6$, sec. ⁻¹							
Experimental	5.48	5.63	7.55	5.87	8.7	10.2	5.26
Theory [eq. (7)]	4.80	4.80	10.9	6.50	7.3	8.3	8.3
$A \times 10^9$ (experimental), sec. ⁻²	2.29	4.86	7.45	0.98	12.9	37.4	19.4
Quantities calculated from exptl.							
A, B, N, P , and t values							
k_t/k_p [eq. (12)]	77	115	29	73	100	92	41
Q at 25% conv. [eq. (15)]	0.58	0.65	0.63	0.54	0.52	0.87	0.60
Q at 60% conv. [eqs. (18) and (19)]	0.96	—	1.25	0.85	0.35	2.16	2.8
Q at 80% conv. [eqs. (18) and (19)]	2.90	—	2.34	1.95	4.00	10.3	5.4
Q at 90% conv. [eqs. (18) and (19)]	1.0	—	—	—	1.67	2.23	2.96
Coefficient of variation, %							
Experimental B	0.002	3	8.2	4.3	4	0.8	10.8
Experimental A	0.01	11	10.6	4.5	20	1.4	1.4

^a The experiments described in this table are also the basis of Table VIII in Part II. The contraction in the dilatometer was 24.5 ± 0.5 cc./100 g. of monomer.

^b This reaction mixture gelled at about 60% conversion and for this reason experimental N value is not available. The k_t/k_p ratio was calculated with the aid of the theoretical N value.

^c The particle radius indicated for this experiment was determined by dissymmetry light scattering.

^d This experiment was run in a three-necked flask; all other experiments were run in a dilatometer. Additional data obtained in this experiment are shown in Table V of Part II and in Tables V and VI and Figures 1, 4, 5, and 6 of this paper.

by the linear time dependence of the difference between conversion and the second-order term in Figure 2. Similarly shaped conversion-time curves were reported for styrene,^{7,12,21,23-25} butadiene,^{14,25,26} isoprene,²² methyl methacrylate,^{7,26-31} methyl acrylate,^{32,33} vinyl acetate,³⁴⁻³⁶ chloroprene,³⁷ vinylidene chloride^{38,39} and vinyl chloride.⁴⁰

An interesting case arises when the conversion-time curves are determined in various recipes in which the temperature, initiator concentration and monomer/water ratio are kept constant but the final particle size is varied by changing the soap concentration or by salt addition. According to the theory [cf. eqs. (6), (10), and (11)] the At^2 term is the same for the interval II conversion-time curves of all such recipes, while Bt decreases

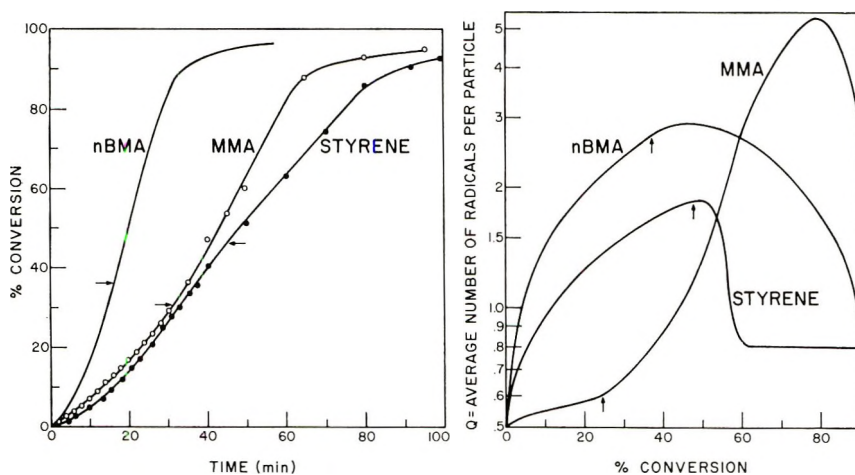


Fig. 1. Interdependence of conversion, time, and average number of radicals per particle. The arrows indicate where the monomer droplets disappear. The methyl methacrylate and styrene curves correspond to the experiments in the last columns of Tables I and II, respectively; the *n*-butyl methacrylate experiment is described in the middle column of Table III. The value of Q is calculated from eqs. (15) and (19). The molecular weight results obtained in this methyl methacrylate experiment are shown in Table V and Fig. 4. Particle size distribution data of the same experiment are shown in Table VI and Figs. 5 and 6.

with increasing final particle size. Thus for latexes of small particle size the Bt term dominates the conversion-time curves in interval II, the conversion is linear with time, and the rate is relatively high. As the particle size is increased, the At^2 and Bt terms become comparable, the conversion at a given time is reduced, and the conversion-time curves become curved, convex to the time axis. Finally, for latexes of very large particle size, the conversion becomes proportional to the square of time because here the At^2 term predominates. Such families of conversion-time curves were obtained for methyl methacrylate,²⁸ vinyl acetate,³⁴ butadiene,²⁶ vinylidene chloride,³⁹ vinyl chloride,⁴⁰ and the copolymerization of butadiene and styrene.²⁶ The predicted proportionality between conversion

TABLE II
Interval II Kinetic Data Obtained with Styrene^a

	Data of Smith ¹²		This work
Reaction conditions			
Temperature, °C.	30.5	50	60
<i>m/w</i>	37/63	37/63	40/60
<i>C_S</i> of SLS, %	—	—	0.67
<i>C_S</i> of SF Flakes, %	0.5	0.5	—
<i>C_I</i> of K ₂ S ₂ O ₈ , %	0.17	0.17	0.24
<i>r</i> × 10 ⁶ at full conversion, cm.			
Experimental (elec. micr.)	7.9	5.8	4.6
Theory [eq. (8)]	8.3	5.8	4.2
<i>B</i> × 10 ⁵ , sec.			
Experimental	0.61	2.97	10.2
Theory [eq. (7)]	0.59	3.55	8.5
<i>A</i> × 10 ⁹ (experimental), sec. ⁻²	0.17	1.52	10.9
Quantities calculated for experimental <i>A</i> , <i>B</i> , and <i>N</i>			
<i>k_t/k_p</i> [Eq. (12)]	15	150	141
<i>Q</i> at 50% conv. [eq. (15)]	1.3	1.6	1.3
Coefficient of variation, %			
Experimental <i>B</i>	39.8	90	8
Experimental <i>A</i>	64.5	190	35

^a Smith's two experiments were run in test tubes; in this laboratory a three-necked flask was used. Additional experimental results are shown in Table VIII of Part II. Table V of this paper shows the variation of molecular weight with conversion for the last two experiments. Figure 1 of this paper shows the conversion-time curve of the experiment of the last column. The SF Flakes used by Smith are a mixture of sodium stearate, oleate, and palmitate with $S/C_S = 5 \times 10^4$ cm.⁻¹/% (cf. Part II). The high coefficient of variation in the *A* and *B* values of the first two columns is due to the fact that Smith gave only few data points in his tables.

and the square of time for large particle sized latexes is demonstrated in Figure 3.

The Value of Parameter *B*

The most rigorous test of the theory is the comparison of the experimental value of *B* [determined from the least-square fit of eq. (11) to the experimental conversion-time curve] to the theoretical value of *B* [calculated from independent parameters by eq. (7)]. For styrene and methyl methacrylate the propagation constants are known and in Part II the theoretical *B* values are given. These values are in satisfactory agreement with the experimental values, as shown in Tables I and II and in the caption of Figure 2.

For butyl methacrylate the available information⁴¹ on propagation constants may not be reliable and is outside the temperature range of the experiments of Table III. As shown in Table III, the propagation constants calculated for this monomer from the experimental *B* and *N* values by eq. (6) are of the right order of magnitude, comparable to the values of other monomers presented in Part II. This indicates that these experi-

TABLE III
 Results Obtained with *n*-Butyl Methacrylate^a

	65°C.	60°C.	45°C.
Reaction conditions			
<i>m/w</i>	40/60	47/53	40/60
<i>C_S</i> of SLS, %	0.68	1.01	0.66
<i>C_I</i> of K ₂ S ₂ O ₈ , %	0.157	0.204	0.35
Experimental results at full conversion			
<i>r</i> × 10 ⁶ (light scatter), cm.	5.69	5.21	6.05
<i>r</i> × 10 ⁶ (elec. micr.), cm.	3.00	—	4.45
Molecular weight × 10 ⁻⁶ , g./mole	5.95	6.91	11.0
Experimental interval II parameters			
<i>A</i> × 10 ⁹ , sec. ⁻²	333	187	3.66
<i>B</i> × 10 ⁵ , sec. ⁻¹	3.51	8.6	4.33
Coeff. of variation of <i>A</i> , %	2.5	13	50
Coeff. of variation of <i>B</i> , %	19.5	27	24
Quantities calculated from experimental <i>A</i> , <i>B</i> , <i>N</i> , <i>P</i> , and <i>t</i> values			
<i>k_p</i> × 10 ⁻⁶ [eq. (6)], cm. ³ /mole-sec.	1.16	1.82	1.75
<i>k_p/k_t</i> [eq. (12)]	4	9	88
<i>Q</i> at 30% conversion [eq. (15)]	7.0	2.4	0.8
<i>Q</i> at 50% conversion [eqs. (18) and (19)]	7.2	2.9	—
<i>Q</i> at 70% conversion [eqs. (18) and (19)]	8.1	2.7	—
<i>Q</i> at 80% conversion [eqs. (18) and (19)]	9.3	1.7	—
<i>M_{SE}</i> × 10 ⁻⁶ [eq. (16)]	0.5	2.4	6.6
\bar{M}_n × 10 ⁻⁶ 80% conv. [eq. (20)]	4.1	9.15	—
\bar{M}_n × 10 ⁻⁶ 90% conv. [eq. (20)]	—	5.3	—
Theoretical <i>r</i> × 10 ⁶ calculated by eqs. (3) and (8) with <i>k_p</i> values shown above, cm.			
	3.4	3.32	4.35

^a For this monomer there are no reliable *k_p* values available so that *B* and *r* cannot be predicted from independent parameters. The density and ϕ_m values used in the calculation are taken from Table III, Part II.

The experimental value of *N* was calculated from the light scatter average radius because the electron microscope may give questionable result for a soft polymer, although the materials were hardened by ultraviolet irradiation prior to exposure.

The experiment at 45°C. was run in three-necked flask, the other two experiments were run in dilatometer. Figure 1 shows additional data for the experiment at 60°C. The contraction in the dilatometer was 19.6 cc./100 g. of monomer.

mental *B* values are plausible. The average particle radii calculated by eqs. (1)–(3) and (8) with the aid of the thus determined propagation constants agree with the experimental values.

The Average Number of Radicals Per Particle *Q*

Figures 1 and 2 and Tables I, II, and III show that the value of *Q* can significantly exceed the Smith-Ewart limit of 0.5 even during interval II for styrene, methyl methacrylate, and butyl methacrylate. The theory and the data are in agreement in that *Q* was found to increase uniformly with conversion during interval II.

At present it is not known how to predict quantitatively the variation of *k_t* with monomer concentration in the particles during interval III; all we

know is that its value decreases with decreasing ϕ_{eff} [cf. eq. (18)], i.e., with increasing conversion and time. Thus at present it is not possible to predict the shape of the conversion-time curve and the variation of Q with conversion during interval II. If the Trommsdorff gel effect⁴² is very strong, as it is for methyl methacrylate, k_t may decrease very rapidly as ϕ_{eff} decreases at the onset of interval III, with the result that Q increases further, beyond the highest value reached in interval II. Actually, Q

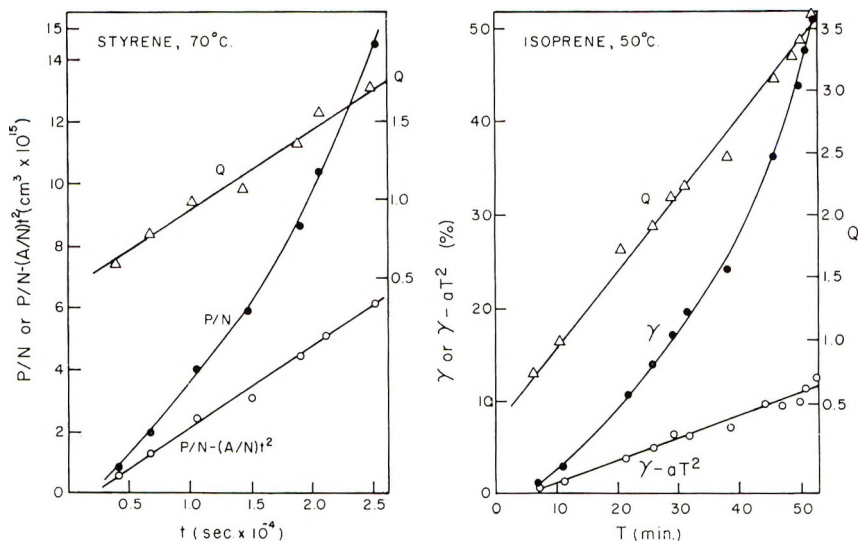


Fig. 2. Analysis of styrene data of Roe and Brass²¹ and isoprene data of Harkins.²² Roe and Brass determined the number-average particle volume (P/N) as a function of time but did not give the fractional conversion to which these values corresponded. These data fit well the equation, $P/N = (A/N)t^2 + (B/N)t$. From the least-square fit values of A/N and B/N , Q was calculated and is shown above. The experiment at 70°C. is expt. 4 of Roe and Brass. It gives an experimental $B/N = 3.44 \times 10^{-21}$ cc./sec., 3.2 times the theoretical value calculated from eqs. (4) and (7). Their expt. 2 at 40°C. gives a pattern of results very similar to that shown above, with experimental $B/N = 3.8 \times 10^{-20}$; the theoretical value is 3.5×10^{-20} . Harkins did not report the particle number or the monomer water ratio. The value of Q was calculated here from the equation: $Q = 0.5[1 + (4a/b^2)\gamma]^{0.5}$. The γ is per cent conversion; in the text, γ stands for fractional conversion.

increases for this monomer faster than ϕ_{eff} decreases and the conversion-time curve remains convex to the time axis even after interval II, up to relatively high conversions within interval III. This is shown in Figure 1. Table I shows that Q can reach values as high as 10.3 for methyl methacrylate at 80% conversion. Only at around 80% conversion is there an inversion point in the conversion-time curve of methyl methacrylate. Gerrens²⁶ and Hummel^{7,31} also found that dP/dt for methyl methacrylate increases not only in interval II but also in the first part of interval III and decreases only at the very end of the reaction.

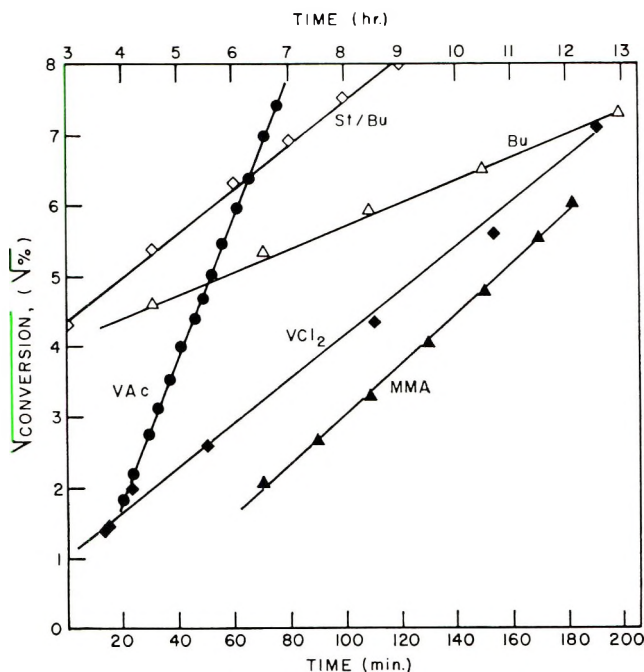


Fig. 3. Time dependence of the square root of conversion for relatively large particle size emulsions: (Δ) butadiene, data of Wall et al.;²⁶ (\diamond) butadiene-styrene copolymer, data of Wall et al.;²⁶ (\bullet) vinyl acetate, data of Napper and Parts;³³ (\blacklozenge) vinylidene chloride, data of Hay et al.;³⁹ (\blacktriangle) methyl methacrylate, data of Zimmt.²⁸ The time is expressed in hours for St/Bu and Bu and in minutes for VAc, VCl₂, and MMA. The data refer to the largest size particle emulsion of each quoted publication.

For styrene and butyl methacrylate there is an inversion point in the conversion-time curve at the onset of interval III, where the monomer droplets disappear. This is shown in Figure 1 and also in the styrene data of Hummel⁷ and Gerrens.⁴³ The existence of an inversion point here indicates that, for these monomers, the reduction of the propagation rate in interval III as ϕ_{eff} decreases is more important than the Trommsdorff effect. If Q increases with increasing conversion, it does so only to a small extent. The present results indicate that for styrene, Q decreases uniformly with increasing conversion within interval III. This is contrary to the findings of Gerrens,⁴³ who found that Q increases with conversion within interval III.

The fate of radicals in the particles at high conversions is of some interest. The data of Figure 1 and Table I suggest that in methyl methacrylate polymerization several radicals can be trapped within each particle at full conversion. To verify this, methyl methacrylate was polymerized isothermally in a three-necked flask at 40°C. by the first recipe of Table I. After having been kept for several hours at 40°C., the fully converted reaction mixture was cooled and treated with an excess of zinc formaldehyde sulfoxylate to destroy the remaining catalyst. This reducing agent probably did not enter the particles and did not affect the radicals existing in

them. Subsequently the latex was diluted with water and more monomer was added to it. After several days standing at room temperature the polymer content of the latex increased 1.5-fold, presumably as a result of polymerization initiated by radicals trapped in the particles.

Ratio between Termination and Propagation Constants in Interval II

The k_t/k_p ratio is calculable by eq. (12) from the easily accessible experimental quantities A , B , N , R , and ϕ_m . Since B , N , and ϕ_m define the value of k_p by eq. (6), the interval II portion of the conversion-time curve yields enough parameters to calculate both fundamental constants, k_p and k_t .

Tables I, II, and III show that the ratio k_t/k_p is of the order of magnitude of 10 to 100 for methyl methacrylate, styrene, and *n*-butyl methacrylate. The precision of the thus calculated values of k_t/k_p is low because each of the five experimental quantities used in the calculation has limited precision. The present theoretical analysis of emulsion polymerization data gives k_t/k_p ratios which are 10^2 – 10^4 times smaller than found for homogeneous polymerization at low conversion.^{44,45} Similar orders of magnitude of k_t/k_p for emulsion polymerization were obtained by Van der Hoff,⁴⁶ Vanderhoff et al.,⁴⁷ and Gerrens et al.⁴⁸ for the emulsion polymerization of styrene; and by Gerrens¹⁷ for the emulsion polymerization of methyl methacrylate. However, these results from the literature cannot be considered to be independent confirmation of the presently found k_t/k_p values because these authors used Stockmayer's⁴⁹ theory in their analysis; and this theory is based on a model which is in many respects similar to that of Part III.⁵

The following independent data indicate that the k_t/k_p ratios presently found for emulsion polymerization are of the correct order of magnitude:

(a) It will be shown below that k_t/k_p , determined from the increase in rate when initiator is post-added, is of the same order of magnitude as k_t/k_p calculated from eq. (12).

(b) The parameters B , N , R , and ϕ_m used in eq. (12) can be checked by independent measurements, as shown in Part II. If independent measurements can also prove the reality of parameter A too, our confidence in the reported k_t/k_p ratios should increase. It will be shown below that the molecular weights calculated with the aid of the parameter A agree with experimental values.

(c) The value of k_t/k_p can be estimated from the increase or decay of conversion rate when emulsion polymerization is initiated by intermittent irradiation. The analysis of such data does not involve a mechanistic model of emulsion polymerization. Using this approach Hummel et al.^{7,9} found k_t/k_p values in the range of 10–100 for several monomers.

(d) It is likely that the relatively low values of k_t/k_p are the result of very high viscosity within the particles, and this in turn is due to the high molecular weight of the polymer and the relatively low concentration of monomer in the particles. Since termination, unlike propagation, is

diffusion-controlled, k_t must be low. Indeed, North et al.^{45,50} determined k_t of homogeneous polymerization in viscous reaction mixtures obtained by dissolving in them inert polymers. Homogeneous methyl methacrylate polymerization at 40°C. and at 120 cp. viscosity yielded $k_t/k_p = 215$, not too different from k_t/k_p results of Table I.

(e) It will be shown in Part V⁵¹ that k_t/k_p has a lowest theoretical limit for very viscous reaction loci; this limit is of the order of 10. The presently found k_t/k_p ratios are often close to this theoretical limit.

Effect of Post-Added Initiators

If Smith and Ewart's assumption of instantaneous termination were correct, the rate in interval II could not be increased by post-added initiator since the value of Q would be half and independent of the initiation rate. Several authors increased the initiation level after the reaction was already in progress and found that the conversion rate was thus increased. Such data were published for butadiene by Morton et al.,⁵² for chloroprene by Morton et al.,³⁷ for vinylidene chloride by Hay et al.,³⁹ for vinyltoluene, vinylxylene, and styrene by Gerrens and Kohnlein.⁴⁸

TABLE IV
Analysis of the Effects of Post-Added Initiators on Styrene
Polymerization Based on the Data of Gerrens and Kohnlein^a

Temperature, °C.	Rate ratio k_t/k_p (calculated) ^b		Rate ratio (experimental) ^c		
	$\epsilon = 5$	$\epsilon = 17.66$	$\epsilon = 5$	$\epsilon = 17.56$	ϕ_m (avg.)
35.3	60	75	1.3	2.0	0.49
40.3	43	—	1.44	—	0.49
45.4	49	68	1.47	2.14	0.52
50.6	41	—	1.48	—	0.47
55.7	42	79	1.5	1.87	0.47

^a In all experiments $m/w = 1/15$ and sulfonated dodecane soap at $C_S = 0.57\%$ were used. The $K_2S_2O_8$ initiator level was increased ϵ -fold at about 20% conversion. The original C_I was 0.0488%. The reported rate ratio is the apparent linear rate after post-addition divided by that prior to post-addition.

^b Calculated from Fig. 6, Part III.

^c Experimental data of Gerrens and Kohnlein.⁴⁸

Some of the styrene data obtained by Gerrens and Kohnlein⁴⁸ are shown in Table IV. The k_t/k_p ratios calculated from these data (with the aid of Figure 6 of Part III) have the same order of magnitude as the independent k_t/k_p data of Table II. Gerrens and Kohnlein⁴⁸ used the steady-state theory of Stockmayer⁴⁹ to calculate k_t and obtained k_t/k_p values somewhat lower than those shown in Table IV. The main reason for this discrepancy is that in their theoretical analysis Gerrens and Kohnlein disregarded the variation of particle volume with time.

MOLECULAR WEIGHT RESULTS

Variation of Molecular Weight with Conversion

The theory of Part III predicts that the molecular weight should increase with conversion during interval II and decrease at the end stage of interval III. Such data were published in the literature for styrene^{12,29,53} and methyl methacrylate,^{28,29} and these data were obtained under experimental conditions consistent with the theoretical model of Part III. Maxima in molecular weight-conversion curves were also obtained^{26,54-57} in recipes containing either redox catalysts or chain transfer agents, i.e., under experimental conditions outside the scope of the theory.

The polystyrene data of Table V show excellent agreement between the calculated and experimentally found molecular weights at increasing conversion. For poly(methyl methacrylate) the calculated molecular weights are 1.5 ± 0.06 times higher than the experimental values. At this point it should be remembered that in the model, and hence in the derivation of

TABLE V
Variation of Molecular Weight with Conversion
in Styrene and Methyl Methacrylate Polymerization^a

	Conversion, %	$\bar{M}_v \times 10^{-6}$		$\bar{M}_n \times 10^{-6}$, calculated	
		Exptl.	Calculated [eq. (14)]	Eq. (13)	Eq. (20)
Styrene, 50°C.	5.1	2.66	3.85	3.49	—
	14.0	3.84	4.35	4.24	—
	31.9	4.68	4.90	4.72	—
	44.0	5.05	5.40	5.17	5.17
	61.0	5.38	—	—	5.62
	73.0	5.28	—	—	5.61
	80.5	5.12	—	—	4.62
Styrene, 60°C.	3.7	1.53	2.34	2.29	—
	12.4	2.3	2.48	2.32	—
	21.2	2.9	2.59	2.54	—
	30.7	3.1	2.72	2.62	—
	38.7	3.3	2.82	2.70	—
MMA, 55°C.	9.8	3.22	4.77	4.10	—
	12.75	3.38	5.22	4.80	—
	16.75	3.70	5.35	5.20	—
	21.40	3.70	5.96	5.35	5.35
	36.05	4.36	—	—	6.3
	59.85	4.65	—	—	7.0
	87.90	4.82	—	—	8.2
	93.3	4.65	—	—	7.25
	93.6	4.11	—	—	6.20

^a The styrene experiments are the ones described in the last two columns of Table II. The methyl methacrylate experiment is the one of the last column of Table I. In calculating the theoretical interval II molecular weights the experimental values of the parameters *A* and *B* were used.

eqs. (13), (14), and (20), termination by combination was assumed. The available data⁵⁸ indicate that combination is indeed the overwhelmingly predominant mode of termination for polystyrene, but not for poly(methyl methacrylate). The difference between viscosity-average and number-average molecular weights may be disregarded and termination by disproportionation can be assumed gives molecules of a weight half of that obtained by combination. If the molecular weight obtained by combination alone (calculated by the theory) is 1.5 times higher than the experimental molecular weight (which is the result of both combination and disproportionation), the fraction of molecules that are formed by combination is 33%. This value, calculated from the present data, compares favorably with the tracer results of Bevington et al.⁵⁹ who found that at 55°C. the fraction of termination events due to combination is 18%.

In Part II data were quoted in which the experimental final molecular weights were about equal to M_{SE} , the interval II molecular weight that would be obtained if termination was instantaneous. It was argued that agreement between M_{SE} and the final molecular weight can be the result of fortuitous compensation between slow termination effects during interval II leading to molecular weights higher than M_{SE} , and slow propagation effects due to low monomer concentration in particles during interval III leading to molecular weights lower than M_{SE} . This argument is confirmed by the data of Table V.

In Part II it was also shown that the theoretical M_{SE} was often higher than the final experimental molecular weight, and this was explained by chain transfer to monomer. The *n*-butyl methacrylate final molecular weights at 65 and 60°C. are considerably higher than the theoretical M_{SE} values, as shown in Table III. Evidently this is the opposite of the expected result if the discrepancy was caused by chain transfer. With this monomer the slow termination effects are overwhelming, even at high conversions. Table III shows that the theoretical molecular weights calculated from eq. (20) for high conversions are in good agreement with the final experimental values.

It is noteworthy that the effects of slow termination become more pronounced at larger particle sizes. It follows that if slow termination is important, the final molecular weight should increase with the monomer/water ratio in the charge. This was indeed found for polystyrene.^{3,19,47}

Molecular Weight Distribution at Persulfate Initiation

¹ There can be several reasons for molecular polydispersity in polymers formed by emulsion polymerization at constant initiation rates.

(1) Due to variation of propagation rate and of termination rate with conversion, the average molecular weight of the material formed at any given instant also varies with conversion. The results shown in Table V reflect this effect.

(2) The material formed at any given instant may be polydisperse because the growing polymer chains can terminate at the same time by

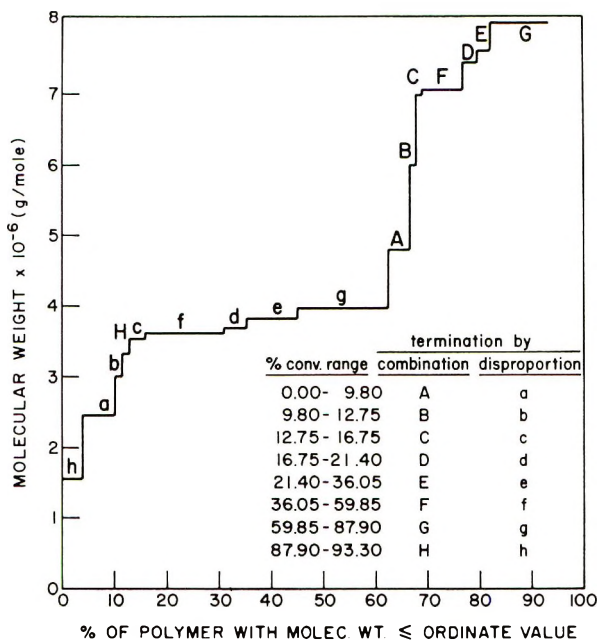


Fig. 4. Molecular weight distribution of the poly(methyl methacrylate) sample of Table V at 93.3% conversion, calculated from the experimental variation of molecular weight with conversion. Method of calculation: let \bar{M}_1 , \bar{M}_2 , and \bar{M}_{12} be the molecular weight of polymer formed up till γ_1 and γ_2 conversion and in the interval between γ_1 and γ_2 , respectively. Then $\bar{M}_{12} = (\gamma_2 \bar{M}_2 - \gamma_1 \bar{M}_1) / (\gamma_2 - \gamma_1)$. One-third of the material formed in the $\gamma_2 - \gamma_1$ interval terminated by combination and has a molecular weight of $1.5 \bar{M}_{12}$; the remainder terminates by disproportionation and has a molecular weight of $0.75 \bar{M}_{12}$. More data on this polymer sample are given in Figs. 1, 5, and 6 and in Tables I, V, and VI.

different modes to give different molecular weights. For example, MMA can terminate by disproportionation and by combination, as discussed earlier.

(3) Molecules formed at the same instant by a given mode of termination may vary in chain length because they may be located in particles of different sizes. Particles larger than average absorb radicals on the average faster than the grand average rate, R/N . This by itself could cause lowering of the molecular weight. However, if larger than average particles contained about average number of radicals, the termination rate in them would be slower than average, since the probability that two radicals meet and cross-terminate in a given time is inversely proportional to the particle volume. Thus in larger particles the termination rate is slower than average and this by itself would increase the molecular weight. This could partially offset the effects of faster than average radical absorption. In fact, Morton et al.⁶⁰ found that the molecular weight was the same for each fraction of a polystyrene emulsion polymer fractionated according to particle size.

(4) Though different particles of equal size should absorb radicals at the same mean rate, the actual intervals between the entry of two radicals can vary due to the random nature of collisions between radicals and particles. Molecules terminated in different equally sized particles by the same termination mode and at the same instant may therefore vary in size.

If the mechanisms (3) and (4) were important, the \bar{M}_n values calculated from the theory could not agree with the experimental values as well as shown in the results of Table V (after suitable correction for disproportionation and combination in the MMA data). Though the results quoted here provide circumstantial evidence for the hypothesis that mechanisms (3) and (4) are not important, this matter is by no means settled. Schulz et al.⁶¹ reported molecular weight distributions of polystyrene emulsion polymers. Their experimental distributions are significantly broader than the distribution calculated from the present poly(methyl methacrylate) data when in these calculations the contribution of mechanisms (3) and (4) are neglected. The distribution calculated from the poly(methyl methacrylate) data of Table V is discussed below.

It was shown in Part III that the \bar{M}_n values can be at most 1.333 times larger than the \bar{M}_v values, if the variation of the average molecular weight with conversion is caused only by changes in termination rate and if this is the sole cause for molecular polydispersity. In calculating the molecular weight distribution at 93.3% conversion from the variation of M_x with conversion it is assumed that the experimental M_x values of Table V approximately equal M_n and that 33% of the molecules terminate by combination, the rest by disproportionation. The thus calculated distribution and the methods of calculating it are shown in Figure 4. Approximately half of the polymer is found to have molecular weights between 3.6 and 4×10^6 . Material terminated by disproportionation at very high conversion (fraction "h") has a much lower molecular weight, 1.5×10^6 . About 8×10^6 is the molecular weight of the fraction G, terminated by combination in the 60–88% conversion range. Figure 1 shows that in the 60–88% conversion range Q passes through a maximum, so that high molecular weights are expected here. One can conclude from the data of Figure 4 that a quite broad molecular weight distribution can be obtained, even if this is caused only by changes in termination and propagation rates and by two different simultaneously occurring termination reactions.

Molecular Weight Distribution at Initiation with Intermittent Irradiation

If the Smith-Ewart assumption of instantaneous termination was generally true, emulsion polymers initiated by suitable intermittent irradiation should be homogeneous in molecular weight since chains would grow only during the dark periods and would be either initiated or terminated during irradiation. This was postulated by Zimm et al.¹⁹ Schulz et al.⁶² investigated polystyrene samples prepared by this method and found several peaks in the differential molecular weight distribution curves. These peaks clearly indicated that radicals could survive several cycles of irradiation.

tion and dark periods. These data provide additional evidence for the fact that the Smith-Ewart instantaneous termination assumption is not tenable.

PARTICLE SIZE DISTRIBUTION

Parameter Defining the Skewness of the Distribution Curve

All particle size distributions of the present work were monododal. They could be fitted to a Gaussian distribution if a certain power of the radius was used. The appropriate power exponent s defines the skewness of the distribution. Its value can be conveniently determined from the median radius, r_m and from the size distribution defined by n_i , the number of particles having r_i radius:

$$r_m^s = \sum n_i r_i^s / \sum n_i \quad (28)$$

It is evident that if $s = 1$, the radii have symmetrical differential distribution. If $s > 1$, the distribution is skew, in that relatively small number of particles have small radii and the rest of the particles are in the large particle radius range. If $s < 1$, the opposite is true.

Below different averages of particle radius will be used. These were defined in Part I.⁴

Variation of Size Distribution with Conversion

In Part III⁵ the distribution of radicals among particles was calculated to be a unique function of the average number of radicals per particle, Q . This distribution was found to be quite broad. For example if $Q = 4$, only about 20% of all particles should actually contain 4 radicals. About 1% of the particles should be "dead" containing no live radicals, about 5% should contain one radical; while at the other extreme, 5% should contain 7 radicals, and 0.2% should contain as many as 10 radicals.

It was also shown in Part III that the distribution of radicals among particles broadens with increasing Q ; the variance of this distribution is about $0.75Q$ at $Q > 1$.

Each particle grows proportionally to the number of radicals in it. Slow termination rates cause Q to rise to values significantly larger than 0.5, and this broadens the distribution of radicals among particles so that the distribution of particle growth rates also broadens. It follows that as Q increases with conversion, the particle size distribution has to broaden.

The theory of Part III also predicts that, as the distribution of radicals among particles broadens, a decreasing number of particles should contain no radical so that they do not grow at all and also a decreasing number of particles should contain few radicals so that they grow slowly. At the same time, more and more particles should contain a relatively large number of radicals so that they grow very fast. With increasing conversion the size distribution should therefore become skew, in that most of the particles should become large while few are small. In other words, the breadth

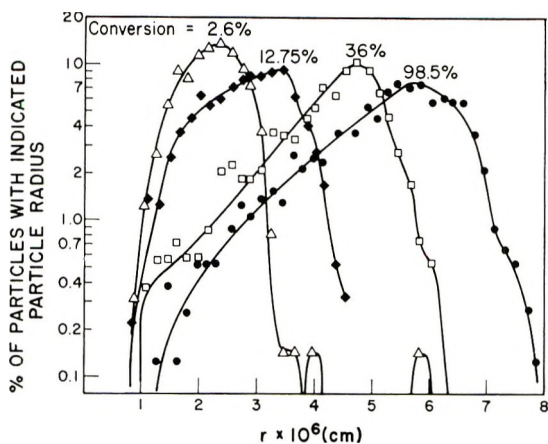


Fig. 5. Variation of differential particle radius distribution with the conversion of methyl methacrylate in the experiment of Table VI. The polymerization details are shown in the last column of Table I. Particles with radii differing by no more than 1.7 to 1.9×10^{-7} cm. were pooled. The points represent the average size of these pooled particles.

of the particle distribution (the standard deviation of the radii), and the skewness factor s of eq. (28) are predicted to increase with conversion, if Q increases with conversion.

Table VI and Figure 5 show that the standard deviation and the breadth of particle size distribution indeed increase with conversion. However, the particle size distribution broadens only in absolute terms, not in relative terms. The ratio of σ/r_n does not vary systematically with conversion; this coefficient of variation is 20-31%. Similarly, the ratio between

TABLE VI
Variation of Particle Size Distribution Parameters with Conversion*

Conversion, %	$r_n \times 10^6$, cm.	$r_w \times 10^6$, cm.	$\sigma \times 10^6$, cm.	s
2.57	2.17	2.57	0.55	0.63
5.25	2.27	2.89	0.71	1.25
12.75	2.76	3.27	0.76	1.4
19.1	2.92	3.75	1.08	1.57
36.05	4.21	4.69	0.94	2.69
45.65	4.66	5.11	0.98	3.04
93.6	5.18	5.67	1.03	2.57
98.6	5.24	5.89	1.26	2.12

* The data describe the methyl methacrylate polymerization experiment also shown in Figures 1, 4, 5, 6, in Table V and in the last column of Table I. Table VI of Part II also gives relevant data.

The data shown below were determined by counting at least 700 particles in the electron micrographs. The averages of radius values are either number (r_n) or weight averages (r_w). The standard deviation is σ . The parameter s is the skewness defined in eq. (28).

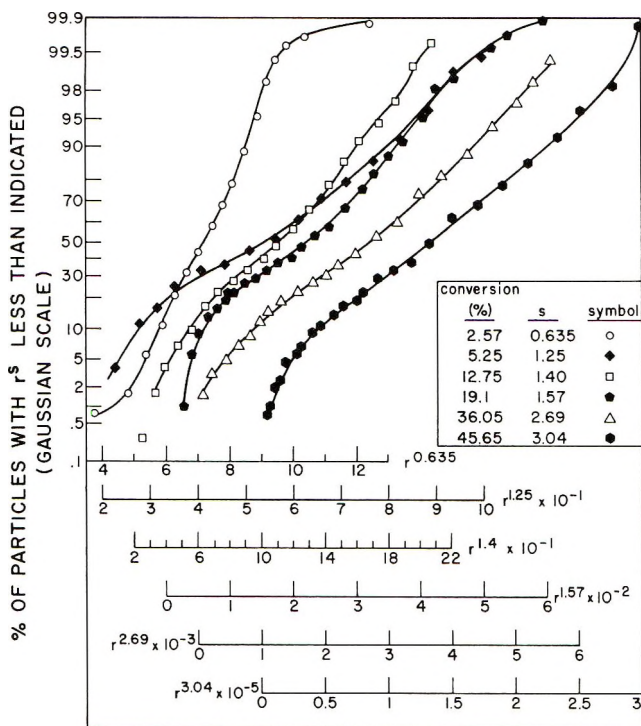


Fig. 6. Variation of cumulative particle size distribution with conversion. The ordinate is probability scale; perfect Gaussian distribution would give straight lines. In the abscissas, r is the particle radius in millimicrons (10^{-7} cm.), and s is the exponent to eliminate skewness, defined in eq. (28). The same data are plotted in Fig. 5.

weight and number-average radii range from 1.09 to 1.28 without any systematic trend.

The variation of skewness with conversion runs parallel with the average number of radicals per particle, Q . The skewness factor s increases from 0.67 to 3.04 below 46% conversion by the data of Table VI. It is shown in Figure 1 that in this conversion range Q increases. At very high conversions s decreases to 2.12, but here Q also decreases. When the cumulative distribution of r^s is plotted on a probability chart, the curves are almost straight lines as shown in Figure 6. This indicates that r^s has Gaussian distribution.

CONCLUSIONS

Slow termination in emulsion polymerization can cause very significant deviations from the theoretical predictions of the Smith-Ewart model. The new nonsteady-state theory proposed in Part III, which takes slow termination rate into account, fits the experimental dependence of conversion on time and also fits well the experimental conversion dependence of molecular weight and of particle size distribution.

Mr. C. L. Killmeier and Mr. E. H. Young determined the experimental conversion-time curves. The particle sizes and their distribution were obtained by Dr. R. Wilkins. The molecular weights were determined by Mr. H. Mason and Mrs. E. Ginsberg. The electrical circuit for the dilatometer was designed and built by Mr. E. M. Sioma. Mr. L. DeFonso was helpful with computer calculations. While the author is responsible for the overall planning and the theory, this work could not have been carried out without the help of these colleagues.

References

1. W. V. Smith and R. H. Ewart, *J. Chem. Phys.*, **16**, 592 (1948).
2. S. S. Medvedev, *Proceedings of the International Symposium Makromolekulare Chemie, Prague, 1957*, Pergamon Press, New York, 1958, pp. 174-190.
3. G. D. Berezhnoi, P. M. Khomikovskii, and S. S. Medvedev, *Vysokomolekul. Soedin.*, **2**, 141 (1960).
4. J. L. Gardon, *J. Polymer Sci. A-1*, **6**, 623 (1968) (Part I).
5. J. L. Gardon, *J. Polymer Sci. A-1*, **6**, 665 (1968) (Part III).
6. J. L. Gardon, *J. Polymer Sci. A-1*, **6**, 643 (1968) (Part II).
7. D. O. Hummel, G. J. Ley, and Ch. Schneider, *Advan. Chem. Ser.*, **34**, 60 (1962).
8. J. Romatowski and G. V. Schulz, *Makromol. Chem.*, **85**, 227 (1965).
9. G. J. Ley, Ch. Schneider, and D. O. Hummel, *Am. Chem. Soc. Polymer Preprints*, **7**, No. 2, 725 (1966).
10. J. Ugelstad, P. C. Mock, P. Dahl, and P. Ragnes, *Am. Chem. Soc. Polymer Preprints*, **7**, No. 2, 628 (1966).
11. J. H. S. Green, *J. Polymer Sci.*, **35**, 514 (1959).
12. W. V. Smith, *J. Am. Chem. Soc.*, **71**, 4077 (1949).
13. B. M. E. Van der Hoff, *J. Phys. Chem.*, **60**, 1250 (1956).
14. W. V. Smith, *J. Am. Chem. Soc.*, **79**, 3695 (1948).
15. F. A. Bovey, I. M. Kolthoff, A. J. Medalia, and E. J. Meehan, *Emulsion Polymerization*, Interscience, New York, 1955, p. 194.
16. A. Rysanek and M. Hlousek, *J. Polymer Sci.*, **52**, 91 (1961).
17. H. Gerrens, *Ber. Bunsenges. Physik. Chem.*, **67**, 741 (1963).
18. J. G. Brodnyan, J. A. Cala, T. Konen, and E. L. Kelley, *J. Colloid Sci.*, **18**, 73 (1963).
19. J. P. Bianchi, F. P. Prize, and B. H. Zimm, *J. Polymer Sci.*, **25**, 27 (1957).
20. K. Giskehaug, *Soc. Chem. Ind. London, Monograph No. 20*, Society of Chemical Industry, London, 1966, pp. 235-48.
21. C. P. Roe and P. D. Brass, *J. Polymer Sci.*, **24**, 401 (1957).
22. W. D. Harkins, *J. Am. Chem. Soc.*, **69**, 1428 (1947).
23. W. V. Smith, *J. Am. Chem. Soc.*, **68**, 2063 (1946).
24. D. J. Williams and E. G. Bobalek, *J. Polymer Sci. A-1*, **4**, 3065 (1966).
25. W. D. Harkins, *J. Polymer Sci.*, **5**, 217 (1950).
26. H. Gerrens, *Dechema-Monograph.*, **49**, 53 (1964).
27. T. Guha and R. S. Palit, *J. Polymer Sci. A*, **1**, 877 (1963).
28. W. S. Zimmt, *J. Appl. Polymer Sci.*, **1**, 323 (1959).
29. J. J. P. Staudinger, *Chem. Ind. (London)*, **1948**, 563.
30. G. J. K. Acres and F. L. Dalton, *J. Polymer Sci. A*, **1**, 3009 (1963).
31. D. Hummel, *Angew. Chem.*, **75**, 330 (1963).
32. R. S. Konar and S. R. Palit, *J. Polymer Sci. A*, **2**, 1731 (1964).
33. C. E. M. Morris, A. E. Alexander, and A. G. Parts, *J. Polymer Sci. A-1*, 985 (1966).
34. D. H. Napper and A. G. Parts, *J. Polymer Sci.*, **61**, 113 (1962).
35. D. H. Napper and A. E. Alexander, *J. Polymer Sci.*, **61**, 127 (1962).
36. A. S. Dumm and P. A. Taylor, *Makromol. Chem.*, **83**, 207 (1965).
37. M. Morton, J. A. Cala, and M. W. Altier, *J. Polymer Sci.*, **19**, 547 (1956).

38. J. C. Light, L. Marker, A. T. Santonicola, and O. S. Sweeting, *J. Appl. Polymer Sci.*, **5**, 31 (1961).
39. P. M. Hay, J. Light, L. Marker, R. W. Murray, A. T. Santonicola, O. J. Sweeting, and J. C. Wepsic, *J. Appl. Polymer Sci.*, **5**, 23 (1961).
40. E. Peggion, F. Testa, and G. Talamini, *Makromol. Chem.*, **71**, 137 (1964).
41. G. M. Burnett, P. Evans, and H. M. Melville, *Trans. Faraday Soc.*, **49**, 1105 (1952).
42. E. Trommsdorff, H. Kohle, and P. Legally, *Makromol. Chem.*, **1**, 169 (1947).
43. H. Gerrens, *Z. Elektrochem.*, **60**, 400 (1956).
44. M. S. Matheson, E. E. Auer, B. B. Bevilacqua, and E. J. Hart, *J. Am. Chem. Soc.*, **73**, 1700, 5395 (1951); *ibid.*, 479, **71**, 2610 (1949).
45. S. W. Benson and A. M. North, *J. Am. Chem. Soc.*, **81**, 1339 (1959).
46. B. M. E. Van der Hoff, *J. Polymer Sci.*, **33**, 487 (1958).
47. J. W. Vanderhoff, E. B. Bradford, H. L. Tarkowsky, and W. B. Wilkinson, *J. Polymer Sci.*, **50**, 265 (1961).
48. H. Gerrens and E. Kohlein, *Z. Elektrochem.*, **64**, 1199 (1960).
49. W. H. Stockmayer, *J. Polymer Sci.*, **24**, 314 (1957).
50. A. M. North and G. A. Reed, *J. Polymer Sci. A*, **1**, 1311 (1963).
51. J. L. Gardon, in preparation (Part V).
52. M. Morton, P. P. Salatiello, and H. Landfield, *J. Polymer Sci.*, **8**, 215 (1952).
53. C. C. Price and C. E. Adams, *J. Am. Chem. Soc.*, **67**, 1674 (1945).
54. W. V. Smith, *J. Am. Chem. Soc.*, **68**, 2059 (1946).
55. M. Morton and T. Piirma, *J. Polymer Sci.*, **19**, 563 (1956).
56. J. W. McFarland and R. Pariser, *J. Appl. Polymer Sci.*, **7**, 675 (1963).
57. W. E. Mochel, *J. Polymer Sci.*, **5**, 583 (1952).
58. C. H. Bamford, W. G. Barb, A. D. Jenkins, and P. F. Onyon, *The Kinetics of Vinyl Polymerization by Radical Mechanism*, Academic Press, New York, 1958, pp. 67-68, 80-81.
59. J. C. Bevington, H. W. Melville, and R. P. Taylor, *J. Polymer Sci.*, **12**, 449 (1954); *ibid.*, **14**, 463 (1954).
60. M. S. Morton, S. Kaizerman, and M. W. Altier, *J. Colloid Sci.*, **9**, 300 (1954).
61. S. Jovanovic, J. Romatowski, and G. V. Schulz, *Makromol. Chem.*, **85**, 187 (1965).
62. G. V. Schulz and J. Romatowski, *Makromol. Chem.*, **85**, 195-226 (1965).

Received May 24, 1967

Revised July 3, 1967

NOTE

*Preparation and Polymerizability of Substituted
 α,β,β -Trifluorostyrenes*

The oxidative instability of polystyrene and its copolymers has been the subject of many reviews and publications for the past three decades. Alternate molecules similar in structure but having greater oxidative resistance (e.g., elimination of benzylic hydrogen) have been sought as replacements for polystyrene, and it is the purpose of this note to review research work directed toward this goal.

Although still expensive, poly- α,β,β -trifluorostyrene is one such alternate material offering good oxidative stability. The monomer α,β,β -trifluorostyrene was first synthesized by Cohen¹ in 1949 and was successfully converted to high molecular weight polymer by Prober,² who described several conversion difficulties encountered. Livingston³ evaluated copolymerizations of α,β,β -trifluorostyrene with styrene and chlorotrifluoroethylene.

This note presents data on the preparations, polymerizability, and copolymerizability of substituted α,β,β -trifluorostyrenes.

Dixon⁴ synthesized α,β,β -trifluorostyrene by reacting phenyl lithium and tetrafluoroethylene, thus discovering a general reaction between organolithiums and fluorinated olefins. We used the Dixon method to prepare the fluorostyrenes listed in Table I. These monomers were then subjected to variable catalysis and medium experiments to determine their polymerizabilities (for both homo- and copolymers). Table II is a summary of the homopolymerizations attempted. Polymers having an intrinsic viscosity of 0.5 dl./g. or higher (measured in benzene at 30°C.) were sought, and those not meeting this requirement are listed as low molecular weight materials.

By heat-induced persulfate decomposition in an emulsions system using 100 g. monomer, 11.69 dodecylamine hydrochloride, 0.44 g. potassium persulfate, all in 600 ml. of distilled water, attempts were made to copolymerize α,β,β -trifluorostyrene with the following monomers: β -chloro- α,β -difluorostyrene, 1-phenylperfluoropropylene, 2-methyl- α,β,β -trifluorostyrene. In each case, only the homopolymer of α,β,β -trifluorostyrene was found, regardless of the ratios of comonomers.

On the other hand, copolymerization of an equimolar mixture of 4-methyl- α,β,β -trifluorostyrene and α,β,β -trifluorostyrene yielded a random copolymer in 80% conversion. No attempt was made to determine reactivity ratios for this copolymerization.

It appears from the results shown that steric hindrance, exerted by groups on or near the substituted vinyl side chain, is the primary factor influencing the ring- and side-chain-substituted fluorostyrenes. The conversion of substituted perfluoro alkyl styrenes to macromolecules by emulsion polymerization is directly related to the size of substituent groups on both the vinyl chain and the ring. For instance, although styrene and α,β,β -trifluorostyrene homopolymerize readily by emulsion techniques, the substitution of even one chloro group for a fluoro group in the β position renders the monomer inactive to free-radical polymerization. Only unreacted monomer was recovered after attempted emulsion polymerizations using this monomer with the larger chloro substituent on the vinyl group.

Also, attempts to bulk polymerize the above monomers by free-radical initiation again showed that the monomers exhibited marked differences in reactivity, α,β,β -trifluorostyrene was converted principally (60–70%) to its dimer (1,3-diphenylperfluorocyclobutane). Dimerization also occurred during attempts to bulk polymerize 4-methyl- α,β,β -trifluorostyrene or 4-fluoro- α,β,β -trifluorostyrene. In contrast, attempted bulk polymerizations of 2-methyl- α,β,β -trifluorostyrene, 1-phenylperfluoropropylene, or

TABLE I
The Boiling Points and Yields of Substituted α,β -Trifluorostyrenes Prepared by the Direct Reaction of Substituted Phenyl Lithium Compounds and Fluoroethylene Monomers⁴





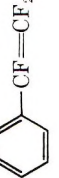
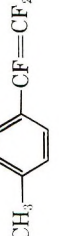
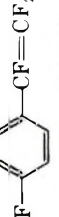
Monomer	Structure	B.p., °C.	% Yield
1. α,β,β -Trifluorostyrene		69/69 mm.	20
2. β -Chloro- α,β -difluorostyrene		77-80/28 mm.	78
3. α,β -Difluorostyrene		87-89/60 mm.	Prepared from 2 by dehydrogenation and dehydrohalogenation
4. 1-Phenyl perfluoropropylene		62-64/31 mm.	35
5. 2-Methyl- α,β,β -trifluorostyrene		60/26.5 mm.	33
6. 4-Methyl- α,β,β -trifluorostyrene		84-86/65 mm.	17
7. 4-Fluoro- α,β,β -trifluorostyrene		47-48/28 mm.	9

TABLE II
The Polymerizability Under Various Conditions of Catalysis for Substituted α,β,β -Trifluorostyrenes

Monomer	Catalyst and reaction conditions	Yield of polymer obtained, %	Intrinsic viscosity of polymer in benzene at 30°C., $[\eta]$, dl./g.	Remarks
α,β,β -Trifluorostyrene	100 g. monomer, 11.6 g. dodecylamine 0.44 g. potassium persulfate, 600 ml. distilled water. temp. = $55 \pm 1^\circ\text{C}$.	82	0.80	
β -Chloro- α,β -difluorostyrene	"	None	—	Monomer recovered
1-Phenyl perfluoropropylene	"	None	—	"
2-Methyl- α,β,β -trifluorostyrene	"	None	—	"
4-Methyl- α,β,β -trifluorostyrene	"	75	0.94	"
4-Fluoro- α,β,β -trifluorostyrene	"	77	1.03	"
α,β,β -Trichlorostyrene	"	None	—	"
α,β,β -Trifluorostyrene	100 g. monomer, 11.6 g. dodecylamine hydrochloride, 0.44 g. potassium persulfate, 0.15 g. potassium hydro- sulfite, 600 ml. distilled water temp. = $27 \pm 1.0^\circ\text{C}$.	69	1.35	
β -Chloro- α,β -difluorostyrene	"	None	—	
1-Phenyl perfluoropropylene	"	None	—	

(continued)

TABLE II (continued)

Monomer	Catalyst and reaction conditions	Yield of polymer obtained, %	Intrinsic viscosity of polymer in benzene at 30°C., $[\eta]$, dl./g.	Remarks
4-Methyl- α,β,β -trifluorostyrene	100 g. monomer, 11.6 g. dodecylamine hydrochloride, 0.44 g. potassium persulfate, 0.15 g. potassium hydro-sulfite, 600 ml. distilled water temp. = $27 \pm 1.0^\circ\text{C}$.	78	Not characterized	
4-Fluoro- α,β,β -trifluorostyrene	"	59	Not characterized	
α,β,β -Trichlorostyrene	"	None	—	
α,β,β -Trifluorostyrene	Bulk polymerization 100 g. monomer 0.075 g. benzoyl peroxide or 0.075 g. azobisisobutyronitrile temp. = $60 \pm 1.0^\circ\text{C}$.	None	—	Nearly quantitative conversion to 1,3-diphenyl perfluorocyclobutane (dimer)
4-Methyl- α,β,β -trifluorostyrene	"	"	—	Nearly quantitative conversion to 1,3-di-4-methyl phenyl perfluorocyclobutan (dimer)
4-Fluoro- α,β,β -trifluorostyrene	"	"	—	Nearly quantitative conversion to 1,3-di-4-fluoro phenyl perfluorocyclobutane
β -Chloro- α,β -difluorostyrene	Bulk polymerization: 100 g. monomer, 0.075 g. benzoyl peroxide or 0.075 g. azobisisobutyronitrile temp. = $60 \pm 1.0^\circ\text{C}$.	None	—	Monomer recovered
α,β -Difluorostyrene	"	"	—	"

1-Phenyl perfluoropropylene	"	—	"	
2-Methyl- α,β,β -trifluorostyrene	"	—	"	
α,β,β -Trichlorostyrene	"	—	"	
α,β -Difluorostyrene	17	0.09	Low MW	gummy polymer
Bulk polymerization: 100 g. monomer, 0.10 g. boron trifluoride ether complex temp. = $27 \pm 1^\circ\text{C}$.				
α,β,β -Trifluorostyrene	None	—		
4-Methyl- α,β,β -trifluorostyrene	"	—		
4-Fluoro- α,β,β -trifluorostyrene	"	—		
β -Chloro- α,β,β -difluorostyrene	"	—		
1-Phenyl perfluoropropylene	"	—		
2-Methyl- α,β,β -trifluorostyrene	None	—		
Bulk polymerization 100 g. monomer 0.075 g. benzoyl peroxide or 0.075 g. azobisisobutyronitrile temp. = $60 \pm 1.0^\circ\text{C}$.				
α,β,β -Trichlorostyrene	"	—		
α,β,β -Trifluorostyrene	"	—		
Anionic catalysts sodium naphthenate or sodium 0.1 g. in 100 g. monomer temp. $27-60 \pm 1.0^\circ\text{C}$.				

(continued)

TABLE II (continued)

Monomer	Catalyst and Reaction conditions	Yield of polymer obtained, %	Intrinsic viscosity of polymer in benzene at 30°C., $[\eta]$, dl./g.	Remarks
4-Fluoro- α,β -trifluorostyrene	"	"	—	
β -Chloro- α,β -difluorostyrene	"	"	—	
α,β -Difluorostyrene	"	"	—	
1-Phenyl perfluoropropylene	"	"	—	
2-Methyl- α,β,β -trifluorostyrene	"	"	—	
α,β,β -Trichlorostyrene	"	"	—	
α,β,β -Trifluorostyrene	Light at 3600 Å.; temp. = $30 \pm 0.1^\circ\text{C}$. time = 88 hr.	None	—	
4-Methyl- α,β,β -trifluorostyrene	"	"	—	
4-Fluoro- α,β,β -trifluorostyrene	"	"	—	
β -Chloro- α,β -difluorostyrene	"	"	—	
α,β -Difluorostyrene	"	"	—	
1-Phenyl perfluoropropylene	"	"	—	
2-Methyl- α,β,β -trifluorostyrene	"	"	—	
α,β,β -Trichlorostyrene	"	"	—	
α,β -Difluorostyrene	Heat ranging between 50 – 100°C . time = 48 hr.	8	Not characterized but <0.05	Sticky solid obtained
α,β,β -Trifluorostyrene	"	None	—	
4-Methyl- α,β,β -trifluorostyrene	"	"	—	
4-Fluoro- α,β,β -trifluorostyrene	"	"	—	
β -Chloro- α,β -difluorostyrene	Heating ranging between 50 – 100°C . time = 48 hr.	None	—	
1-Phenyl perfluoropropylene	"	"	—	
2-Methyl- α,β,β -trifluorostyrene	"	"	—	
α,β,β -Trichlorostyrene	"	"	—	

α,β,β -trichlorostyrene yielded only unreacted monomer. Table II is a summary of these reactions.

Clearly, α,β,β -trifluorostyrene is a monomer which is close to being nonpolymerizable because of steric hindrance, having just enough spacial volume to add monomer and form a high molecular weight linear polymer in a free-radical emulsion system. The substitution of Cl, CF_3 , and presumably any other bulky group larger than H or F on the vinyl group totally inhibits free-radical polymerization in emulsion systems. Such large substituents also prevent dimerization in attempted bulk polymerization by free-radical initiators. The presence of a bulky group on the aromatic ring ortho to the perfluorovinyl group also inhibits emulsion free-radical polymerization as well as bulk free-radical dimerization. However, the same bulky group, when substituted on the aromatic ring in the position para to the perfluorovinyl group, does not interfere with either free-radical emulsion polymerization or free-radical bulk dimerization.

The conversion of substituted perfluorovinylbenzenes to high molecular weight polymers (emulsion system) or dimers (bulk system) is extremely sensitive to steric effects.

References

1. S. G. Cohen, H. T. Wolosinski, and P. J. Schener, *J. Am. Chem. Soc.*, **71**, 3439 (1949).
2. M. Prober, *J. Am. Chem. Soc.*, **75**, 968 (1952).
3. D. I. Livingston, P. M. Kamath, and R. S. Corley, *J. Polymer Sci.*, **20**, 485 (1956).
4. S. Dixon, *J. Org. Chem.*, **21**, 400 (1956).

RUSSELL B. HODGDON, JR.
DAVID I. MACDONALD

Direct Energy Conversion Operation
General Electric Company
West Lynn, Massachusetts

Received October 12, 1966
Revised December 22, 1966

BOOK REVIEW

Die Synthese von einheitlichen Polymeren. J. H. WINTER. Springer-Verlag, Berlin, Heidelberg, New York. Mit 71 Abbildungen. XIV, 415 Seiten Gr. - 8°, 1967.

This book is devoted to recent progress in a field which has experienced some unexpected and spectacular developments, namely the synthesis of polymers which are homogeneous in respect to structural details and to molecular weight.

The first two (brief) chapters serve as general introduction to the core of the presentation which starts with radical initiated addition polymerization of vinyl type monomers (pages 63-84) and emphasizes essentially structural uniformity such as linearity, tacticity, and stereoregularity. The following discussion (pages 85-222) of ionic and Ziegler catalysts adds to it the facts of narrow molecular weight distribution. Polycondensation processes are treated with equal thoroughness together with an account of the uniformity of natural polymers (pages 223-288). Next comes a discussion of chemical reactions and changes with individual polymers (pages 289-310) and the preparation of uniform systems by elution, fractionization, diffusion, and permeation (pages 313-332). Chapters 4 and 5 contain detailed information on the synthesis and analysis of uniform polymers.

The text is concise, clear and encompassing; there are no omissions or bypasses; the emphasis is on completeness and thoroughness. The book makes even interesting casual reading but its real merit and almost indispensable value becomes obvious if one uses it during the work in the laboratory. It is a most welcome time saver and a thoroughly reliable guide through the maze of preparative polymer chemistry.

H. Mark

Polytechnic Institute of Brooklyn
Brooklyn, New York 11201